A TOPICAL WORKSHOP

ORGANIC AND POLYMERIC NONLINEAR OPTICAL MATERIALS

sponsored by

THE DIVISION OF POLYMER CHEMISTRY

AMERICAN CHEMICAL SOCIETY

MAY 16 - 19, 1988

VIRGINIA BEACH, VIRGINIA

A Topical Workshop

ORGANIC AND POLYMERIC NONLINEAR OPTICAL MATERIALS

sponsored by

The Division of Polymer Chemistry

AMERICAN CHEMICAL SOCIETY

May 16-19, 1988

Virginia Beach, VA

Co-Chairmen

Diana Gerbi *Sukant Tripathy*

The generous support of the contributors is gratefully acknowledged: Air Force Office of Scientific Research, Office of Naval Research, Du Pont Company, Hoechst-Celanese and 3M Company.

Monday Evening, May 16, 1988

3:00-9:00 p.m.		REGISTRATION
6:30-9:30 p.m.		WELCOMING RECEPTION

PROGRAM:

Tuesday Morning, May 17, 1988

8:15 A.M.		**Opening Remarks**
8:20-9:10	A.	*"An Overview on Nonlinear Optical Polymer Systems and Devices"* by D.R. Ulrich (Air Force Office of Scientific Research)
9:10-10:00	B.	*"Nonlinear Optical Effects in Polymeric Films"* by P.N. Prasad (State University of New York at Buffalo)
10:00-10:30		**Break**
10:30-11:20	C.	*"Recent Advances in Nonlinear Optical Properties of Organic and Polymer Systems"* by A.F. Garito (University of Pennsylvania)
11:20-12:10	D.	*"Conjugated Polymers and Nonlinear Optics"* by S. Etemad (Bell Communications)
		Lunch

Tuesday Afternoon, May 17, 1988

1:30-2:20	E.	*"Anisotropy of the Third Order Nonlinear Optical Susceptibility in Conjugated Polymers"* by A.J. Heeger (University of California at Santa Barbara)
2:20-3:10	F.	*"Nonlinear Optics in Ordered Molecular Systems"* by K.D. Singer (AT&T)
3:10-3:40		**Break**

3:40-4:30	G.	*"Several Series of Novel Polydiacetylenes for Nonlinear Optics"* by H. Nakanishi (Research Institute for Polymers and Textiles, Japan)
4:30-5:20	H.	*"Resonance Effects in Cubic Hyperpolarisabilities of Conjugated Polymers,* by F. Kajzar (CEN Saclay, France)

Wednesday Morning, May 18, 1988

8:30-9:20	I.	*"Nonlinear Optical Measurements on Liquid Crystals and Quasi-Liquid Crystals"* by Y.R. Shen (University of California at Berkeley)
9:20-10:10	J.	*"Nonlinear Optical Effects in Conjugated Systems"* by D. J. Gerbi (3M Co.)
10:10-10:40		**Break**
10:40-11:30	K.	*"Optical Nonlinearity: Molecules, Assemblies and Wave Phenomena"* by G. R. Meredith (E.I. DuPont DeNemours and Co.)
10:30-12:20	L.	*"Characterization of Polymeric Nonlinear Optical Materials"* by G. Khanarian (Hoechst-Celanese)

LUNCH

Wednesday Afternoon, May 18, 1988

1:30-2:20	M.	*"Preparation and Characterization of Organo-Transition Metal Langmuir-Blodgett Films"* by T. Richardson (University of Oxford, U.K.)
2:20-3:10	N.	*"Optical Properties of Organized Assemblies"* by S.K. Tripathy (University of Lowell)
3:10-3:40		**Break**
3:40-4:30	O.	*"The Nonlinear Optics of Langmiur-Blodgett Films" by I. Peterson (GEC Research, Ltd., Great Britain)*

Wednesday Evening, May 18, 1988

6:00 p.m.		POSTER SESSION Wine & Cheese
8:00 p.m.		BANQUET

Thursday Morning, May 19, 1988

8:30-9:20	P.	*"Advances in Organic Electro-Optic Devices"* by R.S. Lytel (Lockheed Research and Development)
9:20-10:10	Q.	*"Organic Nonlinear Optical Devices and Material Considerations"* by B.K. Nayar (British Telecom Research Laboratories, U.K.)
10:10-10:40		**Break**
10:40-11:30	R.	*"Towards Nonlinear Optical Applications of Polydiacetylenes"* by M. Thakur (AT&T)
11:30-12:20	S.	*"High Resolution Laser Spectroscopy in Polymers" by D. Haarer (Universitat Bayreuth, West Germany)*
12:20		*"Closing Remarks"* byK.J. Wynne(Office of Naval Research)

* *

D. R. Ulrich
Air Force Office of Scientific Research

AN OVERVIEW ON NONLINEAR OPTICAL POLYMER SYSTEMS AND DEVICES

BRIEFER:

Dr. Donald R. Ulrich

Directorate of Chemical & Atmospheric Sciences
AFOSR

NLO Response in Polymers

Molecular Level — Microscopic Polarization Related to Applied Electric Field

$$p(E) = \alpha E + \beta E^2 + \gamma E^3 \ldots$$

Macroscopic NLO — Originates From Polarization Response of Molecular Electrons

$$P(E) = \chi^{(1)}E + \chi^{(2)}E^2 + \chi^{(3)}E^3 + \ldots$$

- $\chi^{(1)}$ — Represents Linear Optics
- $\chi^{(3)}$ — Represents Third Order Nonlinear Process i.e., Third Harmonic Generation, Self-Focusing

First and Third Order Terms of Odd Power of E Common to All Materials — Centrosymmetric

- $\chi^{(2)}$ — Second Order Response i.e., Second Harmonic Generation, Optical Rectification

Only In Noncentrosymmetric Medium — Lacks Center of Inversion Symmetry

Why NLO Polymers?

- Subpicosecond Response Times
- Large, Nonresonant Nonlinearities
- Low DC Dielectric Constants
- Low Switching Energy
- Broadband
- Low Absorption
- Absence of Diffusion Problems
- Potential for Resonant Enhancement
- Ease of Processing and Synthesis Modification
- Room Temperature Operation
- Environmental Stability
- Mechanical and Structural Integrity

Where Will NLO Polymers Fit In?

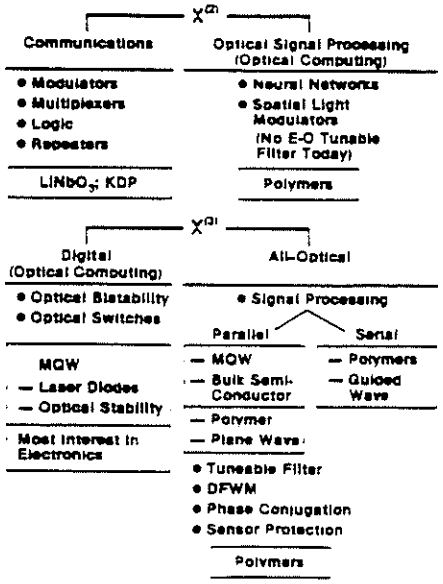

Comparison of Optical Switching Technologies

- Fastest Switches Based on Nonresonant Nonlinearity
- Power Requirements Inversely Proportional to Nonlinearity
- New Organic Polymers May Exceed Optical Device Limits of Resonant Materials
  - Requires Larger n_2 Without Introducing Significant New Absorption
- For $\lambda \neq 0.85$ μm, There are No Alternatives to Organics for Fast Optical Switching

- Power/Bit vs. Switching Time T_s

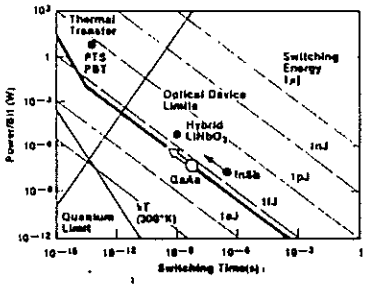

- Extrapolated to λ^2 Cross-Section Devices
- Length Adjusted for Minimum Switching Energy

Optical Performance Comparison

	Polymers	GaAs/GnAlAs
Switch On/ Switch Off, τ (Recovery Period)	• Femtoseconds	• Nanoseconds
Energy Required to Induce Switching	• Moderate N_2 • Nonresonant • Not Defined by λ • Broad Band of Response and Light Sources • Shows all NLO Processes	• High N_2 • Resonance Enhanced • Limited by λ • Close to Bandgap • NLO 3D Order, But Not Optical Amplification or THG
Absorption Coefficient, α Associated With Switching	• $\frac{1}{10^4}$ GaAs	• Large
Figure of Merit FOM = $\frac{n_2}{\alpha\tau}$	• High (1×10^7)	• Moderate (1.5×10^5 on Resonance)

Mechanisms of Four Wave Mixing

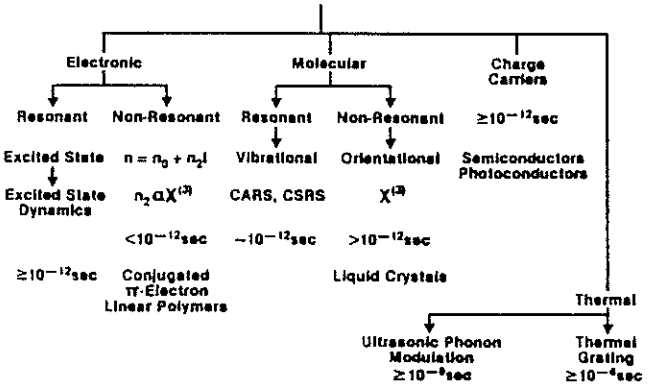

Research Directions NLO Polymer Requirements

- Nonlinear Susceptibilities $\equiv 10^{-8}$ esu
  - Resonant vs Nonresonant
- Ease of Processing
  - Solubility
- Thin Films of Reasonable Optical Quality
  - Transparency
  - Surface Smoothness
- Environmental Stability
- Low Switching Energy (PJ, Diode Lasers)
- Characterization and Separation of Electronic, Molecular, Thermal and Charge Carrier Contribution Mechanisms to Response Time

Status NLO Polymer Classes

Class	Examples	NLO Function
ISO Tropic	Glasses Alloys Composites	$\chi^{(2)}$, $\chi^{(3)}$
Bond Alternation	Ladder Polymers PTL, PQL Polyacetylene Polythiophene	$\chi^{(3)}$
Liquid Crystalline Polymers (LCP)	Side Chain LCPs	$\chi^{(2)}$
Rigid Rod Aromatic Heterocyclics	PBT LCPs PBO BBL	$\chi^{(3)}$
Polydiacetylenes		Mostly $\chi^{(3)}$ Some $\chi^{(2)}$

Second Order Polymers for Electrooptical Devices

- Pendant Side Chain Structure

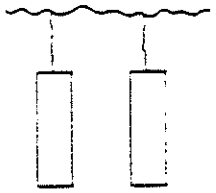

- High Activity

	Polymer	$LiNbO_3$
For SHG	$\chi^{(2)}$ = 120 pm/V	10 pm/V
For Electrooptics	r = 35 pm/V	30 pm/V
FOM = $\frac{r}{\varepsilon}$	10	1

- Excellent Secondary Properties
  - Spin Coatable for Thin Film Waveguides, 2-4 Micron
  - Low Dielectric Constant ($\varepsilon_{Polymer}$ = 3; ε_{LiNbO_3} = 30)
  - Low Loss (< 1 db/cm at 830 nm)
  - Melt Processable for Optics
  - Tg ~ 120 °C

Nonlinear Chromophores Covalently Linked to Glassy Polymer Constructs Noncentrosymmetric Assembly

Synthesis and Poling of Covalently-Functionalized Polymers for Frequency Doubling

I. Functionalization

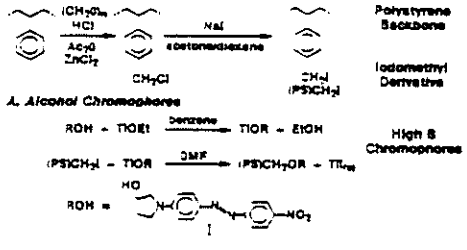

II. Alignment

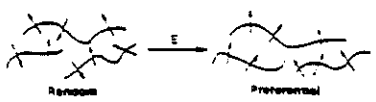

Dependence of SHG On Poling Field

- Significant Non-Random Chromophore Alignment

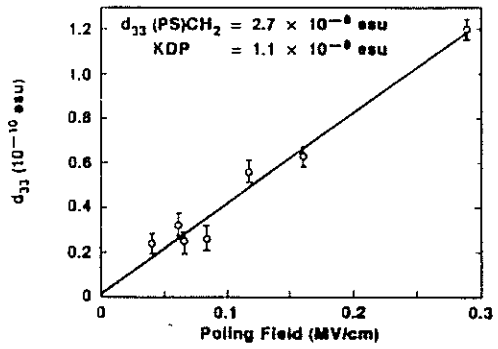

FUNCTIONALIZATION OF POLY(p-HYDROXY-STYRENE) WITH NLO CHROMOPHORES

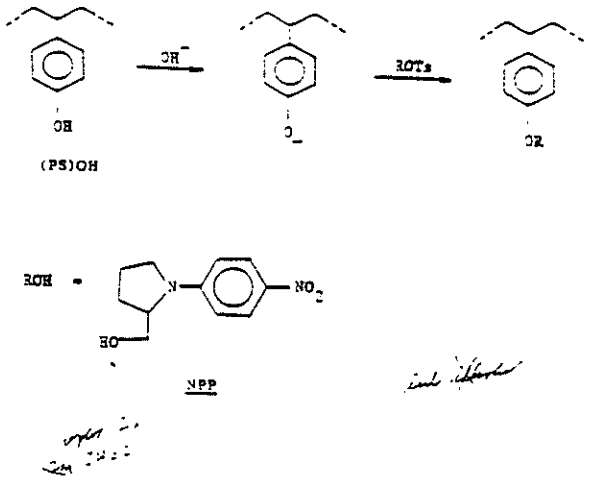

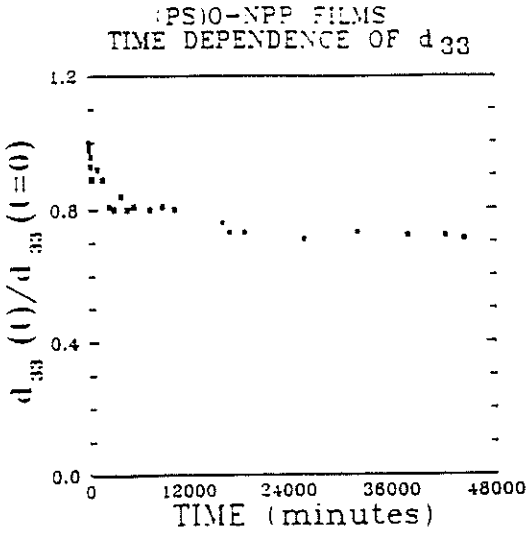

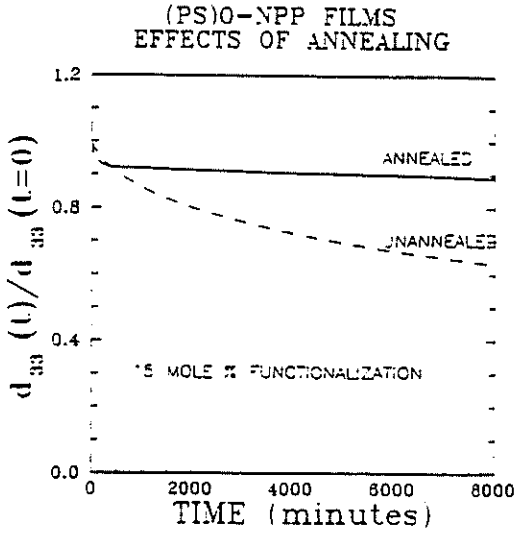

Values for $\chi^{(3)}$, Eg, W From Semiempirical Calculations and Experimentally Determined $\gamma(HOMO)^2$ Delocalization Length for Prototype Ladder Polymers and Polyacetylene

Polymer	Band Gap Eg(eV)	Band Width W(ev)	$\chi^{(3)}$ (esu)	N_d^*
Pristine Trans-PA	1.8	10	6.5×10^{-10}	29
Pristine PXL X = CH Ladder (Chance)	0.7	1.5	5×10^{-10}	26-28
Bipolaron State of PXL X = CH Ladder (Dalton)	0.3	2	10^{-7}	
Protonated PXL	3.8	3	2×10^{-13}	

Implications of $\gamma(HOMO)^2$ Delocalization Experiments For NLO Polymen Synthesis

- Negative Spin Density Confirms Electronic Excitation (Electron Correlation)
- Delocalization Length in Ladder Polymers and Polyacetylene the Same — 26 to 29 Atoms
- Indicates $\chi^{(3)}$ Will Not Increase Beyond 25 Repeat Units (80 Å)
- Ladder Polymers May be Superior to Open Chain Polyanilenes Because Improved π-Orbital Overlap Will Lead to Enhanced Delocalization and Reduced Optical Gap

Dependence of $\gamma(-3\omega, \omega, \omega, \omega)$ On Chain Length

- Finite Chain Limit: $\gamma \propto n^{5.5}$
  - Decreasing Excitation Energy
  - Increasing Number of Spin Correlated States
- Polymer Chains: $\chi^{(3)} \sim 10^{-9}$ esu
  - 25 Repeat Units (80 Å)

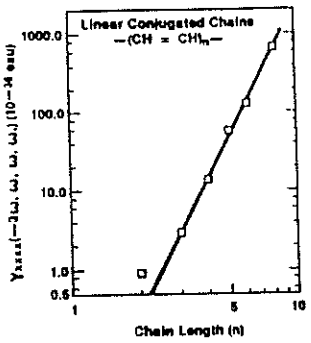

Application of Dalton's Results

- Solubilized Ladder Polymers by Lewis Acid Charge Transfer Complex Forming Agents

Soluble Benzimidazophenanthroline (BBL)

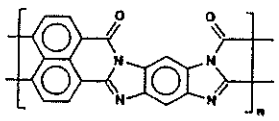

- Soluble in Organic Acids
- Reduces Intermolecular Attractive Forces and Allows Solubilization of Rigid Macromolecules

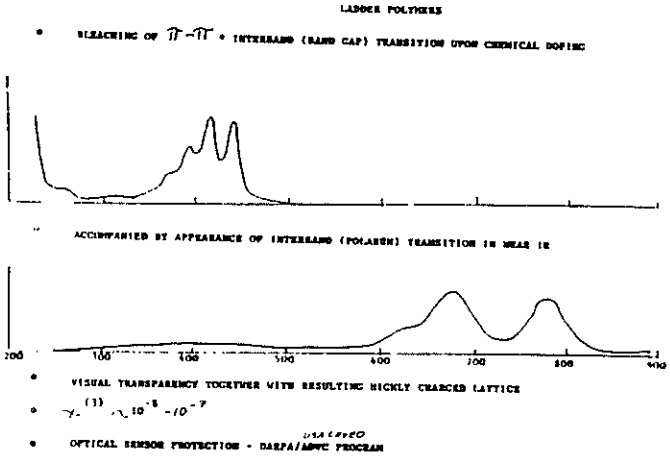

NONLINEAR OPTICAL AND PHOTOCHROMIC POLYMERS

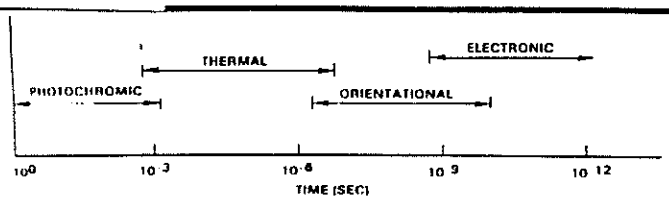

PHOTO-CHROMIC	THERMAL NONLINEARITY	ORIENTATIONAL KERR NONLINEARITY	ELECTRONIC KERR NONLINEARITY
– OPTICAL FUSE	– DYE SENSITIZED THERMAL EFFECT	– LIQUID CRYSTAL POLYMERS	– ELECTRONIC $\chi^{(3)}$ POLYMERS
– 10^{-3} D.C.	– 10^{-3} - 10^{-7} SEC	– 10^{-7} - 10^{-10} SEC	– 10^{-9} - 10^{-12} SEC
THREAT	**THREAT**	**THREAT**	**THREAT**
– GAS LASERS	– PULSED FLASH LAMP PUMPED LASERS	– Q-SWITCHED SOLID STATE LASERS	– Q-SWITCHED SOLID STATE LASERS
– CW SOLID STATE LASERS	– GAS LASERS – CW SOLID STATE LASERS	– PULSED FLASH LAMP PUMPED LASERS	– MODE-LOCKED LASERS

HARDENING TECHNIQUES

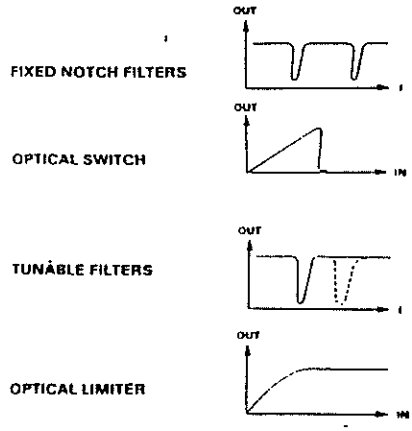

- SUB NANOSECOND RESPONSE TIMES
- MILLISECOND RECOVERY SPEEDS (AT LEAST)
- BROADBAND WAVELENGTH RESPONSE (OVER VISIBLE AND NEAR IR)
- REJECTION EFFICIENCY >99% BEFORE AND AFTER SWITCHING
- HIGH DAMAGE THRESHOLDS (>MW/cm²)
- LOW INSERTION LOSSES AND MINIMAL RETROFIT COMPLEXITIES

SENSOR PROTECTION

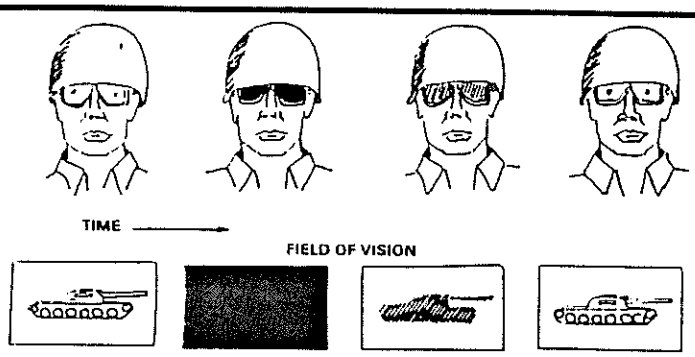

FOCUS IS ON CONCEPTS WHICH CAN:

- PROTECT AGAINST RAPIDLY TUNABLE, PULSED, VISIBLE AND NEAR IR LASER THREATS TO HIGH GAIN OPTICAL SYSTEMS
- USEFUL FOR RANGEFINDERS, VISUAL SENSORS, CAMERAS, AND MOST IMPORTANTLY, THE EYE

Third Order Polymers for Optical Devices

- Planar Structure With Extended π Orbitals

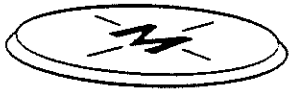

M = Metal Atom

- Shift In Focus From Conjugated Off-Resonance to Systems on Resonance With Narrow Molecular Extinction Coefficients
- High Activity Through Saturable Absorption
  - Effective N_2 Equals AlGaAs MQW Structures
- Excellent Secondary Properties
  - Spin Coatable For Thin Film Structure Applications
    - Optical Bistability
    - Parallel Processing

Phthalocyanines

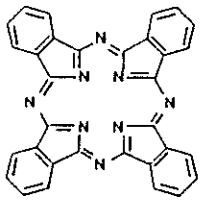

- Large NLO response discovered by A. Garito
- Numerous variants synthesized to tailor
  - NLO activity
  - Fabrication properties

Basic Structure of an Optical Neural Network

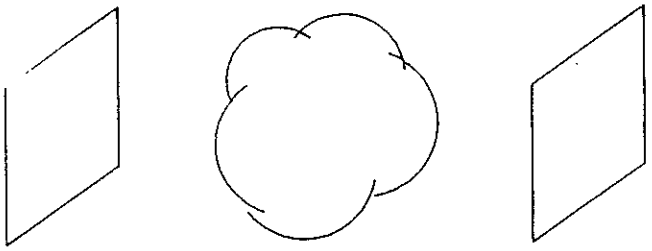

Input Plane of Neurons

N , X (I) 's

Optically Implemented Interconnections

W (I,J) 's

$N^2 \rightarrow N^{3/2}$

Output Plane of Neurons

N , X (J) 's

OPTOELECTRONIC IMPLEMENTATION OF A NEURAL NETWORK

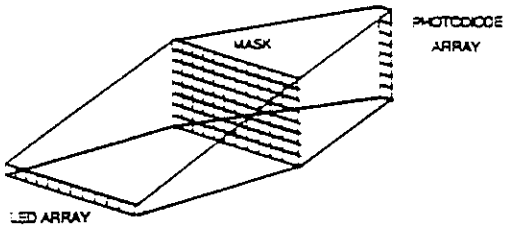

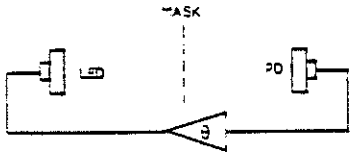

ELECTRONIC FEEDBACK

- DEMONSTRATED STEADY - STATE OPTICAL BISTABILITY COMPARABLE TO GaAs IN FABRY - PEROT ETALON OF 1000Å POLYMER FILM
- LINEAR ARRAY OF OPTICAL BISTABLE ELEMENTS THAT COULD REPLACE PHOTODIODES

Angular Dependence of Reflected $X^{(3)}$ for Oriented Trans-Polyacetylene by Third Harmonic Generation

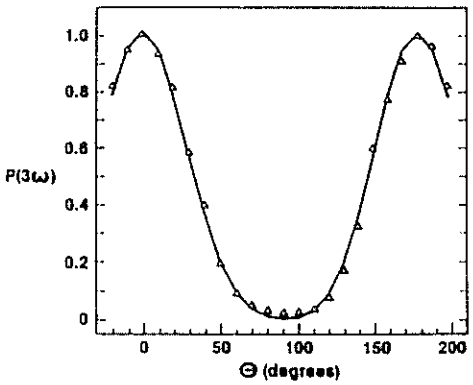

Third Order Response in Polyacetylene

- Resonant Process
  - Photoexcited Nonlinear Excitations
  - Associated Structural Distortions (Solitons, Bipolarons, Polarons) Responsible for Large Shifts of Oscillator Strength Observed With Resonant Pumping Consequence of Electron-Phonon Interaction
  - Electronic Resonant Enhancement
    - Nonradiative Dissipation Produces Slower Responses
- Reflected $X^{(3)}$
  - 9×10^{-10} esu Parallel to Polymer Chain
  - For Devices Polymer Must Be Able to Inherently Transmit or Guide Light

Third Order NLO Response of Ordered Polymers

- Collinear Rigid Rod

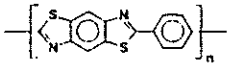

Polybenzobisthiazole (PBT)

- Planar Rigid Rod

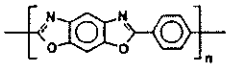

Polybenzobisoxazole (PBO)

COMPARISON			
Uniaxial PBT	— Third Harmonic Generation	—	$\chi^{(3)} \simeq 10^{-10}$ esu
Biaxial PBT	— Degenerate Four Wave Mixing (DFWM)	—	$\chi^{(3)} \simeq 10^{-11}$ esu
Uniaxial PBO	— Degenerate Four Wave Mixing	—	$\chi^{(3)} \simeq 2.5 \times 10^{-11}$ esu

- Requirement for Film Quality — Avoid Inherently Grain or Fibrous Components Which Scatter Light

Degenerate Four Wave Mixing of Biaxial PBT Ordered Polymer Films

Poly (p-phenylenebenzobisthiazole) (PBT)

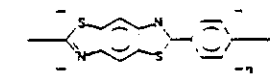

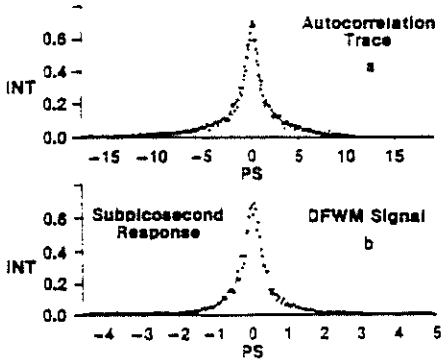

Nonresonant Third Order Susceptibility $\chi^{(3)}$ in Biaxial PBT

- Degenerate Four Wave Mixing

Polar Plot $\chi^{(3)}$ As a Function of Film Rotation Angle

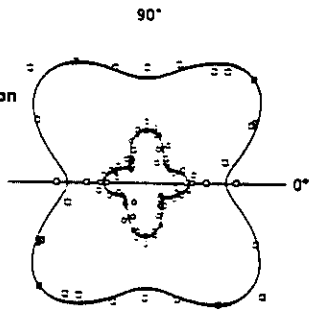

- New Feature for Third Order Devices
- Anisotropic $\chi^{(3)}$ Materials for Optically-Activated Birefringent Film Applications

$\chi^{(3)}$ Polymers for Fibers

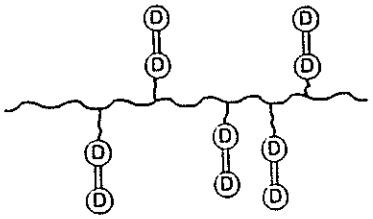

- $\chi^{(3)}$ units have modest activity but very low absorption
- Polymer backbone confers secondary properties
  - Spinability
- Shear and elongational flow yield alignment

$\chi^{(3)}$ Materials

Thin Limit

Properties
- Near reasonance
- High n_2
- High absorption (α)

Material
- Phthalocyanines

Application
- Etalons
- All optical SLM's

Advantages
- Fabrication ease
- Room temperature operation
- Potentially highest n_2 materials

Thick Limit

Properties
- Non resonant
- Lower n_2
- Very low absorption

Material
- Side chain polymer

Application
- NLO fibers
- All optical switching

Advantages
- Fiber spinning ease
- Potentially highest n_2/α materials

POLYALKYLTHIOPHENE

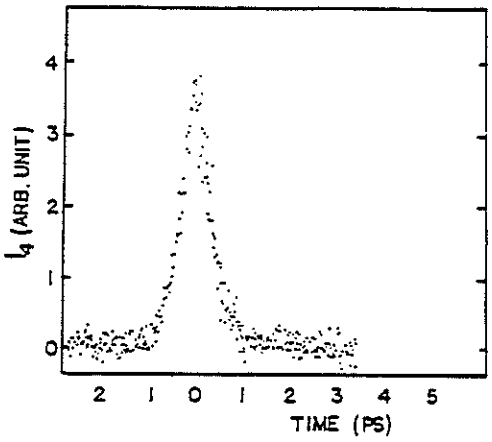

Fig. The degenerate four wave mixing signal obtained for a 20 layer thick Langmuir-Blodgett film of polyalkylthiophene shown as a function of the delay of the backward beam; the wavelength is 602 nm and the excitation pulsewidth is 340 fs.

$\chi^{(3)} \sim 10^{-9}$ esu

POLYMER MULTIPLE QUANTUM WELLS

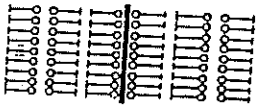

MOLECULAR ARCHITECTURE TAILORING

- o LIQUID CRYSTALLINITY
- o GUEST-HOST BLENDS
- o IN-SITU POLYMERIZATION AND ORDERING
- o RIGID/FLEXIBLE CHAIN CONFORMATIONS

- o NEW HETEROSTRUCTURE ASSEMBLIES
  - GAAS ANALOGS
  - NON GAAS ANALOGS
- o QUANTUM DOT DOMAIN STRUCTURES

CHARGE CARRIER DYNAMICS

- o CHARGE TRANSFER INTERACTIONS
- o REDUCE DIMENSIONALITY OF CHARGE CARRIERS
- o INTERFACE SHG
- o PICOSECOND TRANSIENT ABSORPTION/ GRATING
- o TRANSIENT ETALON EFFECTS/ PHONON INDUCED PROCESSES

LCC Composite

New LCC's

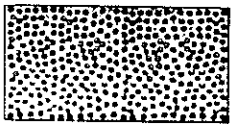

- $d << \lambda$ (Rayleigh scattering regime)
- Randomly oriented LC microdroplets
- Low scattering - hazy blue to transparent
- Kerr material with positive n_2

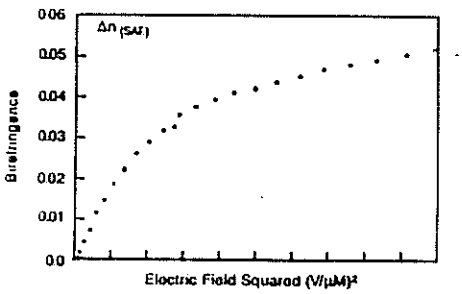

ADVANCED POLYMER BLENDS AND OPTICS

NLO POLYMERS

GENERATION	SECOND ORDER NLO, $\chi^{(2)}$	THIRD ORDER NLO, $\chi^{(3)}$
I (1985 - 1989)	HOMOPOLYMERS	
	o ISOTROPIC	o BOND ALTERNATION
	o POLED	o LADDER
	o ORIENTED	o ORDERED
II (1990 - ?)	POLYMER - POLYMER INTERACTIONS { BLENDS - ALLOYS / MOLECULAR COMPOSITES }	
	o SELF-INDUCED POLARIZATION	o NEAR-OFF RESONANCE
	o SELF-ORGANIZING	o PLANAR

IMPROVEMENTS IN CALCULATION OF NLO SINGLE-MOLECULE PROPERTIES

- PARALLEL COMPUTING
- ABSORPTION LINEWIDTHS

  MOLECULAR CONFORMATIONS AND DEFECTS
- DEVELOPMENT OF ALTERNATIVE METHODOLOGIES, SUCH AS FINITE FIELD APPROACHES

GENERALIZATION OF SINGLE-MOLECULE TO BULK NLO PROPERTIES

STATISTICAL AVERAGING OF ORIENTATION (FROZEN GAS MODEL)

STATISTICAL AVERAGING OF CHAIN LENGTHS

EFFECTS OF INTERMOLECULAR INTERACTIONS ON SINGLE MOLECULE NLO PROPERTIES

EFFECTS OF INTERMOLECULAR INTERACTIONS ON MOLECULAR CONFORMATION AND STRUCTURE

EFFECT OF INTERMOLECULAR INTERACTIONS ON MATERIAL ULTRASTRUCTURE

THE KEY: INTERMOLECULAR INTERACTIONS!

Status of Understanding for Polymer Design

Detailed Mechanism(s) of Nonlinear Optical Activity in Delocalized Electron Polymers Have Yet to Be Defined

- Nonlinear Optical Activity May Not Be Simply Related to Bandgap
- Potential Contributions of D Orbitals to NLO (S-D Cross-Terms)
- Role of Electron-Phonon Interactions
- A Qualitative Correlation Between $\chi^{(3)}$ and Electron Delocalization Length
- Effect of Doping and Intermolecular Charge Transfer Needs to Be Clarified
- Quantitative Theory Lacking to Predict macromolecules With Large Second Order (Beta) and Third Order (Gamma) Molecular Susceptibilities

State-of-Art $\chi^{(2)}$ Devices

- Traveling-Wave Electrode Mach-Zehnder Electrooptic Modulator

	$LiNbO_3$ Modulator	Polymer Modulator
Switching Voltage (V)	3 1/2 – 10 1/2	1.3 (0.7 With Higher $\chi^{(2)}$)
Power Requirement (W)	0.8 – 5	0.03
Maximum Frequency (GHz)	8 – 24	>50

  - No Expected Velocity Mismatch Implies Higher Frequency Devices are Possible With Polymers
- Electrooptic Bragg Cell
  - High Speed Radar Signal Processing
  - 20 GHz as a Target
- Second Harmonic Generation
  - High Efficiency Doubling of a Diode Laser

Waveguide Devices

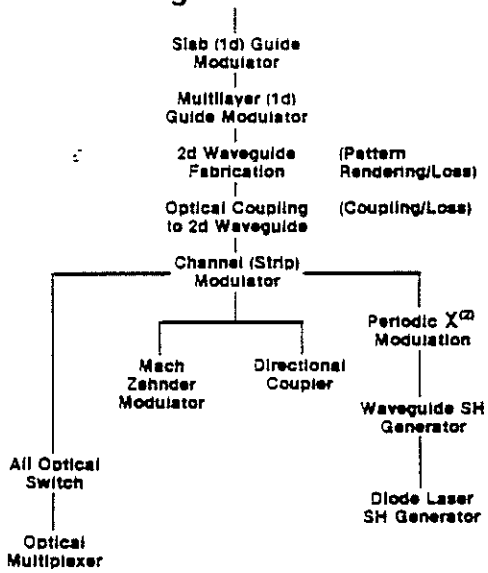

Polymeric Electrooptic Modulator

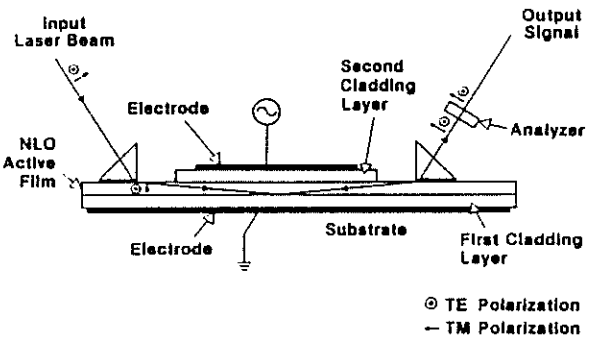

Traveling-Wave Waveguide

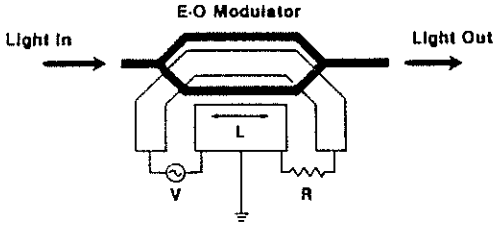

- Voltage Varies Along the Length ($L \gtrsim \lambda$ Electrical)
- Important Device Parameters:
  - Voltage
  - Optical Mode Size
  - Drive Power
  - Speed
  - Length
  - Impedance

State-of-Art $X^{(3)}$ Devices

- Far Less Progress Than $X^{(2)}$
- Large Payoff in Multiplexing and Demultiplexing
  - High Speed
  - Handle Many Inputs
  - Very High $X^{(3)}$
- Can Lead to:
  - All Optical Interferometer and Optical Switch
  - Optical Bistability and Digital Optical Information Processing
  - Optically Induced Dynamic Grating and Real-Time Holography
- Device Performance Depends on Material Properties in a Complicated Way
  - Determined by Device Architecture
  - Parallel/Analog Processing of 2D Image
  - Phase Conjugate Optics and Image Processing
  - Self Focusing/Defocusing Applications

Mach-Zehnder All Optical Modulator

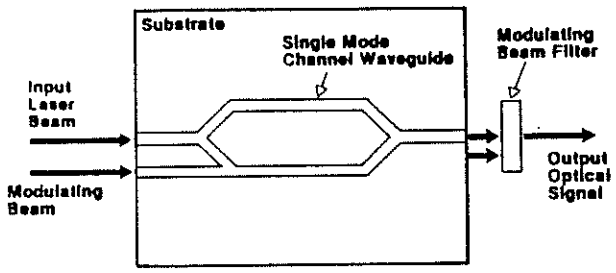

OPTICAL BISTABILITY IN A NONLINEAR POLYMER FABRI-PEROT ETALON

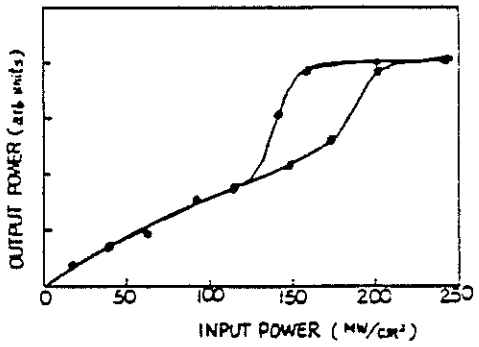

OPTICAL BISTABILITY IN A POLYMER
QUASI WAVE GUIDE INTERFEROMETER

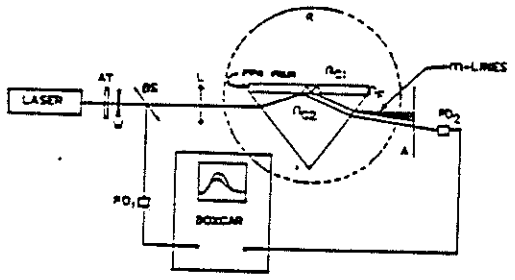

MERITS:

(i) Obtain Linear Refractive Index and Film Thickness

(ii) Obtain Both Magnitude and Sign of $\chi^{(3)}$

REF 23

OPTICAL BISTABILITY IN A
NONLINEAR POLYMER
QUASI-WAVEGUIDE INTERFEROMETER

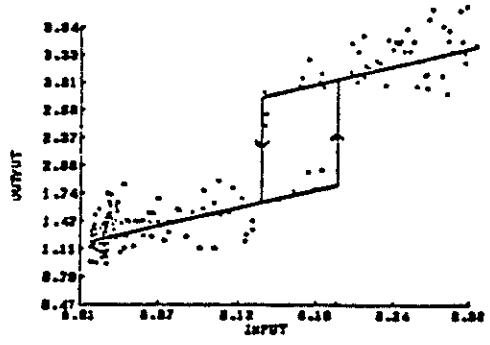

Figure 1. The observed optical bistability behavior in the poly-4-BCMU polymer quasi-waveguide interferometer. The detuning angle is 499°.

Summary

Second Order

- Poled Polymer Films
  - — Close to Achieving Levels of Response for Electrooptic Device Application
- First Polymers Comparable to Lithium Niobate Reported
- Focus for Research to Achieve Optimum Electrooptic Modulation
  - — $X^{(2)}$ Parallel to Film Surface

Third Order

- Nonlinearities of 10^{-9} esu Large for Nonresonance but Still Needs to be Larger ($\approx 10^{-7}$ esu) for Broad Device Application
- State-of-Art of 10^{-9} esu Will Find Applications in Optical Wave Guide Devices Such as Optical Switches and Optically Controlled Modulators
- Thin Film Applications Such as Etalons Unlikely Unless Significant Advances in Larger Nonlinearities, Optical Flatness and Optical Clarity

P. N. Prasad
State University of New York at Buffalo

NONLINEAR OPTICAL EFFECTS IN POLYMERIC FILMS

B-2

NONLINEAR OPTICAL EFFECTS

IN

POLYMERIC FILMS

PARAS N. PRASAD

DEPARTMENT OF CHEMISTRY

STATE UNIVERSITY OF NEW YORK AT BUFFALO

BUFFALO, NEW YORK 14214

SECOND ORDER NONLINEAR OPTICAL PROCESSES

CURRENT STATUS

1. PREDICTABILITY OF STRUCTURE FOR MOLECULAR ENGINEERING
   → REASONABLE

2. LARGE $\chi^{(2)}$
   FAST RESPONSE TIME → ALREADY ACHIEVED
   LOW DC DIELECTRIC CONSTANT

3. GUIDED WAVE PROCESSES - ALREADY DEMONSTRATED

4. POLYMERIC STRUCTURES
   NOT REQUIRED, BUT MAY BE DESIRABLE FOR MATERIALS PROCESSING AND DEVICE APPLICATIONS
   DOPED POLYMERS, LIQUID CRYSTALLINE POLYMERS, ETC.

5. DEVICES (?) : RESTRICTED BY MATERIALS LIMITATION

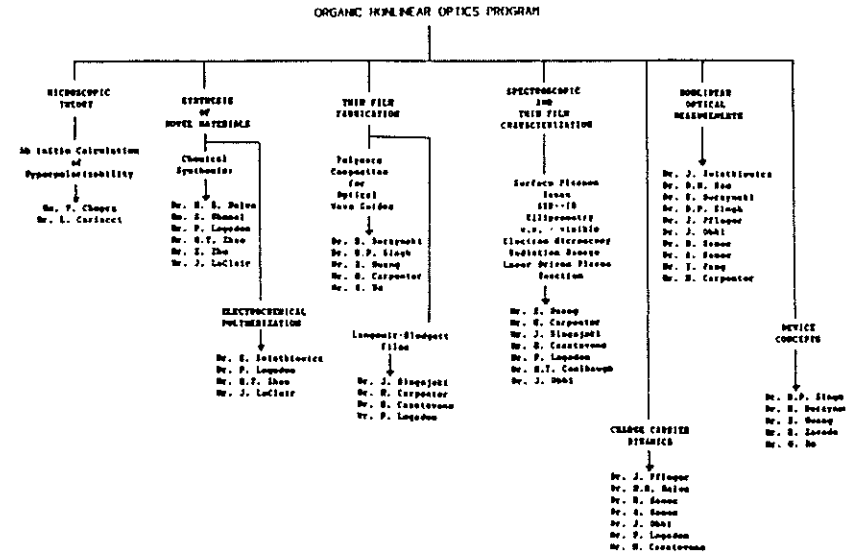

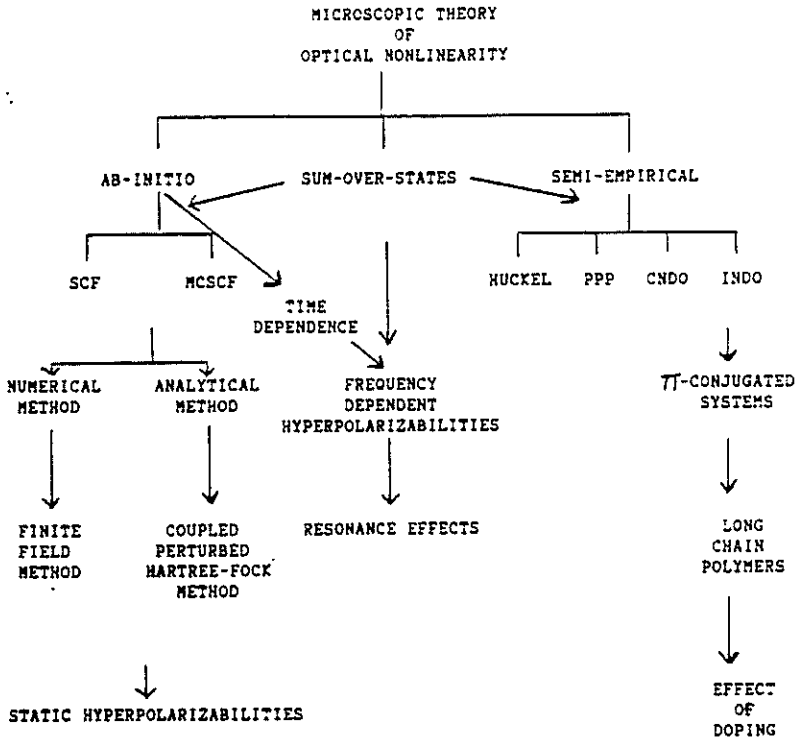

Ab-initio Calculations of Second Hyperpolarizabilities (γ)

OBJECTIVE: Relative importance of σ and π contributions

Comparison of various π electron structures

π-electron conjugation effect

Sign of γ

Anisotropy of γ tensor

Effect of substituents

Conformational effect

Effect of Structural (conformational defects) such as solitons, polarons and bipolarons

⇩

Identify Structural Parameters for enchancing $\chi^{(3)}$

AB-INITIO APPROACH

DEFINE MOLECULAR HAMILTONIAN INCLUDING FIELD DEPENDENT STARK TERM

↓

CONSTRUCT LCAO - MO - SLATER DETERMINANTS WITH A CHOICE OF AO BASIS SET

↓

OPTIMIZE THE GEOMETRY USING SCF

↓

CALCULATE DIPOLE MOMENT AS A FUNCTION OF FIELD

↓

POLYNOMIAL FIT TO GET γ

↓

CHANGE FIELD DIRECTIONS TO CALCULATE DIFFERENT COMPONENTS OF γ

↓

ORBITAL TRANSFORMATION TO SEPARATE σ AND π-CONTRIBUTIONS

↓

CONTOUR PLOTS TO OBTAIN FIELD INDUCED CHARGE REDISTRIBUTION

↓

STATIC SECOND HYPERPOLARIZABILITIES (γ)

↓

NONRESONANT VALUE

MERITS OF THIS APPROACH:

ONLY GROUND STATE PROPERTIES NEED TO BE DEFINED

IN PERTURBATIVE CALCULATIONS INVOLVING EXCITED STATES EXPANSION, EXCITED STATE PROPERTIES NEED TO BE CALCULATED

B-4

SOME CONCLUSIONS OF THEORETICAL STUDIES OF MICROSCOPIC NONLINEARITY

1. THE CHOICE OF BASIS, PARTICULARLY THE INCLUSION OF DIFFUSE POLARIZATION FUNCTIONS, IS IMPORTANT IN DESCRIBING THE HYPERPOLARIZABILITIES OF CONJUGATED SMALL MOLECULES.

2. γ IS ANISOTROPIC, WITH THE COMPONENT γ_{zzzz} ALONG CHAIN GROWING RAPIDLY FOR THE CONJUGATED HYDROCARBONS SERIES POLYENES, POLYYNES AND CUMULENES AS THE CHAIN LENGTH GROWS.

3. FOR POLYENES, CHAIN LENGTH DEPENDENCE OF $N^{3.2}$ IS FOUND. FREE ELECTRON MODEL AND HUCKEL MODEL PREDICT N^{5} AND $N^{5.3}$ RESPECTIVELY.

4. THE CORRESPONDING ORBITAL ANALYSIS SHOWS THAT THE SIGMA AND π-ELECTRON CONTRIBUTIONS TO γ ARE OF OPPOSITE SIGNS.

5. CONTOUR MAP OF THIRD DERIVATIVE OF CHARGE DENSITY WITH RESPECT TO FIELD (REGIONAL CONTRIBUTION ANALYSIS OF γ) CONDUCTED FOR POLYYNES, INDICATES THAT THE NONLINEAR ELECTRONIC DISTORTION IS A CO-OPERATIVE EFFECT WITH A SUBSTANTIAL CHARGE TRANSFER ALONG THE ENTIRE LENGTH OF THE CHAIN.

6. OUR SCF CALCULATION RESULTS FOR α COMPARE WELL WITH THOSE OF THE SOS METHOD, BUT γ VALUES DO NOT AGREE.

7. IN THE SERIES R1 - C≡C - R2, THE LONGITUDINAL COMPONENT γ_{zzzz} INCREASES AS THE ELECTRON WITHDRAWS GROUPS AT R1 OR R2 ARE SUBSTITUTED.

8. A COMPARISON OF γ FOR CIS-BUTADIENE, TRANS-BUTADIENE AND THIOPHENE REVEALS THE FOLLOWING ORDER:

   TRANS-BUTADIENE> THIOPHENE> CIS-BUTADIENE

THIOPHENE OLIGOMERS

REPEAT UNIT DEPENDENCE

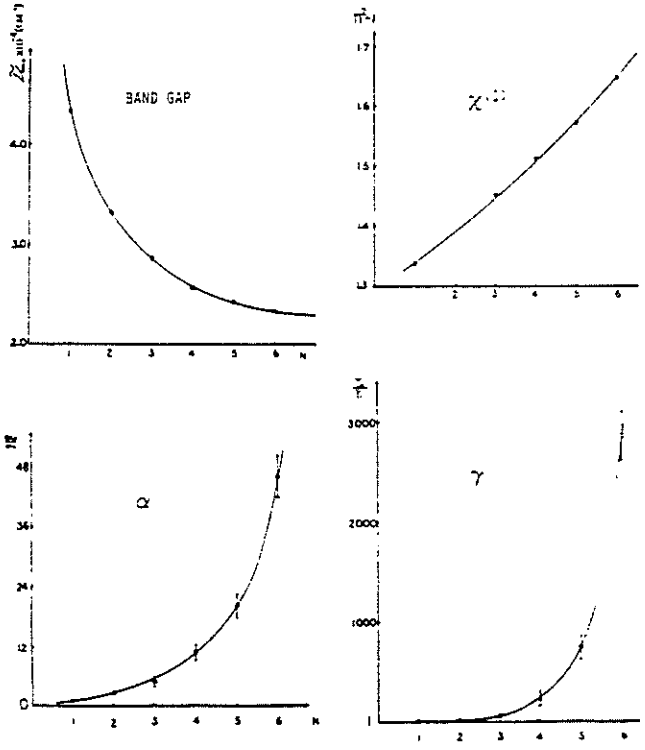

POLYMETHINE OLIGOMERS

DEPENDENCE OF α AND γ ON NUMBER OF REPEAT UNITS (N)

$P = A + B(N - \delta)^C$ $\quad P = \alpha$ OR γ

EXPT.	FOR $\langle\alpha\rangle$	C = 1.69	FOR γ_{HYPER}	C = 4.05
OUR AB-INITIO CALCULATION ON POLYENES	FOR α	C = 1.3 - 1.5	FOR γ	C = 3.2 - 3.4
FREE ELECTRON MODEL	FOR α	C = 3	FOR γ	C = 5
PPP MODEL	α	C = 2.3	γ	C = 5.3

FOR THIOPHENE

	$\langle\alpha\rangle$	$\langle\gamma\rangle$
AB-INITIO CALCULATION	8.21×10^{-24} (cm^3)	1×10^{-36} (esu)
EXPT. VALUE	9.8×10^{-24}	3.5×10^{-36}

FOR BITHIOPHENE

	$\langle\alpha\rangle$
AB-INITIO CALCULATION	1.45×10^{-22}
EXPT. VALUE	2.5×10^{-23}

DEPENDENCE OF $\chi^{(3)}$

RELEVANT PARAMETERS

1. MAGNITUDE OF $\chi^{(3)}$
2. RESPONSE TIME
3. ANISOTROPY OF $\chi^{(3)}$ FOURTH RANK TENSOR
4. SIGN OF $\chi^{(3)}$
5. REAL OR COMPLEX ?
6. LOCAL FIELD EFFECT
7. ELECTRONIC RESONANCE ENHANCEMENT
8. VIBRATIONAL RESONANCE ENHANCEMENT

TECHNIQUES USED

FEMTOSECOND DEGENERATE FOUR WAVE MIXING
OPTICAL WAVEGUIDE
NON-LINEAR FABRY PEROT
SURFACE PLASMON
THIRD HARMONIC GENERATION
KERR GATE EXPERIMENT

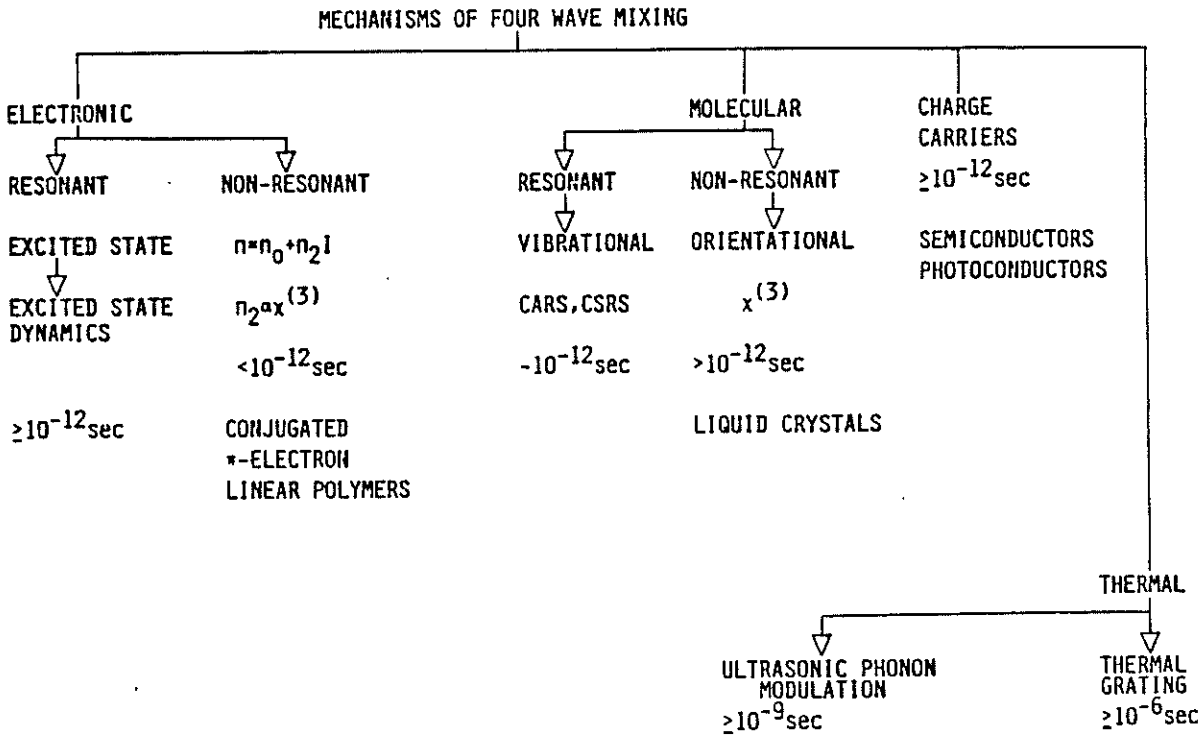

MEASUREMENTS OF $\chi^{(3)}$

RELEVANT PARAMETERS:

1. MAGNITUDE OF $\chi^{(3)}$
2. RESPONSE TIME
3. ANISOTROPY OF $\chi^{(3)}$
   FOURTH RANK TENSOR
4. SIGN OF $\chi^{(3)}$
5. REAL OR COMPLEX (?)
6. LOCAL FIELD EFFECT
7. ELECTRONIC RESONANCE ENHANCEMENT
8. VIBRATIONAL RESONANCE ENHANCEMENT

TECHNIQUES USED:

FEMTOSECOND DEGENERATE FOUR WAVE MIXING
OPTICAL WAVEGUIDE
NON-LINEAR FABRY PEROT
SURFACE PLASMON
THIRD HARMONIC GENERATION
KERR GATE EXPERIMENT

POLAR PLOT: $\chi^{(3)}$ AS A FUNCTION OF FILM ROTATION ANGLE

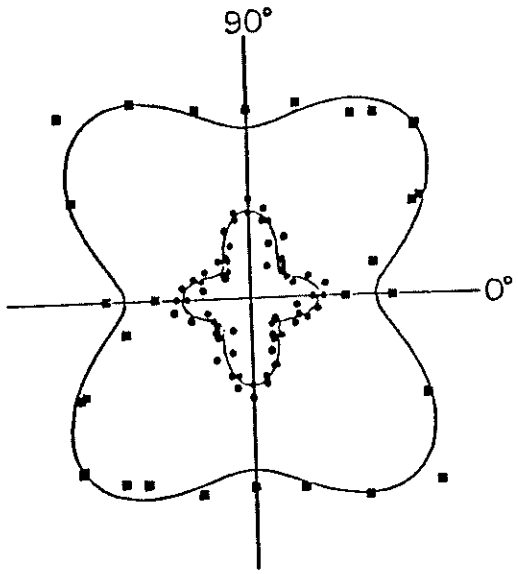

RESONANT $\chi^{(3)}$ BY FIVE WAVE MIXING

ELECTRONIC RESONANCES

SYSTEMS	MECHANISM	RESPONSE TIME	$\chi^{(3)}$
PVK:TNF	CORRELATED ELECTRON-HOLE PAIRS	>100 ps	10^{-11} esu
POLYACETYLENE PHMA	SOLITON/POLARON DYNAMICS	fs	10^{-9} esu
PHTHALOCYANINES (LB FILMS)	EXCITON DYNAMICS	ps	10^{-8} esu
POLYTHIOPHENE (ELECTROCHEMICALLY DEPOSITED)	POLARON DYNAMICS	fs	10^{-9} esu
POLYALKYLTHIOPHENE (SOLUTION CAST FILMS, L-B FILMS)	POLARON DYNAMICS	fs	10^{-8} esu

CAUTION!

$\chi^{(3)}$ DEPENDENT ON PULSE WIDTH GOING FROM 600 fs TO 2 ps INCREASED $\chi^{(3)}$ BY A FACTOR OF 3 IN PHTHALOCYANINES.

B-7

NONLINEAR OPTICAL EFFECTS
IN
CONJUGATED POLYMERS
WITH
CONFORMATIONAL DEFECTS
(Bond Alternation)

NONRESONANT CASE: Charge on Polymer Backbone can be Varied in a Controlled way - Tune $\chi^{(3)}$

RESONANT CASE: Photoinduced Solitons and Bipolarons create Mid Gap States

Redistribution of Oscillator Strength

Large $\chi^{(3)}$ with Fast Response

A NEW PHENOMENON

Chemical or Electrochemical Switching of $\chi^{(3)}$ Between High and Low States

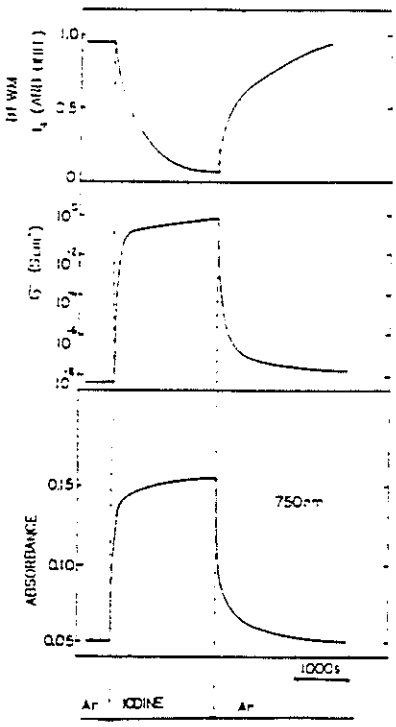

POLYALKYLTHIOPHENE - LB FILMS
IODINE DOPING

IN-SITU ELECTROCHEMICAL STUDY OF $\chi^{(3)}$ IN POLYTHIOPHENE

REDUCED FORM <-> OXIDIZED FORM <-> REDUCED FORM

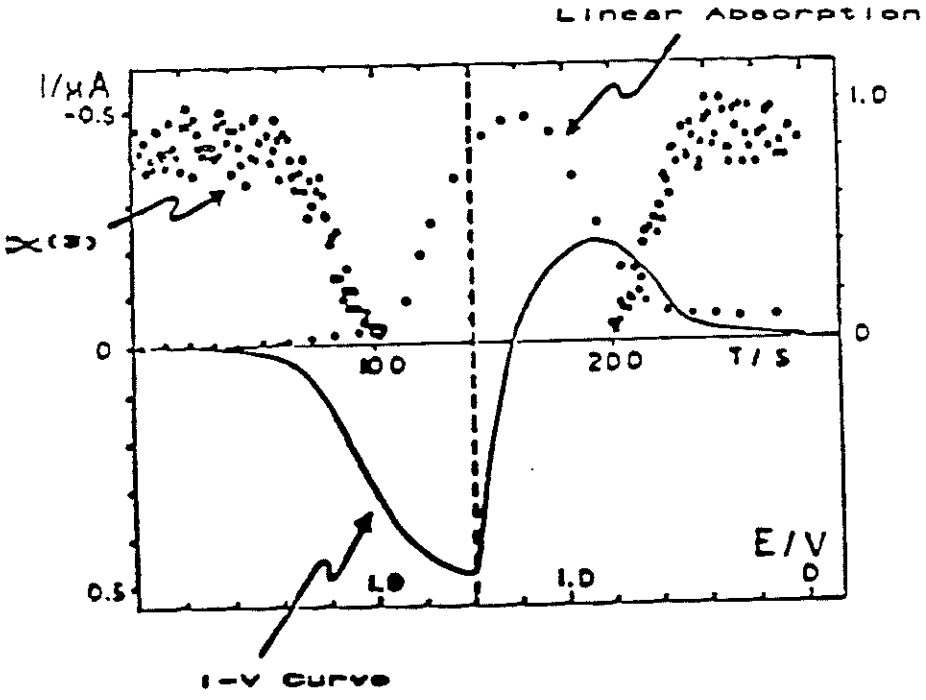

SWIATKIEWICZ, JANISZEWSKA AND PRASAD

B-8

PICOSECOND TIME-RESOLVED COHERENT RAMAN SCATTERING

$\chi^{(3)}$

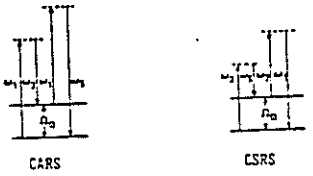

EXPERIMENTAL ARRANGEMENT

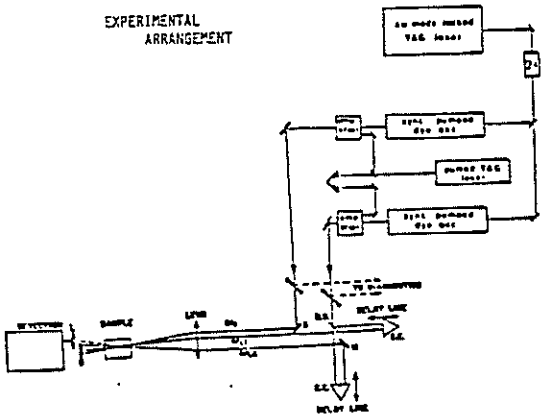

POLY - 4BCMU (LOW MOL. WT), 42 K

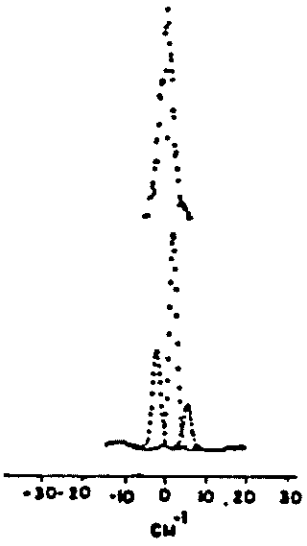

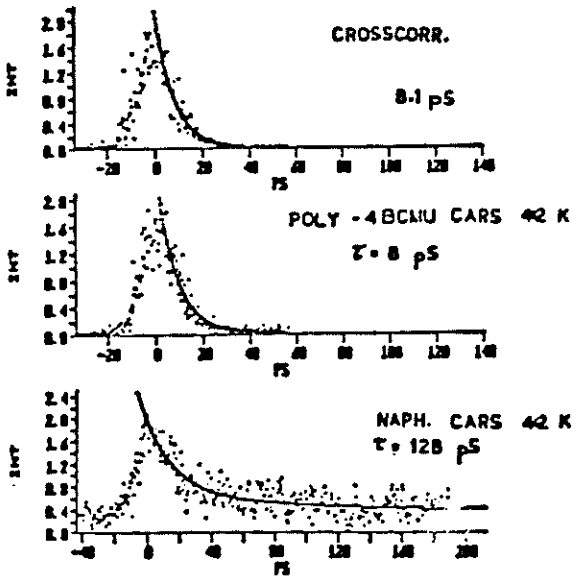

B-9

DEVICE SCHEMES

▽

OPTICAL SWITCHING
OPTICAL BISTABILITY
OPTICAL LIMITER ACTION
LIGHT MODULATION

1.	SURFACE PLASMON	ELECTRO-OPTIC MODULATION IN THE ELECTRICALLY POLED MONOLAYER LANGMUIR-BLODGETT FILMS OF A LIQUID CRYSTALLINE POLYMER
2.	FABRY-PEROT ETALON	OPTICAL SWITCHING AND OPTICAL BISTABILITY BOTH ABSORPTIVE AND DISPERSIVE.
3.	QUASI-WAVEGUIDE INTERFEROMETER	OPTICAL BISTABILITY
4.	WAVEGUIDE	MAY BE ONLY EXAMPLE OF $\chi^{(3)}$ POLYMER WAVEGUIDE LIMITER ACTION (INTENSITY DEPENDENT PHASE SHIFT) INTENSITY DEPENDENT COUPLING ANGLE. FREQUENCY SPECTRUM SHAPING IN WAVEGUIDE PROPAGATION
5.	HOLLOW FIBERS FILLED WITH NONLINEAR MATERIALS	KERR SCATTERING, GAIN AND AMPLIFICATION.

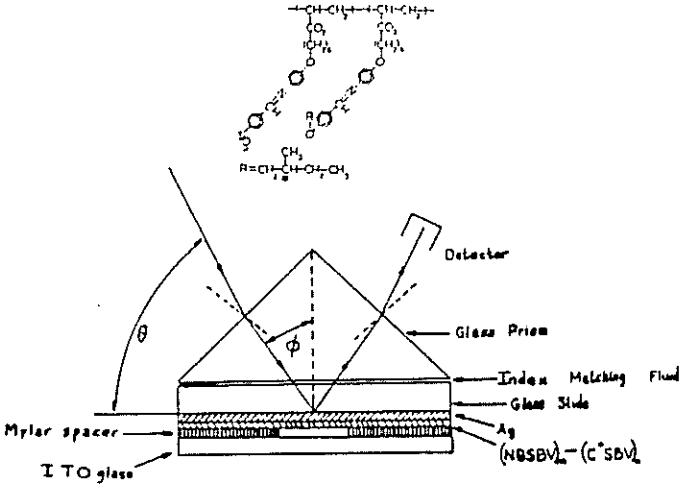

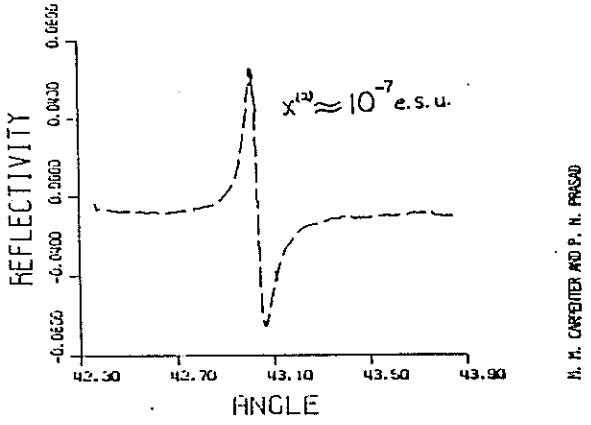

M. M. CARPENTER AND P. N. PRASAD

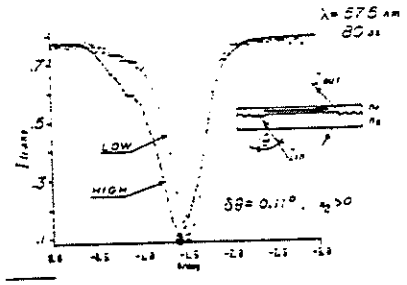

LIMITER ACTION WAVEGUIDE

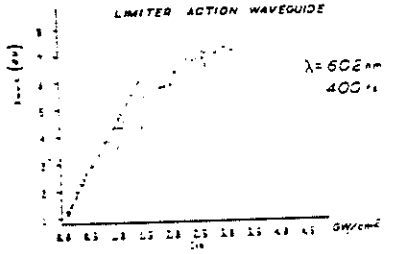

POWER DEPENDENT COUPLING EFFICIENCY

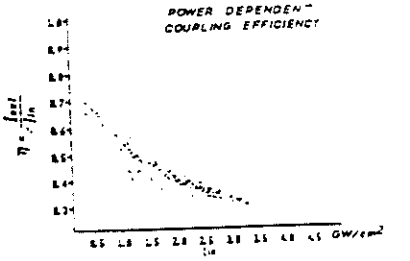

B-10

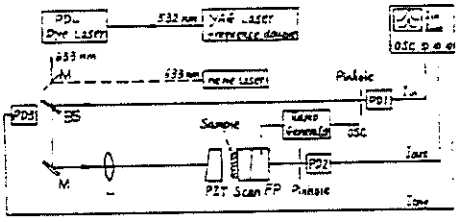

FIG.1. Experimental setup for the observation of optical bistability.

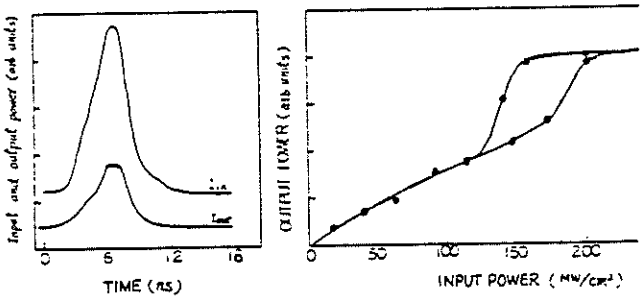

FIG 2 LEFT : INPUT AND OUTPUT PULSES.
RIGHT: INPUT-OUTPUT CHARACTERISTICS.

WHERE DO WE GO NOW?

1. ENHANCEMENT OF $\chi^{(3)}$

(A) DO WE NEED EXTENSIVE π - ELECTRON DELOCALIZATION?

BAND GAP REDUCES. PROBLEM WITH NONRESONANT WINDOW

PROBLEM WITH DISTRIBUTION OF CONJUGATION LENGTH

↓

A BROAD DISTRIBUTION OF BAND GAPS.

(B) DO WE NEED A HIGH MOLECULAR WEIGHT POLYMER?

PROBLEM WITH SOLUBILITY

↓

DERIVATIZE WITH LONG ALKYL CHAIN, REDUCES PACKING DENSITY

PROBLEM WITH DISTRIBUTION OF MOLECULAR WEIGHT

↓

REFRACTIVE INDEX INHOMOGENEITIES

(C) DO WE NEED π - ELECTRONS?

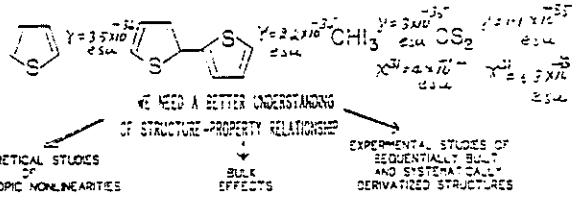

WE NEED A BETTER UNDERSTANDING OF STRUCTURE-PROPERTY RELATIONSHIP

THEORETICAL STUDIES OF MICROSCOPIC NONLINEARITIES

BULK EFFECTS

EXPERIMENTAL STUDIES OF SEQUENTIALLY BUILT AND SYSTEMATICALLY DERIVATIZED STRUCTURES

2. OPTICAL QUALITY MATERIALS

PROCESSABLE MATERIALS

STRUCTURAL CONTROL, CHARACTERIZATION AND MATERIALS PROCESSING FOR LOW OPTICAL LOSS SYSTEMS

3. DEVICE PHYSICS AND DEVICE STRUCTURES

EXPERIMENTS WITH CHANNELED WAVEGUIDES, ETALONS, FIBERS

ACKNOWLEDGEMENT

DR. J. SWIATKIEWICZ
DR. R. BURZYNSKI
DR. S. GHOSHAL
DR. M.S. MALWA
MS. P. CHOPRA
MR. L. CARLACCI
MS. S. GHOSAL
MR. J. ZIEGAJSKI
MR. M.T. COOLBAUGH
MR. R. ZAWADA
DR. D.N. RAO
DR. B.P. SINGH
DR. J. PFLEGER
DR. L. JANISZEWSKA
MR. X. HUANG
MR. Y. PANG
MR. M. CARPENTER
MR. P. LOGSDON
MR. M. CASSTEVENS
MR. M.T. ZHAO

DR. DONALD R. ULRICH (AFOSR)

SUPPORT

AIR FORCE OFFICE OF SCIENTIFIC RESEARCH

A. F. Garito
University of Pennsylvania

RECENT ADVANCES IN NONLINEAR OPTICAL PROPERTIES OF ORGANIC AND POLYMER SYSTEMS

RECENT ADVANCES IN NONLINEAR OPTICAL PROPERTIES OF ORGANIC AND POLYMER SYSTEMS

A.F. Garito
Department of Physics
University of Pennsylvania
Philadelphia, PA 19104-6396

ELECTRON CORRELATED STATES: ORIGIN OF THIRD ORDER NONLINEAR OPTICAL SUSCEPTIBILITY OF CONJUGATED LINEAR CHAINS

FERMI GAS WITH ELECTRON-ELECTRON INTERACTIONS

QFT

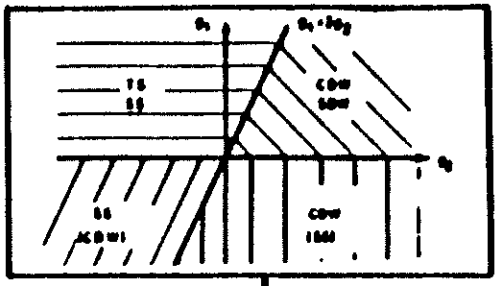

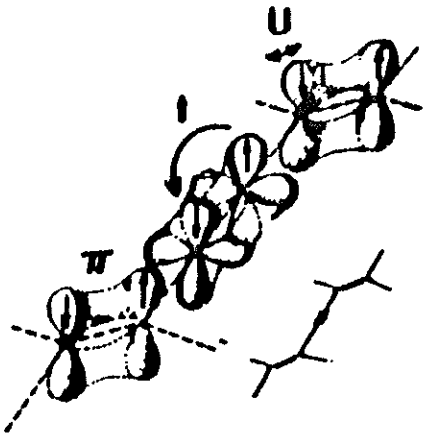

$q_i = q_j$

TIGHT BINDING : HUCKEL

$H = \sum t_{ij} c^{+}_{i\sigma} c_{j\sigma}$

$E = \alpha + 2t \cos ka$

- INDEPENDENT ELECTRONS
- EXCITONS

$U/t \to 0$

U_{ij}

HUBBARD

$H = t \sum c^{+}_{i\sigma} c_{j\sigma} + U \sum n_{i\uparrow} n_{i\downarrow}$

- ELECTRON CORRELATION
- 2 PHOTON STATES
- SDWs
- CDWs

$U/t \to \infty$

SCF - MO - MCI

$H = \sum t_{ij} c^{+}_{i\sigma} c_{j\sigma} + \sum U_{ij} c^{+}_{i\sigma} c_{i\sigma} c^{+}_{j\rho} c_{j\rho} + \sum (-1 - \sum U_{ij}) c^{+}_{i\sigma} c_{i\sigma} + \sum U_{ij}$

- ALL VALENCE ELECTRONS
- S, D, T, Q, ---- CI
- 2 PHOTON STATES

HEISENBERG

$H = \sum J_{ij} \cdot \vec{S}_i \cdot \vec{S}_j$

$J_{ij} = -2 t_{ij}^2 / U$

- 1D MAGNETIC CHAINS
- SDWs

ELECTRON DELOCALIZATION

COMPUTATION

ELECTRON CORRELATION AND RESONANT PROCESSES

- π-ELECTRON STATES DOMINATED BY ELECTRON CORRELATIONS
- TWO PHOTON $2\,^1A_g$ STATE EXISTS BELOW FIRST OPTICALLY ALLOWED $1\,^1B_u$ STATE
- PPP AND HUBBARD MODELS OBTAIN CORRECT STATE ORDERING WITH INCLUSION OF AT LEAST DOUBLY EXCITED CONFIGURATIONS (DCI)

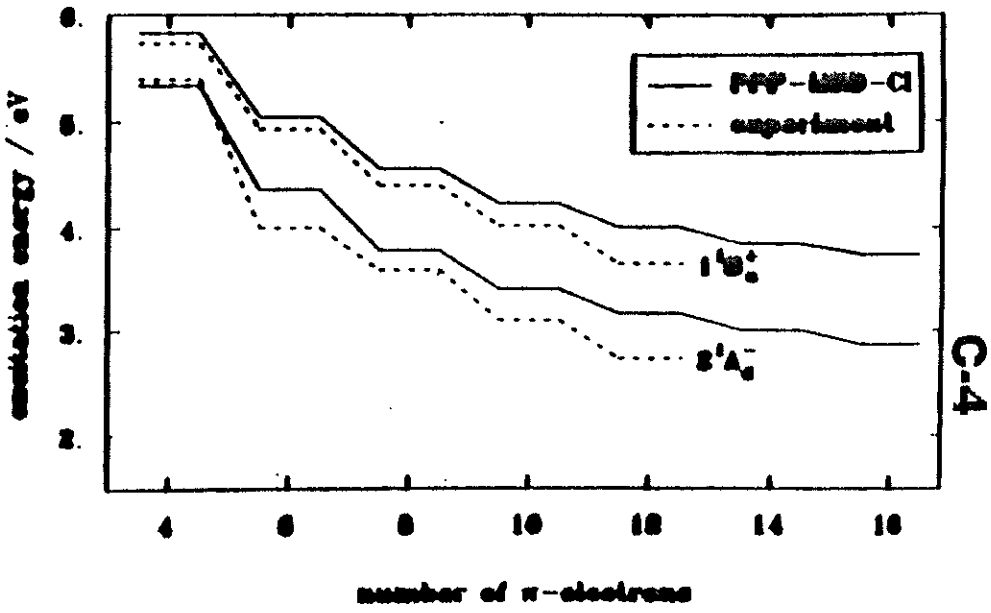

FROM TAVAN AND SCHULTEN, J. CHEM. PHYS. 85, 6602 (1986)

ELECTRONIC STATES OF OT

SYMMETRY	ENERGY (eV)	$\mu_{n,g}$(D)	$\mu_{1^1B_u,n}$(D)
$5\,^1B_u$	7.30	1.14	0.00
$6\,^1A_g$	7.16	0.00	13.24
$4\,^1B_u$	7.01	1.11	0.00
$3\,^1B_u$	6.47	0.01	0.00
$5\,^1A_g$	6.07	0.00	1.11
$4\,^1A_g$	6.00	0.00	2.84
$3\,^1A_g$	5.19	0.00	0.07
$2\,^1B_u$	4.79	0.86	0.00
$1\,^1B_u$	4.42	7.81	0.00
$2\,^1A_g$	4.15	0.00	2.82
$1\,^1A_g$			

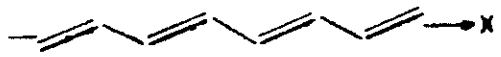

OT (octatetraene)

VERTICAL EXCITATION ENERGIES: CHAIN LENGTH

N(sites)	$1\,^1B_u$ (eV) Exp.	$1\,^1B_u$ (eV) Theo.	$2\,^1A_g$ (eV) Exp.	$2\,^1A_g$ (eV) Theo.
4	5.91	5.77	5.4(0-0)	5.31
6	4.93	4.94	4.0(0-0)	4.59
8	4.40	4.42	3.97	4.15
10	4.02	4.07	3.48	3.90
12	3.65	3.83	2.91	3.74

C-15

- DOMINANT 1 PHOTON STATE: ^1B_u
- LOW-LYING $2\,^1A_g$ EXCITED STATE: ELECTRON CORRELATION

MICROSCOPIC ORIGIN OF $\gamma(-3\omega;\omega,\omega,\omega)$
FOR LINEAR CONJUGATED CHAINS

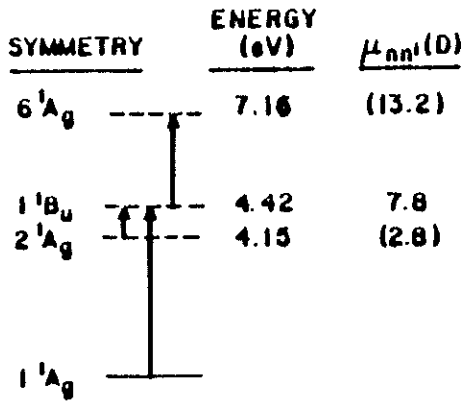

OT

- $\gamma_{xxxx}(-3\omega;\omega,\omega,\omega) = 15.5 \times 10^{-36}$ esu (ω = 0.65 eV/$\hbar$)
  $\gamma_g(-3\omega;\omega,\omega,\omega) = 3.4 \times 10^{-36}$ esu
- ONLY CONTRIBUTIONS: $g \rightarrow {}^1B_u \rightarrow {}^1A_g \rightarrow {}^1B_u \rightarrow g$
- ^1A_g STATES: THOSE WITH LARGEST $\mu_{nn'}$ WITH DOMINANT ^1B_u STATE
- 2 PHOTON ^1A_g STATES CRITICAL IN THIRD ORDER PROCESSES

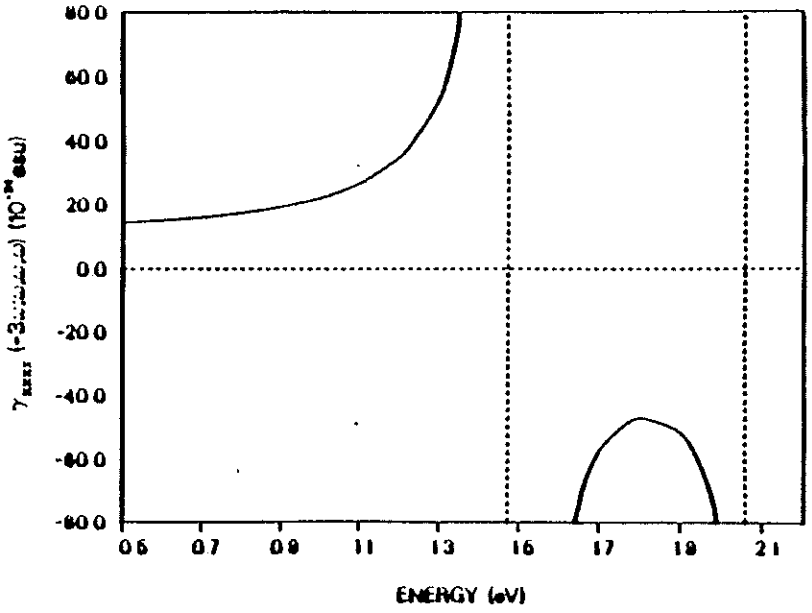

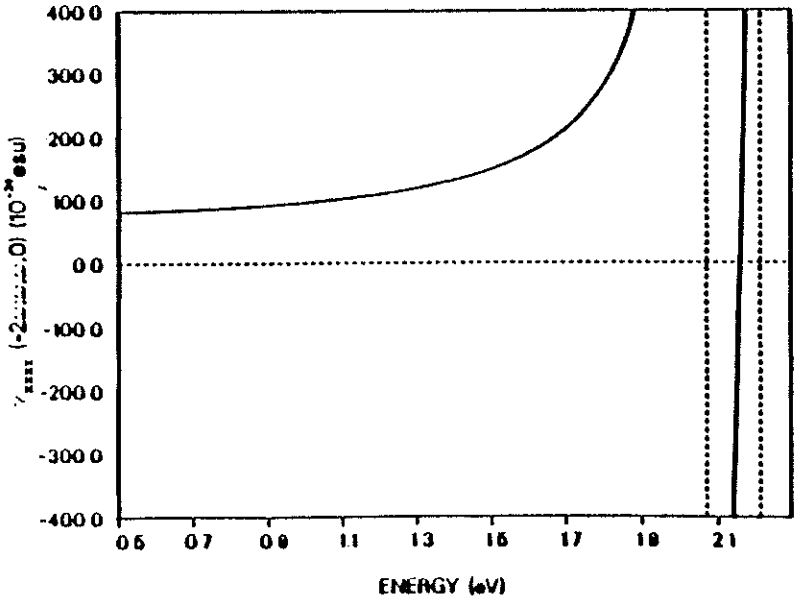

C-6

DC INDUCED SECOND HARMONIC GENERATION AND γ_g

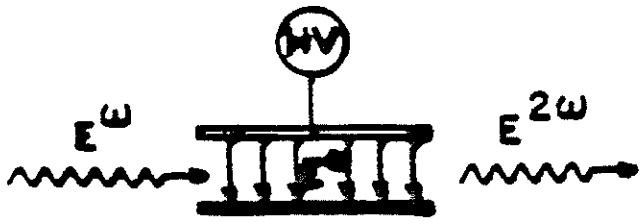

$$P^{2\omega} = \gamma_g(-2\omega,\omega,\omega,0)\, E^{\omega} E^{\omega} E^{0}$$

$$\gamma_g(-2\omega;\omega,\omega,0) = \frac{1}{5}\left[\sum_i \gamma_{iiii} + \frac{1}{3}\sum_{i\neq j}\left(\gamma_{iijj} + \gamma_{ijij} + \gamma_{ijji}\right)\right] + \frac{1}{5}\frac{\mu}{kT}\beta_x(-2\omega;\omega,\omega)$$

- SECOND ORDER CONTRIBUTION β_x VANISHES BY SYMMETRY

γ_g VALUES (IN UNIT OF 10^{-36} esu) AT 1.787 eV:

	γ_g (THEORY)	γ_g (EXPERIMENT)
BUTADIENE (N=4)	3.6	3.45 ± 0.2
HEXATRIENE (N=6) (60% t – 40% c)	13.9 (12.9)	11.3 ± 1.05

- CALCULATED γ_g AGREES WITH EXPERIMENT BOTH FOR THE MAGNITUDE AND SIGN

MICROSCOPIC ELECTRONIC ORIGIN OF $\gamma(-3\omega;\omega,\omega,\omega)$

$$\gamma_{ijkl}(-3\omega;\omega,\omega,\omega) = \frac{e^4}{4\hbar^3} \sum_{m_1 m_2 m_3} \frac{\langle g|r_i|m_3\rangle\langle m_3|r_j|m_2\rangle\langle m_2|r_k|m_1\rangle\langle m_1|r_l|g\rangle}{(\omega_{m_1 g}-\omega)(\omega_{m_2 g}-2\omega)(\omega_{m_3 g}-3\omega)} + \cdots$$

- TWO IMPORTANT TYPES OF CONTRIBUTING TERMS

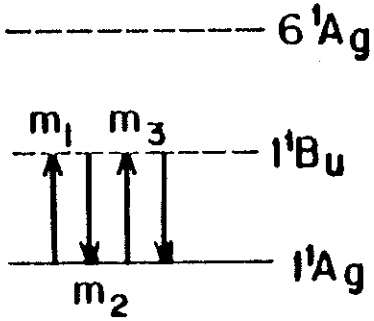

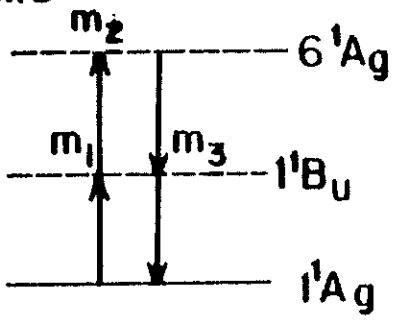

- INTERMEDIATE STATE m_2 IS THE GROUND STATE ITSELF
- NUMERATOR IS POSITIVE
- $(\omega_{gg}-2\omega)$ TERM IN DENOMINATOR IS NEGATIVE
- NEGATIVE CONTRIBUTION TO γ

- INTERMEDIATE STATE m_2 IS THE UPPER 6 ^1A_g STATE
- NUMERATOR IS POSITIVE
- $(\omega_{m_2 g}-2\omega)$ TERM IN DENOMINATOR IS POSITIVE
- POSITIVE CONTRIBUTION TO γ

TRANSITION DENSITY MATRIX DIAGRAMS

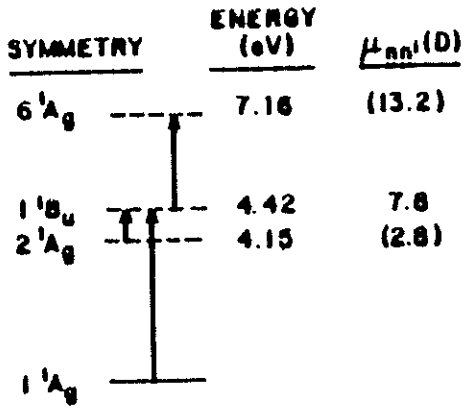

OT

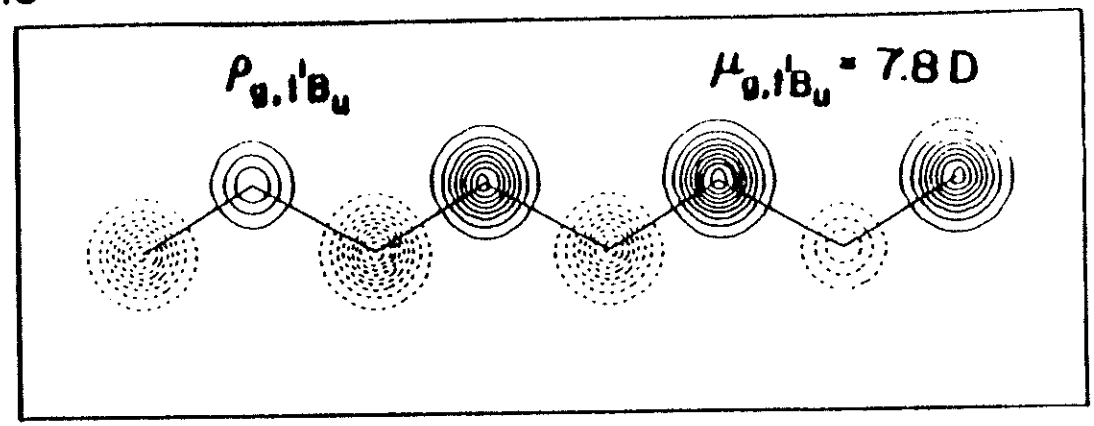

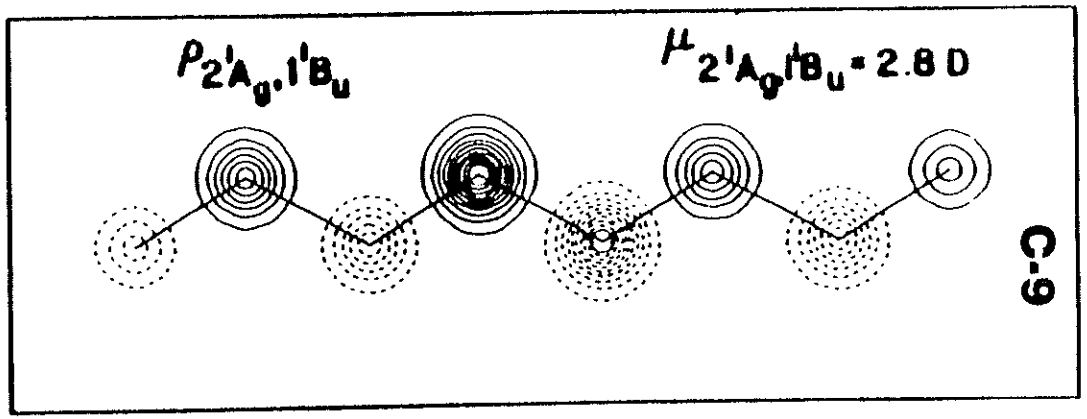

C-9

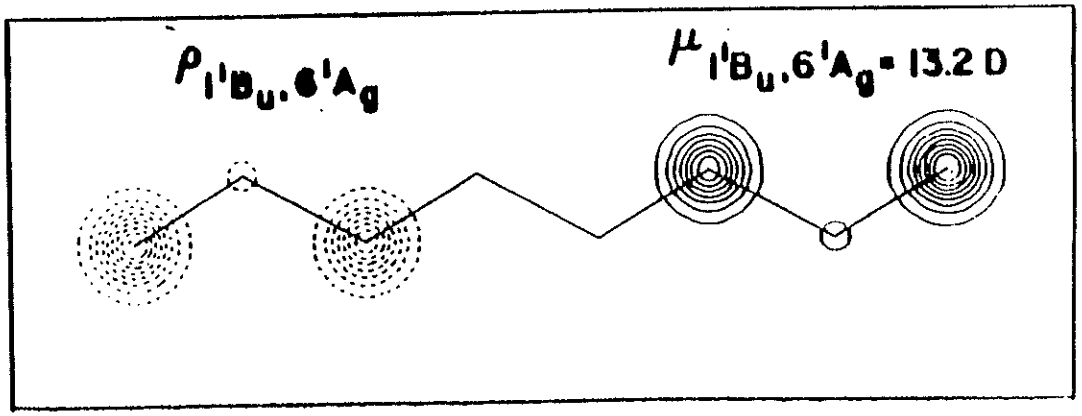

- $\langle \mu_{nn'} \rangle = -e \int r\, \rho_{nn'}(r)\, dr$
- CORRELATION OCCURS ACROSS ENTIRE CHAIN LENGTH
- $\mu_{1^1Bu,6^1A_g} \gg \mu_{2^1Ag,1^1Bu}$: CHARGE SEPARATION IS LARGEST IN $\rho_{1^1B_u,6^1A_g}$

DEPENDENCE OF $\gamma(-3\omega;\omega,\omega,\omega)$ ON NUMBER OF SITES

- FINITE CHAIN LIMIT: POWER LAW DEPENDENCE

$$\gamma_{xxxx} \propto N^{5.4}$$

  - DECREASED EXCITATION ENERGY
  - INCREASED TRANSITION MOMENTS
  - INCREASED NUMBER OF CONTRIBUTING EXCITED STATE TERMS

- POLYMER CHAINS: $\chi^{(3)} \sim 10^{-9}$ esu
  - 50 SITES (60 Å)

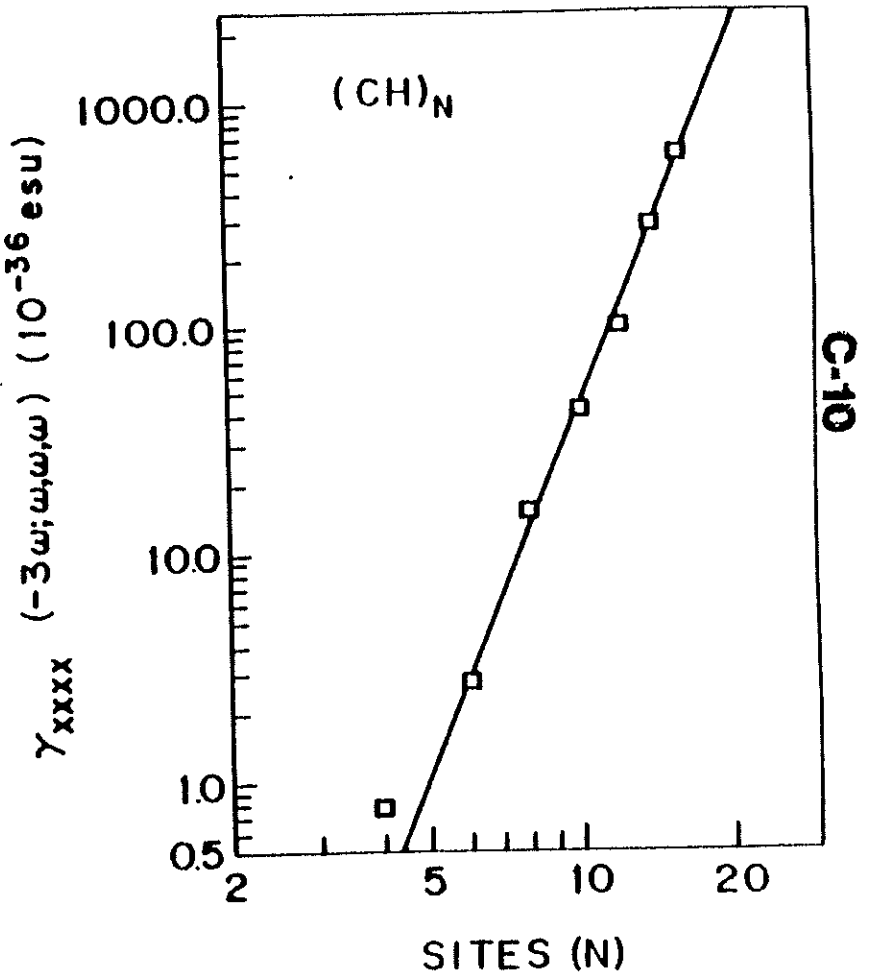

INCOMPLETE DESCRIPTION OF ELECTRON CORRELATION

- SCI ONLY; OTHERWISE IDENTICAL TO FULL SDCI
- NEGATIVE SIGN FOR γ_{xxxx} FOR ALL CHAIN LENGTHS
- SCI POWER LAW EXPONENT IS 3.9 AS COMPARED TO 5.4 OF SDCI

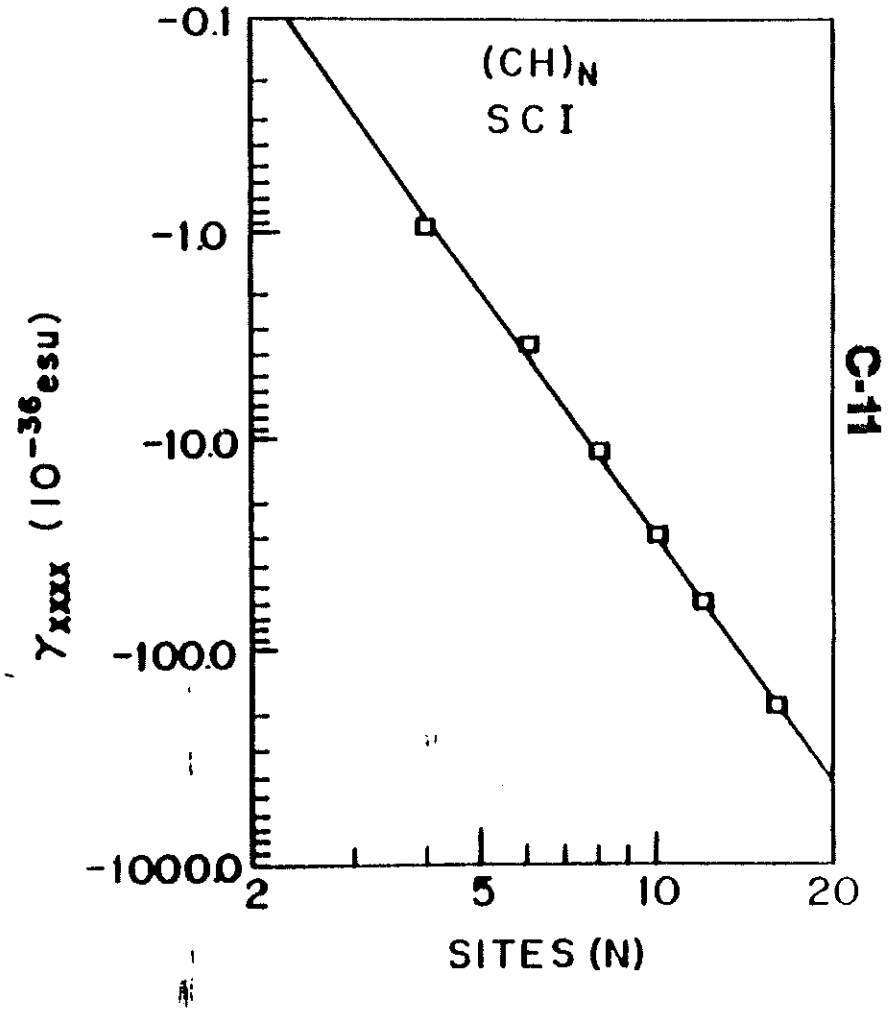

MICROSCOPIC ORIGIN OF $\gamma(-3\omega;\omega,\omega,\omega)$ FOR cis - POLYENES

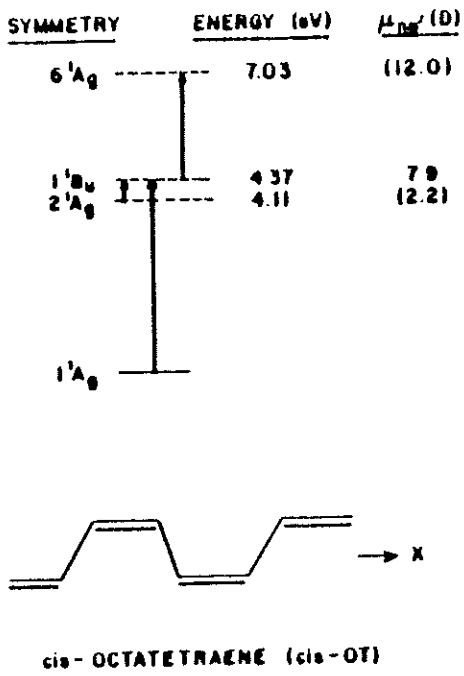

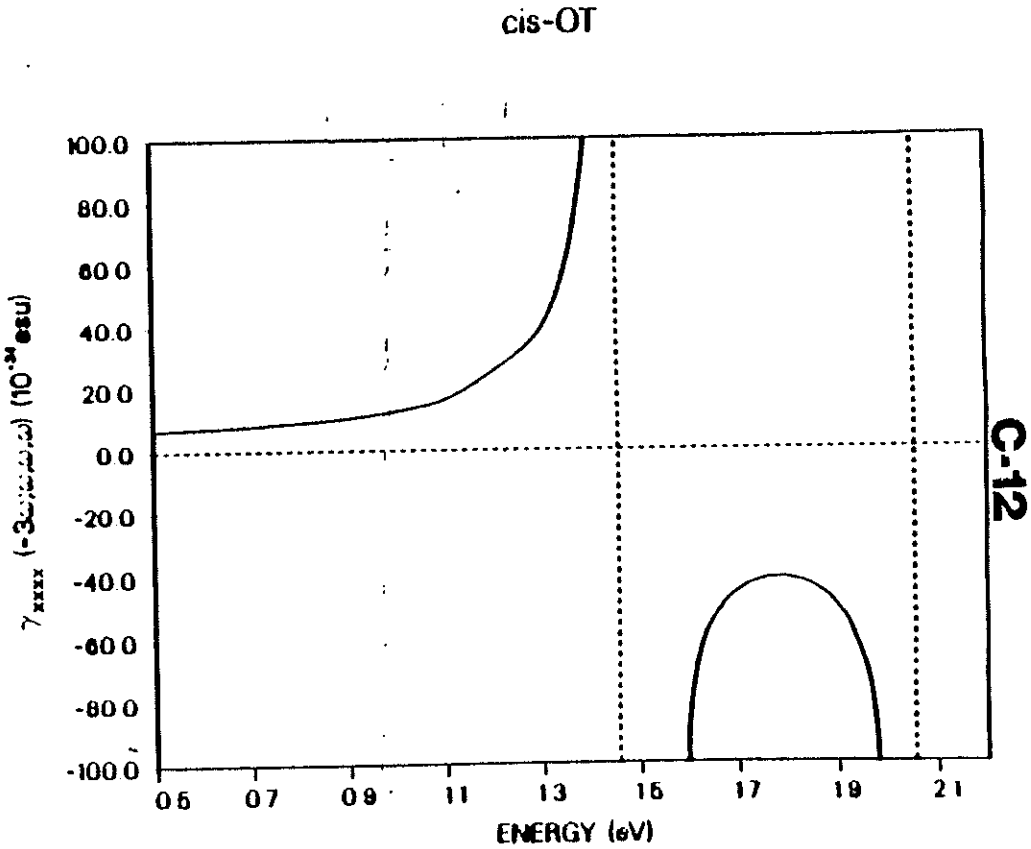

C-12

- $\gamma_{xxxx}(-3\omega;\omega,\omega,\omega) = 7.7 \times 10^{-36}$ esu (ω 0.65 eV/$\hbar$)

  $\gamma_g(-3\omega;\omega,\omega,\omega) = 1.8 \times 10^{-36}$ esu

- ONLY CONTRIBUTIONS: $g \rightarrow {}^1B_u \rightarrow {}^1A_g \rightarrow {}^1B_u \rightarrow g$
- ^1A_g STATES: THOSE WITH LARGEST $\mu_{nn'}$ WITH DOMINANT ^1B_u STATE
- 2 PHOTON ^1A_g STATES CRITICAL IN THIRD ORDER PROCESSES

DEPENDENCE OF $\gamma(-3\omega;\omega,\omega,\omega)$ ON NUMBER OF SITES

- FINITE CHAIN LIMIT: POWER LAW DEPENDENCE

$$\gamma_{xxxx} \propto N^{4.7}$$

  - DECREASED EXCITATION ENERGY
  - INCREASED TRANSITION MOMENTS
  - INCREASED NUMBER OF CONTRIBUTING EXCITED STATE TERMS

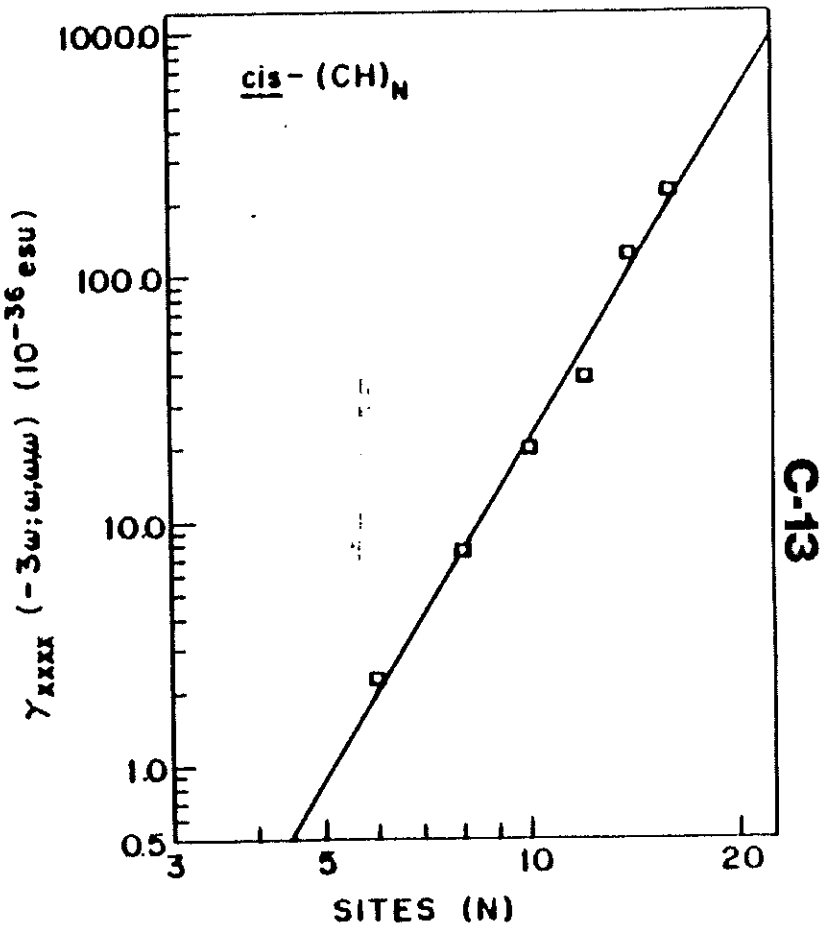

TRANSITION DENSITY MATRIX DIAGRAMS

$\rho_{g,1^1B_u}$

$\mu_{g,1^1B_u} = 7.9D$

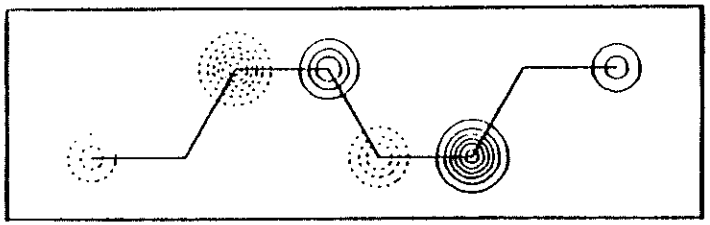

$\mu_{g,1^1B_u} = 7.8D$

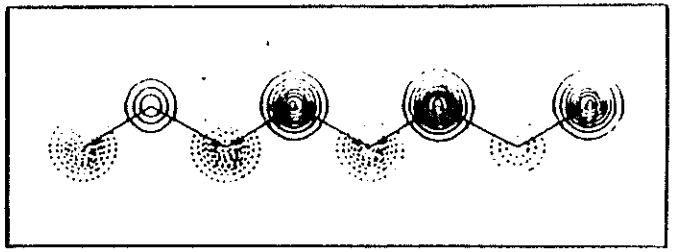

$\rho_{1^1B_u,6^1A_g}$

$\mu_{1^1B_u,6^1A_g} = 12.0D$

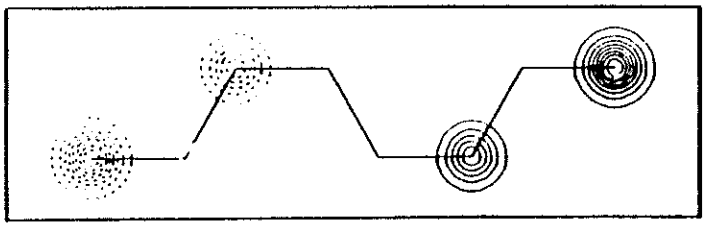

$\mu_{1^1B_u,6^1A_g} = 13.2D$

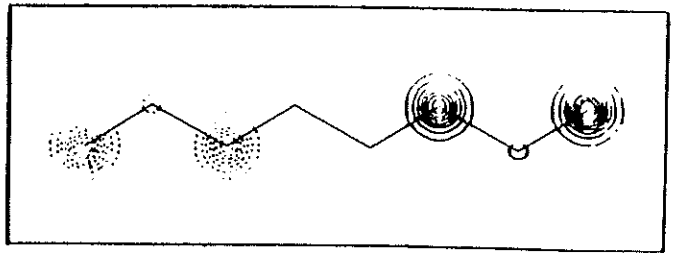

- CHARGE REDISTRIBUTION ESSENTIALLY THE SAME FOR <u>cis</u> AND <u>trans</u> CONFORMATIONS

DEPENDENCE OF $\gamma(-3\omega;\omega,\omega,\omega)$ ON NUMBER OF SITES

- FINITE CHAIN LIMIT: POWER LAW DEPENDENCE

$$\gamma_{xxxx} \propto N^{4.7}$$

  - DECREASED EXCITATION ENERGY
  - INCREASED TRANSITION MOMENTS
  - INCREASED NUMBER OF CONTRIBUTING EXCITED STATE TERMS

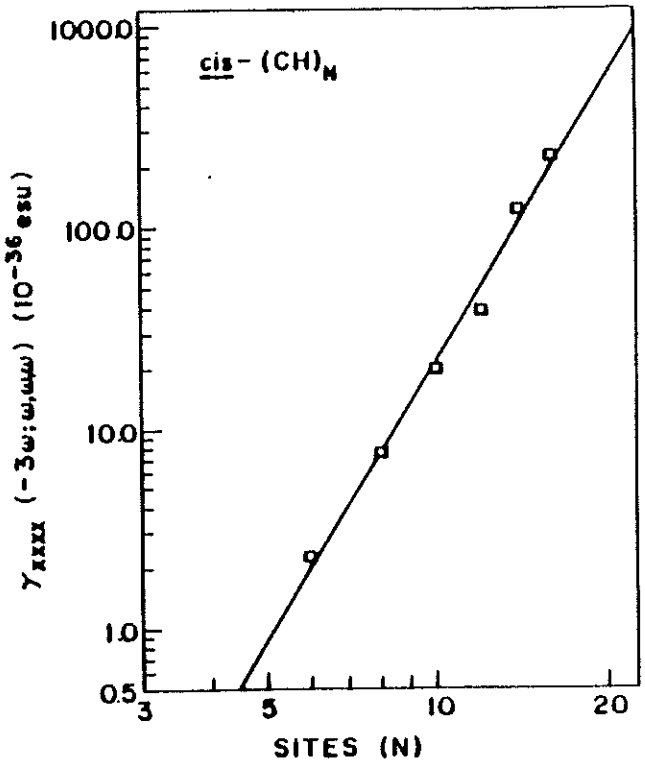

DEPENDENCE OF $\gamma(-3\omega;\omega,\omega,\omega)$ ON CHAIN LENGTH

- FINITE CHAIN LIMIT : $\gamma_{xxxx} \propto L^{4.6}$
- $\gamma_{xxxx}(-3\omega;\omega,\omega,\omega)$ FOR <u>cis</u> IS SMALLER THAN THAT FOR <u>trans</u> OF SAME NUMBER OF SITES
- DIFFERENCE IN $\gamma_{xxxx}(-3\omega;\omega,\omega,\omega)$ IS ACCOUNTED FOR BY DIFFERENCE IN LENGTH IN X-DIRECTION
- $\gamma_{xxxx}(-3\omega;\omega,\omega,\omega)$ MUCH MORE SENSITIVE TO CHAIN LENGTH THAN CONFORMATION

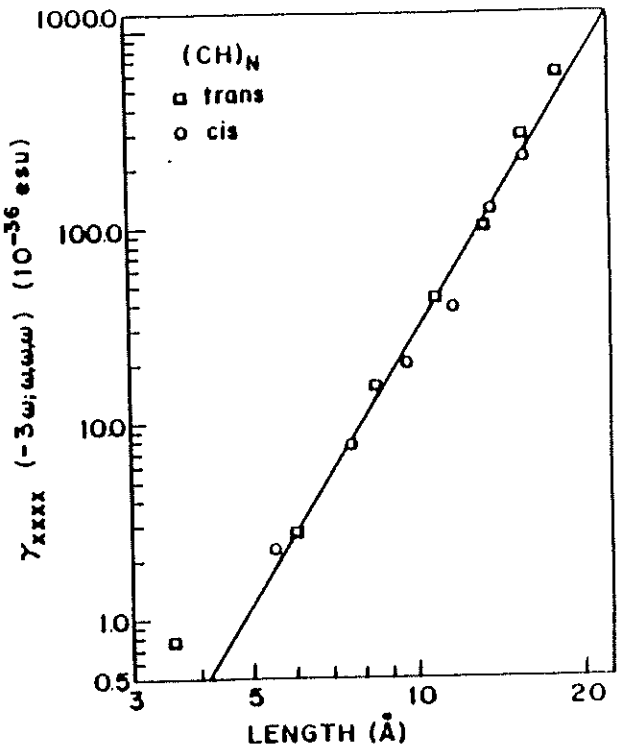

C-17

ELECTRON CORRELATED STATES: ORIGIN OF SECOND ORDER NONLINEAR OPTICAL SUSCEPTIBILITY OF CONJUGATED CYCLIC CHAINS

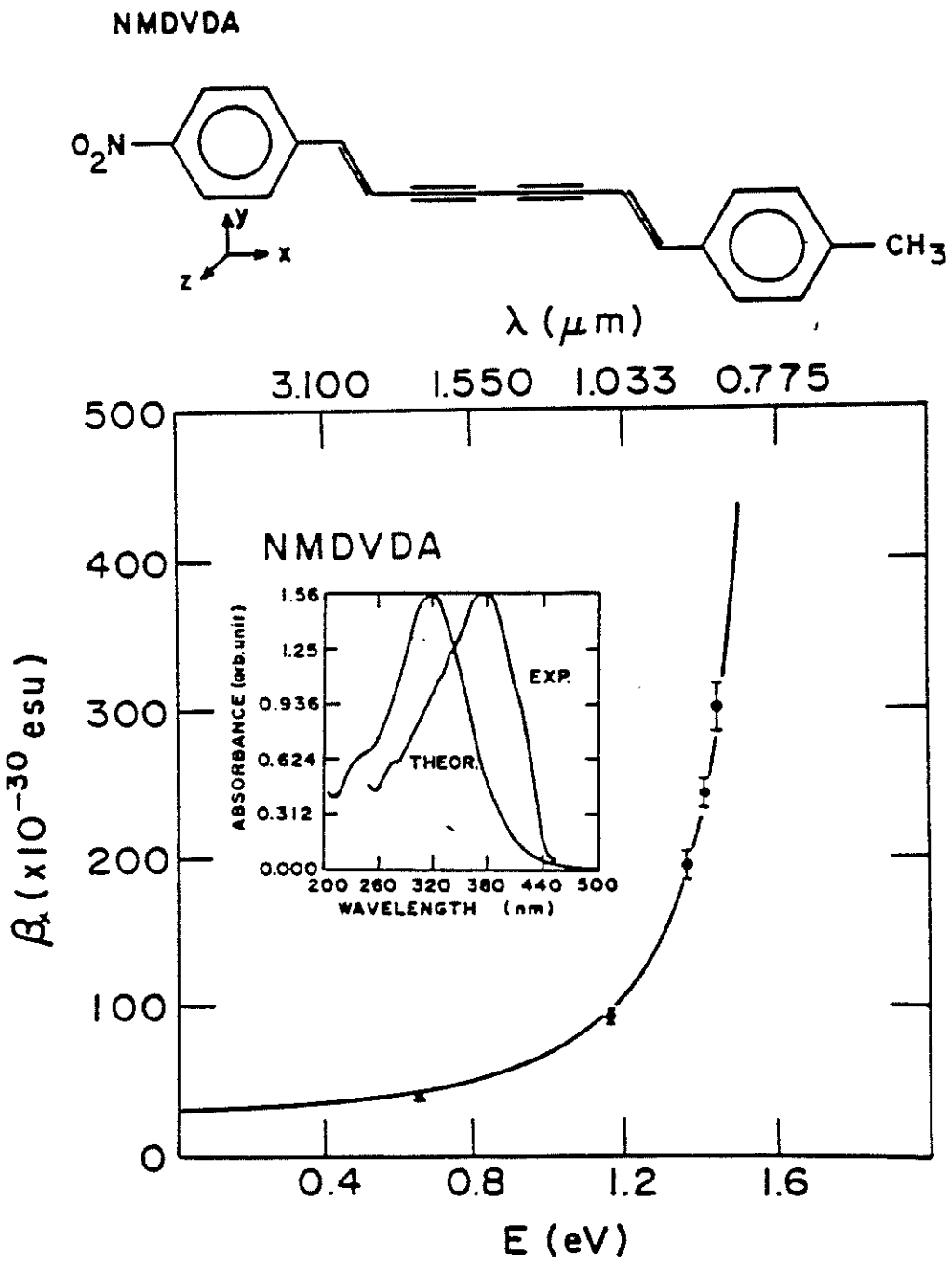

DCNQI

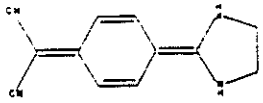

SYMMETRY C_{2v}

	ENERGY (eV)	μ^x_{nq} (D)	$\Delta\mu^x_n$ (D)
$\bullet 3A_1$	3.92	3.1	-6.8
$1B_2$	3.78	0.0	-3.1
$\bullet 2A_1$	2.31	9.0	-4.1
$1A_1$			

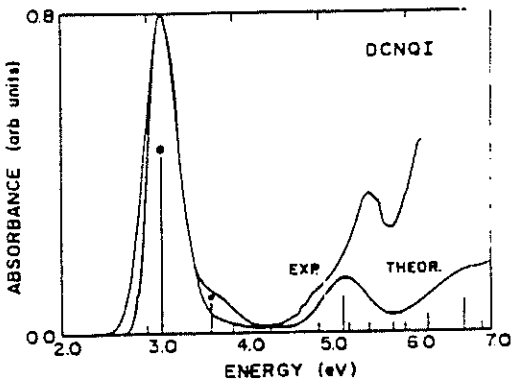

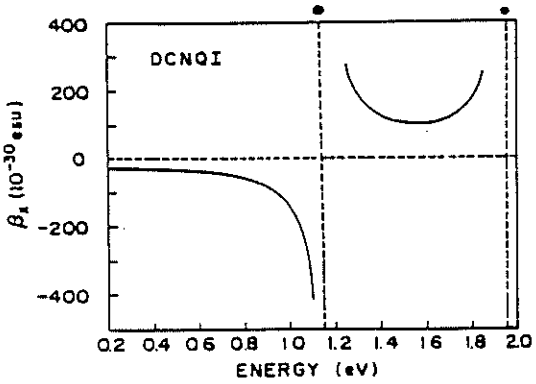

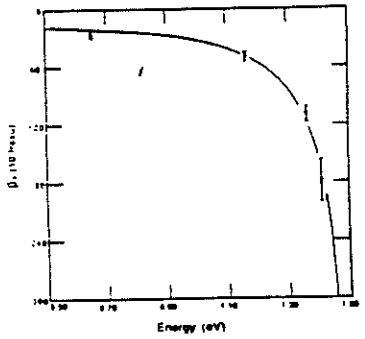

DCNQI	Experimental	SDCI	SCI
μ_x (Debye)	17.5 ±0.8	17	18.4
β_x (10^{-30} esu)	-27 ±3	-19.7	-73.2
$\mu_x \beta_x$ (10^{-48} esu)	-474 ± 52	-335	-1347

Comparison of Experimental and SDCI,SCI Values of Dipole Moment and the Second Order Microscopic Susceptibility at 0.65 eV.

	SDCI	SCI
$\beta^{'nn}_{xxx}$	44%	85%
$\beta^{nn'}_{xxx}$	56%	15%

The percentage Contributions of Diagonal Term and Off-diagonal Term.

MPC

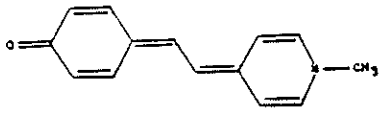

SYMMETRY C_s

	ENERGY (eV)	μ_{ng}^x (D)	$\Delta\mu_n^x$ (D)
5A′	3.69	4.7	-8.3
1A″	3.69	0	-20.0
4A′	3.54	0.4	-13.8
3A′	2.42	0.1	-14.1
2A′	1.92	12.0	-4.4
1A′			

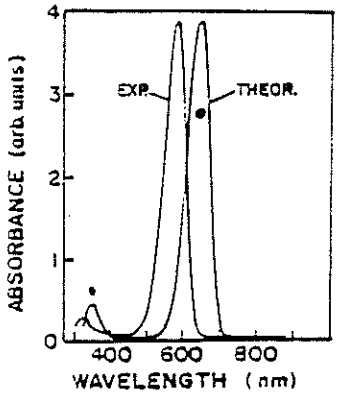

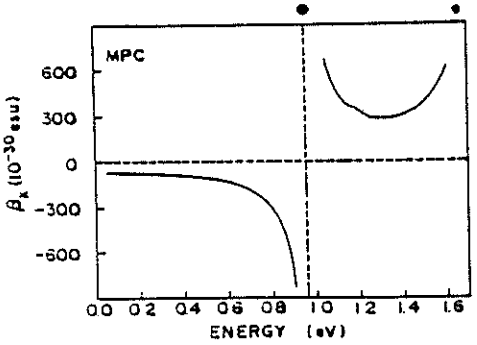

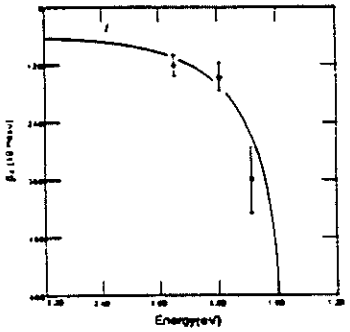

MPC	Experimental	SDCI	SCI
μ_x (Debye)	17.4 ±2.5	21.4	25.1
β_x (10^{-30} esu)	-123 ± 22	-104.7	-236.4
$\mu_x \beta_x$ (10^{-48} esu)	-2140 ± 390	-2240	-5933

Comparison of Experimental and SDCI,SCI Values of Dipole Moment and the Second Order Microscopic Susceptibility at 0.65 eV.

	SDCI	SCI
β_{xxx}^{in}	55.5%	86.4%
β_{xxx}^{off}	44.5%	13.6%

The percentage Contributions of Diagonal Term and Off-diagonal Term.

DPHQ

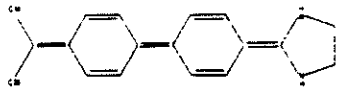

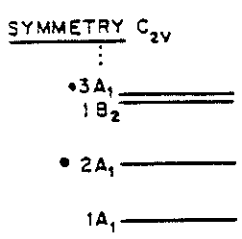

	ENERGY (eV)	μ^x_{ng} (D)	$\Delta\mu^x_n$ (D)
	⋮	⋮	⋮
$3A_1$	3.41	4.2	−8.6
$1B_2$	3.18	0	−9.4
$2A_1$	1.54	14.4	−7.7

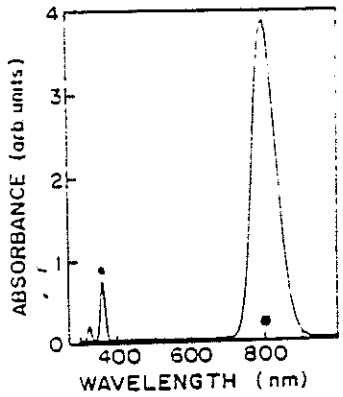

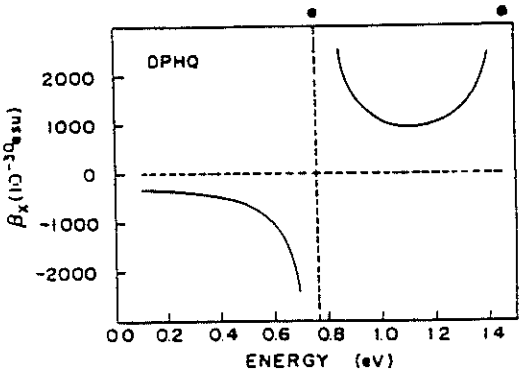

DPHQ	SDCI	SCI
μ_x (Debye)	25.4	30.5
β_x (10^{-30} esu)	-1410	-626
$\mu_x \beta_x$ (10^{-48} esu)	-35800	-19100

Comparison of Experimental and SDCI,SCI Values of Dipole Moment and the Second Order Microscopic Susceptibility at 0.65 eV.

	SDCI	SCI
β^{III}_{xxx}	72%	85%
β^{JIII}_{xxx}	28%	15%

The percentac . Contributions of Diagonal Term and Off-diagonal Term.

ELECTRON DENSITY CORRELATION DIAGRAMS

$$\langle \Delta\mu_n \rangle = e \int_r r \, (\rho_n - \rho_g) \, dr$$

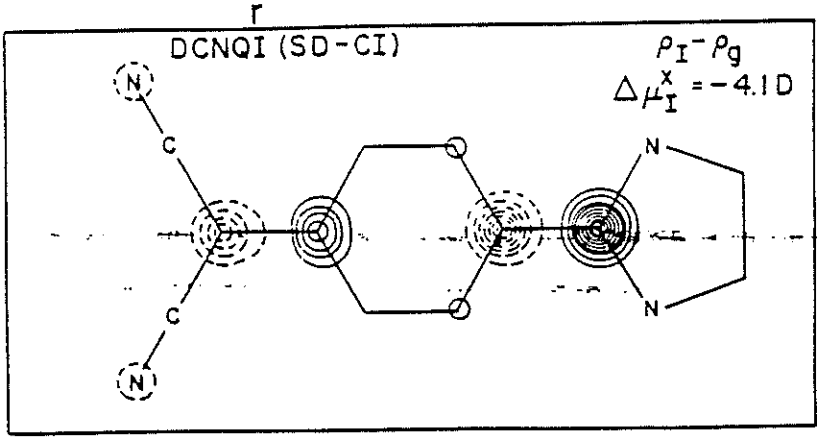

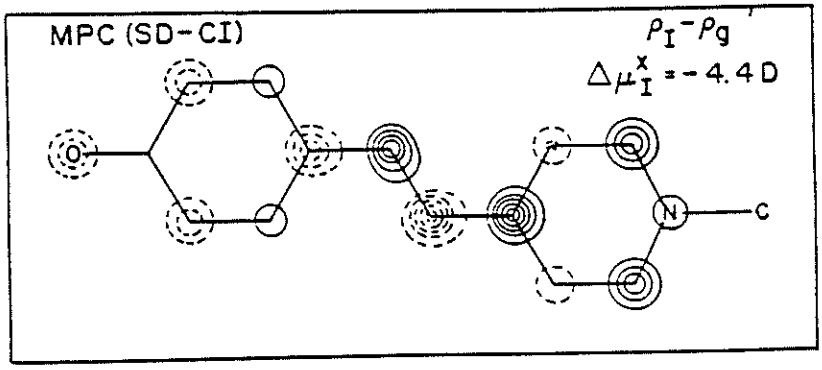

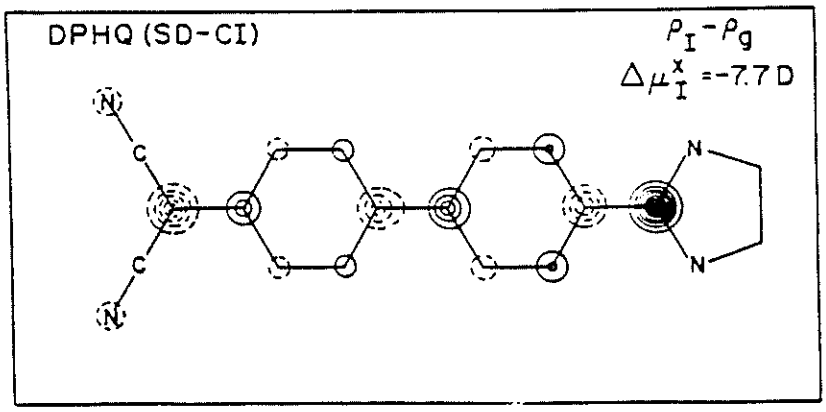

PCLED POLYMER GLASSES

C-22

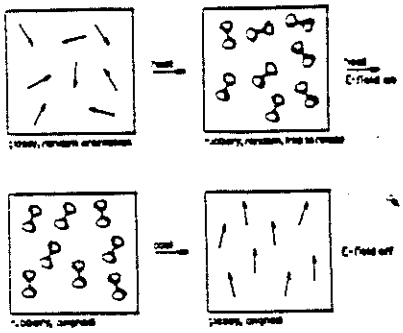

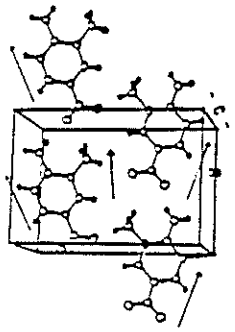

MNA SINGLE CRYSTAL

TIR SLM DEVICES

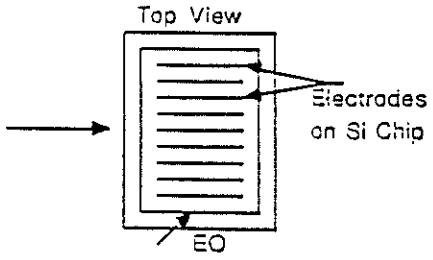

Orientational Order

$$\chi^{(2)}_{111} = N \frac{\beta_{xxx}\mu_x E_x}{k_B T} f^{2\omega} (f^{\omega})^2 \left(\frac{1}{5} + \frac{4}{7}\langle P_2 \rangle + \frac{8}{35}\langle P_4 \rangle \right)$$

CLASS	SYSTEM	$\mu_x\beta_x$ (10^{-30}cm^{5}Desu^{-1})	d_{11}(10^{-9}esu) (λ=1.907μm)	r_{11}(10^{-12}m/V) (λ=0.633μm)
RESONANT RING	MNA	66	0.8	0.3
	AZO DYE	530*	6*	2.5
	MNA SINGLE CRYSTAL		230	67
LINEAR CHAIN	NMDVDA	200	2.3	0.9
CYCLIC CHAIN	MPC	2100	24	10
	DCNQI	470	5.3	2.2
	DPHQ	36000	410	170

*Measured at λ=1.58μm

RELATED REFERENCES

1. Third harmonic generation study of orientational order in nematic liquid crystals, Phys. Rev. A34, 5051 (1986).

2. Microscopic origin of second order nonlinear optical properties of organic structures, in Nonlinear Optical and Electroactive Polymers (Plenum, New York, 1988).

3. Recent developments in microscopic descriptions of the nonlinear optical properties of organic and polymer structures, in Proceedings SPIE 825 (1988).

4. Nonlinear optical properties of linear chains and electron correlation effects, Phys. Rev. B - Rapid Communications (in press).

5. Symmetry controlled electron correlation mechanism for third order nonlinear optical properties of conjugated linear chains, in Electroresponsive Polymers, Special Issue, Mol. Cryst. Liq. Cryst. (1988).

6. Nonlinear optical properties of polyenes: Electron correlation and chain conformation, in Nonlinear Optical Properties of Polymers (Materials Research Society, Boston, 1988) 109, p. 91.

S. Etemad
Bell Communications

CONJUGATED POLYMERS AND NONLINEAR OPTICS

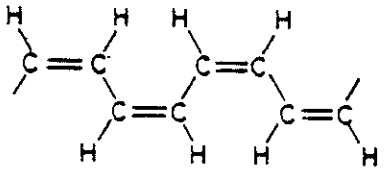

(a)

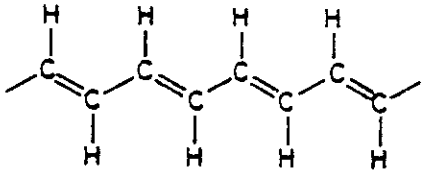

(b)

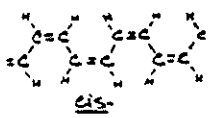

cis-

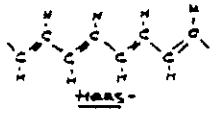

trans-

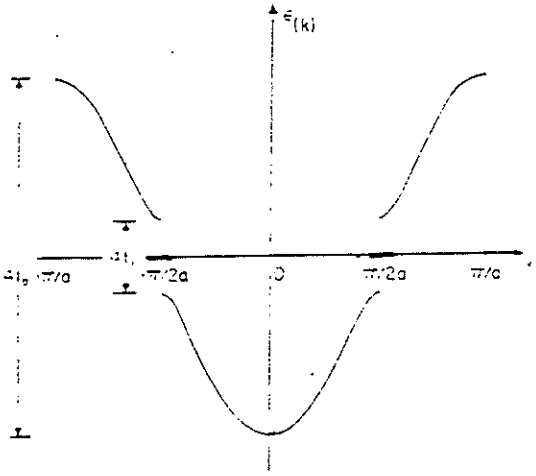

trans - $(CH)_x$

$t_\parallel = 2.5 - 3.0$ eV

$2\Delta = 4t_\perp \approx 1.5$ eV c.f. a-Si

$t_\perp \approx .05$ eV

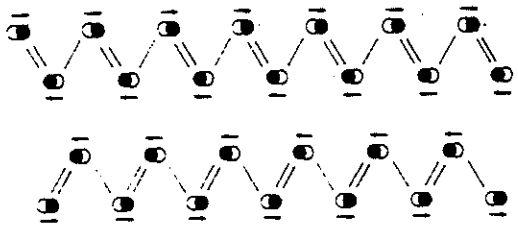

TRANS - $(CH)_x$

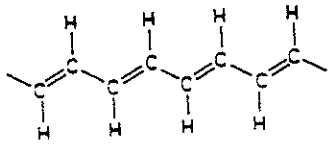

REVERSED CHARGE & SPIN

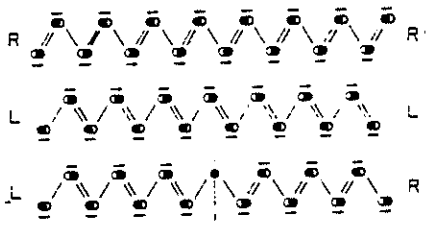

TRANS - $(CH)_x$

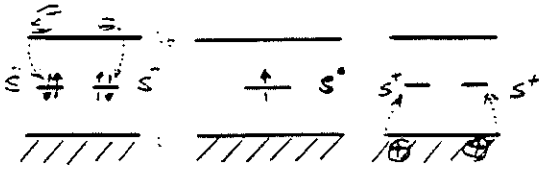

CHEMISTRY VIEW

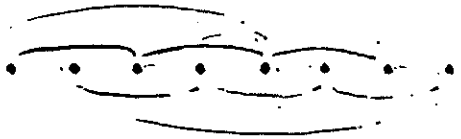

HIGHLY CORRELATED STATES

MANY BODY !

CASE STUDY : FINITE POLYENES

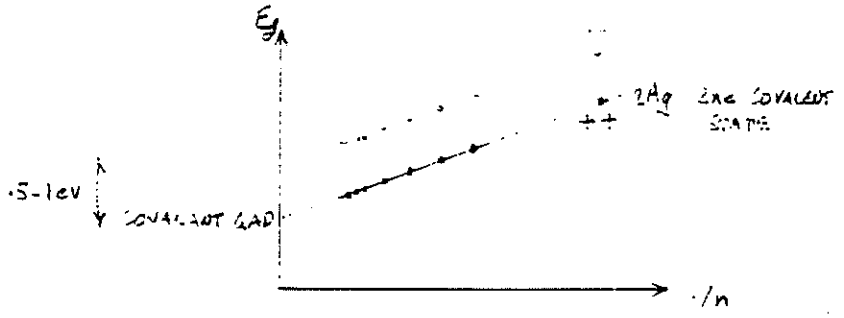

n .S CONJUGATION LENGTH

COULOMB INTERACTIONS

PERTURBATION APPROACH

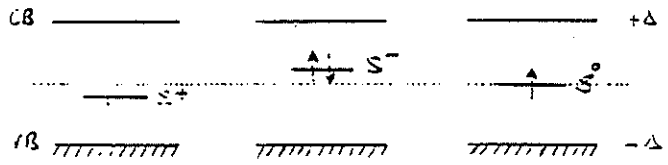

"MID-GAP" TRANSITIONS

HIGHLY CORRELATED STATES

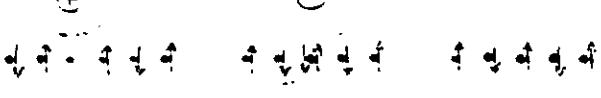

LOWEST ENERGY TRANSITIONS

- S° ABSORPTION AT BAND GAP

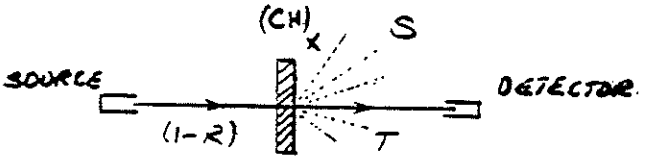

$1-R = T+S+A$

EFFECT OF COMPENSATION WITH NH_3

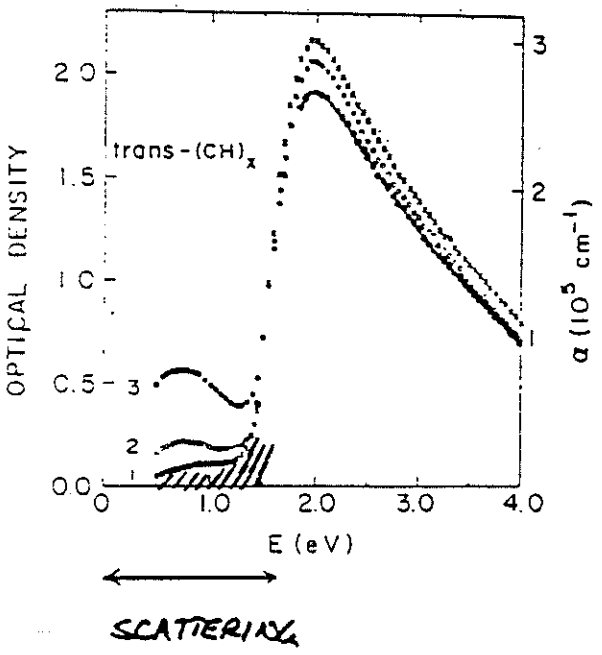

SCATTERING

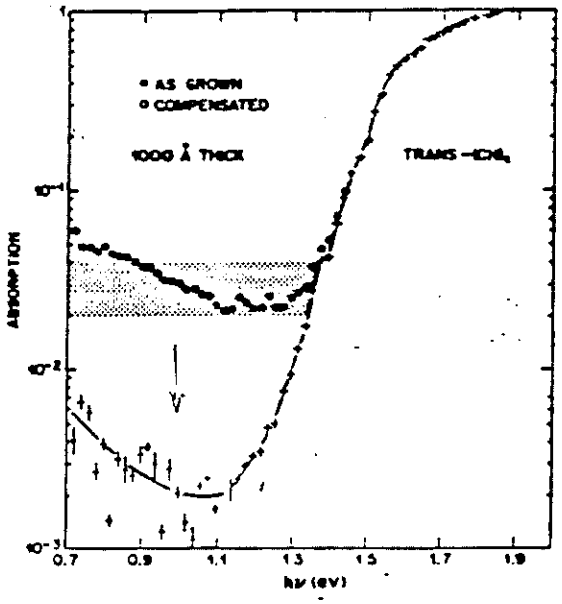

LONG TIME BEHAVIOR

MOL. CRYST. LIQ. CRYST. 117, 275.

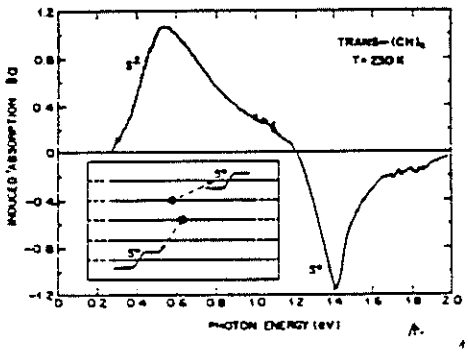

$e/h + 2S^0 \rightarrow 2S^{\pm}$

PRB 30, 786 (84)

IONIC GAP
$^1B \rightarrow {}^1B$
HOMO → LUMO

$S^{\pm}$

S°

COVALENT GAP

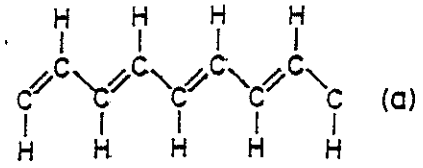

WHERE IS THE $2\,{}^1A_g$ (COVALENT GAP)
WITH RESPECT TO $1\,{}^1B_u$ (IONIC GAP)?

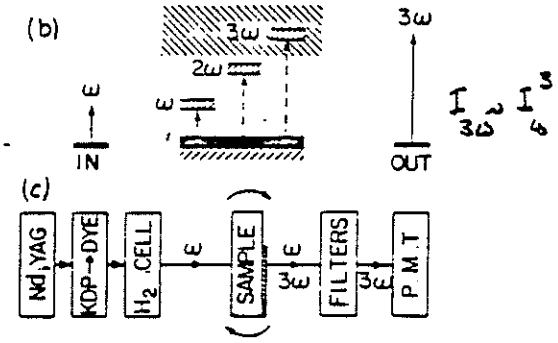

FILM: COMPENSATED $(CH)_x$ Fig 1
700 Å THICK; UNIFORM

THIRD HARMONIC GENERATION

$$\chi^{(3)}(3\omega;\omega,\omega,\omega) = \sum_{nmn'} \Omega_{gn}\Omega_{nm}\Omega_{mn'}\Omega_{n'g}$$

$$\left[\frac{1}{(E_{ng}-3\omega)(E_{mg}-2\omega)(E_{n'g}-\omega)} + \frac{1}{(E_{ng}+\omega)(E_{mg}-2\omega)(E_{n'g}-\omega)} + \frac{1}{(E_{ng}+\omega)(E_{mg}+2\omega)(E_{n'g}-\omega)} + \frac{1}{(E_{ng}+3\omega)(E_{mg}-2\omega)(E_{n'g}+\omega)} \right]$$

TRANSITIONS BETWEEN ALL STATES
IRRESPECTIVE OF SYMMETRY

χ^3 OF $(CH)_x$: CALIBRATION

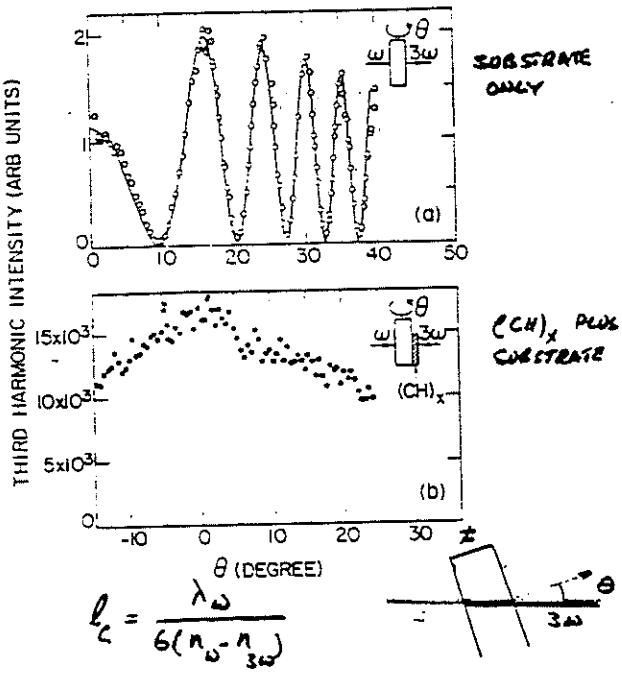

$$l_c = \frac{\lambda_\omega}{6(n_\omega - n_{3\omega})}$$

$$I_{3\omega} \sim I_\omega^3 \cdot |\chi^{(3)}|^2 \cdot \sin^2\left(\frac{L\cos\theta}{2l_c}\right)$$

$\chi^{(3)}_{max}$: VERY LARGE

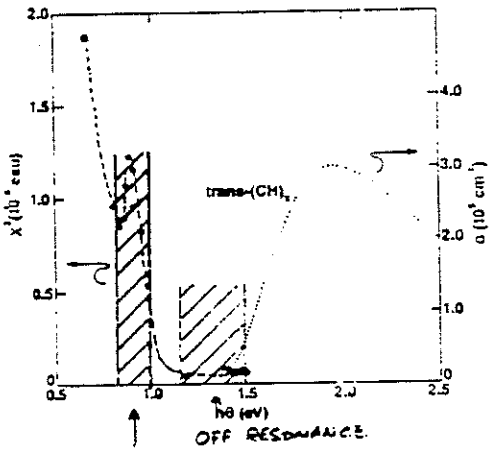

$\chi^{(3)}$ LARGE

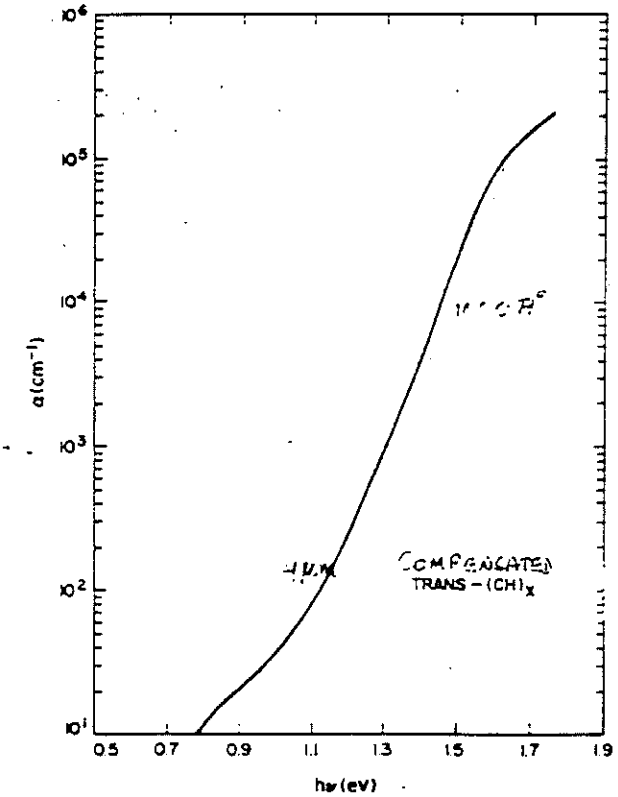

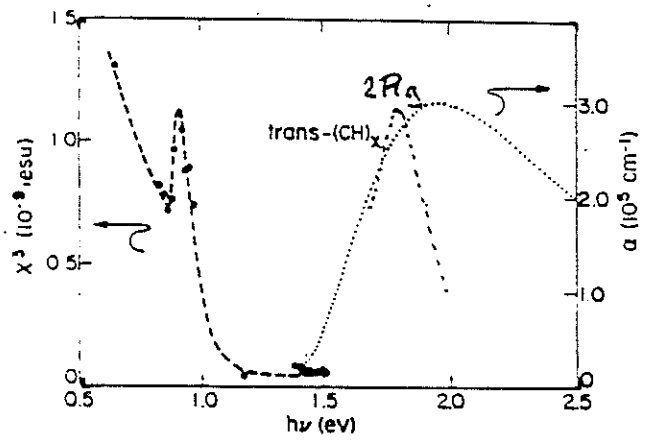

$2A_g$ STATE IS CLOSE TO $1B_u$ STATE?!

FREE ELECTRON LASER (FEL)

INTENSE TUNABLE IR RADIATION

1 → 100 KW IN 2-10 μm RANGE

STANFORD → DUKE

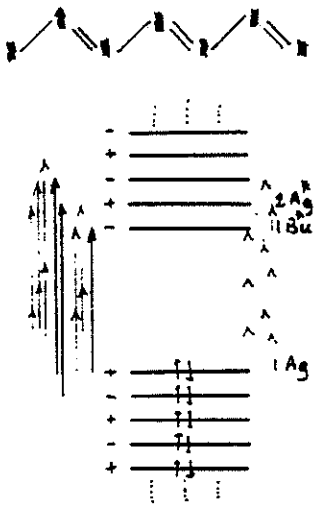

- PARTICLE IN A BOX
- DIMERIZATION
- IONIC ↔ COVALENT STATES

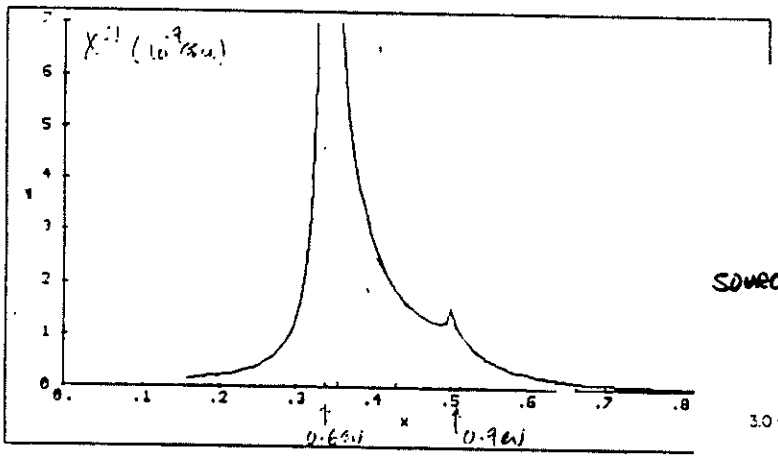

U=0 CALCULATION W. K. Wu

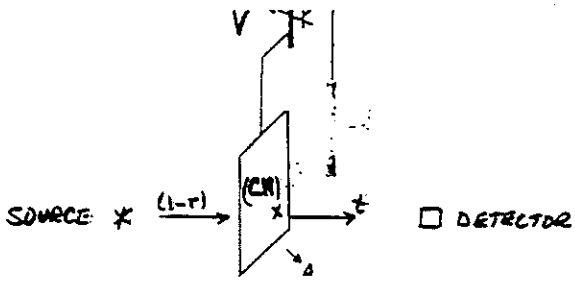

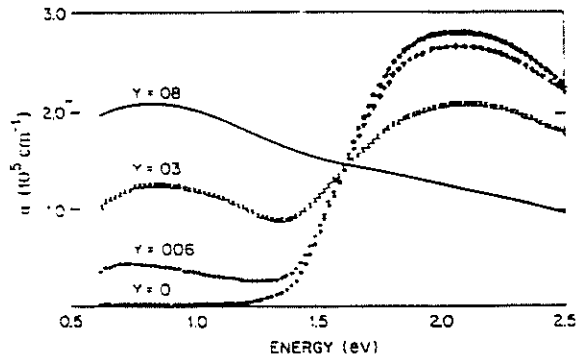

$\xi \cdot \chi_{EL} = 1.1 \times 10^{-17}$ cm^{-1} · eV / injected charge

ENHANCED BY ~ ξ/a

DOPING & SOLITON FORMATION

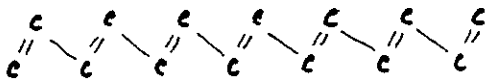

$E = ?\Delta$

$E = 2E_s = 2 \times 2\Delta/\pi$

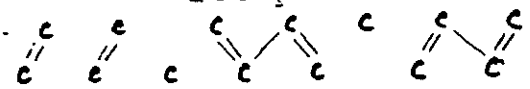

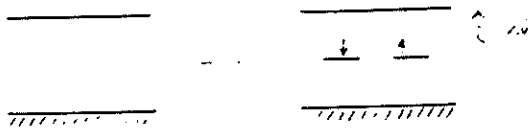

NO SPIN.

SIGNATURES OF SOLITON DOPING

APPEARANCE OF ABSORPTION BAND NEAR MIDGAP

APPEARANCE OF ENHANCED IR ACTIVE LOCAL MODES

NO INCREASE IN χ

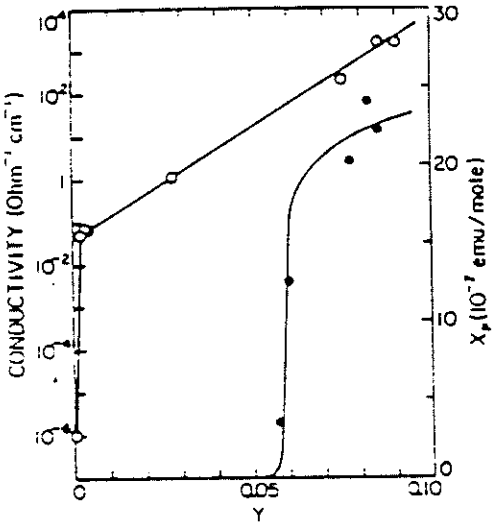

Chiang et al PRB 29, 1341 (1984)

DYNAMICS OF PHOTOEXCITATIONS IN POLYACETYLENE

Su & Schrieffer, Proc. Nat. Acad Sci USA 77, 5626 (1980)

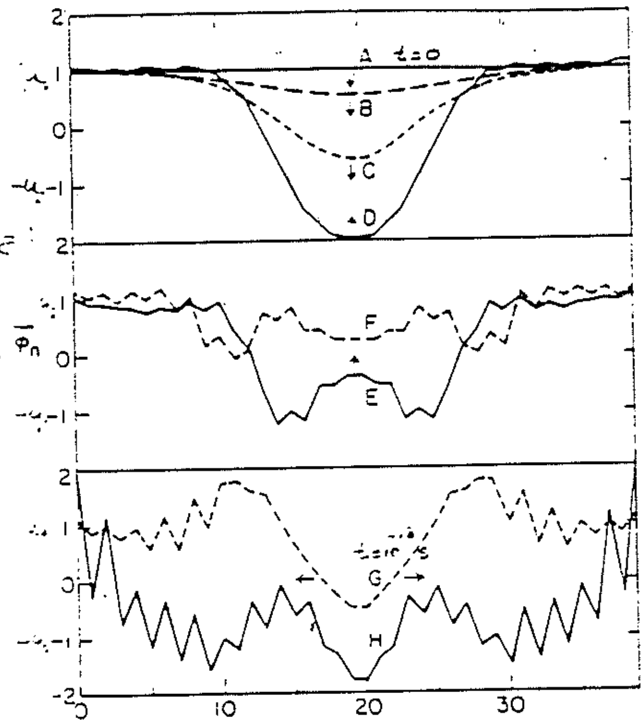

SPEED OF RESPONSE (RESONANCE)

$t > 10^{-2}$ sec.

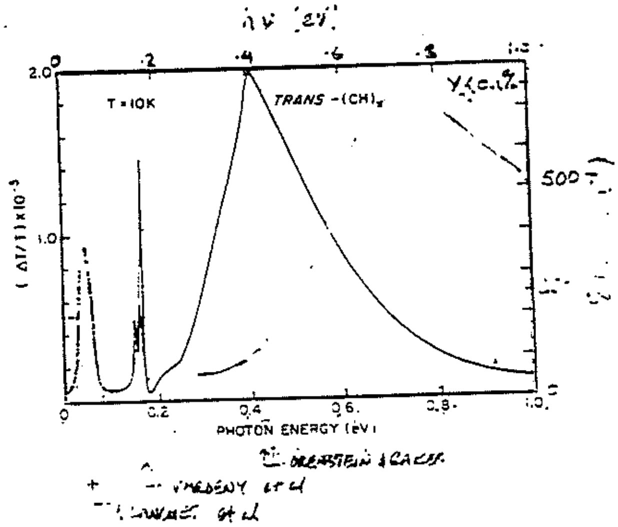

ELECTRONICALLY ENHANCED IR MODES

↳ SELF TRAPPED CHARGE IN CDW

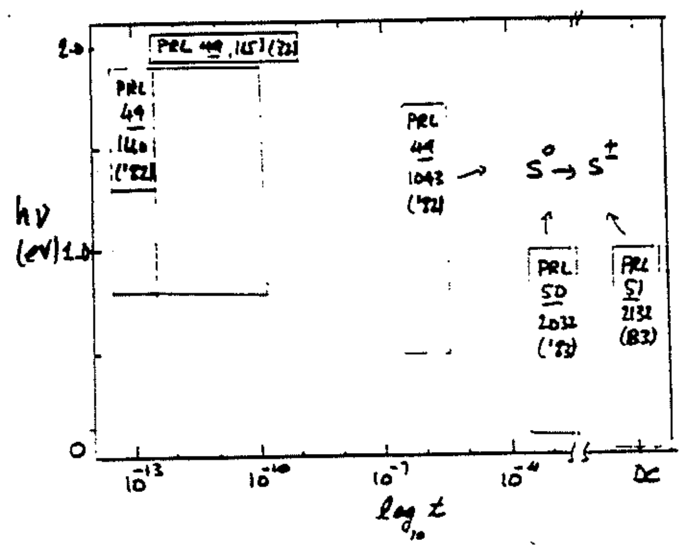

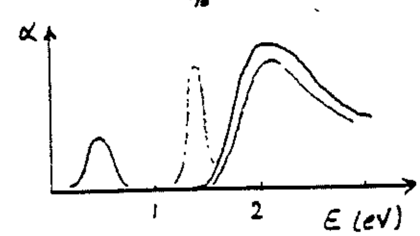

SU & SCHRIEFFER, PROC. NAT. ACAD. SCI 77, 5626 (80)

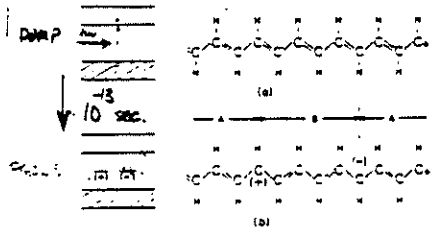

- $E_{e/h} > E_{2S^+}$ $\left(\xi_s \approx \frac{2\Delta}{\pi}\right)$

- $\tau \sim 1/\omega_{ph}$ (10^{-13} sec)

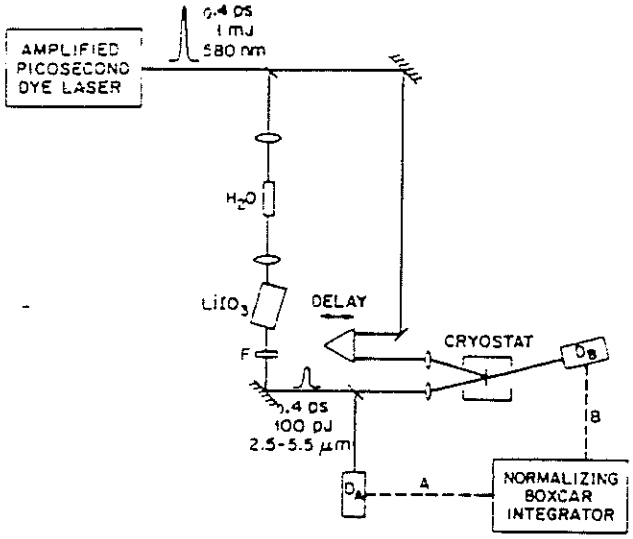

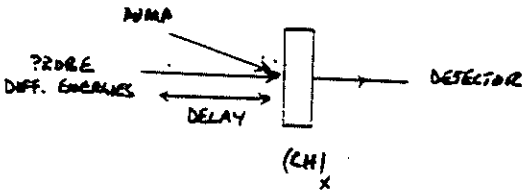

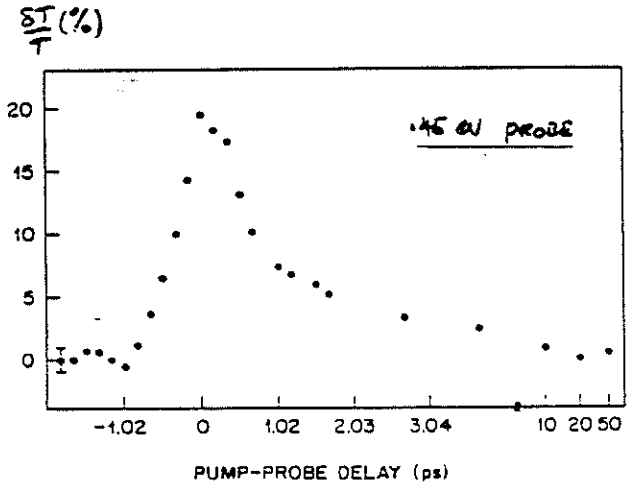

< 0.1 ps RISETIME

~ 0.5 ps LIFETIME

POWER DECAY (1D DIFF. ?)

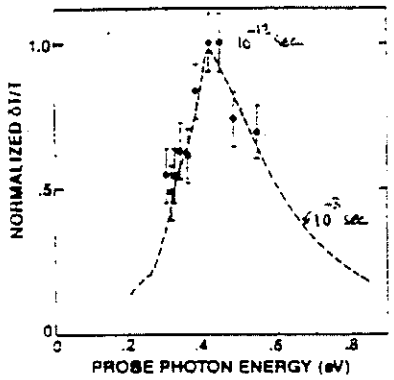

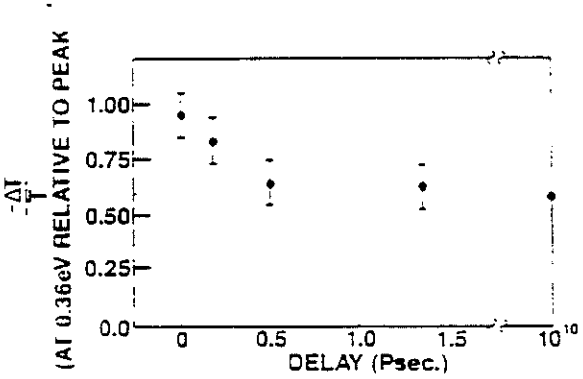

D-11

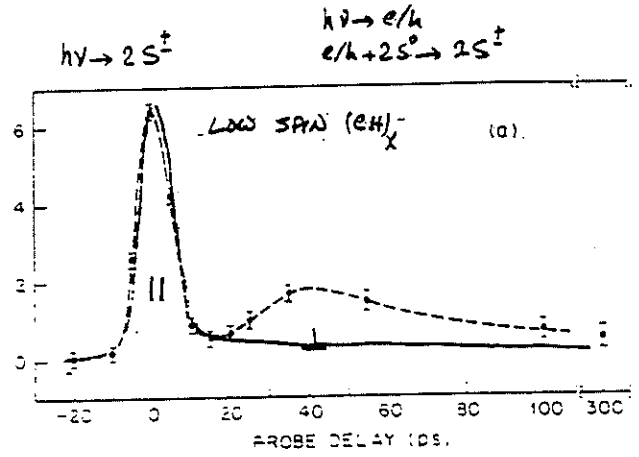

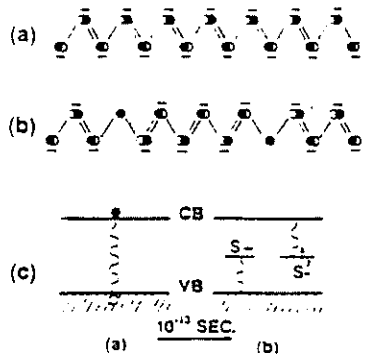

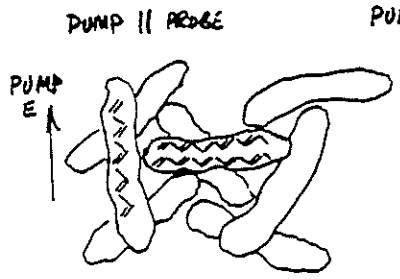

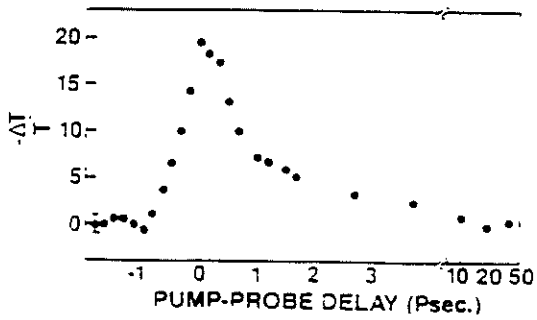

MAGNITUDE OF $\chi^{(3)}$

SHIRAKAWA (CH)$_x$

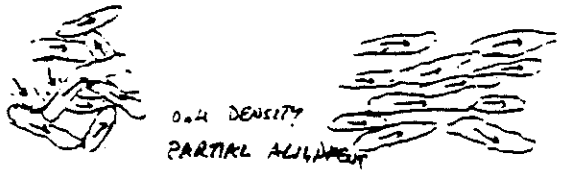

* ESR RESONANCE : TRANSIENT SPIN

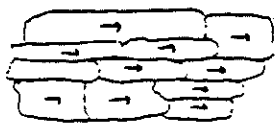

DURHAM (CH)$_x$
100% ALIGNMENT
100% SPACE FILLING
MACROSCOPIC DOMAINS

* POTENTIAL APPLICATIONS

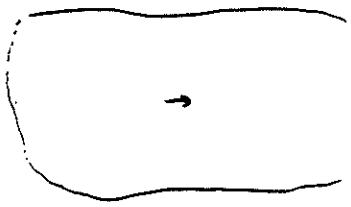

WINNER'S (CH)$_x$

* INTRINSIC ABSORPTION IS SMALL @ 1-3 μ
* SCATTERING LOSS IS MORPHOLOGY DEPENDENT

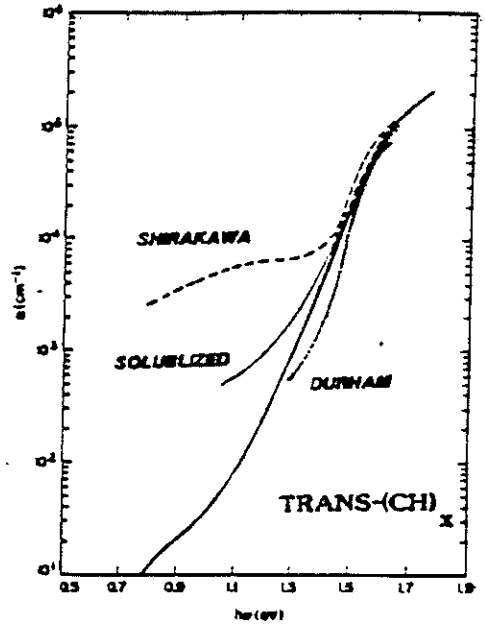

FIGURE OF MERIT

* $\chi^{(3)}/\alpha_{TOTAL}$

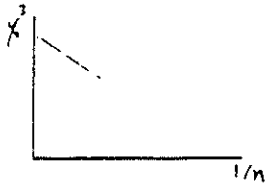

FOR n LARGE DIFFERENTIAL GAIN IS NOT LARGE

* $\alpha_{TOTAL} = \alpha_{abs} + \alpha_{SCATTERING}$

* → PROCESSABILITY (1 μm × 1 μm waveguides)
EASE OF FABRICATION

A. J. Heeger
University of California at Santa Barbara

ANISOTROPY OF THE THIRD ORDER NONLINEAR OPTICAL SUSCEPTIBILITY IN CONJUGATED POLYMERS

"Instantons" as the source of

Nonlinear Optical Properties

of Polyacetylene

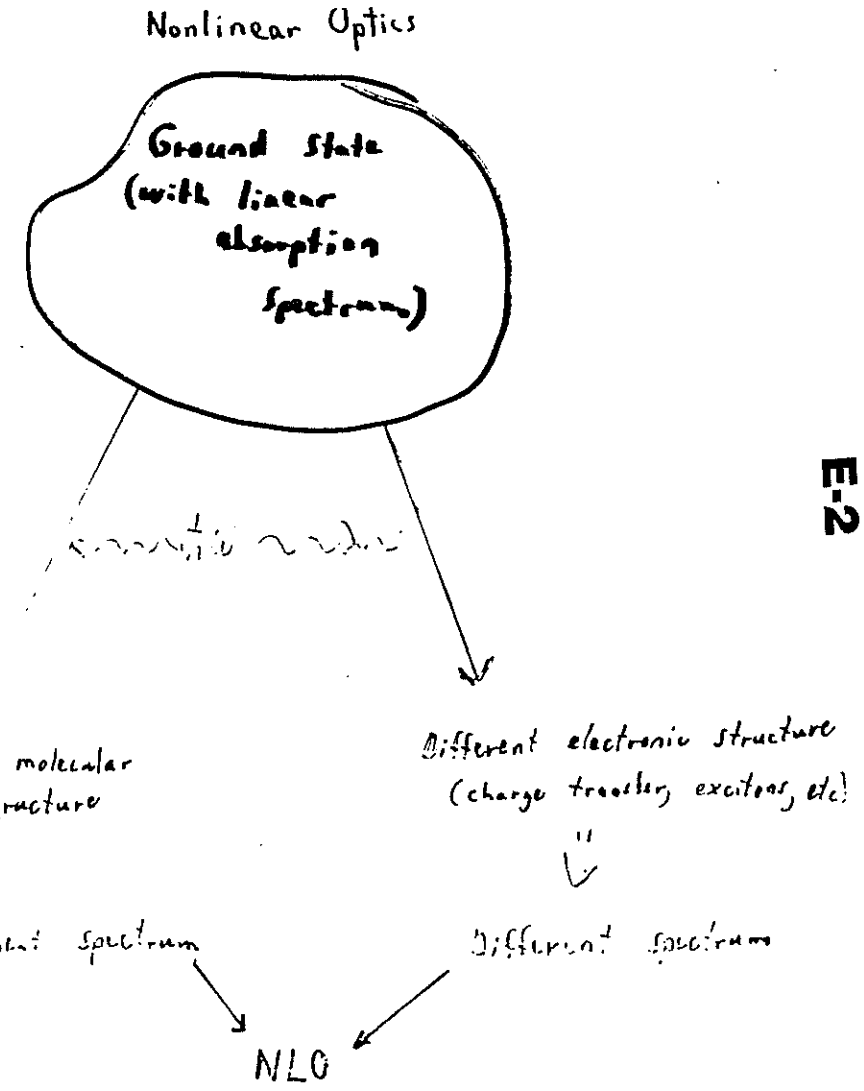

Acknowledgement:
M. Sinclair
D. Moses
W.-P. Su

trans-$(CH)_x$

Broken symmetry with 2-fold degenerate ground state

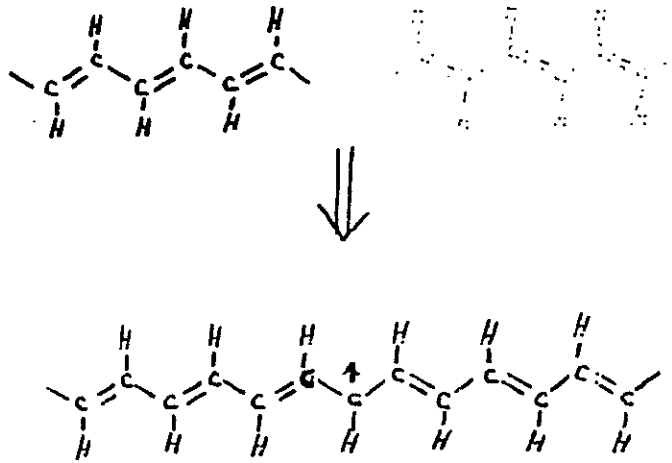

Bond-alternation domain wall or "Soliton"

≡ "particle" consisting of structural alternation

plus

localized non-bonding electronic state

$m_s \sim 5\, m_e$

$\pm$trans-$(CH)_x$: two-fold degenerate ground state

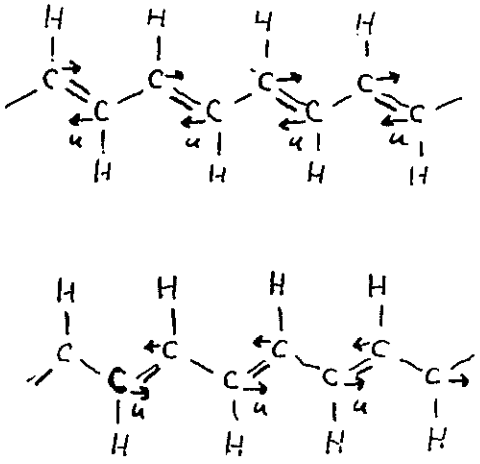

Quantum (zero point) fluctuations are important!

"Instantons" as the Source of $\chi^{(3)}_{\parallel}$ in Trans-$(CH)_x$

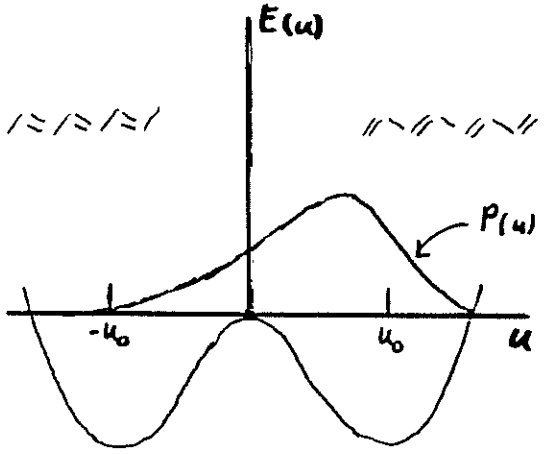

Order parameter $\varphi = \pm(-1)^n u_n \overset{\text{(classical)}}{=} \pm u_0$

Classical:

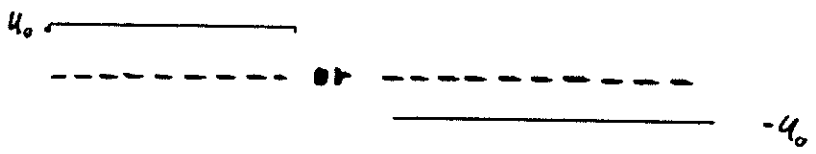

Quantum:

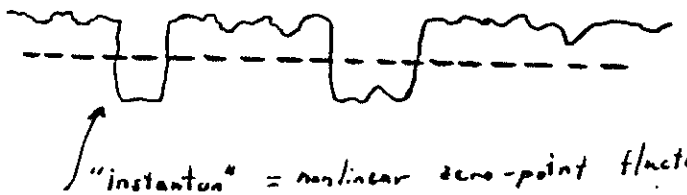

Instantons in polyacetylene

The effect of *nonlinear* ground state fluctuations on the photoproduction of charged solitons

Creation energy for soliton-antisoliton pair

$$2E_s = \frac{2}{\pi} E_g < E_g$$

Can one get direct photogeneration of Solitons for $\hbar\omega < E_g$?

Yes --- with help from ground state fluctuations !!

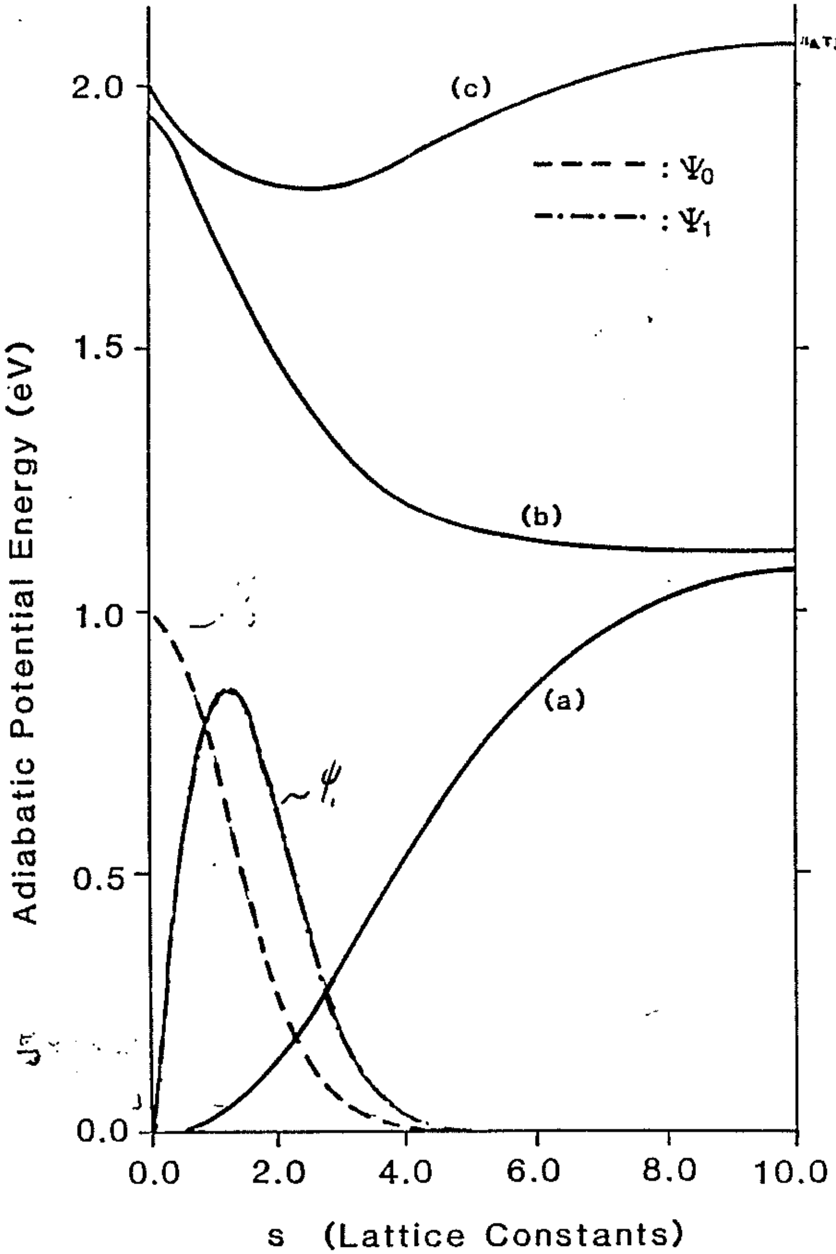

Vu, Matsuoka & Su

$\phi(x=na) = \phi_0\{1 - \tanh(2s/\xi)[\tanh(x-s/\xi) - \tanh(x+s/\xi)]\}$

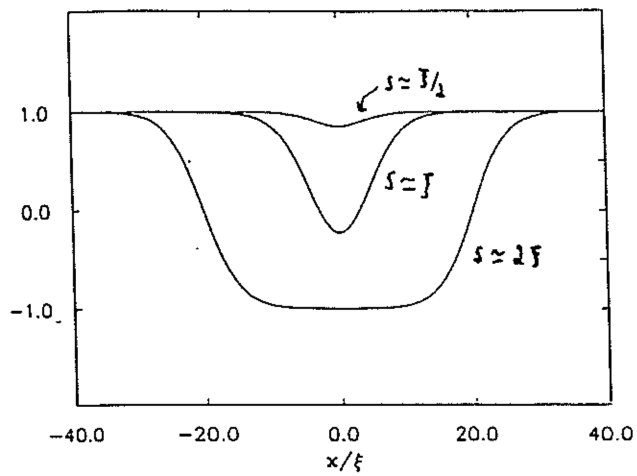

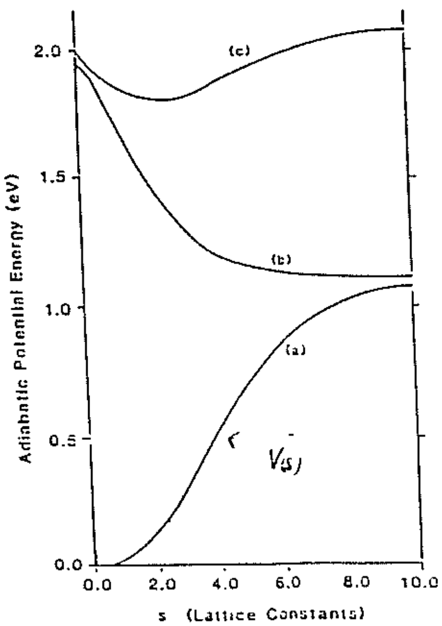

$U(s) = \frac{1}{2} m (\dot{s})^2 - V(s)$

& solve

[illegible] = [illegible]

straightforward [illegible] problem

E-5

E-6

For each δ ---- gap states appear

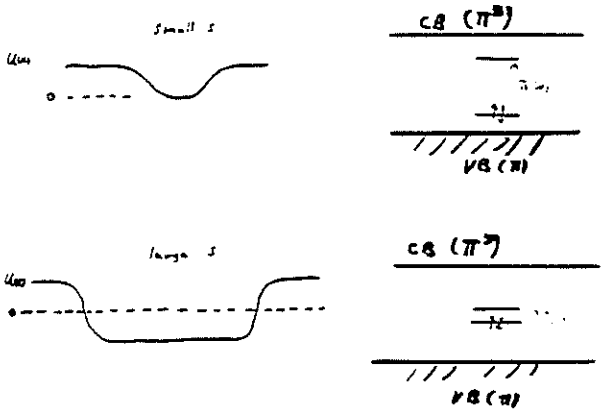

$$\Delta E = \frac{4}{\pi}\Delta + \hbar\omega_0(\delta)$$

$E_g = 2\Delta \simeq 1.8 - 1.9\,eV$

$\frac{4}{\pi}\Delta \simeq 1.15\,eV$ (threshold)

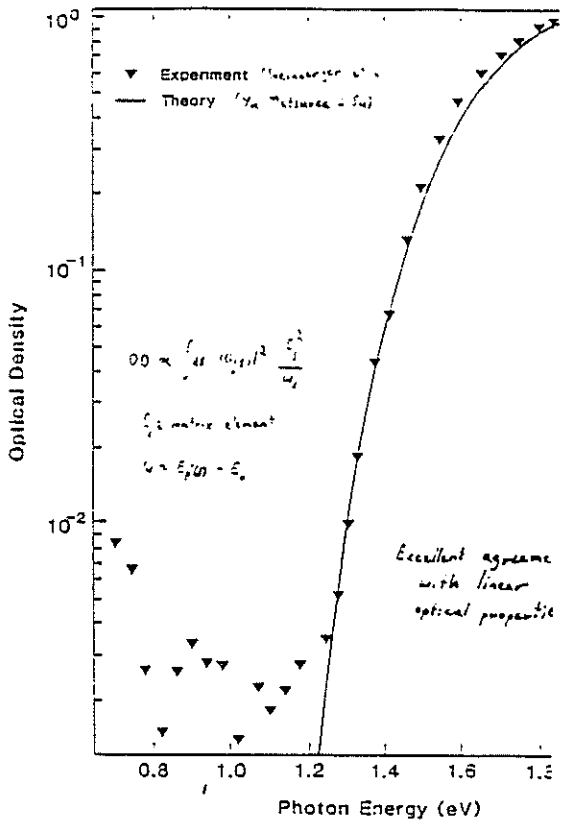

The connection to resonant

nonlinear optical properties

Soliton Photogeneration & Confinement in $(CH)_x$

Dynamical calculations (Su & Schrieffer) show that after photogeneration of e-h pair, lattice distortion forms in very short time ($\sim 10^{-13}$ sec) leading to photogenerated S^+ and S^- pairs

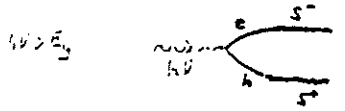

Photogeneration in trans

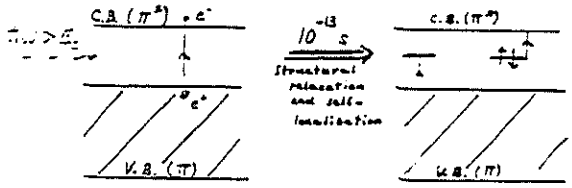

trans-$(CH)_x$

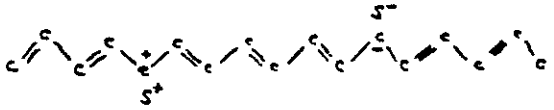

Two states are equivalent --- S^+ and S^- "free"

Sum rule:

$$\int_\omega \left[\alpha_{\text{Higher energy region}}\right] d\omega = \int_\omega \left[\alpha\right] d\omega \Rightarrow \chi^{(3)} \simeq 5\times10^{-2}\ \text{esu}$$

(resonant)

Nonlinear Optics!

Index of refraction is different after absorption of $\parallel$ photon

Higher energy region

cis-$(CH)_x$

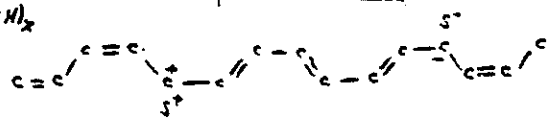

S^+ and S^- are "confined"

Resonant $\Lambda\Lambda C$ process

Vardeny, Strait, Moses, Chung + AJH

PRL (1983)

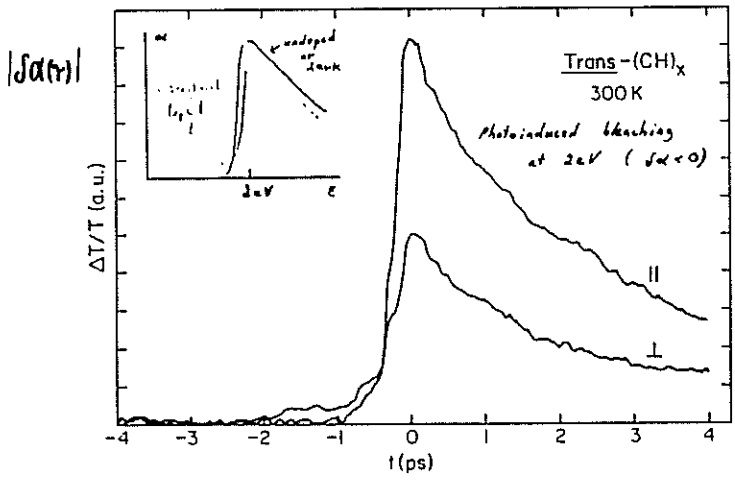

E-8

Rubbing, Etemad et al

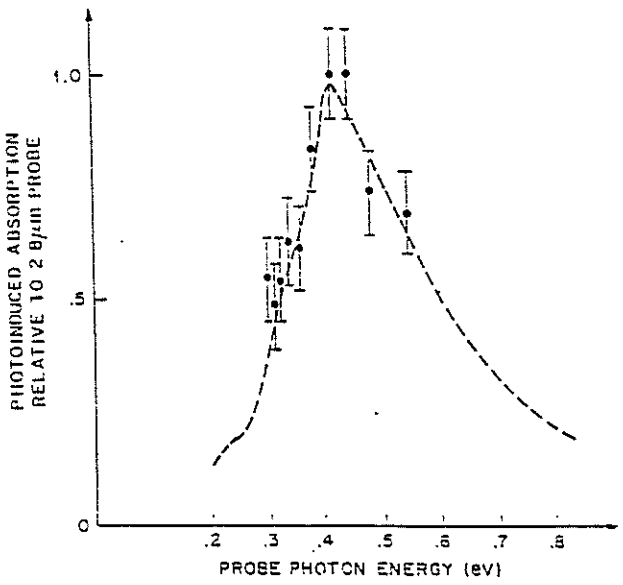

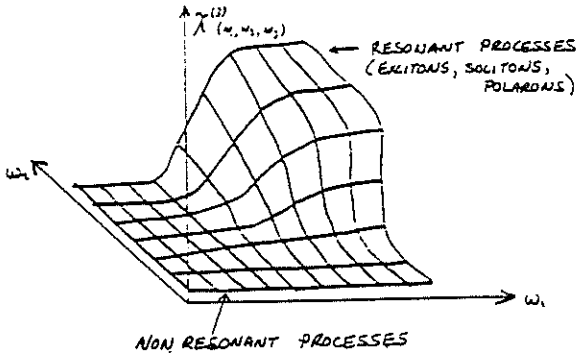

We have seen how solitons lead directly to resonant NLO

What about non-resonant NLO ?

(i.e. for $\hbar\omega < \frac{E_g}{2}$ ---- ω ---- $\frac{E_g}{2}$)

Yes ---- Instantons

THIRD HARMONIC GENERATION IN ORIENTED $\frac{1}{2}$-(CH)$_x$

$$P(3\omega) \propto \chi^{(3)}_{\parallel} E^6_{\parallel} = \chi^{(3)}_{\parallel} E^6 \cos^6\theta$$

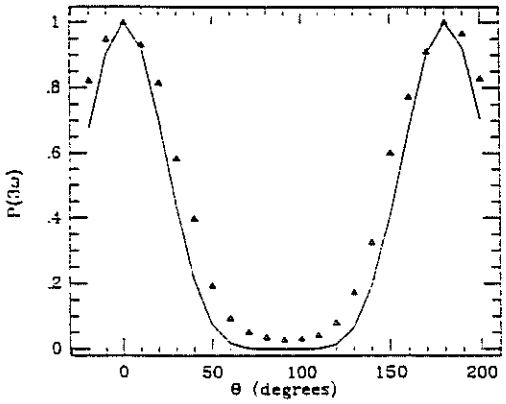

Alignment Direction

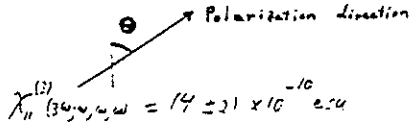

$\chi^{(3)}_{\parallel}(3\omega;\omega,\omega,\omega) = 14 \pm 3) \times 10^{-10}$ esu

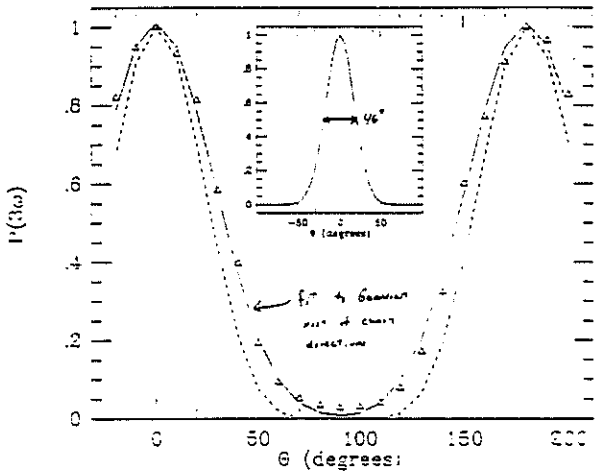

All nonlinearity associated with

Nonlinear: $\chi^{(3)}(3\omega;\omega,\omega,\omega)$

Third order perturbation theory on the excited states of the s-configurations yields

$$\chi^{(3)} = N_0\Sigma_{mn}\langle g|n\rangle\langle n|m\rangle\langle m|g\rangle \times$$
$$[(1/(E_{ng}-3\omega)(E_{mg}-2\omega)(E_{lg}-\omega) + 1/(E_{ng}+\omega)(E_{mg}-2\omega)(E_{lg}-\omega)$$
$$+ 1/(E_{ng}+\omega)(E_{mg}+2\omega)(E_{lg}-\omega) + 1/(E_{ng}+\omega)(E_{mg}+2\omega)(E_{lg}+3\omega)]$$

where $E_{ng}=E_{s,n} - E_{s,g}$,

$E_{s,g}$ is the ground state energy

$E_{s,\alpha}$ (α=n,m, l are the energies of excited states of the s-configurations

$f_{\alpha\beta}$ are the dipole matrix elements

$N_0=n_0\rho_c$ where $n_0=(L/2\xi)$ is the phase space for soliton pairs on a chain of length L and ρ_c is the density of chains per unit area.

In the sum, n and l denote excited states with symmetry opposite to g, and m is an excited state with the same symmetry as g.

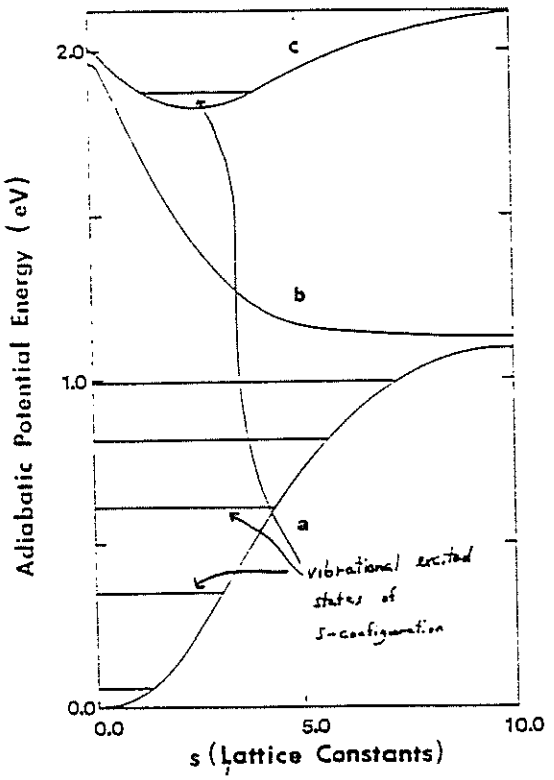

To estimate the magnitude of $\chi_\perp^{(3)}$ we consider the term in the full sum where the matrix elements go from $g \to E_n(s) \to g \to E_n(s) \to g$; i.e we ignore the various vibrational states of the s-configuration and consider only this single contribution ($\chi_\perp^{(3)}|_0$):

$$\chi_\perp^{(3)}|_0 = N_0\Sigma_{ss'}|\phi_0(s)|^2|\phi_0(s')|^2(|f_s|^2|f_{s'}|^2/2\omega) \times$$
$$[-(1/(E_s-3\omega)(E_s-\omega) + 1/(E_s+\omega)(E_s-3\omega)].$$

For $3\omega<E_s$

$$\chi_\perp^{(3)}|_0 = -4N_0\Sigma_{ss'}|\phi_0(s)|^2|\phi_0(s')|^2(|f_s|^2|f_{s'}|^2/E_s^2E_{s'}$$

where f_s is the matrix element between the ground state with wave function $\phi_0(s)$ and the excited state with energy E_s relative to the ground state

Since

$$\alpha = N_0\Sigma_s|\phi_0(s)|^2\alpha_s$$

is the linear term in the polarizability,

$$\chi_\perp^{(3)}|_0 = -(4\alpha)\Sigma_s|\phi_0(s)|^2(\alpha_s/E_s)$$

$$\chi_\perp^{(3)}|_0 \sim (8\xi/a)(N\rho_c)^{-1}\alpha^2/E_0$$

$$\chi_\perp^{(3)}|_0 \sim 3\times10^{-10} \text{ esu}$$

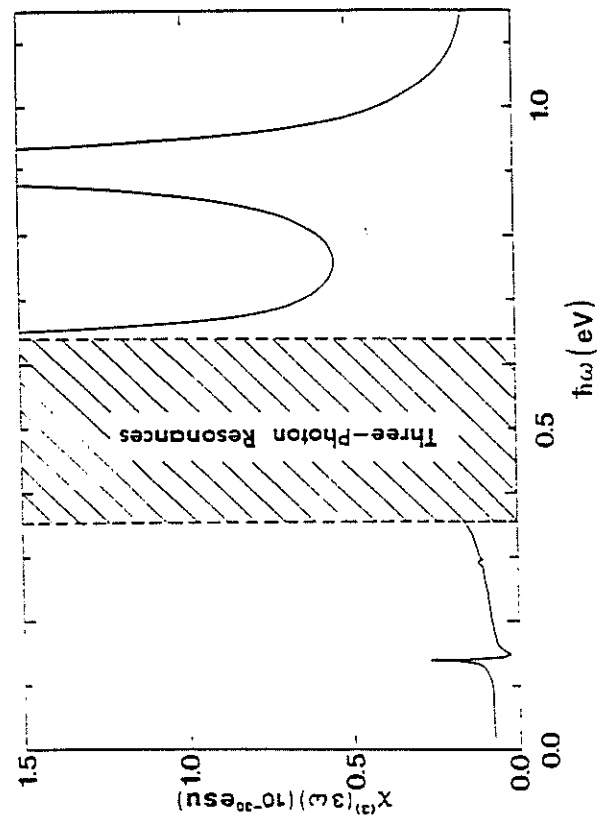

E-10

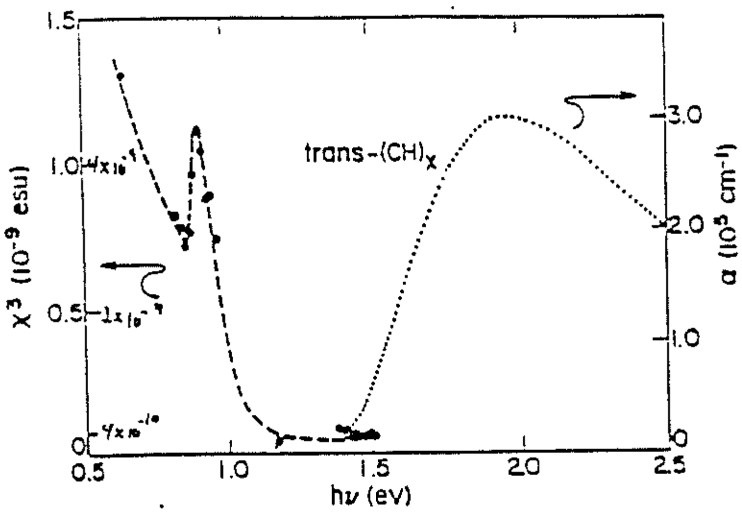

Kajzar, Etemad, Messier & Baker
Synth. Met. 17, 563 (1987)

[illegible] the ground-state degeneracy

Not equivalent

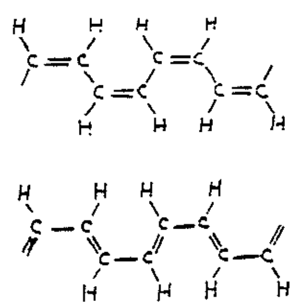

A phase

B phase

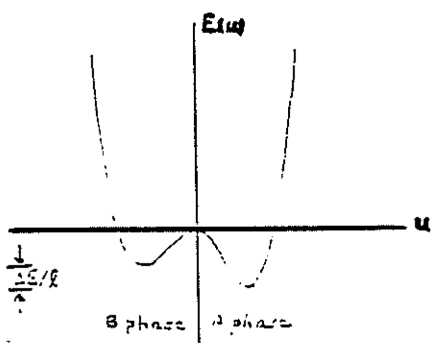

Symmetry Specific Origin of $\chi^{(3)}$: Comparative Measurements of $\chi^{(3)}$ in cis and trans-(CH)x

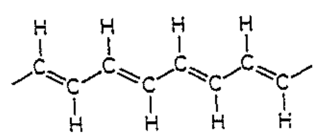

TRANS

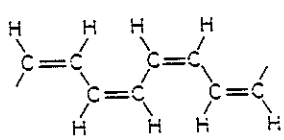

CIS

Result: $\chi^{(3)}_{(3\omega)}\big|_{cis} < \frac{1}{16}\,\chi^{(3)}_{(3\omega)}\big|_{trans}$

Best number: $\chi^{(3)}\big|_{trans} = (15\text{–}20)\,\chi^{(3)}\big|_{cis}$

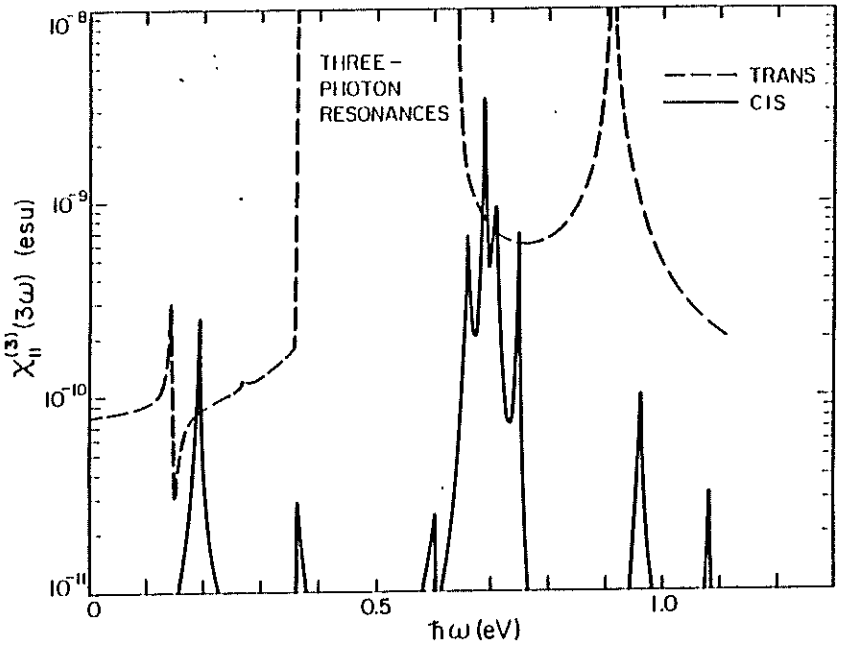

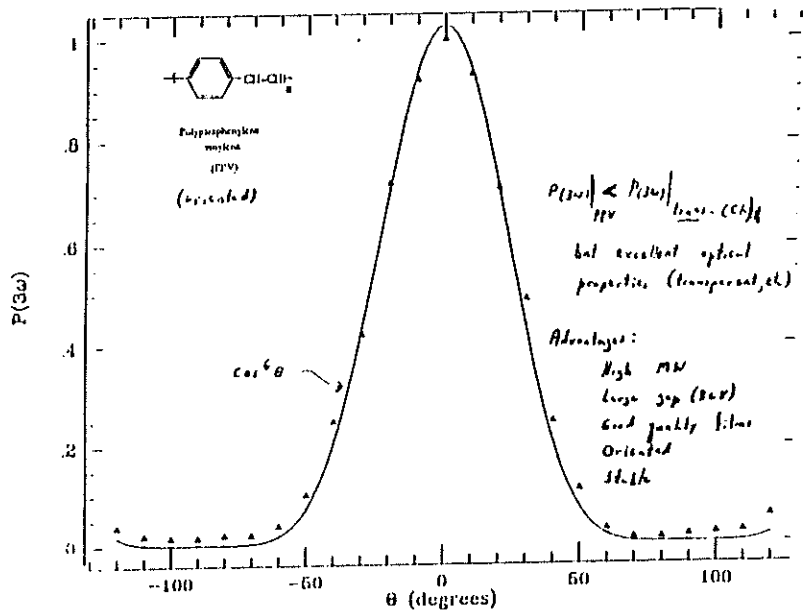

Conclusions:

1) Large $\gamma^{(3)}$'s are a general feature of conjugated polymers

2) Nonlinearity is associated with the π-electrons

3) At 1.06 μm $\left|\gamma^{(3)}_{(3\omega)}\right|_{trans\text{-}(CH)_x} \simeq \left|\gamma^{(3)}_{(3\omega)}\right|_{PDA}$

At longer wavelengths $\left|\gamma^{(3)}_{(3\omega)}\right|_{trans\text{-}(CH)_x}$ is certainly larger by considerable factor

4) For polyacetylene $|\gamma^{(3)}|_{trans} > 10\ |\gamma^{(3)}|_{cis}$

5) Nonlinearity from rigid band structure is not dominant contribution for [illegible] $trans\text{-}(CH)_x$ [illegible] $(CH)_x$

Questions:

1) Why is $trans\text{-}(CH)_x$ special?

2) How to connect measurement $\chi^{(3)}$'s to known resonant properties?

E-11

K. D. Singer

AT&T

NONLINEAR OPTICS IN ORDERED MOLECULAR SYSTEMS

F-2

NONLINEAR OPTICS IN ORDERED MOLECULAR SYSTEMS

K.D. SINGER and M.G. KUZYK
AT&T Engineering Research Center, Princeton, NJ

OUTLINE

R.B. COMIZZOLI

D.L. FISH

W.R. HOLLAND

H.E. KATZ

L.A. KING

M.L. SCHILLING

J.E. SOHN

- NONLINEAR OPTICS IN MOLECULAR ENSEMBLES
- FILMS POLED UNDER UNIAXIAL STRESS
- NEW POLYMERS
  - MATERIALS
  - CORONA POLING
  - NONLINEAR OPTICAL PROPERTIES
  - MOLECULAR ORIENTATION DISTRIBUTION

MOLECULAR MATERIALS

- MACROSCOPIC POLARIZATION

$$P_i(t) = \chi_i^{(0)} + \chi_{ij}^{(1)}(t)E_j(t) + \chi_{ijk}^{(2)}(t)E_j(t)E_k(t) + \chi_{ijkl}^{(3)}(t)E_j(t)E_k(t)E_l(t) + \cdots$$

- MICROSCOPIC POLARIZATION

$$p_I(t) = \mu_I^{(0)} + \alpha_{IJ}(t)F_J(t) + \beta_{IJK}(t)F_J(t)F_K(t) + \gamma_{IJKL}(t)F_J(t)F_K(t)F_L(t) + \cdots$$

- VAN DER WAALS MATERIALS

$$P_i(t) = \frac{1}{V}\langle p_I(t)\rangle_i$$

F-3

MATERIAL CLASSES

Crystal

Langmuir-Blodgett

Smectic LC

Nematic LC

Orientational Order

Liquid

MOLECULAR ORDER

- MOLECULES FIXED IN LATTICE

$$\chi^{(n)}_{ijkl\ldots} = N_u \sum_{I,J,K,L\ldots s=1}^{n} a_{iI(s)} a_{jJ(s)} a_{kK(s)} \cdots \xi^{*}_{IJKL\ldots}(s)$$

- THERMODYNAMIC ENSEMBLE

$$\chi^{(n)}_{ijkl\ldots} = N \langle \xi^{*}_{IJKL\ldots} \rangle_{ijkl\ldots}$$

$$\langle \xi^{*}_{IJKL\ldots} \rangle_{ijkl\ldots} = \int_0^{2\pi} d\phi \int_0^{\pi} \sin\theta d\theta \int_0^{2\pi} d\psi \, \xi^{*}_{IJKL\ldots} a_{iI} a_{jJ} a_{kK} \cdots G(\phi,\theta,\psi)$$

EULER ANGLES

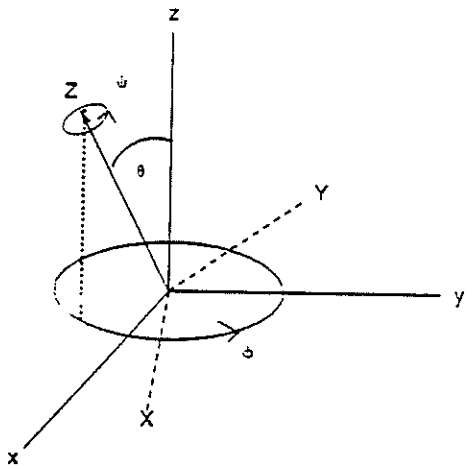

SYMMETRY CLASSES

$\chi^{(2)}$ components for point group ∞mm

	1	2	3
1	0	0	$\chi_{311}^{(2)}$
2	0	0	$\chi_{322}^{(2)}$
3	0	0	$\chi_{333}^{(2)}$
4	0	$\chi_{123}^{(2)}$	0
5	$\chi_{113}^{(2)}$	0	0
6	0	0	0

$\chi^{(3)}$ components for point group ∞/mmm

	1	2	3	4	5	6
1	$\chi_{1111}^{(3)}$	$\chi_{1122}^{(3)}$	$\chi_{1133}^{(3)}$	0	0	0
2	$\chi_{2211}^{(3)}$	$\chi_{2222}^{(3)}$	$\chi_{2233}^{(3)}$	0	0	0
3	$\chi_{3311}^{(3)}$	$\chi_{3322}^{(3)}$	$\chi_{3333}^{(3)}$	0	0	0
4	0	0	0	$\chi_{2323}^{(3)}$	0	0
5	0	0	0	0	$\chi_{1313}^{(3)}$	0
6	0	0	0	0	0	$\frac{1}{2}(\chi_{1111}^{(3)} - \chi_{1122}^{(3)})$

Row and column labels: 1 = 11; 2 = 22; 3 = 33; 4 = 23,32; 5 = 31,13; 6 = 12,21

DISTRIBUTION FUNCTION

$$G(\theta) = \sum_{l=0}^{\infty} \frac{(2l-1)}{2} A_l P_l(\cos\theta)$$

LEGENDRE POLYNOMIALS

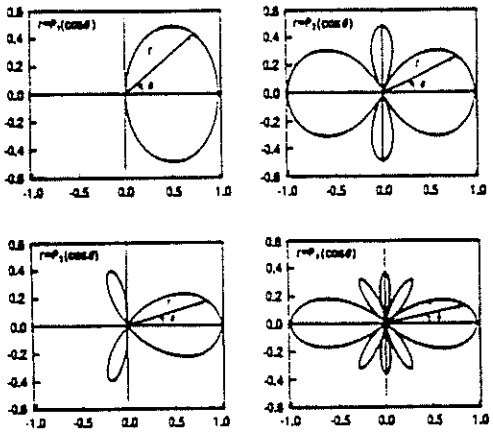

SUSCEPTIBILITIES

$$\chi_{ijkl\ldots}^{(2n)} = \sum_{m=0}^{n} u_{ijkl\ldots}^{(2m-1)} \langle P_{2m-1} \rangle$$

$$\chi_{ijkl\ldots}^{(2n-1)} = \sum_{m=0}^{n-1} u_{ijkl\ldots}^{(2m)} \langle P_{2m} \rangle$$

- SECOND ORDER

$$\chi_{333}^{(2)} = N\beta_{zzz}^{*}\left(\frac{3}{5}\langle P_1 \rangle - \frac{2}{5}\langle P_3 \rangle\right)$$

$$\chi_{113}^{(2)} = \chi_{131}^{(2)} = \chi_{311}^{(2)} = N\beta_{zzz}^{*}\left(\frac{1}{5}\langle P_1 \rangle - \frac{1}{5}\langle P_3 \rangle\right)$$

- THIRD ORDER

$$\chi_{3333}^{(3)} = N\gamma_{zzzz}^{*}\left(\frac{1}{5} - \frac{4}{7}\langle P_2 \rangle - \frac{8}{35}\langle P_4 \rangle\right)$$

ELECTRIC FIELD POLING

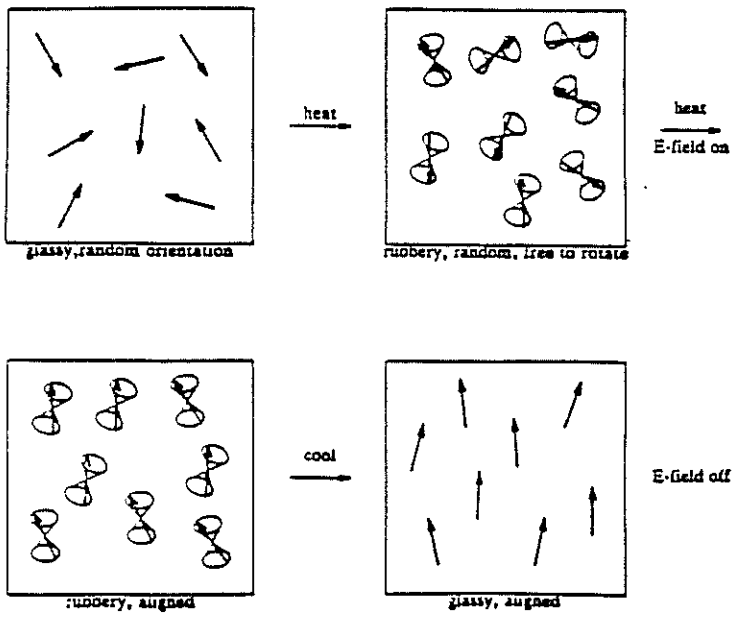

F-5

POLED MATERIALS

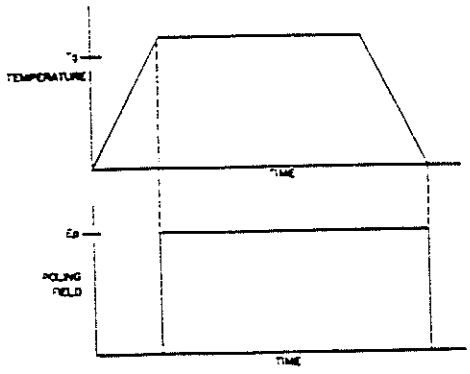

POLING UNDER UNIAXIAL STRESS

- SECOND HARMONIC TENSOR PROPERTIES
- MOLECULAR DISTRIBUTION

$$G_u(\Omega,E_p) = \frac{\exp[-\frac{1}{kT}(\sum_v U_{uv} - \mathbf{m}_u^* \cdot \mathbf{E}_p)]}{\int d\Omega \exp[-\frac{1}{kT}(\sum_v U_{uv} - \mathbf{m}_u^* \cdot \mathbf{E}_p)]}$$

SECOND HARMONIC GENERATION

$$\chi_{ijk}^{(2)} = \nu_{ijk}^{(0)} \langle P_0 \rangle + \nu_{ijk}^{(2)} \langle P_2 \rangle + \nu_{ijk}^{(4)} \langle P_4 \rangle$$

$$P_1^{(2)}(2\omega) = 2d_{31}(-2\omega;\omega,\omega)E_1(\omega)E_3(\omega)$$

$$P_2^{(2)}(2\omega) = 2d_{31}(-2\omega;\omega,\omega)E_2(\omega)E_3(\omega)$$

$$P_3^{(2)}(2\omega) = d_{31}(-2\omega;\omega,\omega)\left[E_1^2(\omega) + E_2^2(\omega)\right] + d_{33}(-2\omega;\omega,\omega)E_3^2(\omega)$$

EXPERIMENTAL GEOMETRY

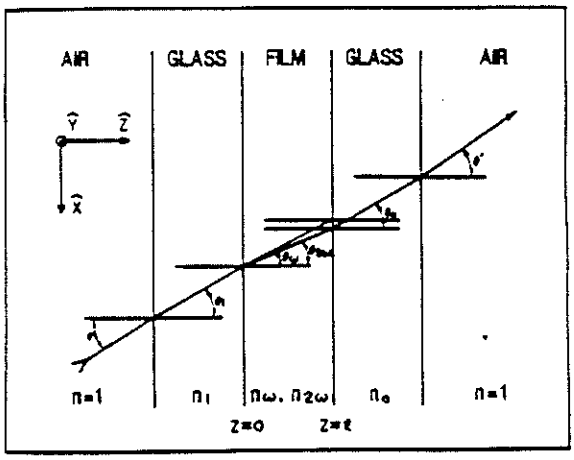

SECOND HARMONIC INTENSITY

$$P_T = \frac{512\pi^3}{A}|d_{33}|^2 t_1^4 t_\omega^4 T_{2\omega} t_o^2 p^2(\theta) I_\omega^2 \left[\frac{1}{n_\omega^2 - n_{2\omega}^2}\right]^2 \sin^2\psi$$

- P-POLARIZED INCIDENT LIGHT

$$p(\theta) = (a\cos^2\theta_\omega + \sin^2\theta_\omega)\sin\theta_{2\omega} + 2a\cos\theta_\omega \sin\theta_\omega \cos\theta_{2\omega}$$

- S-POLARIZED INCIDENT LIGHT

$$p(\theta) = a\sin(\theta_{2\omega})$$

$$\text{where} \quad a = \frac{d_{31}}{d_{33}}$$

ORDERING ENERGY

$$G_u(\Omega) = \frac{\exp[-\frac{U}{kT}]}{\int d\Omega \exp[-\frac{U}{kT}]}$$

- ELECTRIC FIELD POLING

$U_E = \mathbf{m}_u^* \cdot \mathbf{E}_p$

$$\chi^{(2)}_{333} = N\beta^*_{zzz}\frac{m_z^* E_p}{kT}\left(\frac{1}{5} + \frac{4}{7}\langle P_2\rangle + \frac{8}{35}\langle P_4\rangle\right)$$

$$\chi^{(2)}_{113} = \chi^{(2)}_{131} = \chi^{(2)}_{311} = N\beta^*_{zzz}\frac{m_z^* E_p}{kT}\left(\frac{1}{15} + \frac{1}{21}\langle P_2\rangle - \frac{4}{35}\langle P_4\rangle\right)$$

- UNIAXIAL STRESS

$U_T = U_P + U_E = bP_2(\cos\theta) - m^* E_p P_1(\cos\theta)$

ORDERING ENERGY

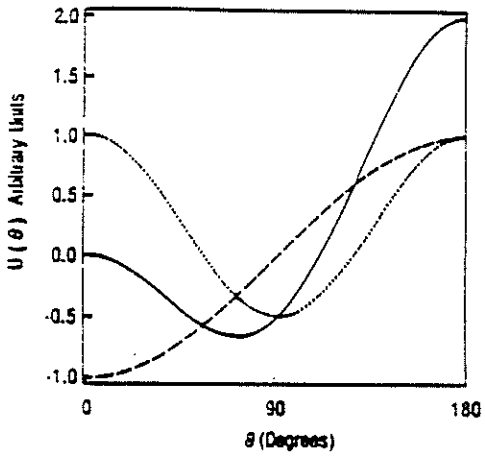

STRESS POTENTIAL

$$\frac{\exp\left[-\frac{(U_P - U_E)}{kT}\right]}{\left(\frac{m^* E}{kT}\right)} = a_1(\frac{b}{kT})P_1(\cos\theta) + a_3(\frac{b}{kT})P_3(\cos\theta)$$

$$\frac{\langle P_3\rangle}{\langle P_1\rangle} = \frac{3}{5}\frac{a_3}{a_1}$$

b = magnitude of stress potential

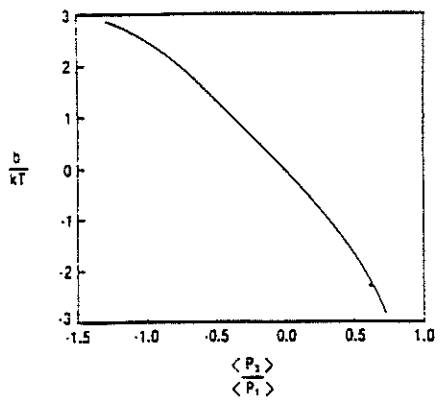

DISTRIBUTION FUNCTION

$$\langle P_1\rangle = \frac{2}{3}\frac{m^* E_p}{kT}\frac{a_1}{A_n}$$

$$\frac{\langle P_3\rangle}{\langle P_1\rangle} = \frac{1-3a}{1+2a}$$

$$\langle P_2\rangle = \frac{1}{2}\left(\frac{\langle P_1\rangle}{\left[\frac{m^* E_p}{3kT}\right]} - 1\right)$$

$$\langle P_4\rangle = \frac{1}{4}\left(\frac{\langle P_3\rangle}{\left[\frac{m^* E_p}{7kT}\right]} - 3\langle P_2\rangle\right)$$

FILMS POLED UNDER STRESS

- DISPERSE RED 1 DYE DISSOLVED IN PMMA

Film #	Dye Number Density $N\ (10^{20}/cm^3)$	Thickness $l(\mu m)$	Poling Field $E_p(MV/cm)$	Stress $\sigma(dyne/cm^2 \times 10^7)$
1	2.42	4.0	0.60	0.00
2	1.08	4.9	0.25	3.71

- RESULTS

Film #	a	$\frac{\mu^* E_p}{kT}$	$\frac{b}{kT}$	$<P_1>$	$<P_2>$	$<P_3>$	$<P_4>$	Δn
1	0.33	0.50	0.00	0.16	-0.020	0.00	0.015	0.0014
2	0.7	0.20	1.2	0.041	-0.20	-0.019	-0.02	-0.0043

NEW MATERIALS

DISTRIBUTION FUNCTION

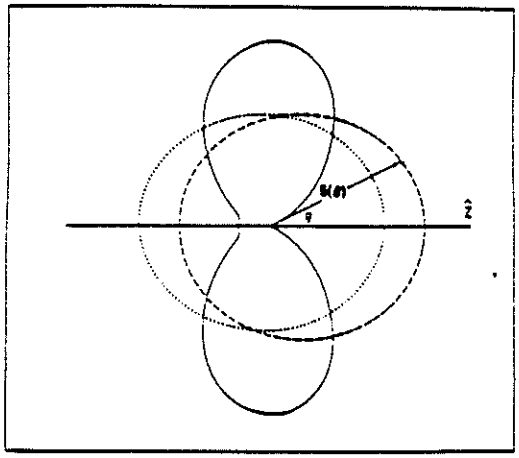

..... ISOTROPIC

------- POLED

——— STRESS + POLED

$r \propto d \propto N\ \beta\ \mu\ E_p$

- MOLECULES
- CORONA POLING
- POLYMERS

MOLECULES

$\beta\mu$ MEASURED BY EFISH

- DIRECT MEASUREMENT IN DIPOLAR SOLVENT, DMSO
- INFINITE DILUTION TECHNIQUE

RESULTS

Molecule		βμ*
DR1	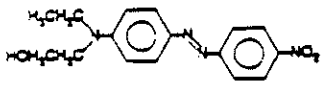	1090†
DCV	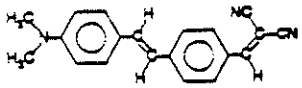	2850†
TCV	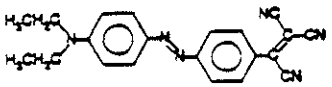	4110#

* βμ in $10^{-30} cm^5 D/esu$
† λ = 1.356μm
# λ = 1.58μm

CORONA POLING

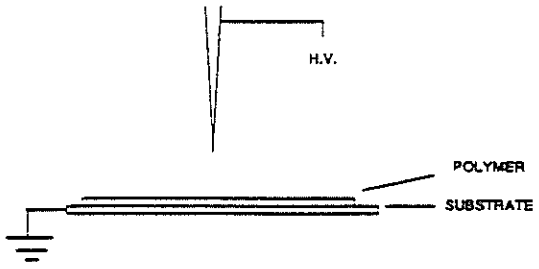

- NO ELECTRODE DEPOSITION
- HIGHER POLING FIELD

H. Nakanishi

Research Institute
for Polymers and Textiles, Japan

SEVERAL SERIES OF NOVEL POLYDIACETYLENES FOR NONLINEAR OPTICS

F. Kajzar
CEN Saclay, France

RESONANCE EFFECTS IN CUBIC HYPERPOLARISABILITIES OF CONJUGATED POLYMERS

RESONANCE EFFECTS IN CUBIC HYPERPOLARISABILITIES OF CONJUGATED POLYMERS

François KAJZAR

Commissariat à l'Energie Atomique
Institut de Recherche Technologique et de Développement Industr
Division d'Electronique, de Technologie et d'Instrumentation
Département d'Electronique et d'Instrumentation Nucléaire
Laboratoire de Physique Electronique des Matériaux
CEN Saclay, 91191 GIF SUR YVETTE, France

- THIN FILM PREPARIATION TECHNIQUES (polydiacetylenes)
- THIRD ORDER OPTICAL HYPERPOLARISABILITY DETERMINATION TECHNIQUES
  - Third Harmonic Generation
  - Electric Field Induced Second Harmonic Generation
- NONLINEAR SPECTROSCOPY IN PDA THIN FILMS
  - Multiphoton resonances
  - Two photon resonance → Kerr susceptibility → intensity dependent index of refraction
  - Temperature variation of cubic susceptibility
  - Nonlinear Optical Dichroism
- POLARISATION EFFECTS IN PDA THIN FILMS

PDA THIN FILM PREPARATION TECHNIQUES :

- Langmuir - Blodgett technique
- Solution casting
- Dipping technique from a polymer solution
- Evaporation technique (sublimation, epitaxy
- Shear technique (thin monocrystalline films

Why thin films (0.003 µm up a few tens of microns)?

- Nonlinear optical properties characterisation

$l \ll l_c$ $\quad l_c = \lambda_p / 2(n_H - n_F)$

$J = \begin{cases} 2 & \text{EFISH} \\ 3 & \text{THG} \end{cases}$

$I_{2\omega} \sim l^2 I_\omega^2$

$I_{3\omega} \sim l^2 I_\omega^3$ "phase matching"

- Nonlinear spectroscopy
  - harmonic light within absorption range
- Integrated optics
- Thin film devices

LANGMUIR- BLODGETT METHOD OF THIN FILM DEPOSITION

Diacetylene monomers :

$R_1 - C \equiv C - C \equiv C - R_2$

$R_1 = (CH_2)_n COOH$ $\quad n=0, 8$

$R_2 = CH_2 - (CH_2)_m CH_3$ $\quad m=10,\ldots,15$

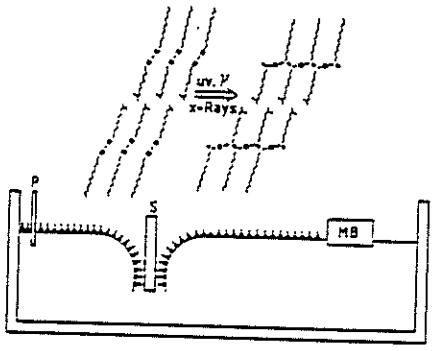

P-pressure sensor MB - mobile barrier S - substrat

Transfer layer by layer of monomer film
Polymerisation of monomer film by UV, , X-Ray radiation

Polymerisation of the monomer film on water subphase
Transfer of polymer monolayer ~30Å thick on a substrat

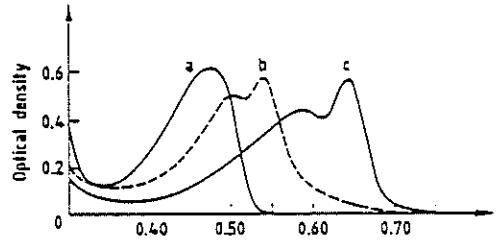

Optical absorption spectra of different diacetylene polymers:

a - yellow form (polymer solution oremorphous phase)

b - red form (stable)

c - blue form

H-3

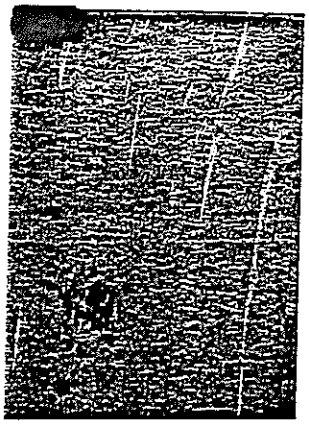

Electron micrograph of a polydiacetylene monolayer

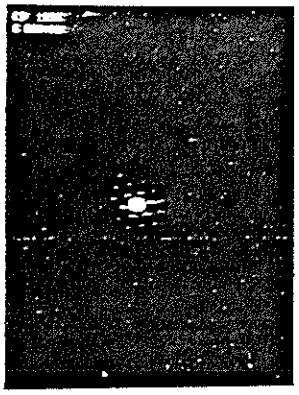

Electron diffraction patterns of a polydiacetylene monolayer

PRINCIPAL PROPERTIES OF LB FILMS

- Centrosymetric thin films with controllable thickness (each layer ~ 30Å thick)
- Thickness limited to a few thousand of Ångstroms
- Two-dimensional order
- Films composed from polycrystallites
  large light scattering

SOLUTION CASTING

Soluble polymers

$$R_1 - C \overset{\nearrow}{\underset{\searrow}{=}} C - C \equiv C - C \overset{\nearrow}{\underset{\searrow}{=}} C - R_2$$

3-BCMU $R_1=R_2=(CH_2)_{13}OCONHCH_2COOC_3H_9$

4-BCMU $R_1=R_2=(CH_2)_{14}OCONHCH_2COOC_3H_9$

TS-12 $R_1=R_2=(CH_2)_4OSO_2C_6H_4CH_3$

Thin films with thickness varying from a few thousands ångstrom to a few tens of microns

Crystallites - large light scattering

Large surface roughness - light scattering by surface

Surface light scattering effects in solution cast 4-BCMU film (red form)

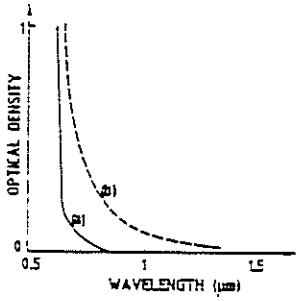

Tail of optical absorption spectrum of a 50 μm thick native 4-BCMU film (b) and after an annealing at 400° C under vacuum and a simultaneous sealing of a silica plate on free film face (a).

H-4

DIPPING TECHNIQUE

from a polymer solution

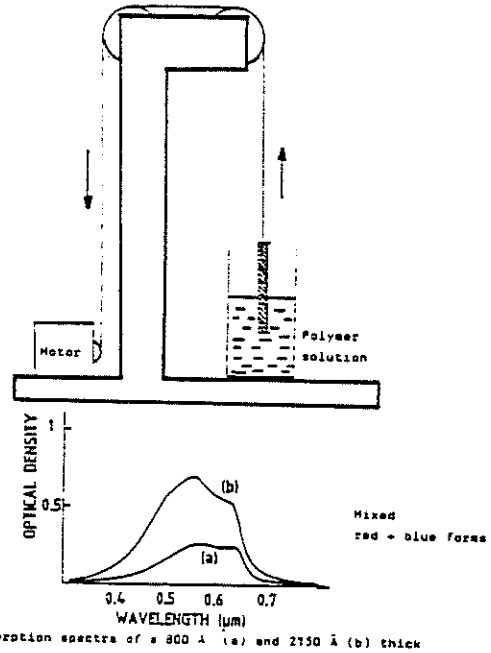

Absorption spectra of a 800 Å (a) and 2750 Å (b) thick polymer films obtained by dipping technique from 3-BCMU solution in $CHCl_3$.

MONOMER EVAPORATION TECHNIQUE SUBLIMATION

High vacuum $\sim 10^{-6}$ Torr

Works for practically all DA monomers delicate in the case of monomers polymerising thermally like TS-n PTS, DCH

Yields homogenous thin films with thickness varying from a few hundreds to a few tens of microns.

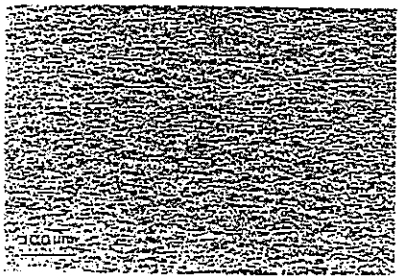

Electron micrograph of a poly-DCH $R_1R_2CH_2NC_6H_5$ thin film showing an isotropic orientation of crystallites.

Light scattering by crystallites - this can be reduced by a cooling of substrate (diminution of the crystallites size).

EPITAXY

KBr single crystal substrate

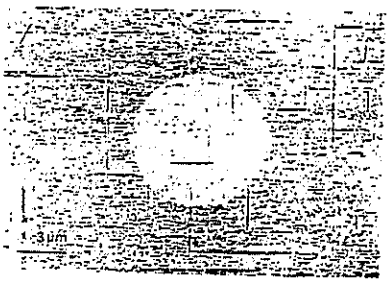

Electron micrograph of a bi-oriented pDCH film (250 Å) evaporated on KBr single crystal substrate

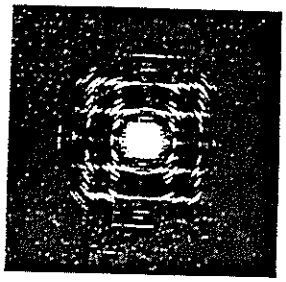

Electron diffraction of a central part of bi-oriented 250 Å thick p-DCH film

THIRD HARMONIC GENERATION EXPERIMENTS

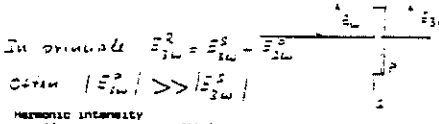

Harmonic intensity (for a transparent film)

$$J_{3\omega} = \frac{2304\pi^4}{C^2}\left(\frac{\chi^{(3)}}{(n_\omega^2 - n_{3\omega}^2)}\right)^2\left(\frac{l}{\lambda_\omega}\right)^2 |A|^2 J_\omega^3$$

does not depend on the refractive index dispersion "phase matching"

For an absorbing film at harmonic frequency

$$J_{3\omega} = \frac{2304\pi^4}{C^2}\chi^{(3)2}|A|^2 J_{3\omega}^3 f_\lambda \qquad f_\lambda = \frac{(1-\exp(-\alpha_{3\omega}l/2))^2 + 4\exp(-\alpha_{3\omega}l/2)\sin^2(\Delta\varphi/2)}{[(n_{3\omega}^2 - n_\omega^2)^2 + k_{3\omega}^2 k_\omega^2]^{1/2}[(n_{3\omega}^2 - n_\omega^2)^2 + (k_{3\omega}^2 - k_\omega^2)^2]^{1/2}}$$

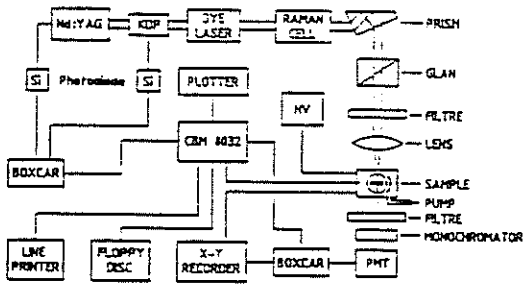

Experimental set-up for third harmonic generation measurements.

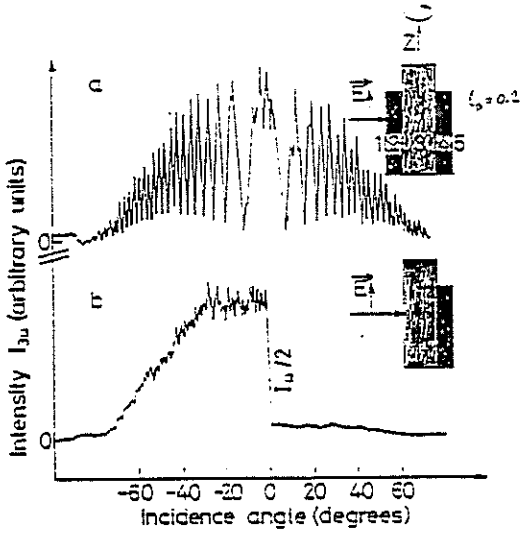

Third harmonic intensity from an .8 PVA film in function of rotation angle.

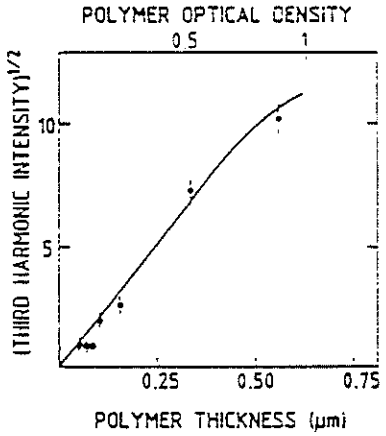

$\chi^{(3)}(-3\omega;\omega,\omega,\omega)$ phase determination

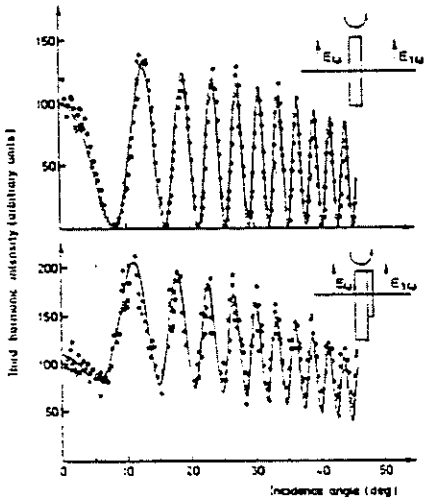

FIG. 4. Third harmonic intensity as function of incidence angle for (a) silica plate and (b) silica plate + polymer film in vacuum. Points represent measured values and solid lines the calculated ones with tabulated values of refractive indices for silica.[7]

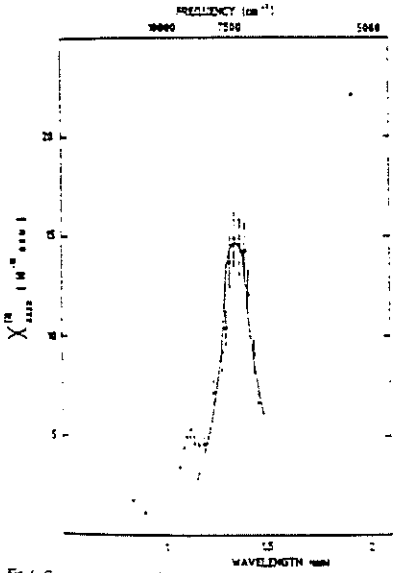

Fig. 5. Cubic susceptibility [illegible] corrected for crystal absorber, as a function of the third fundamental wavelength. The continuous line is a least-squares fit as described in the text.

H-6

ELECTRIC FIELD INDUCED OPTICAL SECOND HARMONIC GENERATION

Polydiacetylenes - centrosymmetric structure

no second harmonic generation

By applying an external DC field

centrosymmetry broken

second harmonic generation

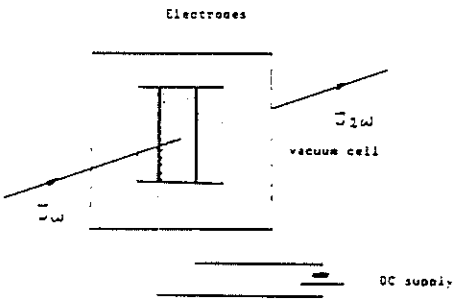

Comparison with a single crystal quartz standard (Q)

$$\langle \chi_{zzz}^{(3)}(-2\omega;\omega,\omega,0)\rangle = \frac{2\,l_2}{3\varepsilon\,l_1\,\delta_{ac}} \times \frac{1.13\,DD_{(\omega)}}{1+\exp(-1.13\,DD_{(2\omega)})} \frac{n_3}{n_1} \left(\frac{n_1+n_2}{n_2+n_3}\right)^2 \chi_Q^{(2)}(2\omega;\omega,\omega)$$

(e.s.u.)

f - polymer film

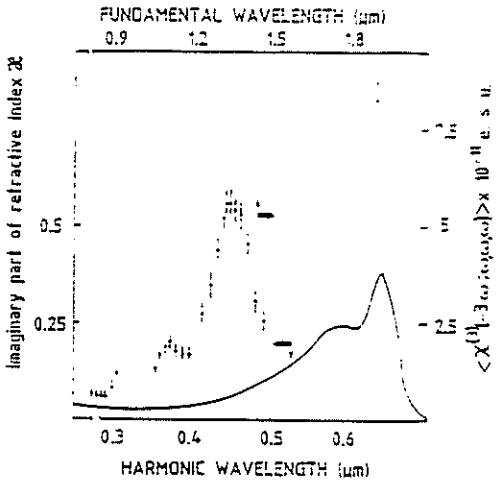

C_{16-5} LB film - blue form

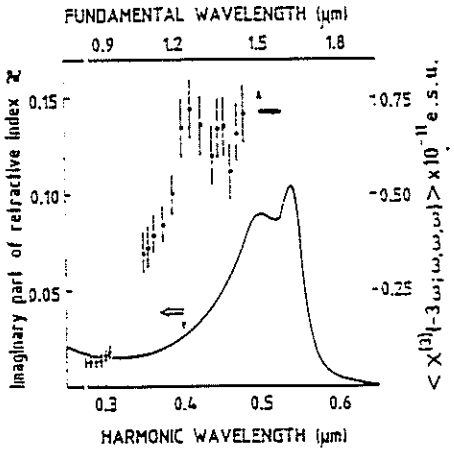

C_{16-5} LB film - red form

Evaporated under vacuum films

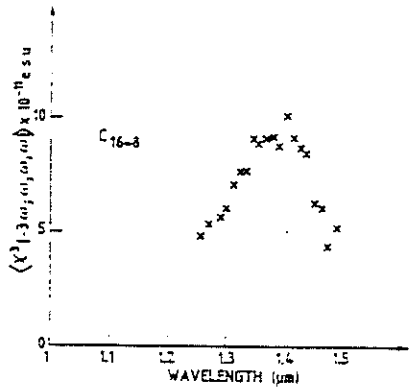

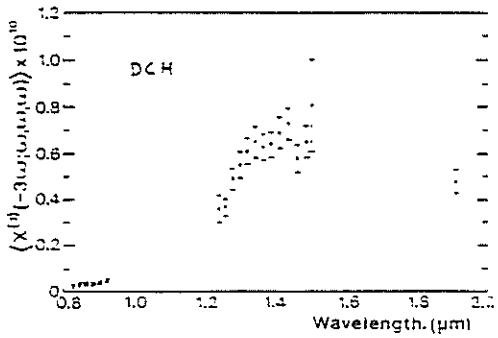

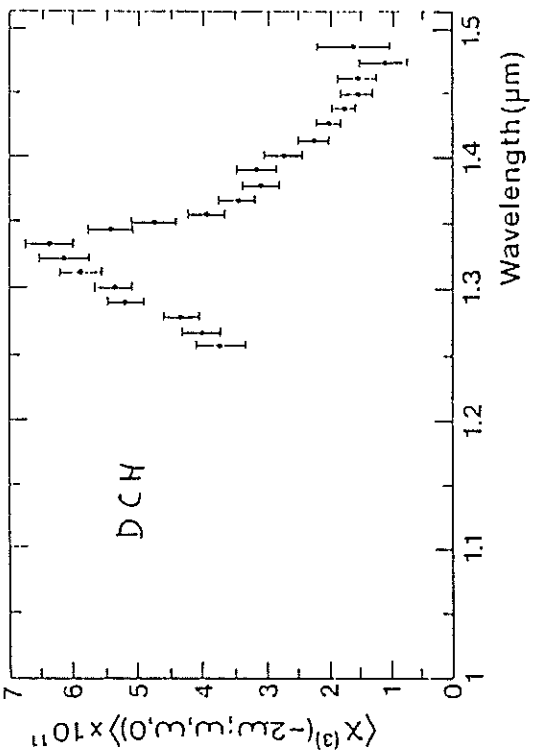

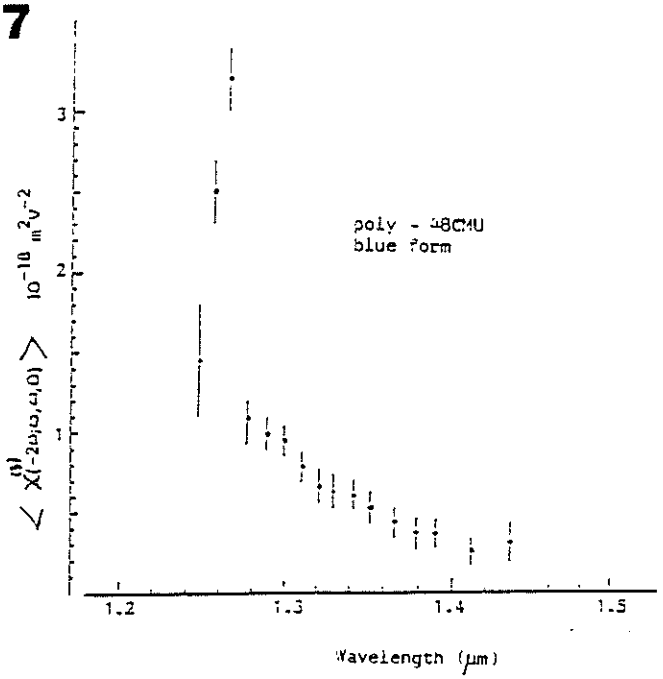

Tensor elements contributing to $\chi^{(3)}(-3w;w,w,w)$ (THG)

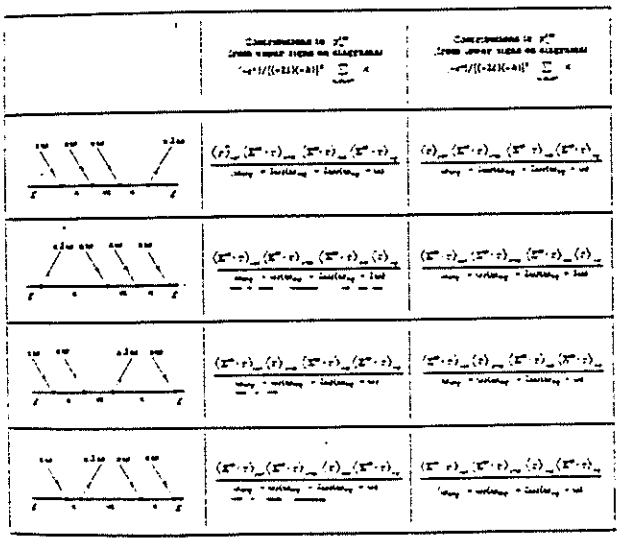

J. F. Ward , Rev. Mod. Phys., 37, 1(1965)

Tensor elements contributing to $\chi^{(3)}(-2w;w,w,0)$ (EFISHG)

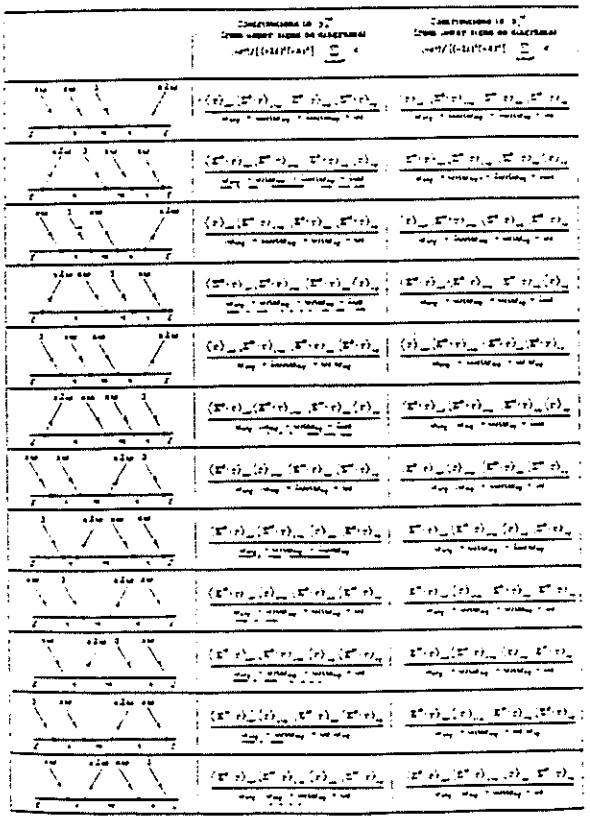

J. F. Ward, Rev. Mod. Phys., 37, 1(1965)

- two photon resonance
- two photon resonance with a (same symmetry as fundamental) level
- three photon resonance
- one photon resonance

H-8

Tensor elements contributing to optical Kerr susceptibility $\chi^{(3)}(-w;w,w,-w)$

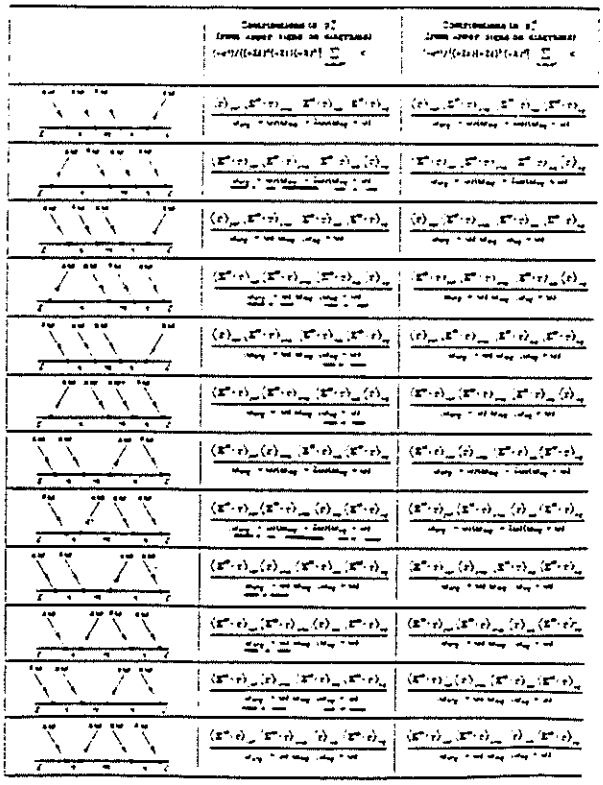

J.F. Ward, Rev. Mod. Phys. 37,1(1965)

—— - two photon resonan

- . - one photon resonan

Intensity dependent index of refraction

$$n = n_0 + n_2 I^{\omega}$$

$$n_2 = 12\pi^2 \chi^{(3)}(-\omega;\omega,\omega,-\omega)/n_0^2 c$$

At two photon resonance - $\chi^{(3)}(-3w;w,w,-w)$ complex

↓

active optical bistability

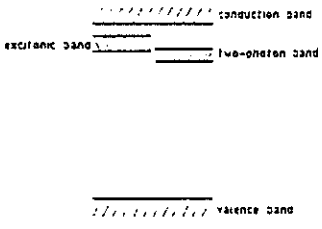

Band structure of the PDA multilayers.

Temperature variation of $\chi^{(3)}(-3w;w,w,-w)$

T=7K

resonance narrowing

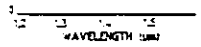

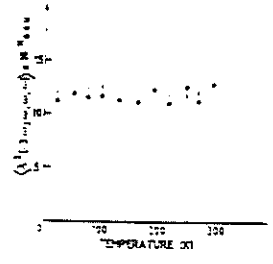

Constancy of $\chi^{(3)}(-3w;w,w,-w)$ vs temperature - excitonic origin of cubic hyperpolarisability (phase space filling model -Schmitt-Rink et al Phys. Rev. B32(1985)

H-9

NONLINEAR OPTICAL DICHROISM

Enhanced $\chi^{(3)}$ -/w/w/w/w e.g. in direction of polymer chain

θ = angle between incident electric field and polymer chain

Harmonic intensity

$$I_{3\omega} \sim \cos^{8}\theta \; I_{\omega}^{3}$$

Example: epitaxied OCH thin film

Bi-axe orientation of polymer chains mutually perpendicular.

In linear optics (crossed polarizers, linear optics, dichroism

$$I_{\perp} = I_{\omega}\left[\cos^2\theta \cdot \cos^2(90°-\theta)\right] = I_{\omega}$$

In THG experiments

$$E_{3\omega} = A(\cos^3\theta - \sin^3\theta)\, E^3_{\omega} \qquad \text{Harmonic field}$$

$$I_{3\omega} \propto |E_{3\omega}|^2 = |A|^2 \,(\cos^3\theta - \sin^3\theta)^2\, I_{\omega}^3 \qquad \text{Harmonic intensity}$$

θ = angle between incident electric field and polymer chain.

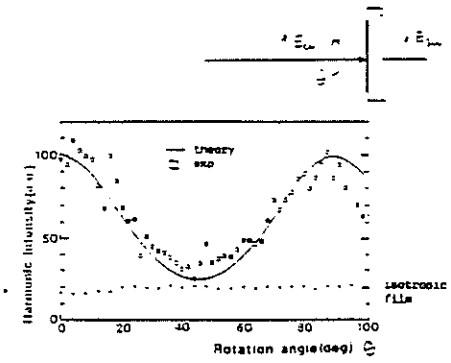

Third harmonic intensity from a bi-oriented p-OCH thin film obtained by epitaxy on a KBr single crystal substrate.

POLARIZATION EFFECTS

LB film

"Y-type" LB film $R = C-C\equiv C-C-$

$Z = (CH_2)_8 \; COO\,Cd_{1/2}$ $Z' = (CH_2)_{15}\,CH_3$

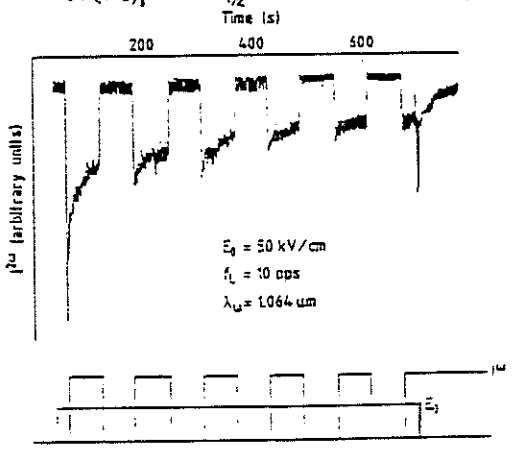

Decrease of SH intensity due to an internal polarization creation of e-h pairs and their separation in external DC field

H-10

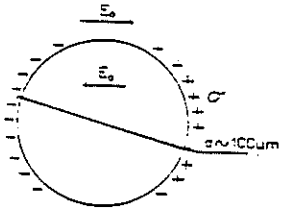

Setting of the internal polarization by charge drainage at the laser spot boundaries.

CONCLUSIONS

ADVANTAGES

Large $\chi^{(3)}$ with fast response time (< 25 ps)
Two photon resonance in telecommunications window (1.3 - 1.6 µm)
Active optical bistability
Logic systems
Thin film feasibility by different techniques
Oriented thin films
Epitaxy
Optical gap and physico-chemical properties can be modified by a choice of side groups

PROBLEMS

Light scattering
Amorphous thin films (?)
Photodecomposition
Chemical stability (PTS)
Blue-red transformation (in some cases)

COWORKERS

Jean MESSIER	- chief of the laboratory
Pierre-Alain CHOLLET	
Dominique GREC	
Jean-Michel MUNZI	
Fabrice CHARRA	- graduate student
Jacques BANIDE	
Roger GRAS	- technical staff
André LORIN	

EXTERNAL COLLABORATIONS

Isabelle LEDOUX	
Joseph ZYSS	CNET Bagneux
Alain BOUDET	CNRS Toulouse
Jacques LEMOIGNE	
Anne THIERRY	CRM Strasbourg
Shahab ETEMAD	Bellcore
Lewis ROTHBERG	AT&T Murray Hill
Michel DUMONT	
Jean-Claude LOULERGUE	Institut d'Optique Orsay
Yves LEVY	
Gerhard WEGNER	MPI Mainz

Y. R. Shen

University of California at Berkeley

NONLINEAR OPTICAL MEASUREMENTS ON LIQUID CRYSTALS AND QUASI-LIQUID CRYSTALS

Optical Nonlinearities of Liquid Crystals and Quasi-Liquid Crystals

Motivation:

- Liquid crystal molecules are highly nonlinear
- Existence of many liquid crystals with different molecular structures
- Dependence of nonlinearities on molecular structure

Gary Buskovic
Theo Rasing

Technique for measuring $\overleftrightarrow{\alpha}^{(2)}$

SHG from molecular monolayer spread on water

$$\chi^{(2)}_{ijk} = N L_{ii} L_{jj} L_{kk} \langle G^{\alpha\beta\gamma}_{ijk}(\Omega) \rangle \alpha^{(2)}_{\alpha\beta\gamma}$$

If $\Omega \equiv \theta$ and L's are known, then the n elements of $\overleftrightarrow{\alpha}^{(2)}$ can be deduced from measurements of $n+1$ independent components of $\overleftrightarrow{\chi}^{(2)}$.

Advantages:

1. Molecular density can be a variable.
2. Local field effect could be less important.

Disadvantages:

1. Not all molecules are spreadable on water.
2. Molecules could interact with water.

ALKYL-CYANO-(POLY)-PHENYLS

I 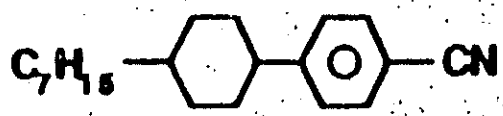

II 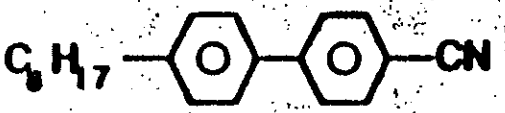

III 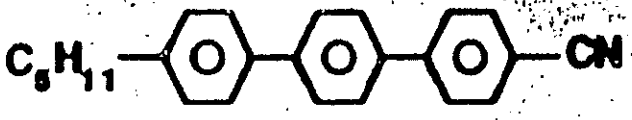

ALKYL-CYANO-PHENYLPYRIMIDINES

IV 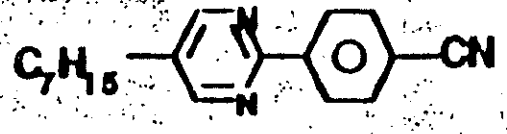

V 

ALKOXY-CYANO-BIPHENYL

VI 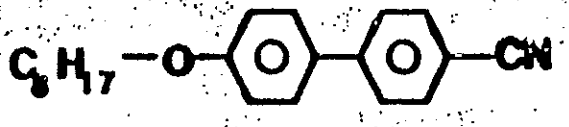

14

TABLE 1 Second order polarizabilities, $\alpha_{zzz}^{(2)}$, for molecules I - VI. θ_0 is the average orientation angle of the molecular long axis to the surface normal, as calculated from the SHG data.

	$\lvert\alpha_{zzz}^{(2)}\rvert$ (10^{-30} esu)		θ_0 (°)
	at 2ω resonance	at 1.06 μm	
I	4	a	80 ± 10
II	25	3	71 ± 2
III	13	a	60 ± 2
IV	8	a	79 ± 3
V	8	a	82 ± 4
VI	40	5	78 ± 2

Results:

1. $\alpha^{(2)} \sim 10^{-29}$ esu
2. CN is a better electron donor than COOH.
3. Interruption of electron delocalization decreases $\alpha^{(2)}$
4. Triphenyl is worse than biphenyl presumably because of twist between phenyl rings.

Nonlinearities of Hemicyanine Dyes and the Environmental Effect

G. Marowsky
L. F. Chi
D. Möbius
R. Steinhoff
D. Dorsch
B. Rieger

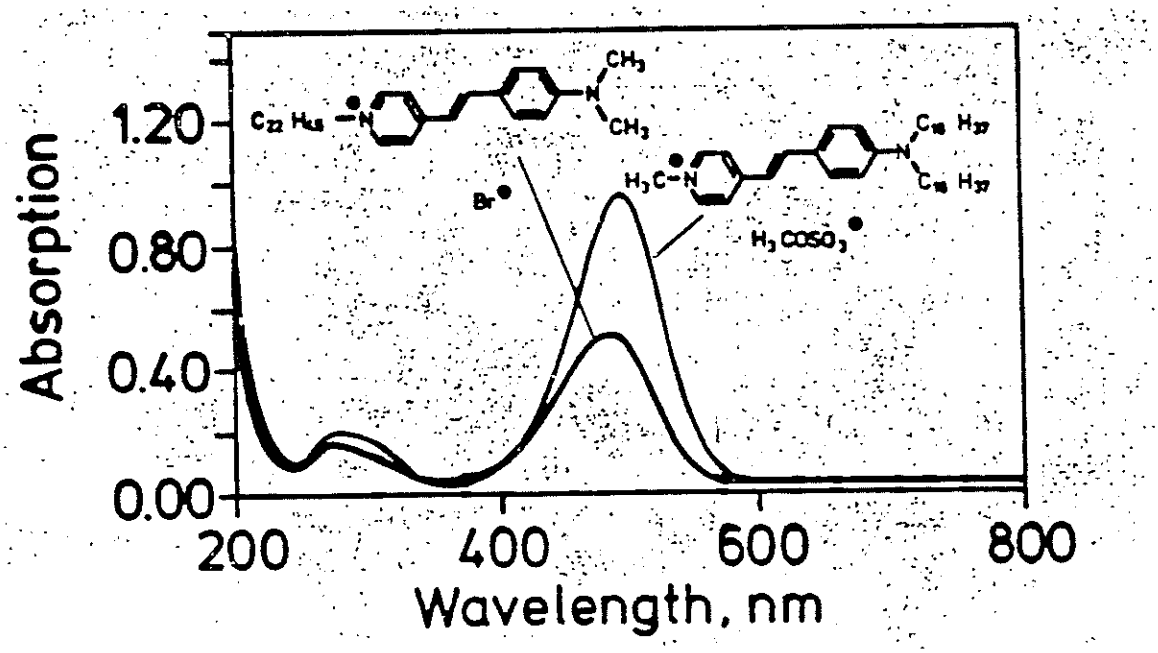

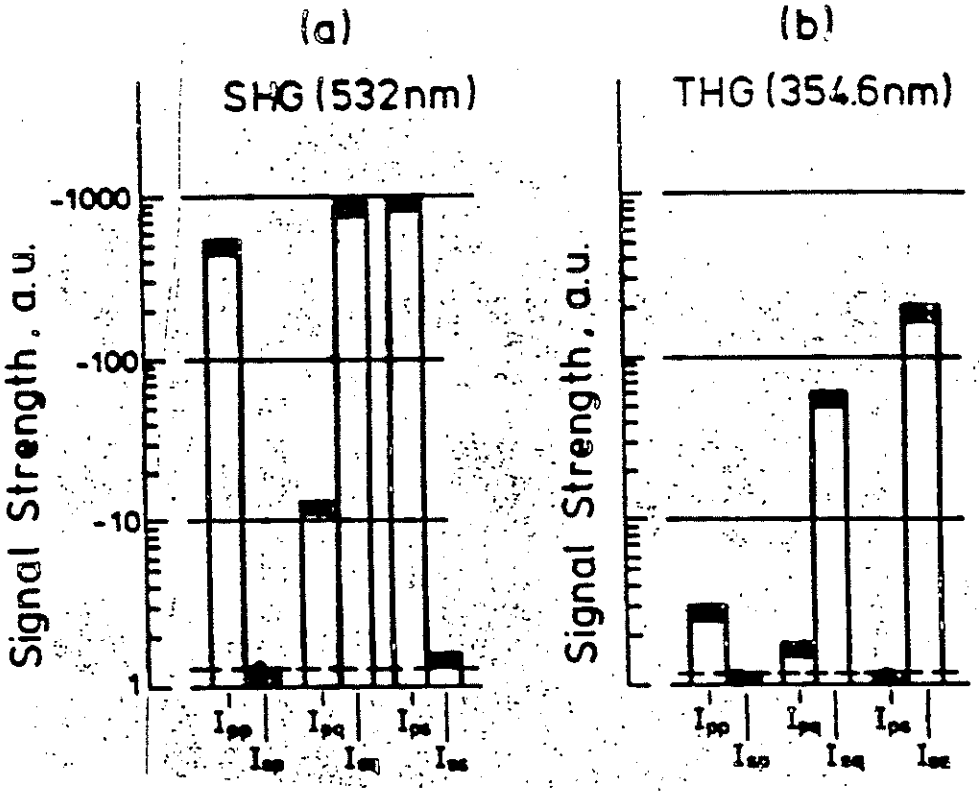

Marowsky, Chi, Möbius, Steinhoff, Shen, Dorsch, Rieger: Nonlinear Optical Properties ...
Fig. 2

Effects of Protonation.

1. Suppresses charge-transfer absorption
2. Drastically reduces $\chi^{(2)}$.
3. $\chi^{(2)} \propto$ Charge-transfer absorption
   $\propto N_{\text{Unprotonated}}$
4. UV absorption band has little effect on $\chi^{(2)}$.

Marowsky, Chi, Möbius, Steinhoff,
Shon, Dorsch, Rieger: Nonlinear
Optical Properties ...

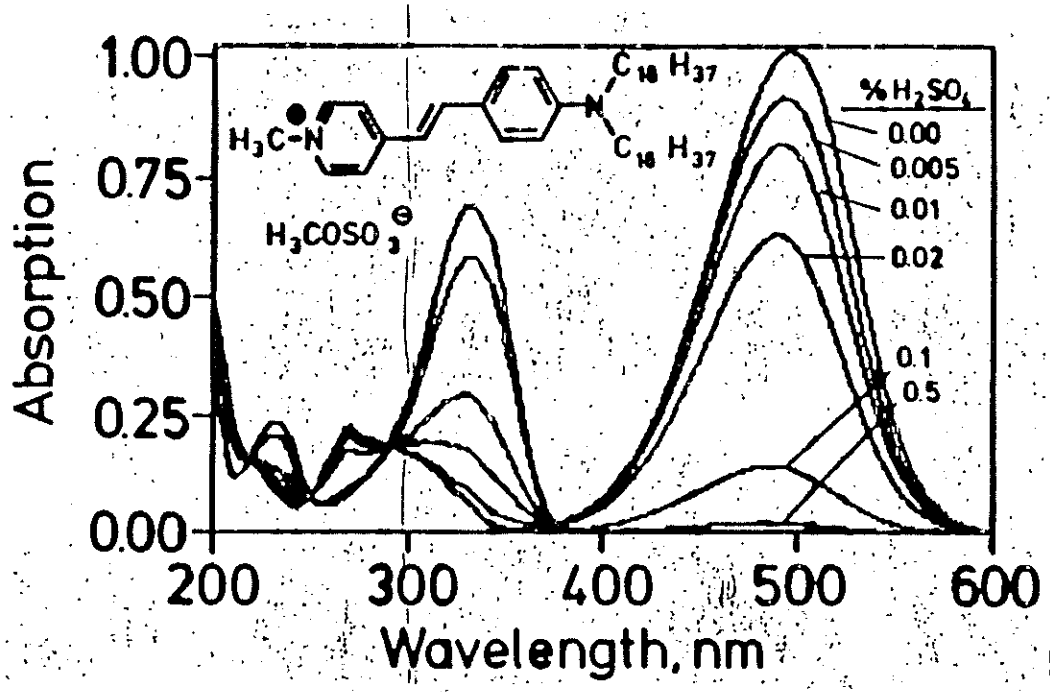

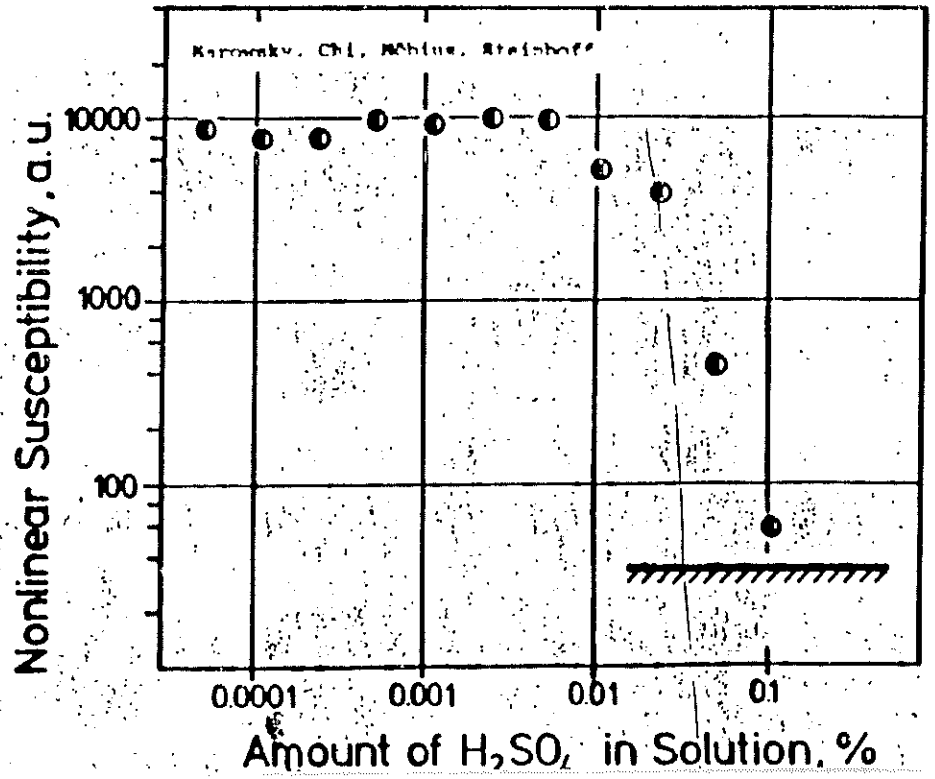

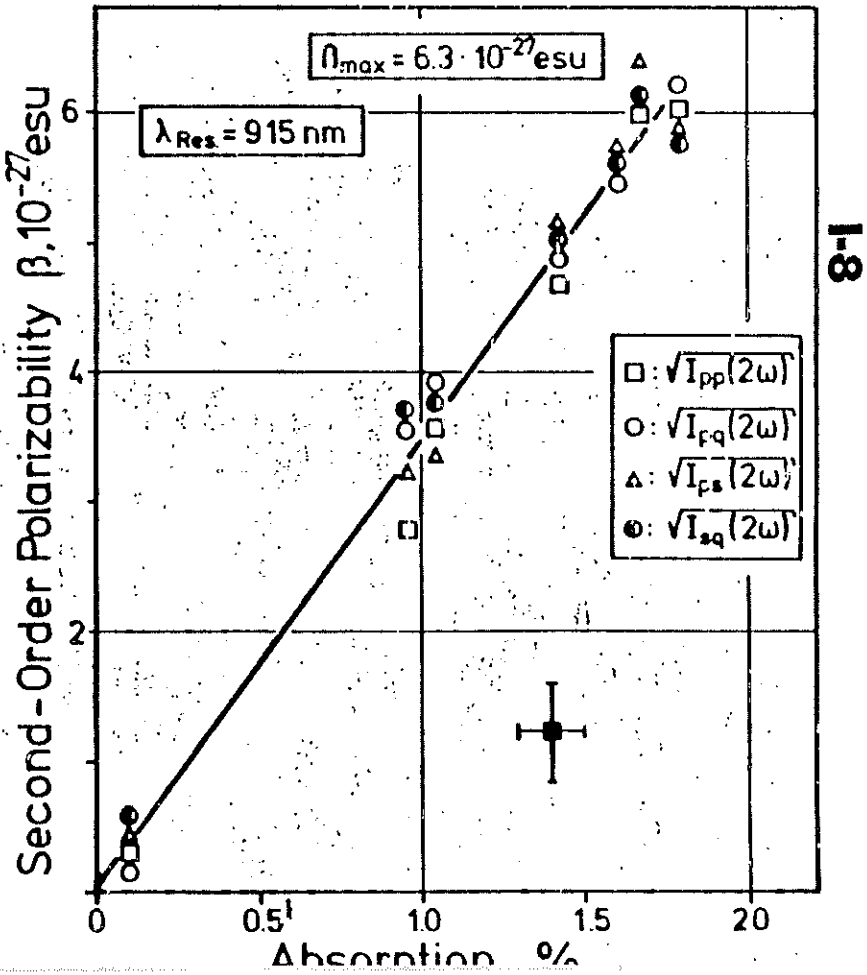

I-8

Poling

on

Quasi Liquid Crystal Films

H. Hsiung
T. Rasing
F.P. Shvartzman
I.R. Cabrera
V.A. Krongauz

Theory of Poling.

Assume $\overleftrightarrow{\alpha}^{(2)}$ and $\vec{p}$ dominated by $\alpha^{(2)}_{zzz}$ and p_z. $\vec{E}$ along $\hat{x}$.

$$\chi^{(2)}_{xxx} \propto \alpha^{(2)}_{zzz} \langle \cos^3\theta \rangle$$

$$\chi^{(2)}_{yyx} \propto \alpha^{(2)}_{zzz} [\langle \cos\theta \rangle - \langle \cos^3\theta \rangle]$$

$$\langle \cos^n\theta \rangle = \int_{-1}^{1} \cos^n\theta \, e^{-V/kT} d(\cos\theta) / Z$$

$$V = V_N - u\cos\theta - pE\cos\theta$$

$$V_N = -u_2 P_2(\cos\theta) - u_4 P_4(\cos^4\theta) - \cdots$$

$$\langle \cos^n\theta \rangle \cong \int_{-1}^{1} \cos^n\theta \left(1 + \frac{u + pE}{kT}\cos\theta\right) e^{V_N/kT} \times d(\cos\theta) / Z_N$$

$$= \langle \cos^n\theta \rangle_0 \qquad n \text{ even}$$

$$= \frac{u + pE}{kT} \langle \cos^{n+1}\theta \rangle_0 \qquad n \text{ odd}$$

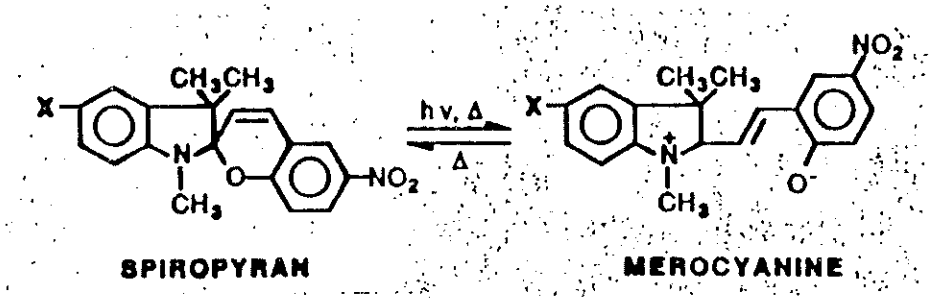

$\langle \cos^2\theta \rangle = \langle \cos^2\theta \rangle_0$ indep of E

$\langle P_2(\cos\theta) \rangle = \frac{1}{2}(3\langle \cos^2\theta \rangle - 1) = \langle P_2(\cos\theta) \rangle_0$

$\equiv S$

obtained from birefringence

$\langle \cos\theta \rangle = \langle \cos^2\theta \rangle_0 \left(\frac{u + pE}{kT}\right)$

$\langle \cos^3\theta \rangle = \langle \cos^4\theta \rangle_0 \left(\frac{u + pE}{kT}\right)$

$\chi^{(2)}_{xxx} \propto \langle \cos^4\theta \rangle_0 \left(\frac{u + pE}{kT}\right)$

$\chi^{(2)}_{yyx} \propto [\langle \cos^2\theta \rangle_0 - \langle \cos^4\theta \rangle_0] \left(\frac{u + pE}{kT}\right)$

Measurements of $\chi^{(2)}_{xxx}$ and $\chi^{(2)}_{yyx}$ versus E allow the determination of $\langle \cos^4\theta \rangle_0$, u, and p.

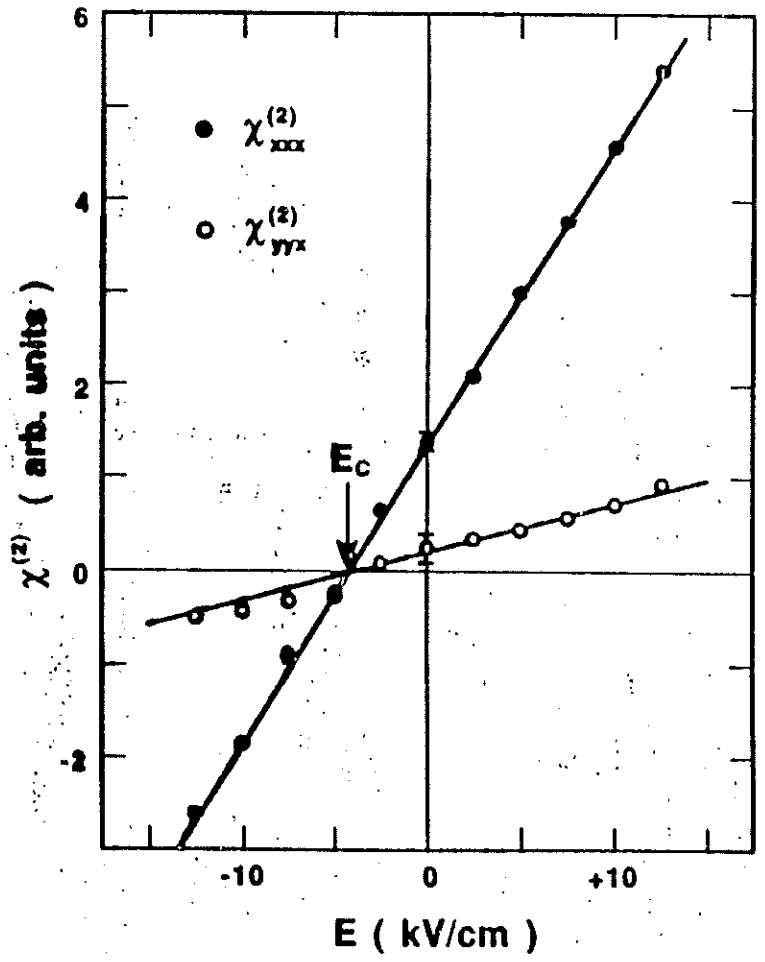

D. J. Gerbi

3M Co.

NONLINEAR OPTICAL EFFECTS IN CONJUGATED SYSTEMS

SECOND ORDER NONLINEAR OPTICAL EFFECTS IN CONJUGATED SYSTEMS

DIANA GERBI

G. T. BOYD

D. A. ENDER

R. M. HENRY

K. K. KAM

P. C. W. LEUNG

J. J. STOFKO

ADVANCED OPTICAL MATERIALS
SCIENCE RESEARCH LABORATORY
3M CORPORATE RESEARCH LABORATORIES

ADVANCED OPTICAL MATERIALS PROGRAM (ORGANIC-BASED DEVICES)

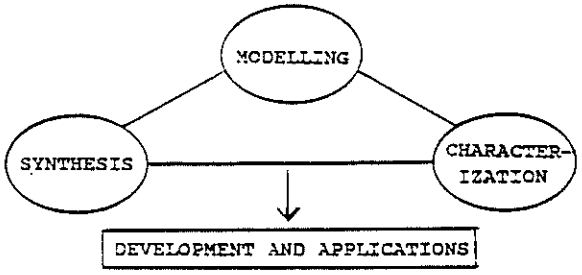

- IDENTIFY CANDIDATE MATERIALS
- UNDERSTAND AND MAINTAIN MOLECULAR ORDER
- DETERMINE APPLICATIONS OF MATERIALS. FEASIBILITY IN DEVICES

$\chi^{(2)}$

OPTICAL COMMUNICATIONS

FIBER OPTICS LAB
TELCOMM
3M DORRAN
EOTEC

SENSORS

FIBER OPTICS LAB

$\chi^{(3)}$

OPTICAL SIGNAL PROCESSING

INFORMATION AND IMAGING TECHNOLOGIES

OPTICAL SIGNAL PROCESSING
OPTICAL SENSOR PROTECTION

AFOSR

OUTLINE

I. REVIEW OF SECOND ORDER NONLINEAR OPTICS, CHARACTERIZATION METHODS AND DEVICE CONFIGURATIONS

II. ADVANTAGES OF ORGANIC NONLINEAR OPTICAL MATERIALS

III. MATERIALS PROCESSING/APPLICATIONS

IV. ELECTRO-OPTIC MATERIALS - CRYSTALS AND POLED POLYMER SYSTEMS

MACROSCOPIC POLARIZATION:

$$P_i = P_{o_i} + X^{(1)}_{ij} E_j + X^{(2)}_{ijk} E_j E_k + X^{(3)}_{ijkl} E_j E_k E_l \cdots$$

MICROSCOPIC POLARIZATION:

$$p_i = p_{o_i} + \alpha_{ij} E_j + \beta_{ijk} E_j E_k + \gamma_{ijkl} E_j E_k E_l \cdots$$

REVIEW OF SECOND ORDER NONLINEAR OPTICAL EFFECTS

ELECTRO-OPTIC EFFECT:

Index of refraction changes with applied voltage

$$n = n_o + \Delta n(E)$$

$$\Delta n \propto X^{(2)}$$

SUM FREQUENCY GENERATION:

Output frequency = sum of input frequencies

$$w(out) = w_1 + w_2$$

SHG: $I(2w) \propto [X^{(2)}]^2 [I(w)]^2$

DIFFERENCE FREQUENCY GENERATION:

Output frequency = difference of input frequencies

$$w(out) = w_1 - w_2$$

CHARACTERIZATION METHODS
FOR
SECOND ORDER NONLINEAR OPTICAL MATERIALS

POWDER SHG

SINGLE CRYSTAL SHG

EFISH

POLYMER POLING

ELECTRO-OPTIC EFFECT

POWDER SHG

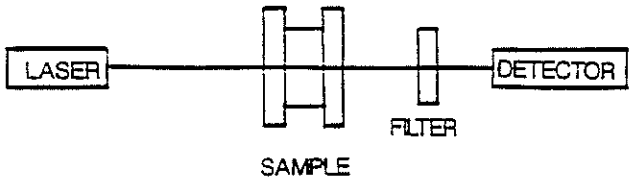

$$\eta = \frac{I(2w)sample}{I(2w)urea}$$

MATERIAL FORM: MICROCRYSTALLINE POWDER

ADVANTAGES: USEFUL FOR SCREENING

DISADVANTAGES: CANNOT RESOLVE MICRO- AND MACROSCOPIC CONTRIBUTIONS TO NONLINEARITY

EFISH

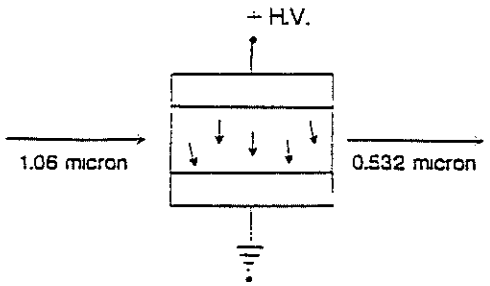

MATERIAL FORM: SOLUTION (LOW POLARITY SOLVENTS)

ADVANTAGES: OBTAIN MOLECULAR PROPERTIES, COMPARISONS

DISADVANTAGES: MOLECULAR PROPERTIES ARE SUBJECT TO ENVIRONMENT

SINGLE CRYSTAL SHG

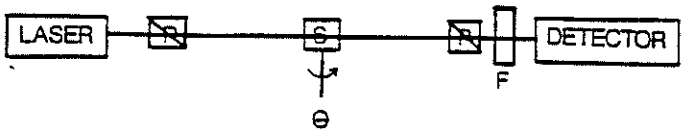

MAKER FRINGE

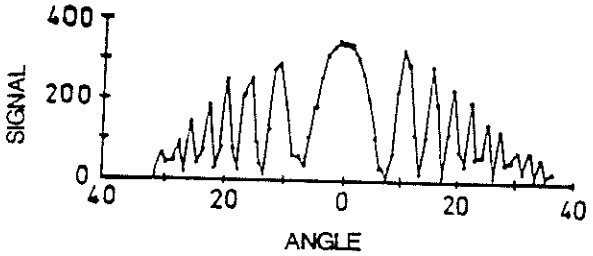

MATERIAL FORM: LARGE SINGLE CRYSTAL (mm to cm)

ADVANTAGES: MEASURES TENSOR ELEMENTS $X^{(2)}_{ijk}$

DISADVANTAGES: REQUIRES CRYSTAL ORIENTATION, INDICES OF REFRACTION, POLISHING

POLYMER POLING

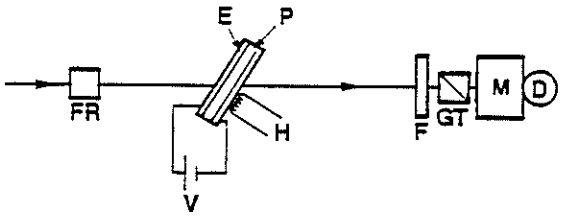

Figure 2. Experimental set-up for thin film SHG measurement using Fresnel rhomb FR, transparent electrodes E, polymer film P, poling voltage V, heater H, color filter F, Glan-Thompson prism GT, monochromator M and detector D.

MATERIAL FORM: POLYMER SYSTEM

ADVANTAGES: REAL LIFE ENVIRONMENT, EASY SIGNAL DISCRIMINATION

DISADVANTAGE: NOT A DIRECT MEASUREMENT FOR E-O

ELECTRO-OPTIC EFFECT

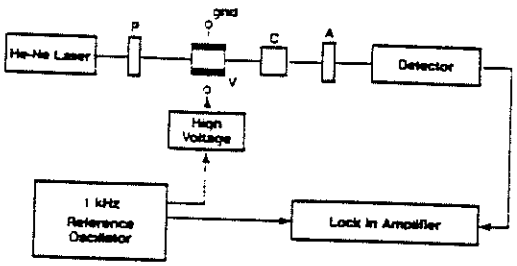

Figure 1. Experimental set-up for electro-optic measurement using polariser P, analyzer A, and Babinet-Soleil compensator C.

MATERIAL FORM: POLYMER SYSTEMS, CRYSTALS

ADVANTAGES: DIRECT MEASUREMENT (DEVICE FORM)

DISADVANTAGES: LESS SENSITIVE THAN SHG
NOT AN IN-SITU TEST
CRYSTALLOGRAPHIC ORIENTATION FOR CRYSTALS

ADVANTAGES OF ORGANIC MATERIALS

- SYNTHETIC TAILORABILITY VIA DELOCALIZATION/SUBSTITUENTS
- SUBPICOSECOND RESPONSE TIMES
- TRANSPARENCY
- MECHANICAL AND STRUCTURAL STABILITY
- HIGH RADIATION DAMAGE THRESHOLD
- ENVIRONMENTAL STABILITY
- PROCESSABILITY
- ROOM TEMPERATURE OPERATION OF DEVICES

MATERIALS PROCESSING

SPIN-COATED POLYMERS

e.g. CHANNEL WAVEGUIDES

- REQUIRES LOW LOSS (<1 dB/cm)
- REPRODUCIBLE, WELL-KNOWN TECHNIQUES AVAILABLE
- INDUCE ORDER RATHER THAN RELY ON CRYSTAL PACKING

CRYSTALS

e.g. BULK CRYSTALS
CHANNEL WAVEGUIDES
VAPOR DEPOSITED FILMS

- REQUIRES LOW LOSS (<1 dB/cm)
- BULK CRYSTALS MUST BE DURABLE ENOUGH FOR CUTTING AND POLISHING
- COMPLETE CRYSTALLOGRAPHIC ORIENTATION IS REQUIRED
- PRINCIPAL OPTIC INDICES AND AXES RELATIVE TO EXTERNAL MORPHOLOGY MUST BE DETERMINED

SECOND HARMONIC GENERATION APPLICATIONS

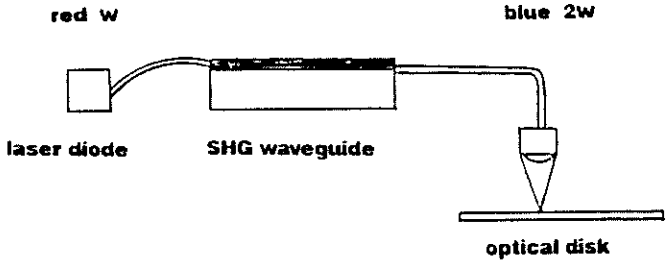

doubling optical frequency gives 4x storage density

APPLICATIONS — ELECTRO-OPTIC EFFECT

modulator

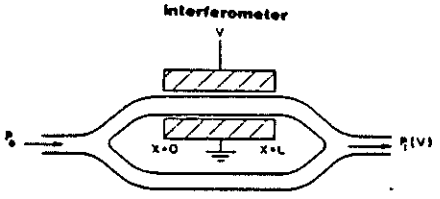

directional coupler

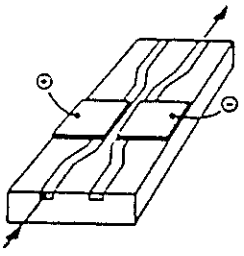

ELECTRO-OPTIC PHASE SHIFTER

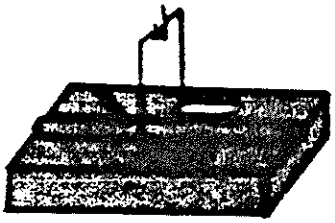

MODULATOR, GYRO

* COMPARE $LiNbO_3$

λ = 850 nm

Insertion loss 6dB

BW = 3 GHz

V_π = 5V (4 cm)

Room Temperature

ELECTRO-OPTIC PHASE SHIFTER

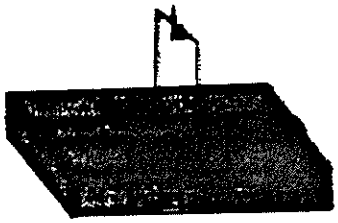

[illegible] CRYSTAL

$$\chi_{33}^{(2)} = \frac{\lambda n_e d}{2V_\pi L}$$

$\chi_{33}^{(2)} \approx 3 \times 10^{-7}$ esu $\approx 30 \cdot \chi^{(2)}$ (urea)

POLED POLYMER

$\chi^{(2)} = c\, N\, \mu\beta\, E$ N = 1 Molar

E = 0.4 MV/cm

$\Rightarrow \mu\beta \sim 50 \cdot \mu\beta$ (DNA)

$A < 0.1/cm$ (1 dB/cm)

HALONITROANILINES	RELATIVE EFFICIENCY (UREA)	μ (DEBYE
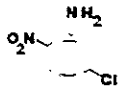	20	4.471
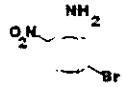	≤0.001	—
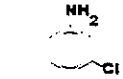	≤0.001	9.403
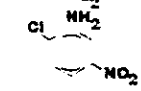	≤0.001	4.433
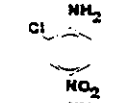	2	7.722
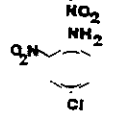	0.03	5.281
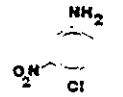	≤0.001	8.023

MATERIAL	SPACE GROUP	a	b	c	α	β	γ	Z
5-chloro-2-nitroaniline (phase I)	$Pna2_1$	30.844 Å	3.852 Å	6.004 Å	90°	90°	90°	4
5-bromo-2-nitroaniline (5-chloro-2-nitroaniline) (phase II)	$P\bar{1}$	7.344	7.844	7.091	97.95	116.69	83.23	2
2-chloro-4-nitroaniline*	$Pna2_1$	11.25	16.85	3.87	90	90	90	4
3-chloro-4-nitroaniline	$P2_1/C$	3.813	12.531	14.467	90	91.20	90	4

* A. T. McPhil and G. A. Sim, J. Chem. Soc., 227 (1965)

MOLECULAR MODELLING

HOMO

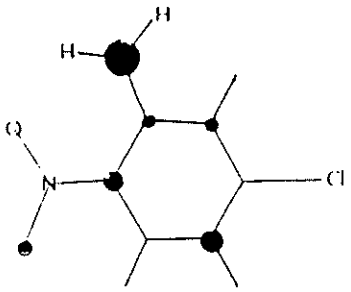

LUMO

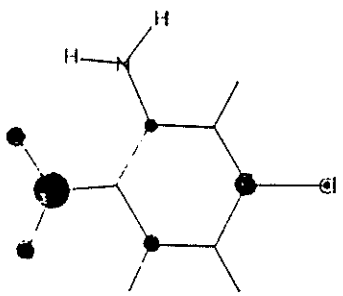

$\beta \propto$ difference in ground state and excited state dipole moments

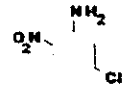

5-CHLORO-2-NITROANILINE

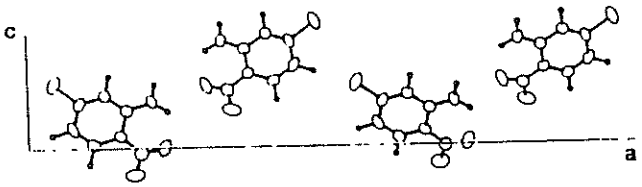

a = 30.844 Å
b = 3.852
c = 6.004

SPACE GROUP
$Pna2_1$

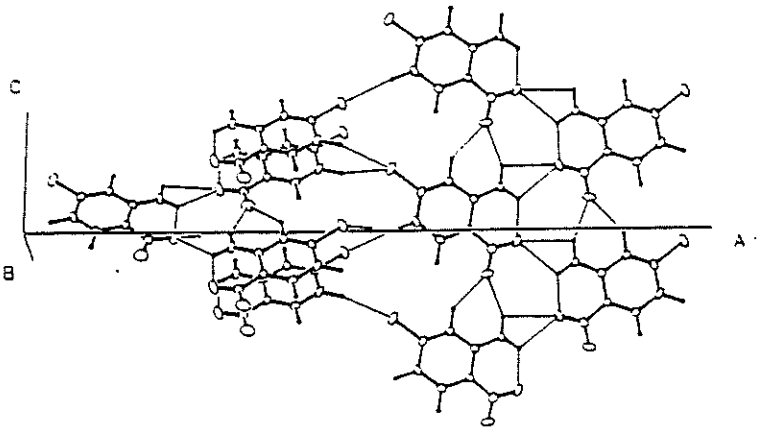

Figure 4. An illustration of the crystal structure of 5-chloro-2-nitroaniline. Significant intra- and intermolecular hydrogen bonding indicated by thin lines.

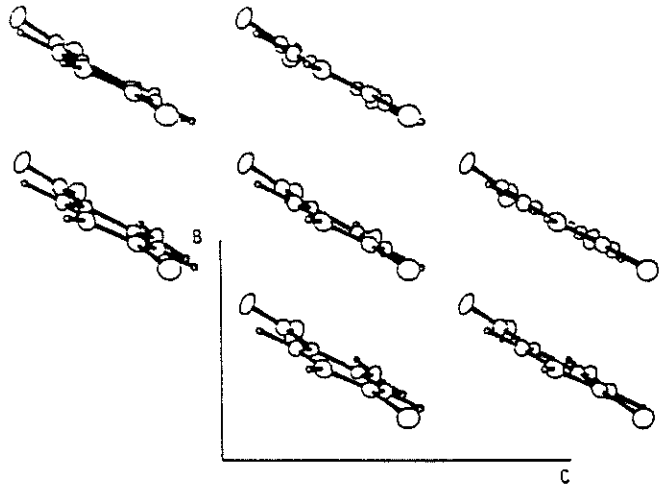

Figure 5. A projection of the ribbon-like packing structure of 5-chloro-2-nitroaniline. Molecules in each row are connected by significant intermolecular hydrogen bonding.

5-CHLORO-2-NITROANILINE

SPACE GROUP $Pna2_1$

polarization axis ∥ C-axis

$P \propto \chi(333) \propto \beta(zzz)\cos^3\theta$

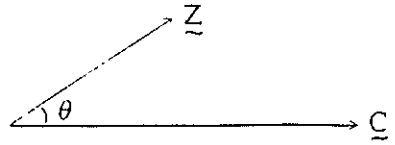

$\underset{\sim}{Z}$ ∥ polarization axis of molecule

$\underset{\sim}{C}$ ∥ polarization of crystal

$\underset{\sim}{Z} \cdot \underset{\sim}{C} = \cos\theta = 0.906$

SHG PACKING EFFICIENCY ≈ 0.74

2-CHLORO-4-NITROANILINE

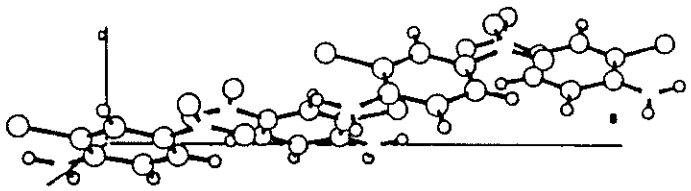

ELECTRODE CONFIGURATION
FOR MEASURING E-O EFFECT

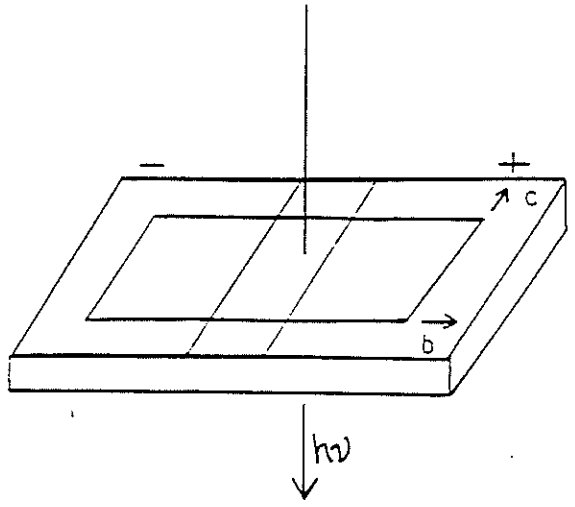

FIGURE OF MERIT = $\frac{1}{2}| n_1^3 r_{13} - n_2^3 r_{23} | = 18$ pm/v

$E^{DC} = \hat{y}$

EFISH on 3-CHLORO-4-NITROANILINE

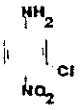

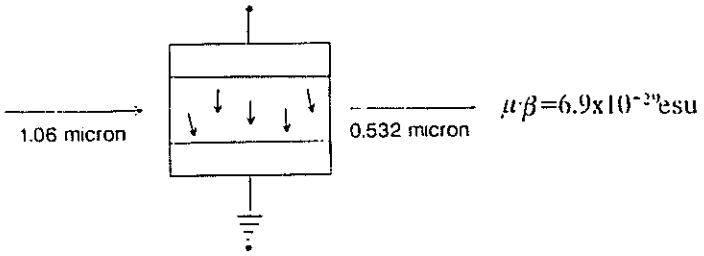

SHG STUDIES OF POLED POLYMERS

PRINCIPLE OF POLING GUEST/HOST SYSTEMS

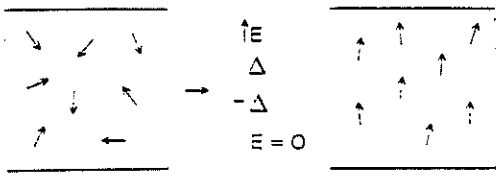

INVESTIGATE:

- Extent of ordering
- In-situ β
- Poling dynamics

CONDITIONS FOR POLING

3-CHLORO-4-NITROANILINE IN PMMA

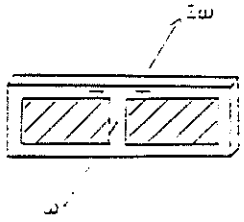

$I_{SHG} \propto E^2$ local poling

- 0.7 M in PMMA (10% by wt)
- E = 6 x 10^5 v/cm
- T = 110° C

RESULTS OF POLING EXPERIMENTS

- CALCULATED β AGREES WITH MEASURED
- OBSERVED DECREASE OF $X^{(2)}$ WITH TIME

CONDITIONS	$X^{(2)}$ (esu)
E, 110° C	1 X 10^{-10}
E, RT	1 X 10^{-10}
E = 0 (30 sec), RT	0.5 X 10^{-10}
E = 0 (65 hr), RT	0.39 X 10^{-10}

POLED POLYMER SYSTEMS FOR ELECTRO-OPTIC EFFECT

GUEST	$\mu \cdot \beta$ (x 10^{-28} D-esu) at 1.58 microns	A/molar 810 nm	1000 nm	1300 nm	1500 nm
3MX-40	37	84	51	30	27
3MX-3	19	1.5	0.13	0.09	0.1
3MX-36	18	0.6	0.3	0.3	0.3
3MX-2	15	0.5	0.6	0.6	0.6
3MX-1	11	0.07	0.06	0.05	0.07
3MX-8	10	0.03	0.04	0.04	0.04

G. R. Meredith
E. I. Dupont DeNemours and Co.

OPTICAL NONLINEARITY: MOLECULES, ASSEMBLIES AND WAVE PHENOMENA

G. Khanarian
Hoechst-Celanese

CHARACTERIZATION OF POLYMERIC NONLINEAR OPTICAL MATERIALS

L-2

Characterization of Nonlinear Optical Organic Materials

G. Khanarian
Hoechst Celanese Corporation
Summit, New Jersey 07901

T. CHE
R. DEMARTINO
D. HAAS
T. LESLIE
H. MAN
J. STAMATOFF
C. TENG
H. YOON

ACS Workshop
Virginia Beach, May, 1988

OUTLINE

- Molecular Miller's Rule
- Polymer Structure and $\chi^{(2)}$
- Measurement of $\chi^{(2)}$ by Second Harmonic Generation
- Measurement of $\chi^{(2)}$ by the Pockels Effect
- Results for MNA/PMMA
- MNA/PMMA/Sol-Gel Glasses - Role of Molecular Motion
- Langmuir Blodgett Films - Role of Internal Optical Field
- Application to Devices

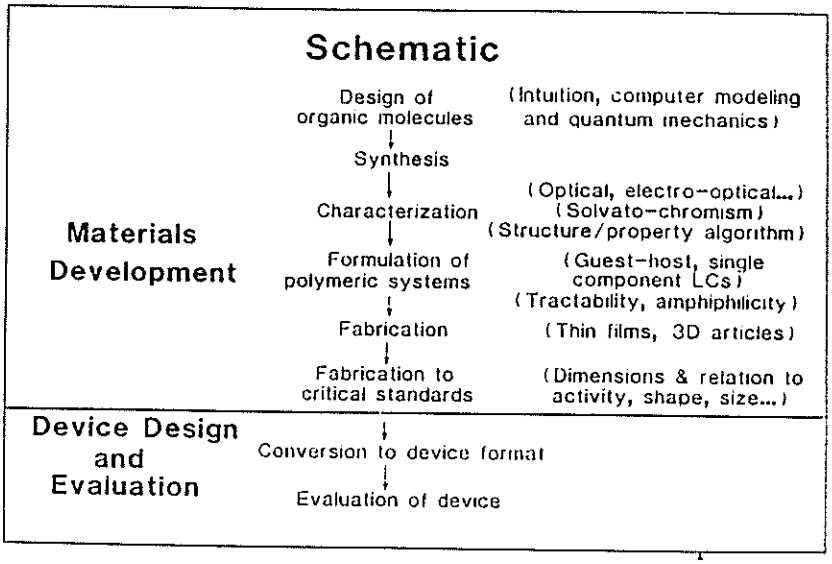

L-3

BASIC PHYSICS

MOLECULAR

$$p = \mu_0 + \alpha E + \beta E^2 + \gamma E^3$$

MATERIAL

$$P = \chi^{(1)} E + \chi^{(2)} E^2 + \chi^{(3)} E^3$$

$$\frac{d^2r}{dt^2} + 2\gamma \frac{dr}{dt} + \omega_0^2 r - \xi r^3 = -\frac{e}{m} E$$

$$\chi^{(1)}(\omega_\sigma) = \frac{Ne^2}{m} \frac{1}{\omega_0^2 - 2i\gamma\omega_\sigma - \omega_\sigma^2}$$

$$\chi^{(3)}(\omega_\sigma, \omega_m) = -\frac{m\xi}{Ne^4} [\chi^{(1)}(\omega_\sigma)][\chi^{(1)}(\omega_m)][\chi^{(1)}(\omega_\sigma + \omega_m)]$$

ANHARMONIC OSCILLATOR MODEL

$$\delta_{zzz} = \frac{-m\xi}{Ne^4} \alpha^3_{zz}$$

m mass of electron

e charge of electron

N oscillator strength

ξ anharmonic constant

$$= \frac{1}{L^2}$$

ω angular frequency

L length of molecule

	Exp. (10^{37} esu)	Theory (10^{37} esu)
$\frac{m\xi}{Ne^4}$	1	3.0

$\log_e \beta_{zzz}$ versus $\log_e \alpha_{zz}$

Verification of molecular Miller's Rule

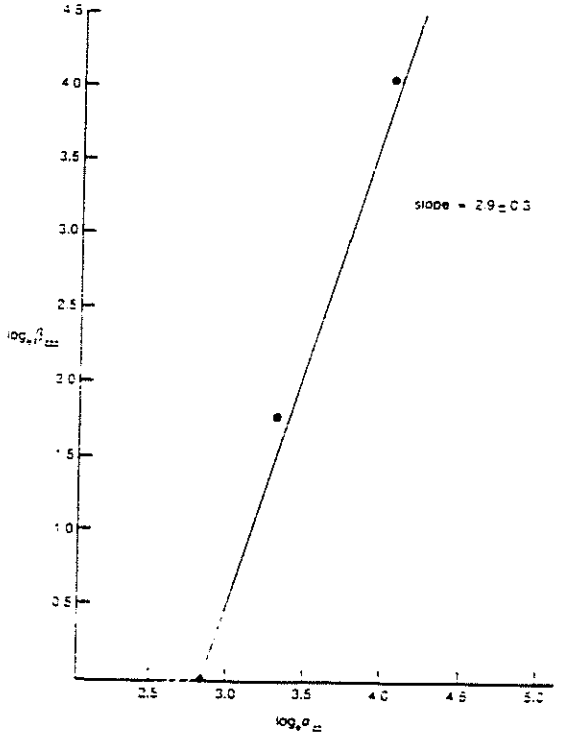

$$n^{K} = \frac{(n_0 - n_s)}{(n_0^2 + 2)^2 (n_s + 2)^2}$$

- M = molecular weight
- n = refractive index
- λ = wavelength of light
- ε = dielectric constant
- d = density
- B = Kerr constant
- n^K = molar Kerr constant

$$n^K = \frac{n_0 - N_A}{310} \left[\frac{3\mu_z^2 \bar{\alpha}}{(kT)^2} + \frac{3(\alpha_{zz} - \bar{\alpha})}{kT} + \frac{10\mu_z \beta_z}{3kT} + 10\gamma \right]$$

$$\bar{\alpha}_{zz} = \alpha_{zz} - \bar{\alpha}$$

$$\mathrm{tr}(\hat{\alpha}\hat{\alpha}) = \hat{\alpha}_{zz}\hat{\alpha}_{zz} + \hat{\alpha}_{xx}\hat{\alpha}_{xx} + \hat{\alpha}_{yy}\hat{\alpha}_{yy} + \ldots$$

$$\beta_z = \beta_{zzz} + \beta_{zxx} + \beta_{zyy} \quad \text{(1st hyperpolarizability)}$$

- γ = mean 2nd hyperpolarizability
- N_A = Avogadro's number
- k = Boltzmann's constant
- T = temperature
- $\bar{\alpha}$ = mean polarizability
- μ_z = dipole moment

TABLE I

Molar Kerr constants ${}_mK$ (x 10 ^{9} esu), linear polarizability α_{zz} (x 10 ^{24} esu) and β_{zzz} (x 10 ^{30} esu)

Compound	${}_mK$	α_{zz}	β_{zzz}
	0 985	13 2	1 0
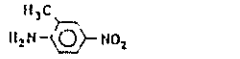	6 850	18.7	5.7
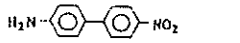	14 5	29 5	20
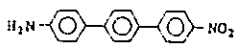	16.9	39 6	51

${}_mK$ values are at 0 633 µm. α_{zz} has been deduced from equation 3, and literature values for the dipole moment μ_z and the average polarizability. α_{zz} values reported above are at 1 9 µm A dispersion formula has been used to go from 0 633 to 1.91 µm β_{zzz} are also at 1 91 µm.

Types of Molecular Packing

Packing	Type	Order	Magnitude
	Non-centric	Second	Moderate
	Non-centric	Second	Strong
	Centric	Third	Strong
	Centric	Third	Weak

Direction of dipole moment

$\chi^{(2)}$ OF POLED FLEXIBLE DIPOLAR POLYMERS

- Theory same as for efish
- Exact calculations can be done for single chains - Flory Theory

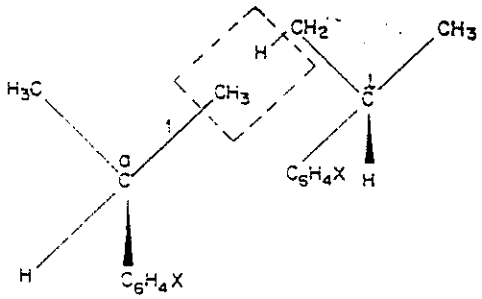

FIG. 2. Designation of bonds of PPNS, $X = NO_2$.

TABLE II. $\langle \mu \cdot \beta \rangle / x$ ($\times 10^{-48}$ cm^5) and $\langle \mu^2 \rangle / X$ ($\times 10^{-36}$ SC^2 cm^2) of poly(*p*-nitrostyrene) vs tacticity p_r, $T = 298$ K, $x = 200$ repeat units.

P_r	$\frac{\langle \mu \cdot \beta \rangle}{x}$	$\langle \mu^2 \rangle / x$
0.0 (isotactic)	21.5	10.7
0.2	16.6	8.27
0.4	16.3	8.12
0.6	16.8	8.36
0.8	16.4	8.17
1.0 (syndiotactic)	12.5	6.23

J. KHANARIAN, J. CHEM. PHYS., 77, 1982, P. 2586

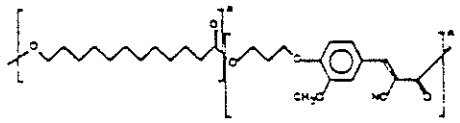

Table 2: Average Monomer Susceptibilities for Various Molecular Weight Copolymers.

Molecular Weight,[a] $\overline{M}_n$	Calculated Number of Monomer Units, *n*	$M_z B_z / n$ (10^{-48} esu)	Enhancement factor, G
NLO chromophore[b]	—	57	—
17,000	37	830	15
70,000	152	1140	20

[a] Determined by GPC relative to polystyrene.

[b] Structure II from Table 1.

C. S. Willand, S. E. Feth, M. Scozzafava, and D. J. Williams
Corporate Research Laboratories, Eastman Kodak Company, Rochester, N. Y.

G. D. Green,* J. I. Weinschenk, III, H. K. Hall, Jr., and J. E. Mulvaney
C. S. Marvel Laboratories, Department of Chemistry, University of Arizona, Tucson, Az.

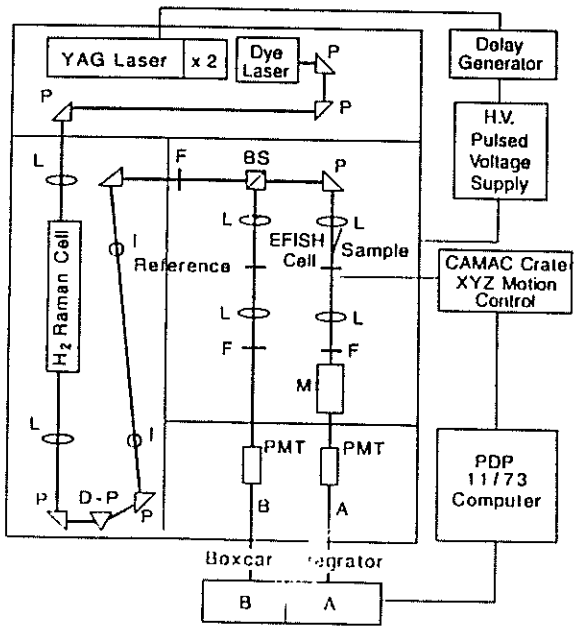

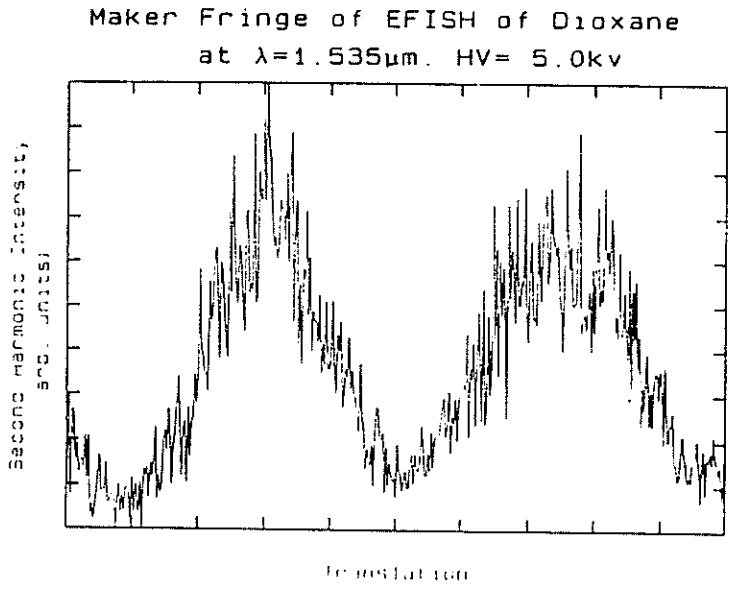

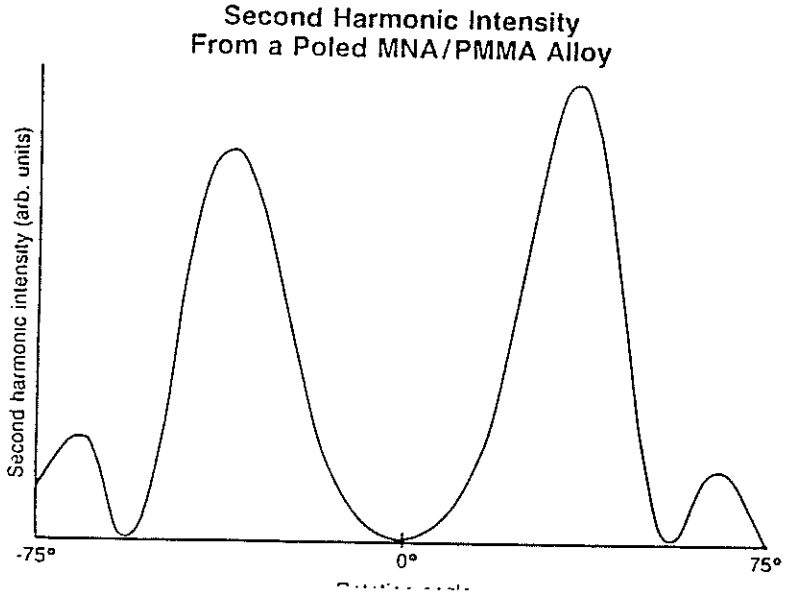

SECOND HARMONIC GENERATION FROM POLED POLYMERS

The second harmonic intensity is given by

$$\frac{I(2\omega)}{[I(\omega)]^2} \propto t^4 T d_{33}^2 p^2 l_c^2 \sin^2\left(\frac{\pi}{2}\frac{L}{lc}\frac{n}{(n^2-\sin^2\theta)^{1/2}}\right)$$

t, T	Fresnel transmission factors
d	Second harmonic coefficient
p	Projection factor of d tensor onto optical electric field
l_c	Coherence length
n	Refractive index
L	Thickness of sample
θ	Angle of rotation

$\chi^{(2)}(-2\omega, \omega, \omega) = 2d$

When $\theta = 0$, $p = 0$ and there is no component of d along E, and there is no second harmonic observed

The Maker fringe arises from an interference between the fundamental beam and generated harmonic wave

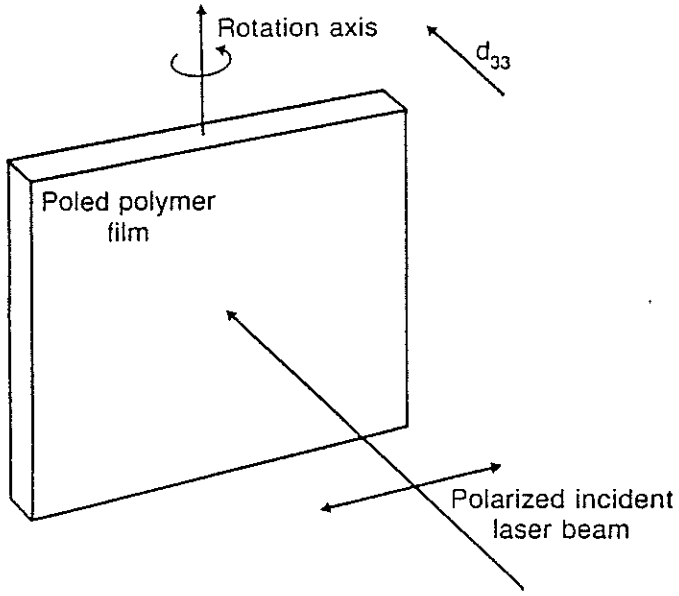

THEORY OF MEASUREMENT FOR POCKELS AND KERR EFFECT

The birefringence Δn induced in a Kerr cell is:

$$\Delta n = \lambda B E^2$$

and in a Pockel cell:

$$\Delta n = 1/2\ n^3 E$$

The birefringence results in a retardation Γ

$$\Gamma = \frac{2\pi \Delta n l}{\lambda}$$

In the small angle approximation, Equation 4 becomes:

$$\frac{I}{I_o} = \frac{1}{2}[1 + \Gamma]$$

A sinusoidal voltage is applied across the electro-optic cell

$$V = Vo \sin\omega t$$

Substituting Equation 7 into Equation 5

$$\frac{I}{I_o} = \frac{1}{2} + \frac{\Gamma \text{ Kerr}}{2} + \frac{\Gamma \text{ Pockel } \sin\omega t}{2} - \frac{\Gamma \text{ Kerr } \cos 2\omega t}{2}$$

The apparent angular dependence of the Pockels effect arises from change of optical path length

$$\frac{d}{\cos\theta}$$

where d is the thickness of the sample

The analyzing light beam sees a different birefringence as a function of angle

$$\Delta n\ (\theta) = \Delta n\ (\theta = 90°) \sin^2\theta$$

θ is the angle between the normal axis of sample and the light beam

POCKELS EFFECT

The optical retardation is

$$\Gamma = \frac{2\pi}{\lambda} l\ \Delta n$$

- l Optical path length
- Δn Induced birefringence
- λ Wavelength of light

The induced birefringence

$$\Delta n = \frac{1}{2}(n_1^3 r_{33} - n_2^3 r_{31})\ E$$

- r Pockels constant
- n Refractive index
- E Applied electric field

For poled materials

$$r_{31} \cong \frac{r_{33}}{3}$$

This result is obtained from a thermodynamic model for poling

- Boltzmann statistics

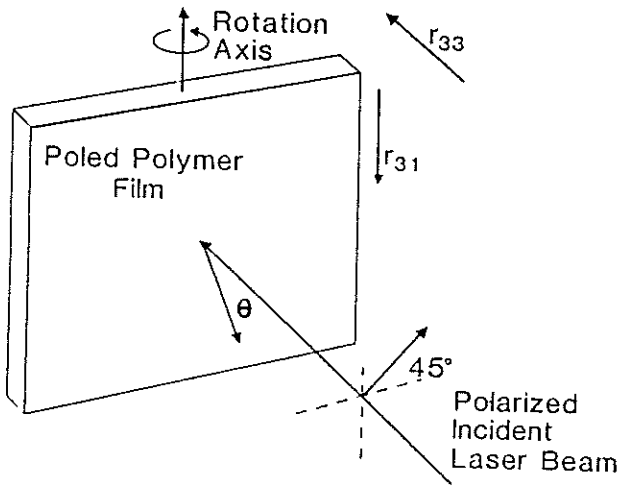

SCHEMATIC OF ELECTROOPTIC APPARATUS

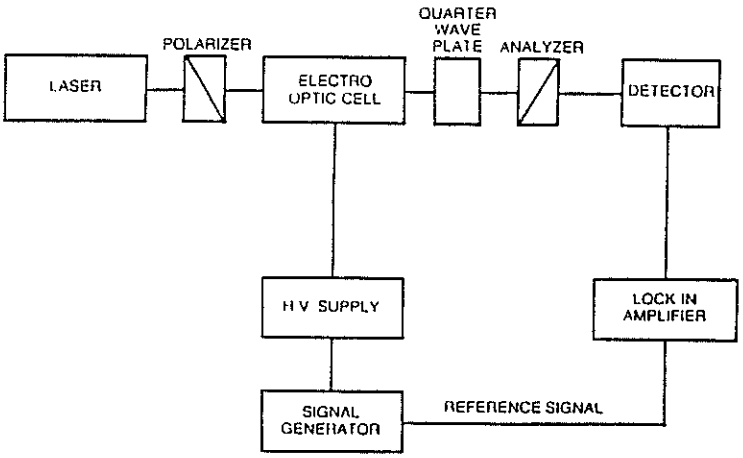

Pockels Effect from Poled MNA/PMMA Sample

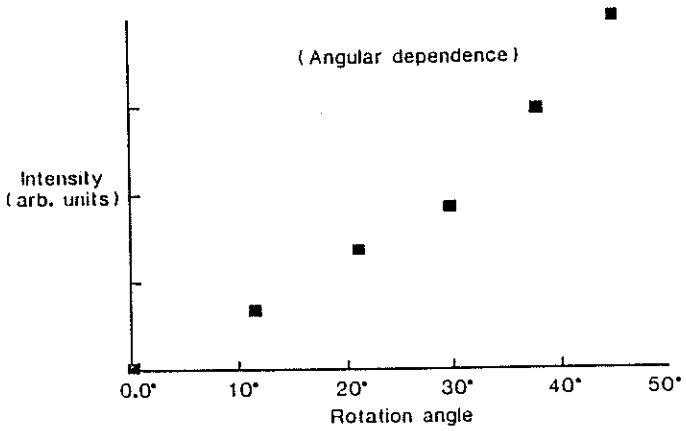

Pockels Linear Electro-optic Effect From a $\chi^{(2)}$ Polymer

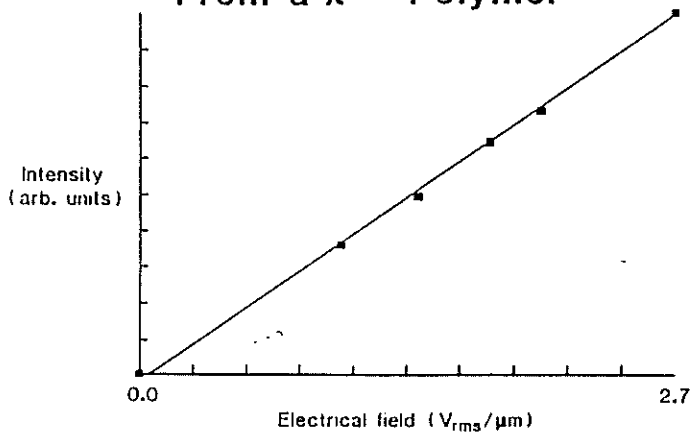

SOL-GEL TECHNOLOGY

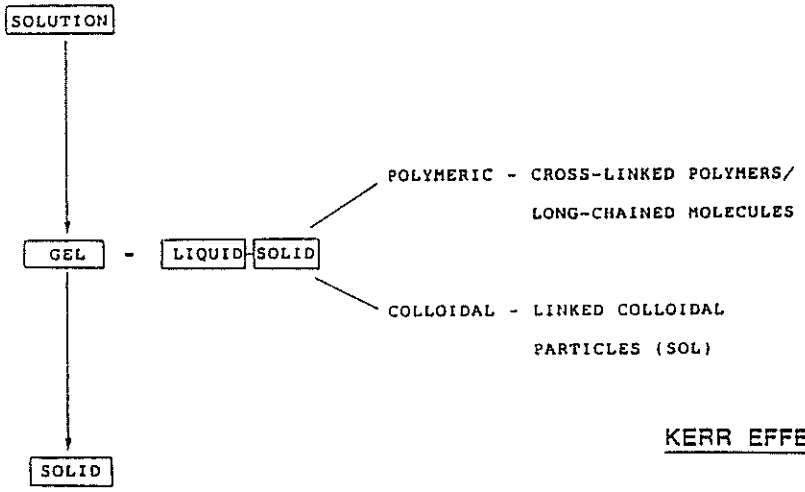

KERR EFFECT OF SOL-GEL GLASS

MNA added to sol-gel glass

PMMA is added to sol gel glass to give mechanical strength

Slab was cut and polished for electro-optic measurement

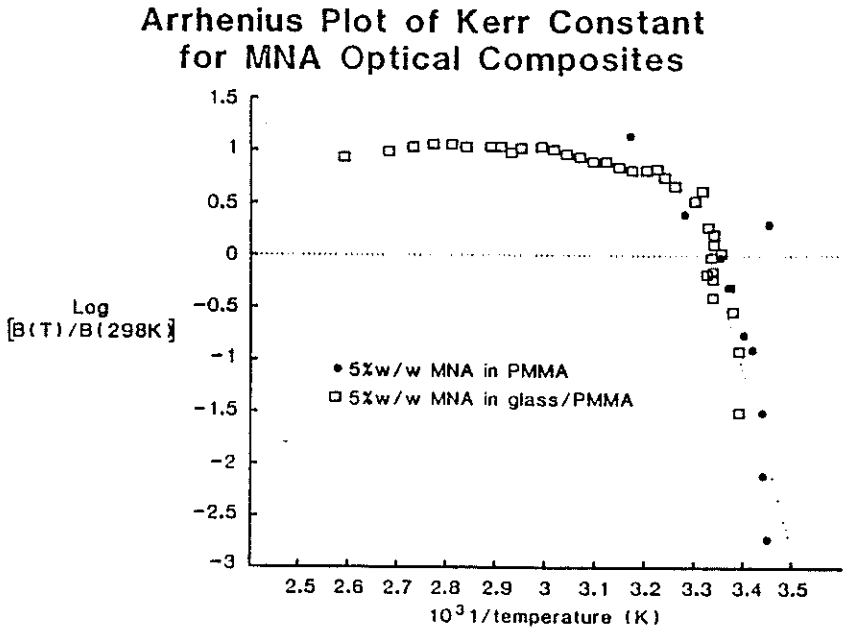

THERMODYNAMIC MODEL

Assume that nonlinear optical molecules are distributed orientationally according to Boltzmann statistics.

$$\chi^{(2)}_{zzz}(-2\omega,\omega,\omega) = Nf^3 s \frac{\epsilon(n^2+2)}{n^2+2\epsilon} \frac{\mu E}{5kT}$$

N	number density
f	internal field
s	hyperpolarizability
μ	dipole moment
E	poling field
k	Boltzmann constant
T	temperature
ϵ	dielectric constant
n	refractive index

RESULTS

Sample	$\chi^{(2)}(-2\omega,\omega,\omega)$	$\chi^{(2)}(-\omega,\omega,0)$	$\chi^{(2)}$(calc)
10% MNA/PMMA	1.6	1.5	0.6

All $\chi^{(2)}$ values are $\times 10^{-9}$ esu and are at 1.06 μm

$\chi^{(2)}(-2\omega,\omega,\omega)$ measured at 1.06 μm

$\chi^{(2)}(-\omega,\omega,0)$ measured at 0.63 μm and a dispersion relation was used to obtain values at 1.06 μm

$\chi^{(2)}$(calc) used the thermodynamic model

NLO Side Chain Polymers
First Generation

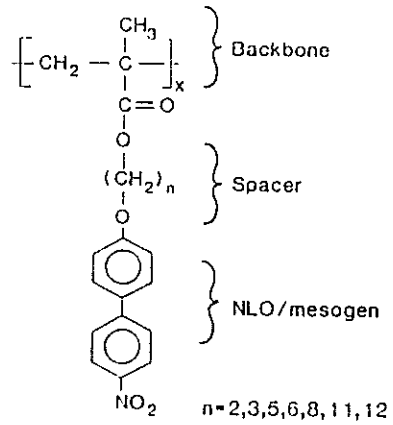

n=2,3,5,6,8,11,12

Dependence of Glass and Clearing Temperatures on Carbon Spacer Length

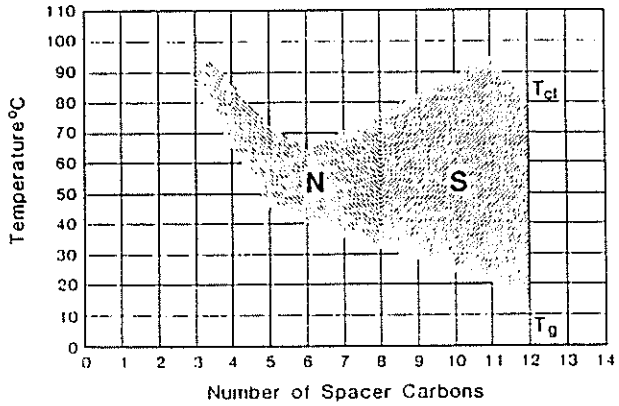

NLO Polymer Properties

$\chi^{(2)}$ at 1.3 μm	> 50 pm/V
r (calculated)	> 14 pm/V
n (1.3 μm)	1.57
ε (DC)	3.5
ε (n^2)	2.6
waveguide loss at 1.3 μm	0.9 dB/cm

Spin coatable from common solvents

Poled for application
Stable (<10% loss) at >50°C for 5 years

LANGMUIR BLODGETT FILMS

- 2D Material
- Orientation of Molecules by Surface
- Useful for Fundamental Studies of:
  - Interaction of radiation with molecules (spectroscopy)
  - Tilt angles
  - Hyperpolarizability
  - Molecule/surface interactions
  - Interaction between layers
  - Local optical electric field effects

Langmuir-Blodgett Film (LBF) Formation

- Is the deposition on a surface of a single molecular layer at a highly ordered state
- Sequential deposition leads to periodically structured films
- It is done by transfer of a compressed molecular surface layer on a liquid onto a solid surface by dipping

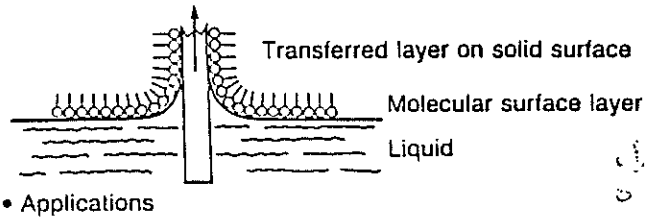

- Applications
  - — Nonlinear optics: Bistable switches, Thin film SH and TH generation
  - — Electro-optics: Thin film light modulator
  - — Integrated optics: Planar dielectric wave guides

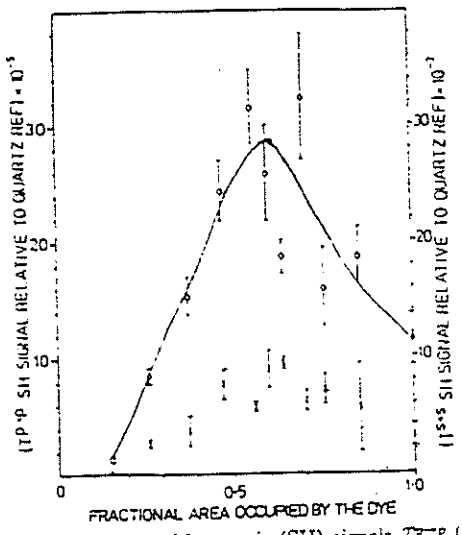

5. Plot of the second-harmonic (SH) signals T^{pp} (○) and T^{ss} (×) relative to the quartz reference slab versus the area fraction occupied by the dye in the mixed monolayer.

J.R. DURING ET AL JOSA B, 1987, VOL. ., P. 950

Local Optical Electric Field

$$p_z = \mu_z + (\alpha_{zz}) F_z + (\beta_{zzz}) F_z^2 + (\gamma_{zzzz}) F_z^3$$

$$F_z = E_z + \sum_j T_{zz}^{ij} p_z$$

$$T_{zz}^{ij} = \frac{-1}{r_{ij}^3}$$

μ, α, β and γ are the dipole moments and polarizabilities

Z axis is normal to glass surface

Linear Mean Field Approximation

* Neglect fluctuation in dipole moment
* Assume that linear polarizability alone changes local dynamic optical field.

$$\sum_j T^{ij} = \rho \int_a^\infty \frac{2\pi r\, dr}{r^3}$$

$$= \frac{2\pi\rho}{a}$$

ρ = surface density of dipoles

a = radius of nonlinear optical molecule

Results for the nonlinear susecptibility

$$\chi_{zzz} = \frac{3a}{2\pi\alpha_{zz}} \frac{x}{(1+x)^2} - \frac{3\gamma\mu a}{2\pi\alpha_{zz}^2} \frac{x^2}{(1+x)^2}$$

$$x = \frac{2\pi\alpha_{zz}\rho}{a}$$

Variation of effective χ_{zzz} of a Langmuir Blodgett Film versus normalized concentration of active nonlinear optical molecule

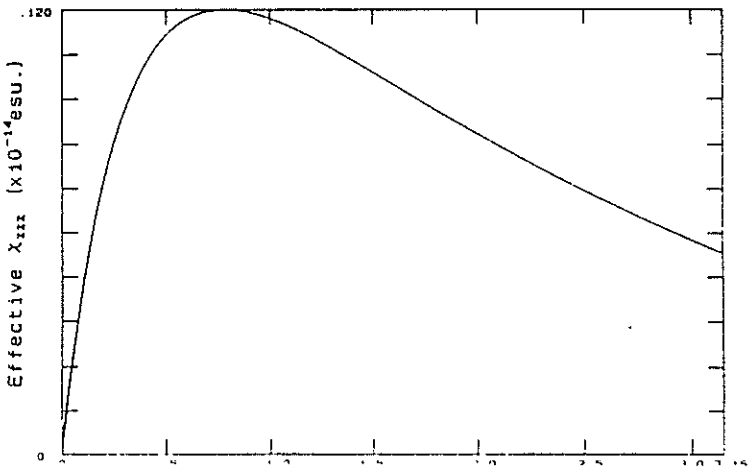

CLASSES OF ORGANIC NLO DEVICES

- Electro-Optic Devices
  - Control of light with electronics
  - Based on the second order NLO susceptibility $\chi^{(3)}$
  - Applications: Hybrid optical processing and optical communications
- All Optical Devices
  - Control of light with light
  - Based on the third order NLO susceptibility $\chi^{(3)}$
  - Applications: All optical computing and ultra-fast optical communications

POLYMER GUIDE FABRICATION PROCESS

COMPONENTS

- Spin Coating (thin film formation)
- Buffer Layer and Substrate Materials
- Patterning
- Metallizing
- Beam Coupling

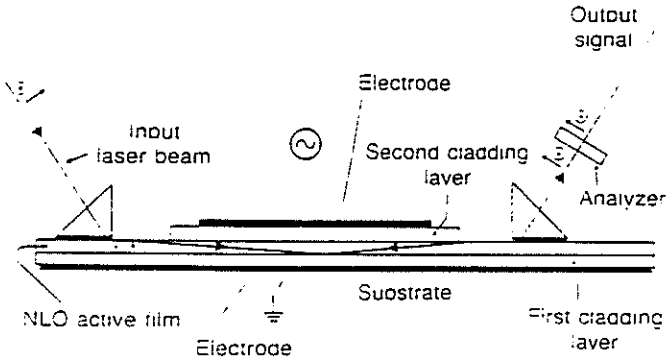

TE Polarization
TM Polarization

MODULATOR RESULTS

MATERIAL	LENGTH (CM.)	V_π (V)	Λ (nm)	F_{MAX} (MHz)	r_{33} (pm/V)
PMMA: pNA	1.0	450	633	30	.5
HCC #0520	1.0	45	633	0.5	3.5
HCC #1622	2.0	30	830	10*	3.75
HCC #1238	1.5	4.0	830	1	20

$$r_{33} = \frac{3 \lambda G}{2n^3 L V_\pi \Gamma}$$

$\Gamma \approx .85$ to $.95$ for these structures

OTHER MATERIAL PROPERTIES

> N FROM 1.51 TO 1.66

> ε (100 KHZ) $\approx$ 3.6

SUMMARY

- Organic NLO research at HCC has developed outstanding NLO and EO polymers
- These materials, additionally, exhibit combination of excellent performance characteristics and fabrication properties for NLO and EO devices
- Initiative to develop a series of important NLO devices has been undertaken at HCC
- Fabrication science and technology for the materials is a key component of the initiative

T. Richardson

University of Oxford, U. K.

PREPARATION AND CHARACTERIZATION OF ORGANO-TRANSITION METAL LANGMUIR-BLODGETT FILMS

M-2

THE PREPARATION AND CHARACTERISATION OF ORGANO-TRANSITION METAL LANGMUIR-BLODGETT FILMS

T. RICHARDSON, G.G.ROBERTS
UNIVERSITY OF OXFORD
DEPARTMENT OF ENGINEERING SCIENCE
PARKS ROAD, OXFORD, OX1 3PJ, ENGLAND

M.E.C. POLYWKA, S.G. DAVIES
DYSON PERRINS LABORATORIES
UNIVERSITY OF OXFORD
SOUTH PARKS ROAD, OXFORD, OX1 3QY, ENGLAND

A SERIES OF NOVEL RUTHENIUM COMPOUNDS HAVE BEEN DEVELOPED FOR USE WITH THE LANGMUIR-BLODGETT DEPOSITION TECHNIQUE. COMPLEXING OF A N- [RUTHENIUM (CYCLOPENTADIENYL-BIS TRIPHENYLPHOSPHINE)] HEAD GROUP TO A CYANOTERPHENYL LIQUID CRYSTAL MOLECULE HAS BEEN SHOWN TO INCREASE THE SECOND-ORDER NON-LINEAR OPTICAL HYPERPOLARIZABILITY AND FURTHERMORE INDUCE MULTILAYER FORMATION. OPTICAL ABSORPTION DATA HAVE REVEALED THE EXCELLENT REPRODUCIBILITY OF SUCCESSIVE MONOLAYER TRANSFER. SECOND HARMONIC GENERATION HAS BEEN OBSERVED AND THE EFFECT HAS BEEN INCREASED BY INCORPORATING UNSUBSTITUTED LIQUID CRYSTAL MOLECULES INTO THE VOIDS BETWEEN THE TERPHENYL CHAINS OF ADJACENT RUTHENIUM SUBSTITUTED MOLECULES. WE HAVE FURTHER OPTIMISED THE NON-LINEAR RESPONSE BY SYSTEMATICALLY VARYING THE ELECTRON-RELEASING CHEMICAL GROUP AND THE CONJUGATION WITHIN THE MOLECULE.

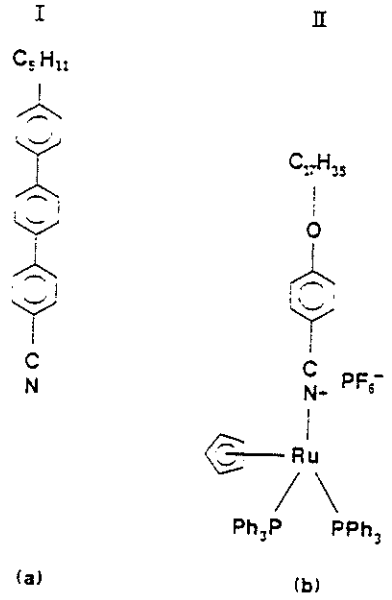

FIGURE 1

(A) A TYPICAL CYANO-TERPHENYL MOLECULE (I).

(B) THE $[(C_5H_5)\ Ru\ (PPh_3)_2]$ SUBSTITUTED MOLECULE POSSESSES A LARGER SECOND-ORDER NON-LINEAR OPTICAL HYPERPOLARIZABILITY THAN COMPOUND I.

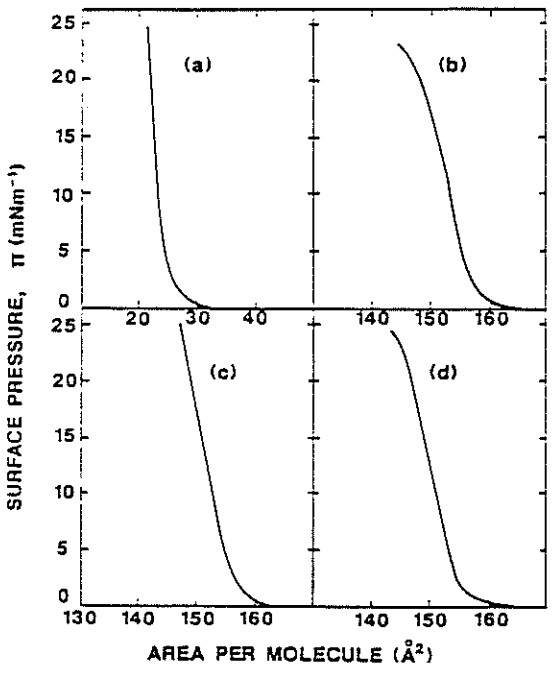

FIGURE 2

THE BEHAVIOUR OFMOLECULES OF COMPLEX I AND II UNDERGOING COMPRESSION ON THE WATER SURFACE. (A) COMPLEX I AT PH 5.8, (B, C AND D) COMPLEX II AT PH 3.8, 5.8 AND 8.7 RESPECTIVELY. THE MOLECULAR AREAS AT RELATIVELY HIGH SURFACE PRESSURE (20 mNm^{-1}) CORRESPOND ACCURATELY TO THE MEASURED CROSS-SECTIONAL AREA OF THE RUTHENIUM HEAD GROUP.

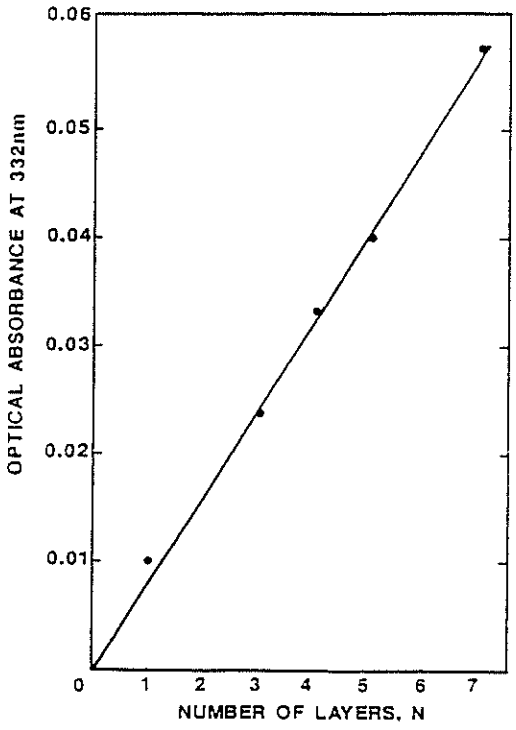

FIGURE 3

OPTICAL ABSORPTION VERSUS THE NUMBER OF TRANSFERRED MONOLAYERS. THE LINEAR RELATIONSHIP INDICATES THE REPRODUCIBILITY OF SUCCESSIVE MONOLAYER DEPOSITION.

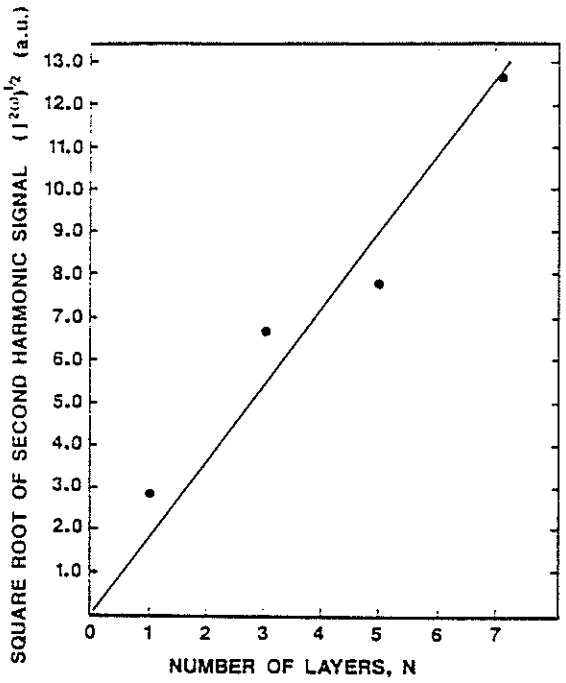

FIGURE 4

THE RELATIONSHIP BETWEEN THE SQUARE ROOT OF THE SECOND HARMONIC GENERATION SIGNAL AND STRENGTH THE THICKNESS OF THE FILM. THE APPROXIMATELY LINEAR RELATIONSHIP IMPLIES THE UNIDIRECTIONAL ALIGNMENT OF THE MOLECULES.

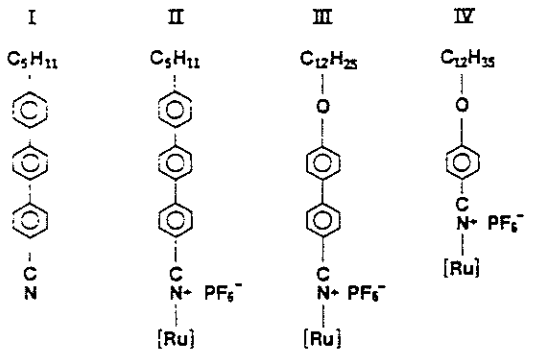

COMPLEX	SHG SIGNAL NORMALIZED TO II
II	1.0
II/I	1.5
III	11.0
IV	77.0

FIGURE 6

OPTIMISATION OF NON-LINEAR RESPONSE. THE SECOND HARMONIC SIGNAL IS HIGHLY DEPENDENT UPON THE ELECTRON DONOR AND THE DEGREE OF CONJUGATION.

(a) NO INCORPORATION

(b) INCORPORATED CTP MOLECULES

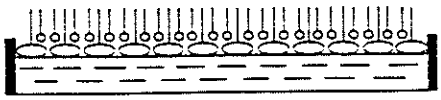

FIGURE 5

HIGH PACKING DENSITY STRUCTURES.

(A) THE LIQUID CRYSTAL MOLECULES MAY REMAIN ON THE WATER SURFACE,
OR
(B) THEY MAY BE INCORPORATED INTO THE MATRIX FORMED BY THE RUTHENIUM SUBSTITUTED MOLECULES.

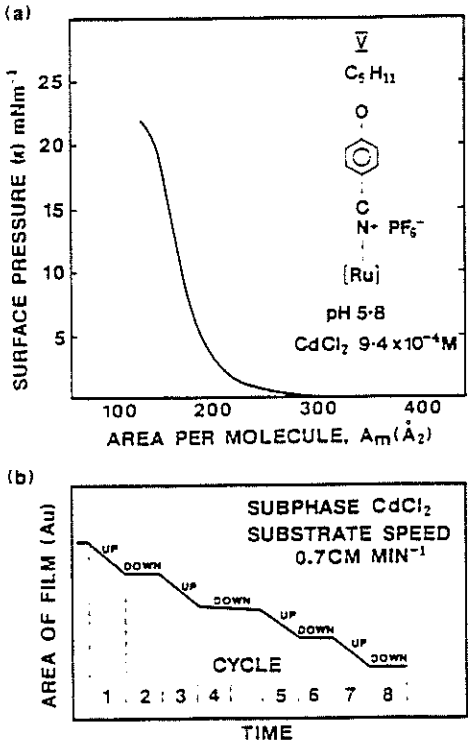

FIGURE 7

OPTIMISATION OF THE CARBON CHAIN LENGTH:-

(A) I VS.A_M PLOT FOR COMPLEX V, SHOWN IN INSERT

(B) THE Z-TYPE DEPOSITION OF COMPLEX V. HIGHER RATES OF DEPOSITION ARE POSSIBLE WITH $CdCl_2$ IN THE SUBPHASE.

S. K. Tripathy
University of Lowell

OPTICAL PROPERTIES OF ORGANIZED ASSEMBLIES

OPTICAL PROPERTIES OF MOLECULAR ASSEMBLIES

SUKANT TRIPATHY
UNIVERSITY OF LOWELL
LOWELL, MA 01854

- Selected conjugated molecular and Macromolecular systems
- Organized mono and multilayer assemblies
- Characterization of microstructure and morphology
- Measurement and anticipation of electronic and optical properties

Selection of materials

1. **Linked donor-acceptor molecules.**

   anticipated large 2nd order effects.
   example MNA

2. **Polymers with delocalized backbone electronic structure.**

   anticipated large 3rd order susceptibilities.
   example Polydiacetylenes

POLYDIACETYLENES

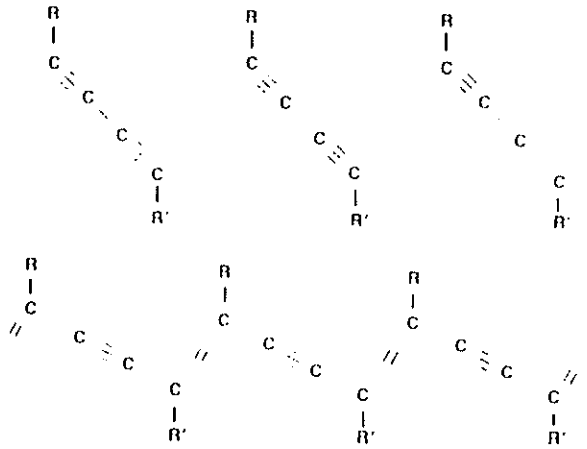

- Backbone Responsible for the Optical and the Nonlinear Optical Properties
- The Side Groups Provide a Handle for Fabrication and Structure Control

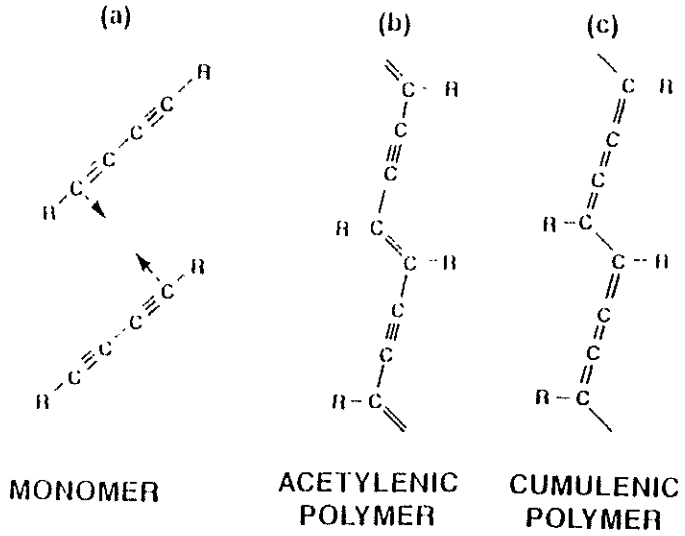
(a)
(b)
(c)
MONOMER
ACETYLENIC POLYMER
CUMULENIC POLYMER

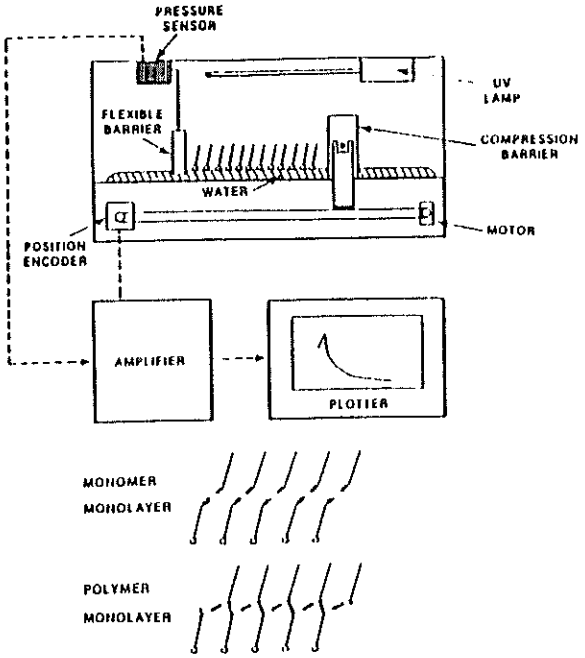
PRESSURE SENSOR
UV LAMP
FLEXIBLE BARRIER
COMPRESSION BARRIER
WATER
MOTOR
POSITION ENCODER
AMPLIFIER
PLOTTER
MONOMER MONOLAYER
POLYMER MONOLAYER

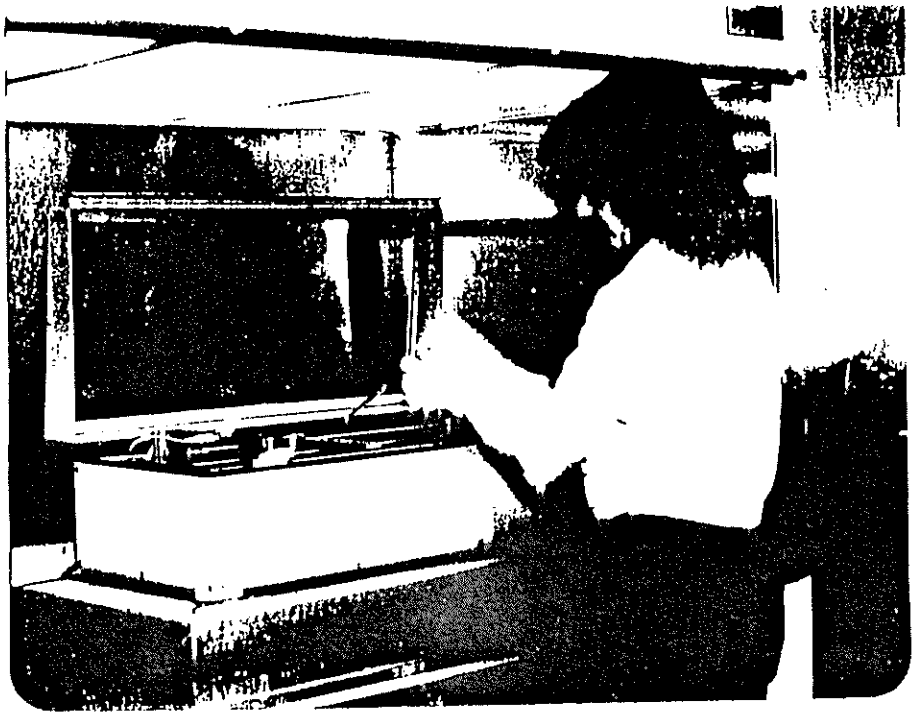

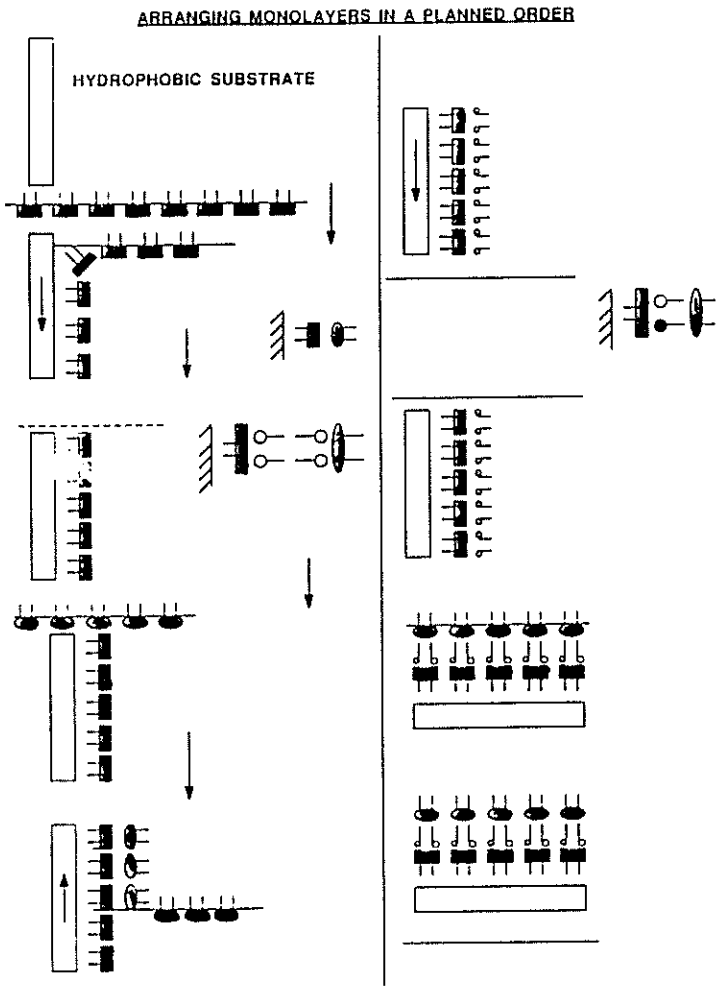

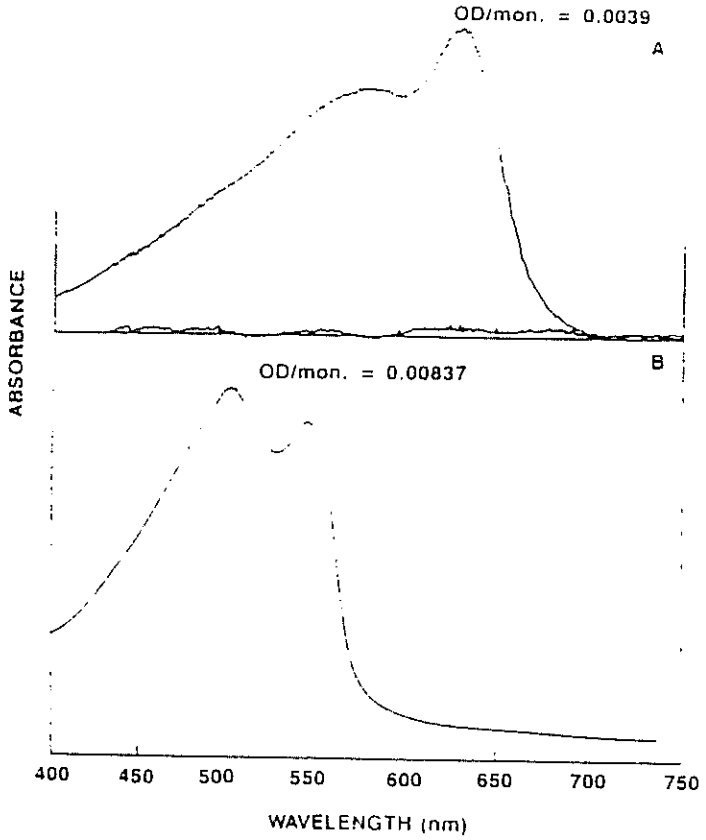

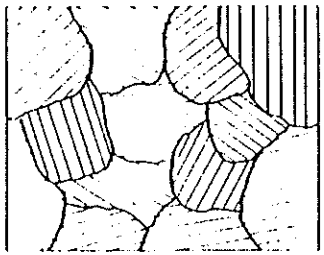

POLY CRYSTALLINE

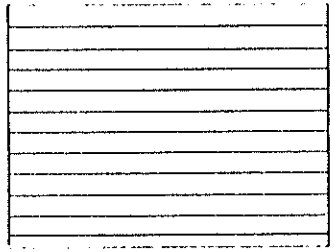

ORIENTED SINGLE CRYSTALLINE

N-4

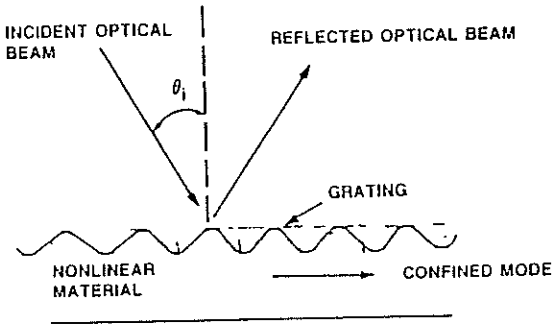

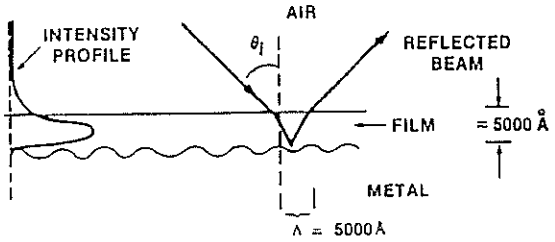

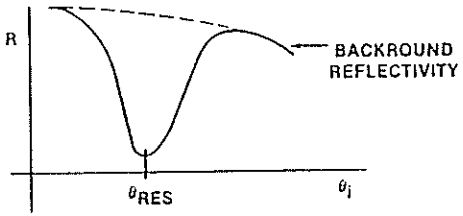

$$n_g = \lambda_o/\Lambda \pm \sin(\theta_{RES})$$

$$(n_g \equiv k_g/k_o)$$

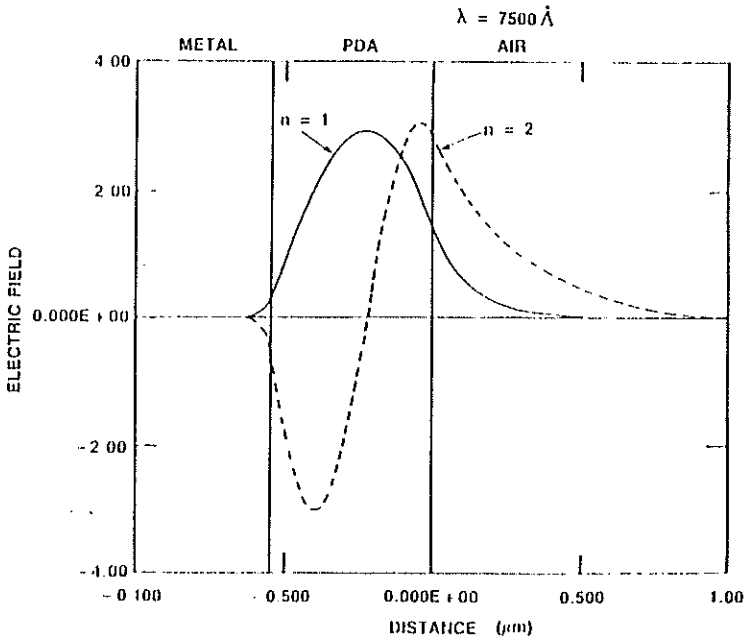

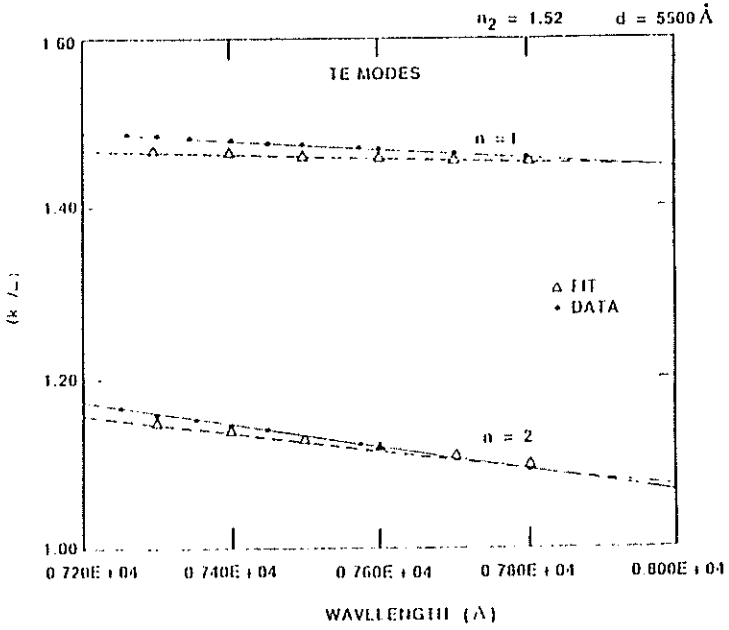

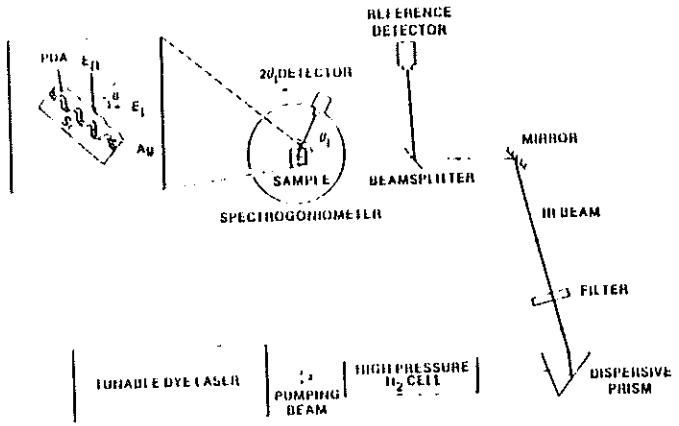
REFERENCE DETECTOR
PDA
$2\theta_i$ DETECTOR
E_{II}
$E_\perp$
Au
θ_i
SAMPLE
BEAMSPLITTER
MIRROR
SPECTROGONIOMETER
IR BEAM
FILTER
TUNABLE DYE LASER
PUMPING BEAM
HIGH PRESSURE H_2 CELL
DISPERSIVE PRISM

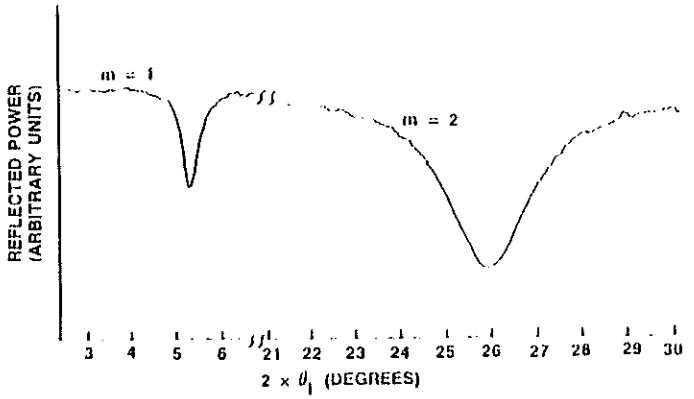
REFLECTED POWER (ARBITRARY UNITS)
m = 1
m = 2
3 4 5 6 21 22 23 24 25 26 27 28 29 30
2 x θ_i (DEGREES)

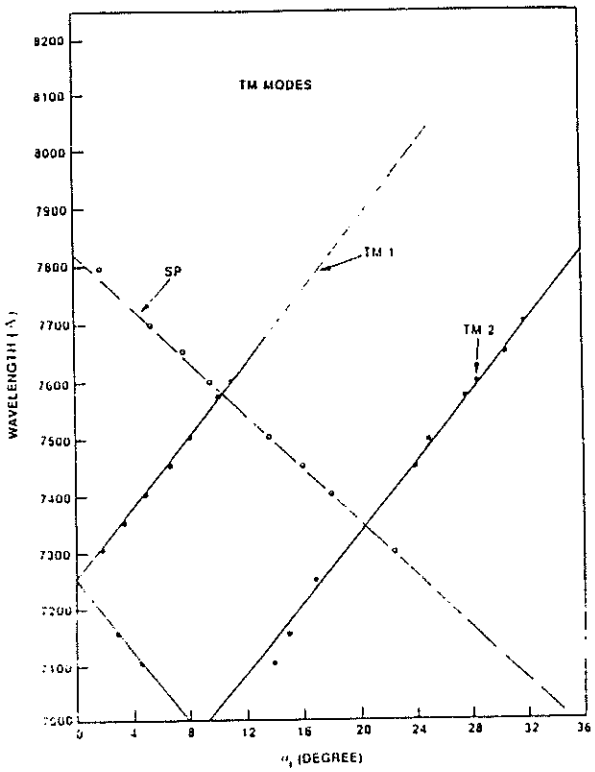
TM MODES
SP
TM 1
TM 2
WAVELENGTH (Å)
8200
8100
8000
7900
7800
7700
7600
7500
7400
7300
0 4 8 12 16 20 24 28 32 36
θ_i (DEGREE)

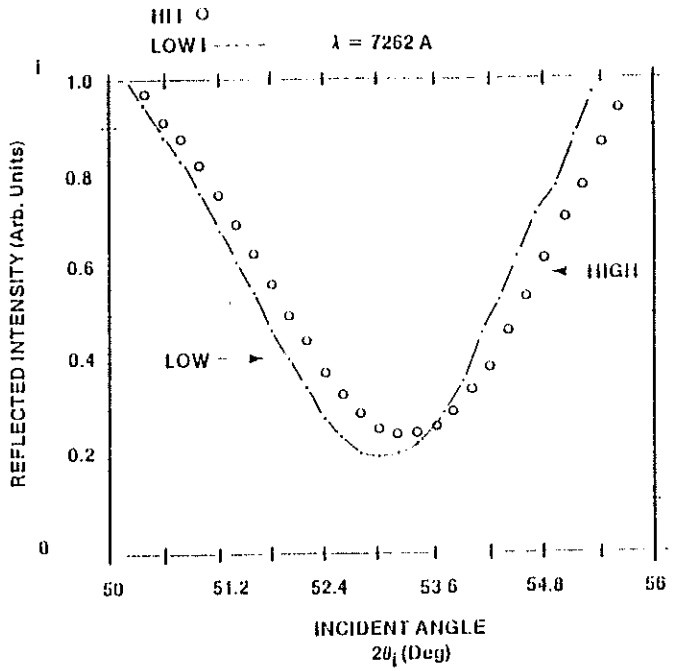
HIGH
LOW
λ = 7262 A
REFLECTED INTENSITY (Arb. Units)
1.0
0.8
0.6
0.4
0.2
0
50 51.2 52.4 53.6 54.8 56
INCIDENT ANGLE
$2\theta_i$ (Deg)

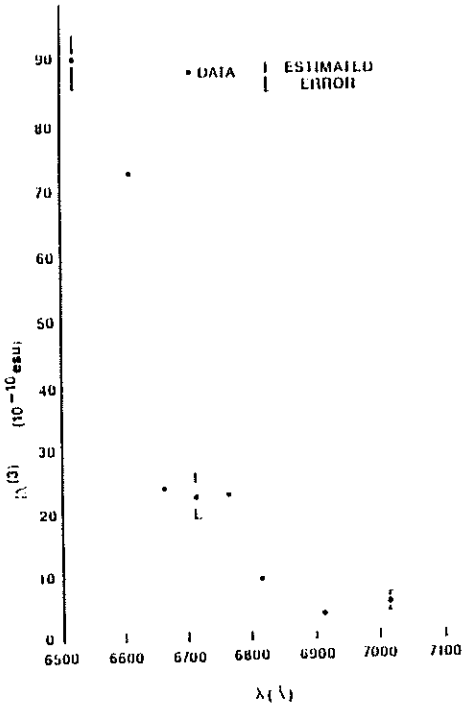
DATA
ESTIMATED ERROR
90
80
70
60
50
40
30
20
10
0
6500
6600
6700
6800
6900
7000
7100

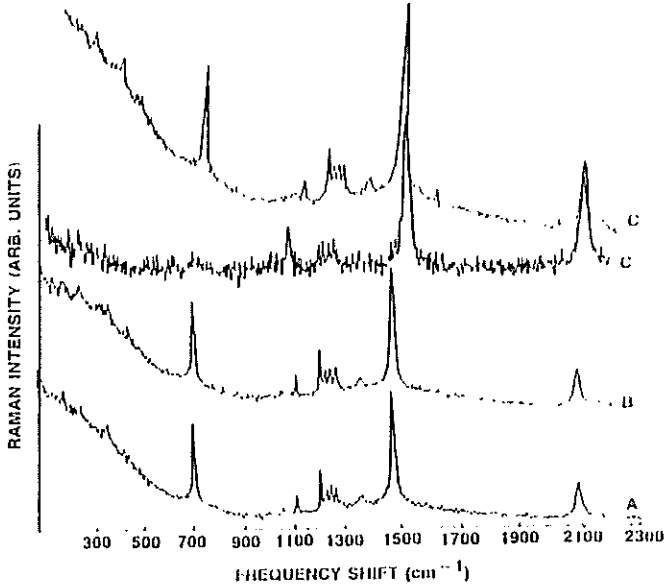
RAMAN INTENSITY (ARB. UNITS)
C
C
B
A
300 500 700 900 1100 1300 1500 1700 1900 2100 2300
FREQUENCY SHIFT (cm⁻¹)

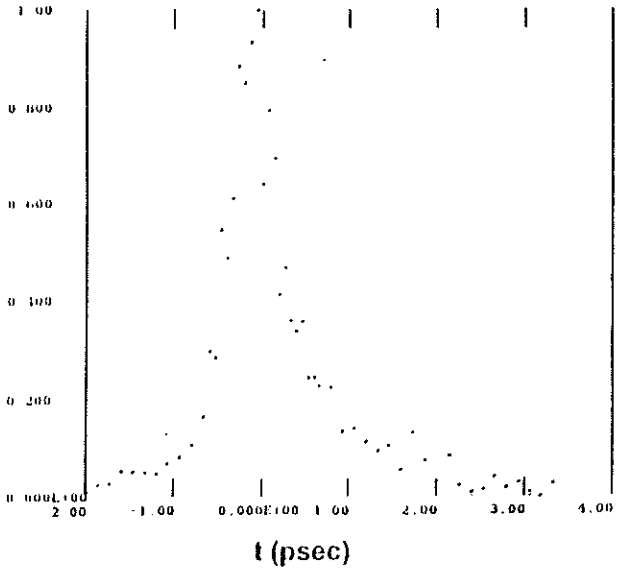
-1.00
0.000E+00
1.00
2.00
3.00
4.00
t (psec)

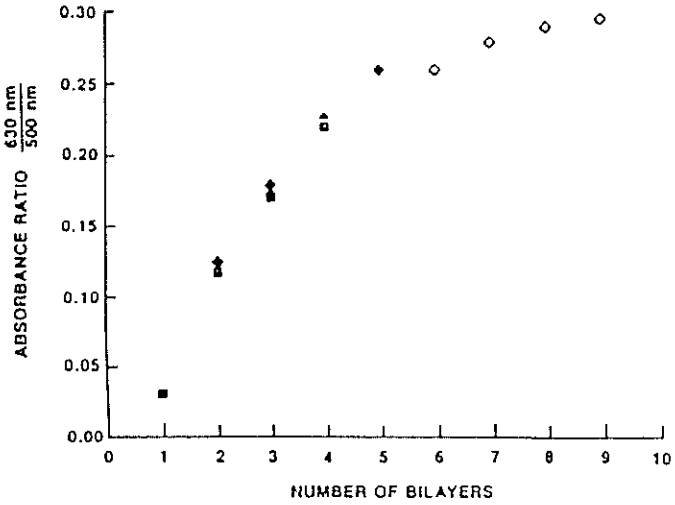
ABSORBANCE RATIO 630 nm / 500 nm
0.30
0.25
0.20
0.15
0.10
0.05
0.00
0 1 2 3 4 5 6 7 8 9 10
NUMBER OF BILAYERS

N-7

PUMP–PROBE: SATURATED ABSORPTION

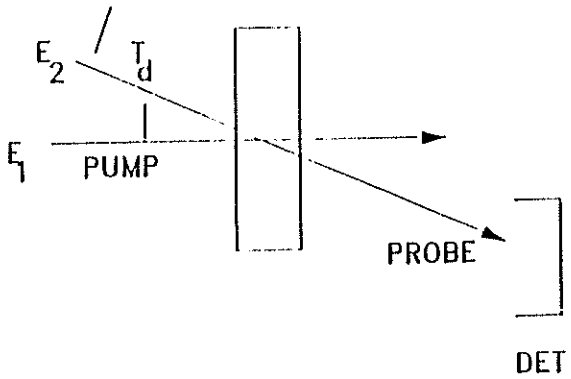

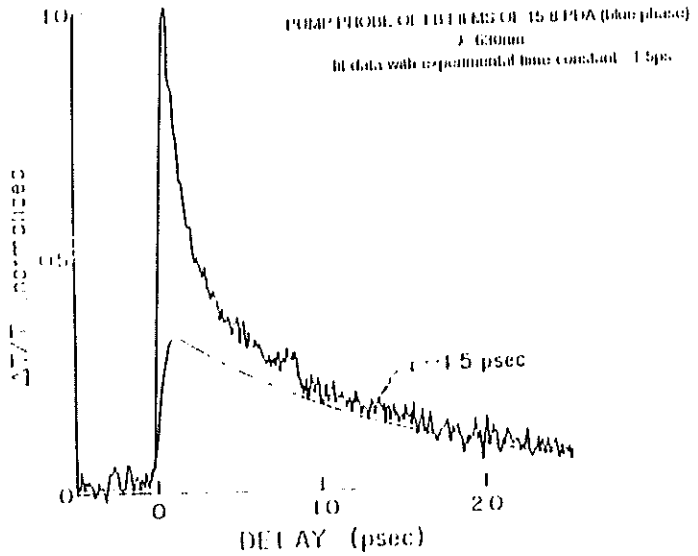

EXPERIMENTAL SCHEMATIC

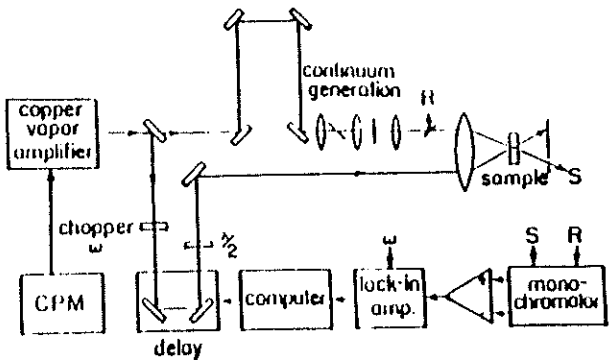

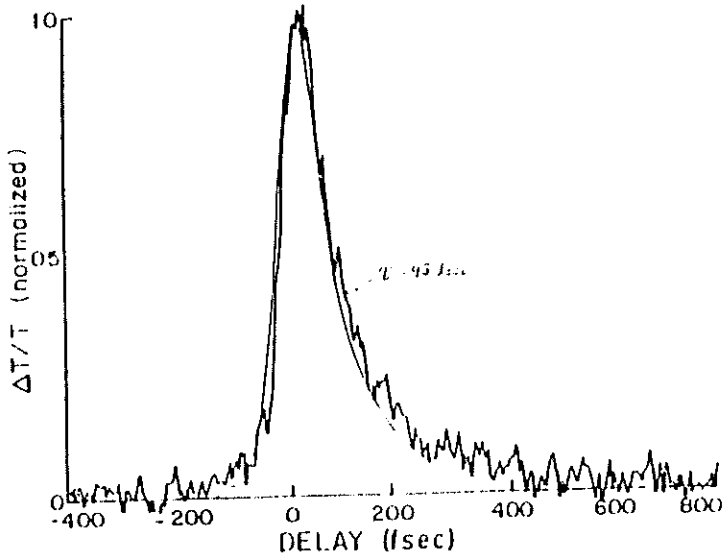

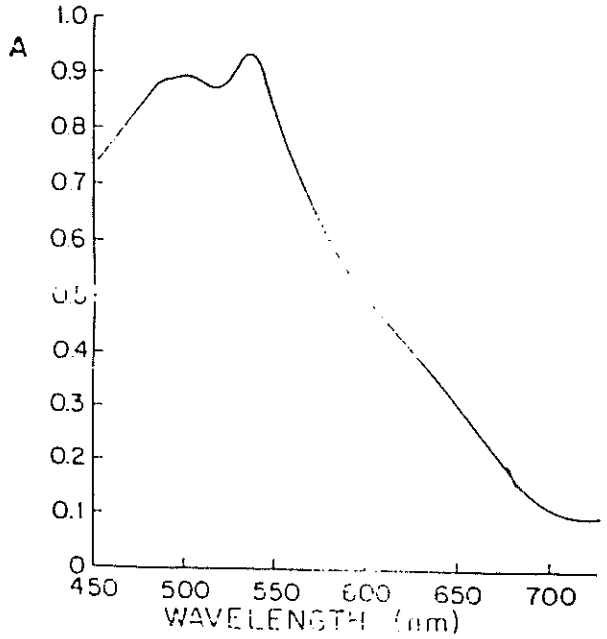

LINEAR ABSORPTION SPECTRUM OF LASER-INDUCED RED PHASE LB FILMS OF PDA 15-8

SCF ab initio Hartree Rock

Semi empirical (EH)

VEH gives ab initio quality results

σ and π bonds treated equally

MNDO - Excellent geometry all electrons.

	ΔH_f	Etot
PDA	498.6	-106275.8
PBT		-106159.7

Δ/rep. = 14.5 Kcals/Mole.

6-N

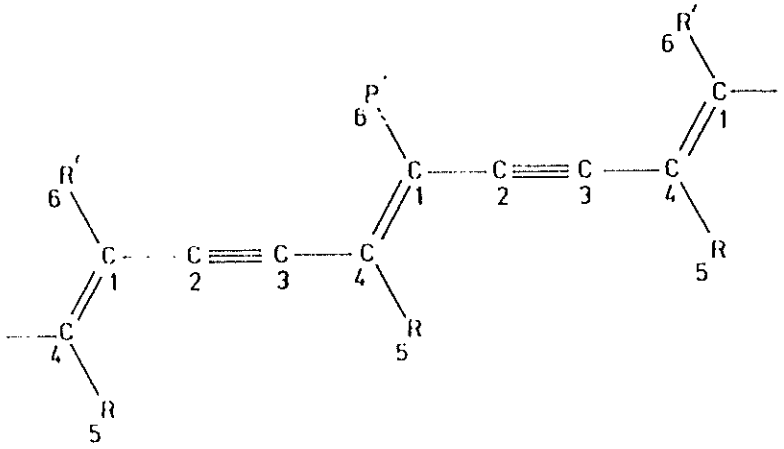

Structure of the polydiacetylene backbone. The numbers label the carbon atoms on the backbone and the single masses representing the sidegroups R and R' in the vibrational model.

BANDGAP OF PDA AS A FUNCTION OF NONPLANARITY

	0°	5°	10°	15°	20°
eV	2.596	2.558	2.585	2.612	2.721
cm^{-1}	20938	20631	20850	21070	21947
nm	478	485	480	475	456

EFFECT OF SUBSTITUENTS ON PDA ELECTRONIC STRUCTURE

	BW	E_g	E_{ip}
PDA	3.972	2.596	5.338
	(32043)	(20938)	(43056)
$+_2^-$ PDA	1.115	1.769	4.903
	(8998)	(14266)	(39544)
$(CH_3)_2^-$ PDA	3.265	2.449	5.039
	(26337)	(19753)	(40642)

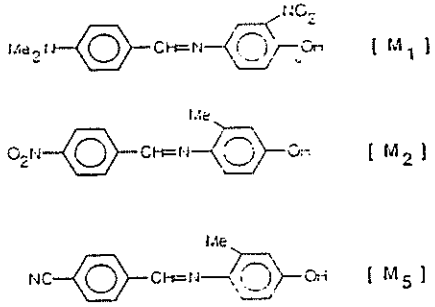

Molecular Structures of Some Representative Molecules

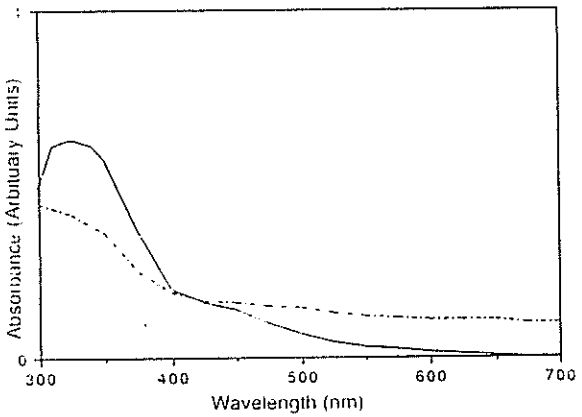

Visible Spectra of Partially Oxidized Polypyrrole in Solution

Part-I

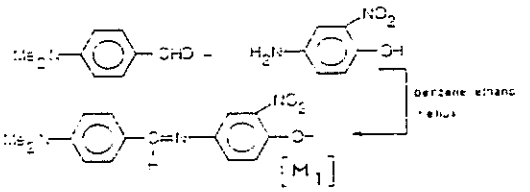

Part-II

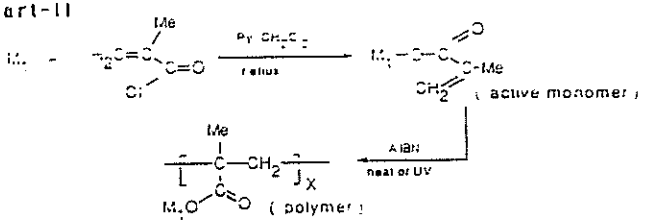

Part-III

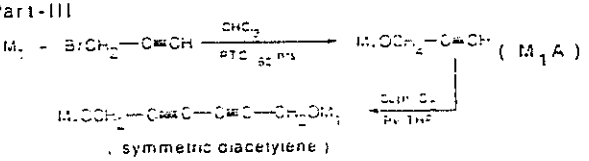

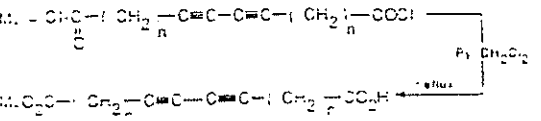

Synthetic Scheme

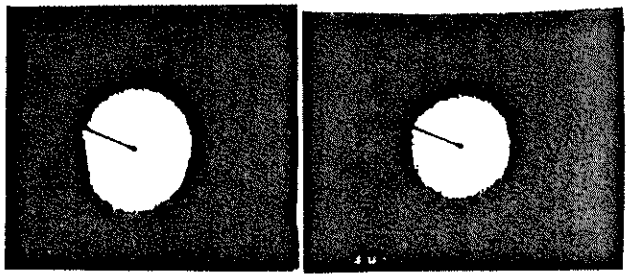

PYRROLE: HDP=500: 1 POLYPYRROLE

d_1=2.58A d_1=2.54A

d_2=1.55A d_2=1.55A

d_3=1.33A

d_4=1.01A

d_5=0.90A

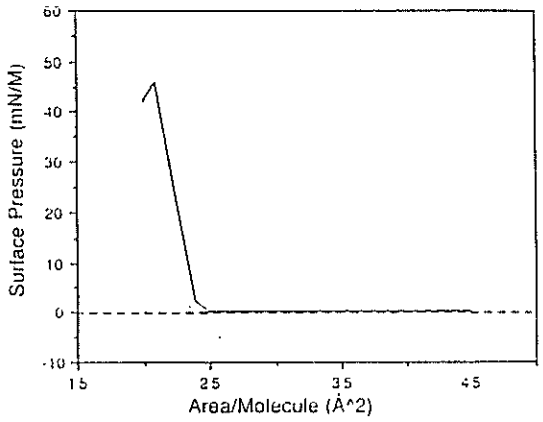

Isotherms of 3-Hexadecyl Pyrrole

(mixed monolayers with pyrrole monomer)

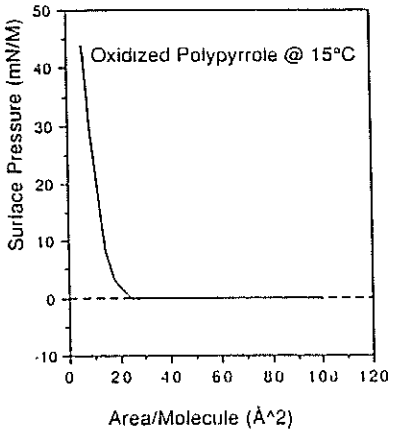

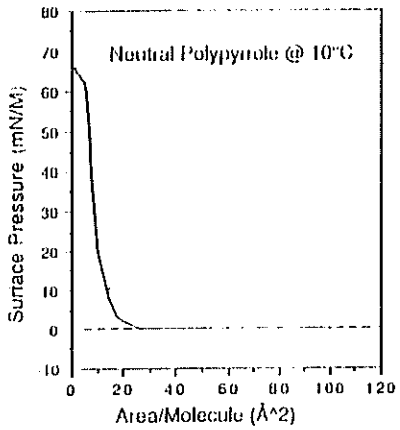

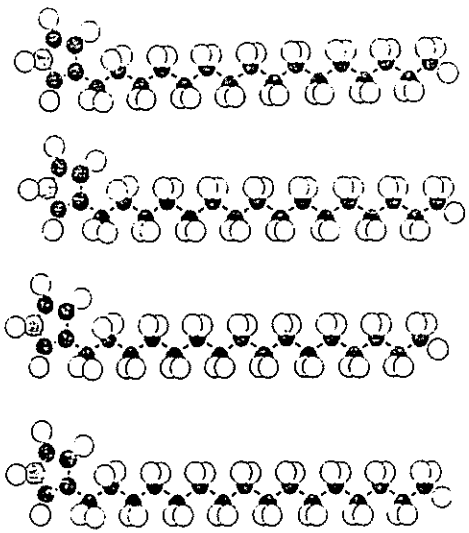

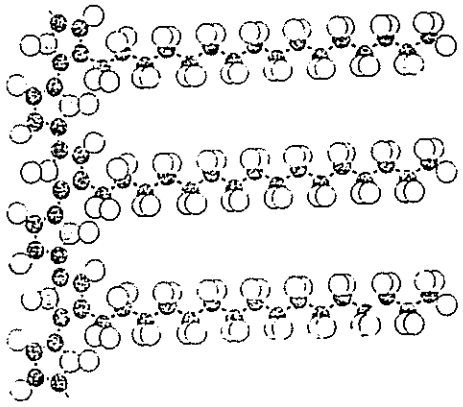

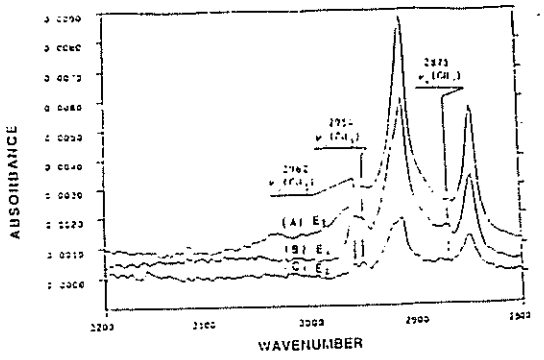

IR SPECTRA OF $C_{18}H_{33}$-PYRROLE LB FILMS IN THE C-H STRETCHING REGION.

(A) TRANSMISSION OF 5 MONOLAYERS ON ZnSe

(B) GIR OF 5 MONOLAYERS ON Pt

(C) GIR OF 1 MONOLAYER ON Pt

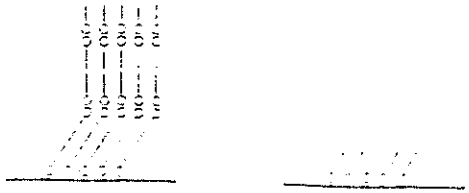

I. Peterson
GEC Research, Ltd., Great Britain

THE NONLINEAR OPTICS OF LANGMUIR-BLODGETT FILMS

THE NONLINEAR OPTICS OF LANGMUIR-BLODGETT FILMS

Theoretical advantages:

- Good geometry
- Chromophore alignment
- Dense packing

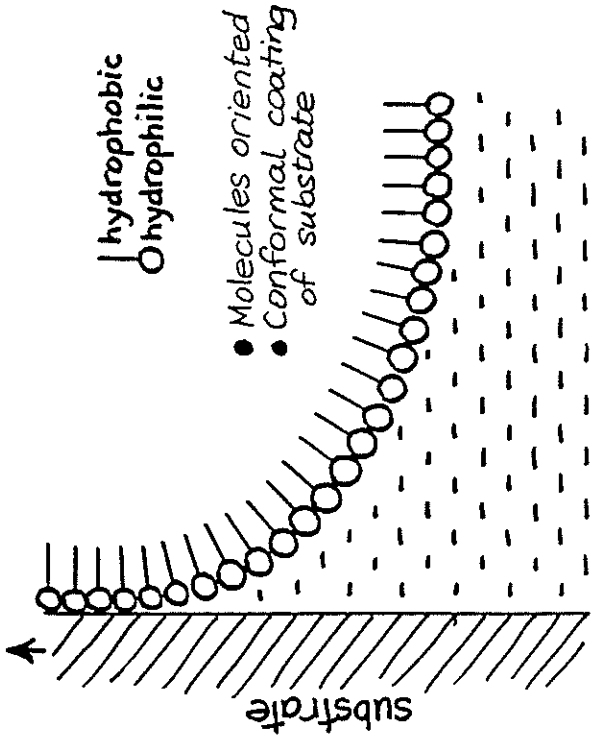

Building up thick films

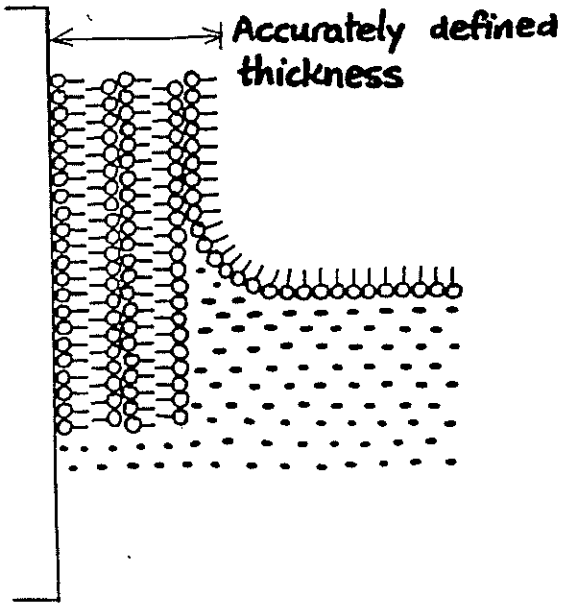

Geometry

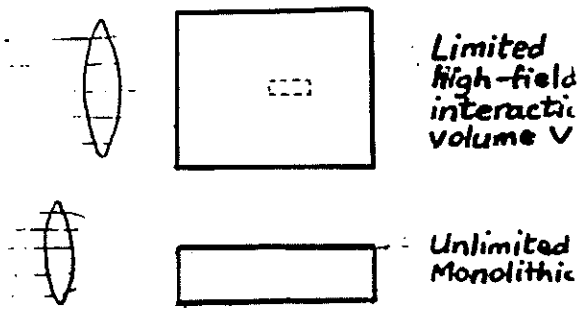

Overlay structure

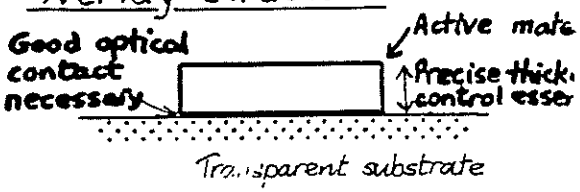

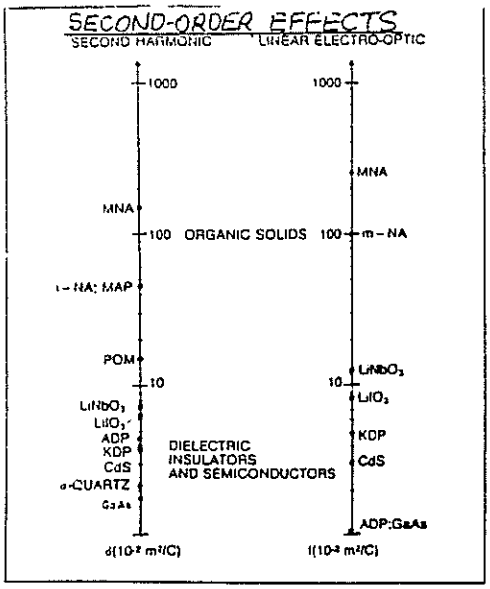

Fig 1 *Comparison of nonlinear optical figures of merit for organic and inorganic solids. (d is measured at 1.06 μm; l is the strain-free quantity measured at 0.633 μm, except for GaAs where it is measured at 0.9 μm)*

FGarito & KDSinger
Laser Focus 80(1982)59

WHAT MOLECULE?

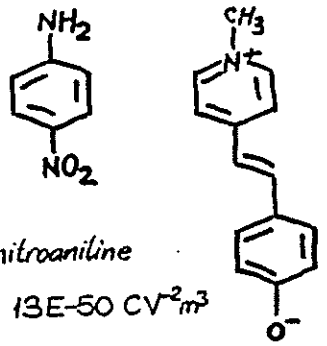

p-nitroaniline
β = 13E-50 $CV^{-2}m^3$

'Gedye'
merocyanine
β = 370E-50 $CV^{-2}m^3$

$\frac{\beta}{\xi_0 V}$ 65 pm/V 1100 pm/V

cf $LiNbO_3$ $\chi^{(2)}_{SHG}$ = 10 pm/V

Two-state Approximation

$$\beta = \frac{3e^2\hbar^2}{2m} \cdot \frac{W_0}{(W_0^2 - 4W^2)(W_0^2 - W^2)} \cdot f\Delta\mu$$

W_0	State transition energy
W	Photon energy $\hbar\omega$
f	Oscillator strength
$\Delta\mu$	Dipole moment difference

The best materials have

- Long-wavelength absorption
- Strong absorption
- Charge transfer

Ian Girling
Graham Cross
John Earls
} GEC Hirst Researc

JOERS (LB nonlinear opt

Durham	Mike Petty
Lancaster	Richard Tredgold
Hull	George Gray
Plessey	Jack Brettle
British Telecom	Roger Heckingbott

My new address.....

Institut für phys. Chemie
Universität Mainz FRG

Y-type film

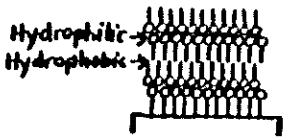

Stable but $\chi^{(2)}$-inactive

X- and Z-type films

X

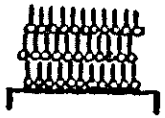

$\chi^{(2)}$-active but unstable

Z

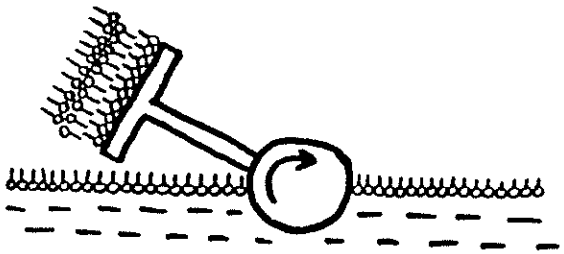

Deposition of $\chi^{(2)}$-active

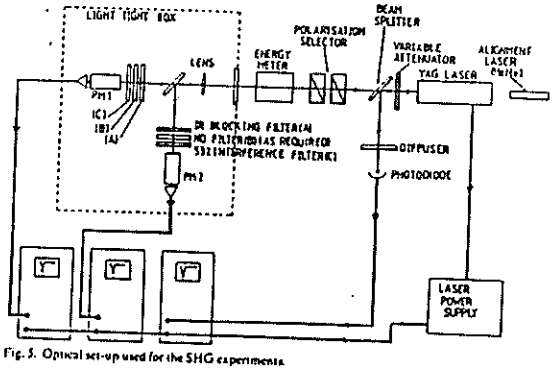

Fig. 5. Optical set-up used for the SHG experiments

Second Harmonic Generation

GEDYE MEROCYANINE MONOLAYERS

	$\chi^{(2)}$(pm/V) $\theta°$	
Low π	250	15
High π	1300	9

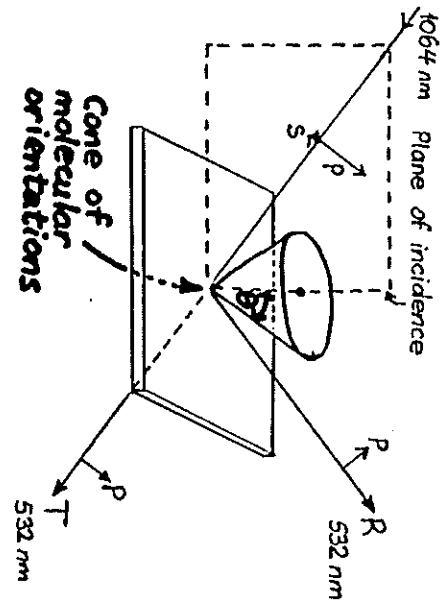

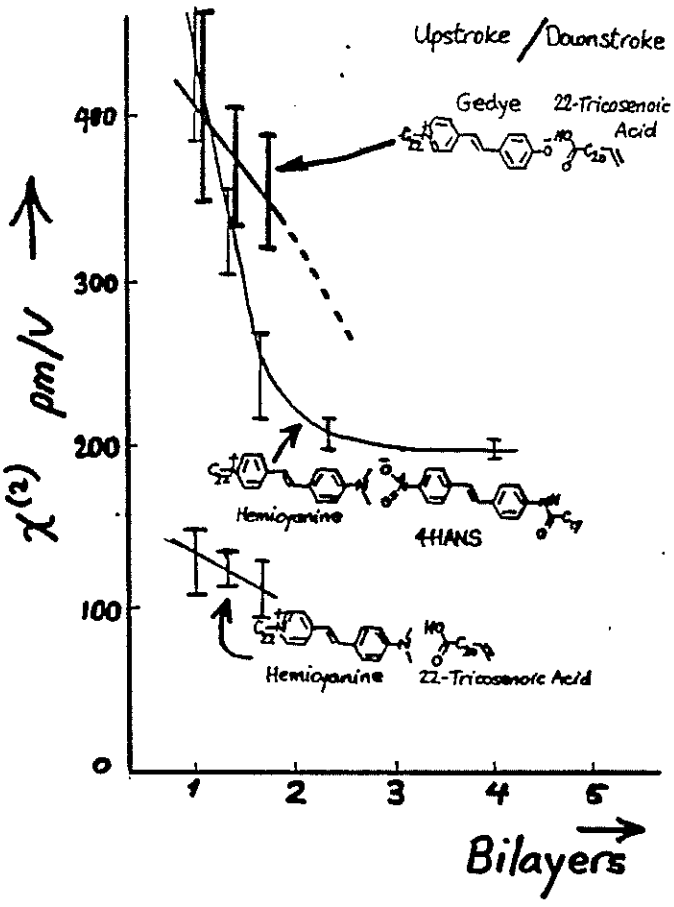

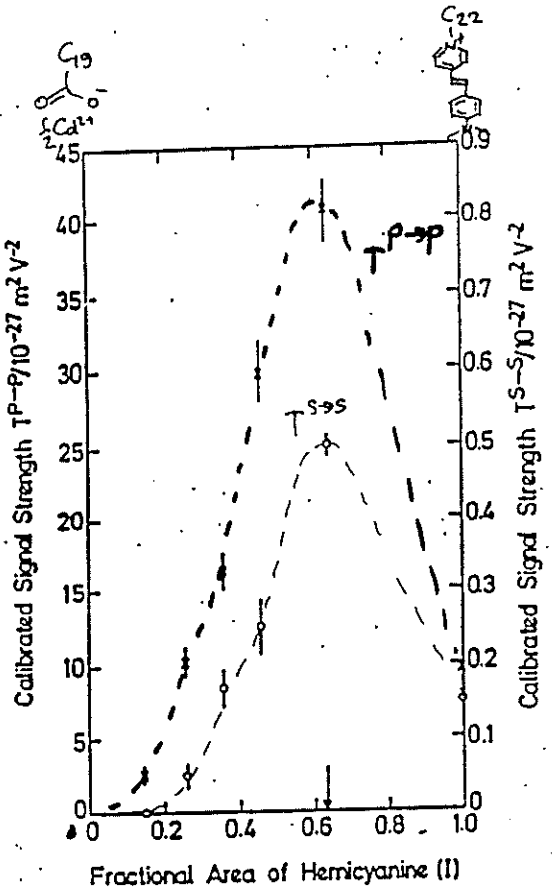

4 $T^{p\to p}$(x) and $T^{s\to s}$(o) second harmonic signal (10^{-27} m^2V^{-2}) from mixed monolayer

Measurement of refractive index

Surface plasmon Attenuated Total Reflection

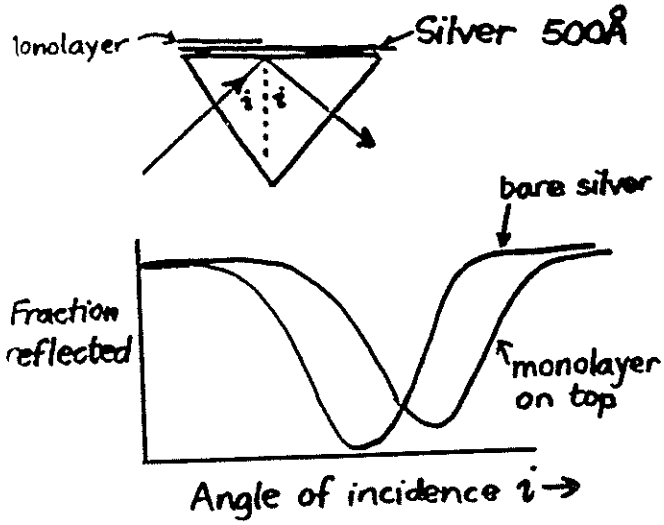

Pockels-ATR Technique

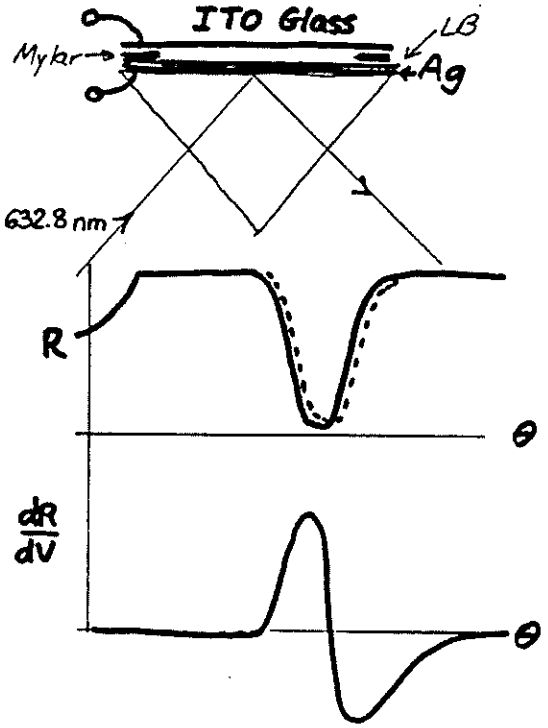

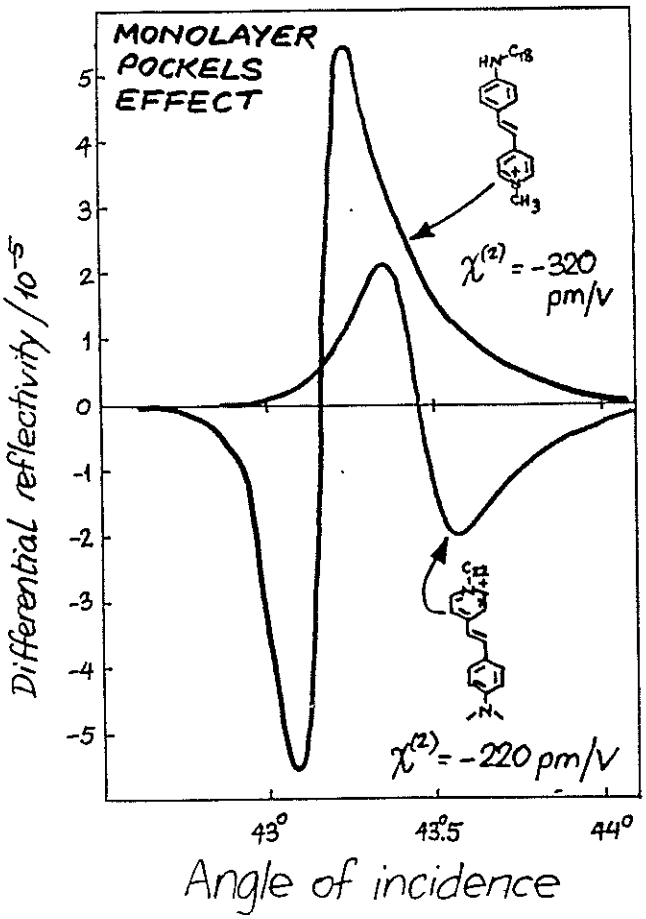

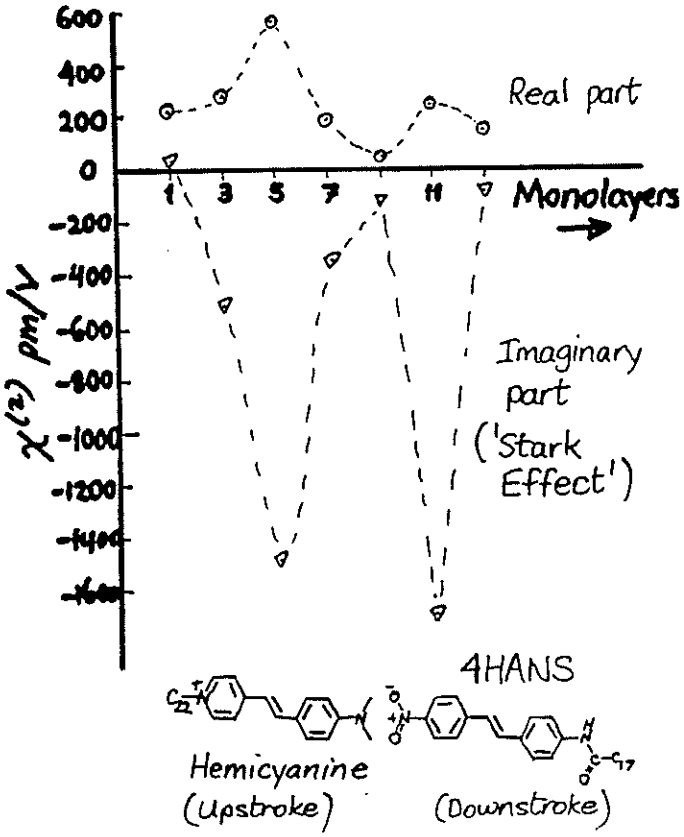

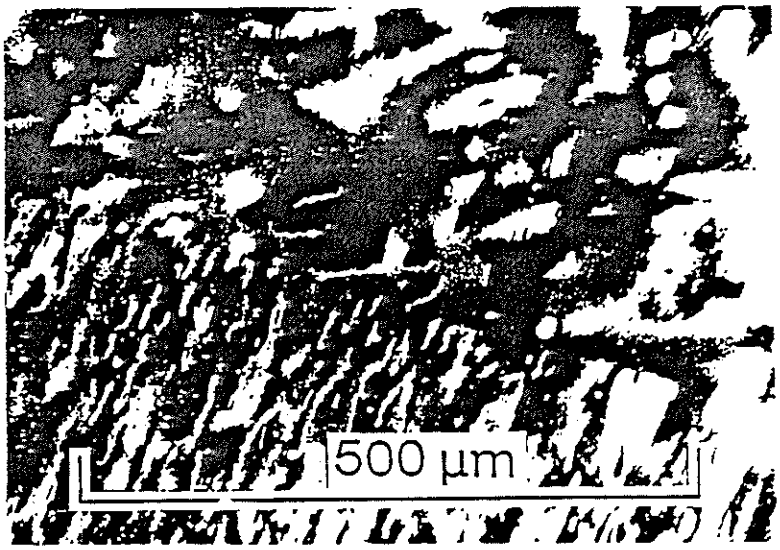
500 µm

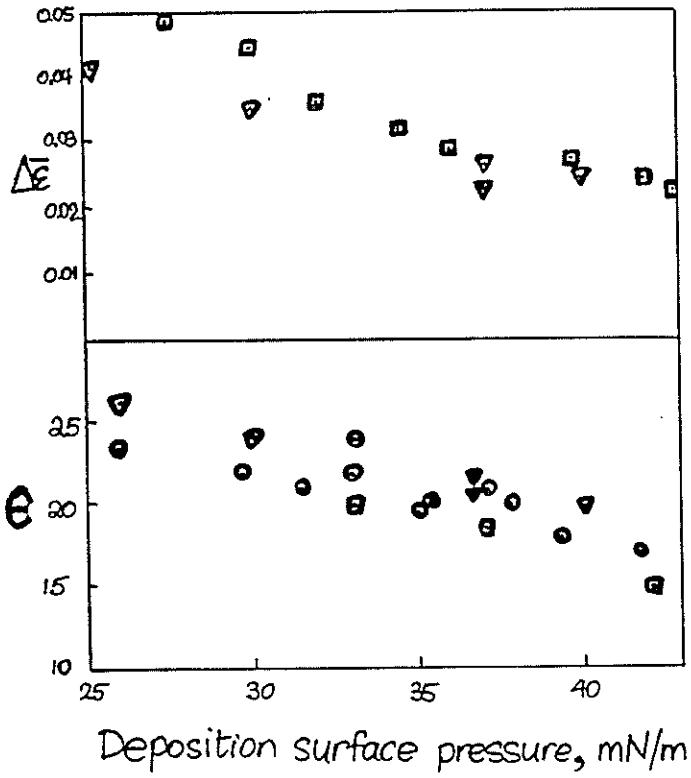
0.05
0.04
0.03
0.02
0.01
Δε
25
20
15
10
ε
25
30
35
40
Deposition surface pressure, mN/m

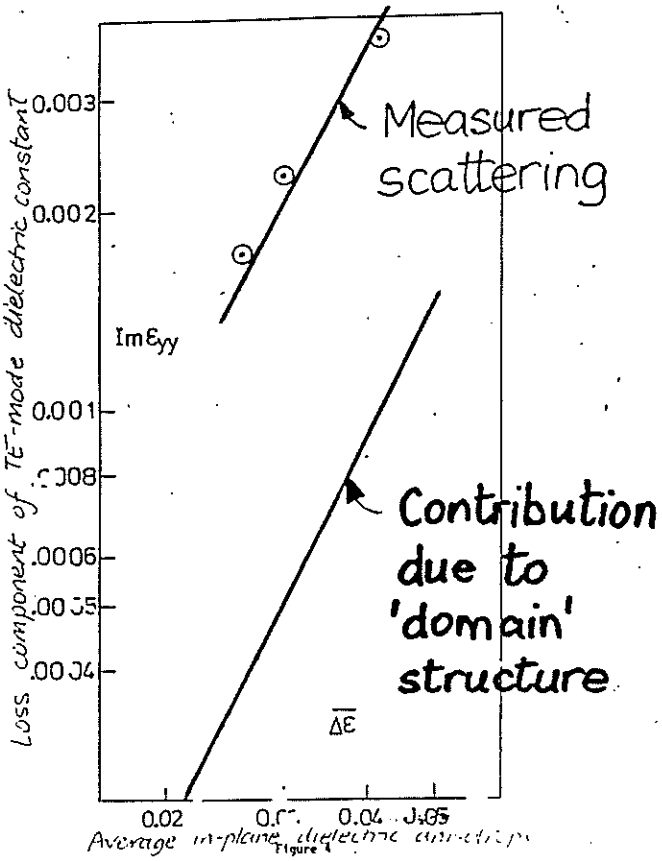
Loss component of TE-mode dielectric constant
0.003
0.002
0.001
Im εyy
Measured scattering
Contribution due to 'domain' structure
Δε
0.02
0.04
Average in-plane dielectric anisotropy

Figure 4

R. S. Lytel
Lockheed Research and Development

ADVANCES IN ORGANIC ELECTRO-OPTIC DEVICES

R&DD
ORGANICS

LOCKHEED

ADVANCES IN ORGANIC ELECTRO-OPTIC DEVICES

MAY 19, 1988

R. LYTEL

Lockheed Research and Development Division
LOCKHEED MISSILES AND SPACE COMPANY, INC.
3251 Hanover St., Palo Alto, California 94304

R&DD
ORGANICS
3/88

ACKNOWLEDGEMENTS

LOCKHEED

DARPA
* J. NEFF

AFOSR
* D. ULRICH

AFWAL/AFML
* P. LAND

U.S. ARMY
* E. SHARP
* W. EISER

U. PENN
* A.F. GARITO

HOECHST-CELANESE
* J. STAMATOFF
* R. DEMARTINO
* H. YOON

U. S. MISS.
* A. GRIFFIN

R&DD
ORGANICS
3/88

THE LOCKHEED ORGANIC DEVICES GROUP

LOCKHEED

SYNTHESIS

S. ERMER
M. STILLER

ANALYSIS

S. KWIATKOWSKI
G.F. LIPSCOMB
R. LYTEL
D. SWANSON
A. TICKNOR

GRATINGS/FILTERS

M. STILLER
B. SULLIVAN

CHARACTERIZATION

J. ALTMAN
K. ARON
P. ELIZONDO
G. HANSEN
G.F. LIPSCOMB
R. STONE

WAVEGUIDES

G.F. LIPSCOMB
R. LYTEL
M. STILLER
J. THACKARA
A. TICKNOR

SPATIAL LIGHT MODULATORS

D. ARMITAGE
W. EADES
M. STILLER
J. THACKARA

R&DD
ORGANICS
3/88

MAJOR BENEFITS OF NONLINEAR ORGANIC/POLYMERIC MATERIALS

LOCKHEED

* ORGANIC/POLYMERIC MATERIALS OFFER UNIQUE OPTICAL AND STRUCTURAL FEATURES FOR DEVICE APPLICATIONS

* MOLECULAR PROPERTIES CAN BE ENGINEERED TO ACHIEVE DESIRED MACROSCOPIC PROPERTIES

STRUCTURAL	OPTICAL
* MOLECULAR ENGINEERING	* LARGE, NONRESONANT RESPONSE
* THIN FILMS AND BULK CRYSTALS	* LOW DC DIELECTRIC CONSTANTS
* ROOM-TEMPERATURE OPERATION	* FAST NLO RESPONSE
* CHEMICAL/STRUCTURAL STABILITY	* HIGH OPTICAL DAMAGE THRESHOLD
* INTERNAL GRATINGS/STRUCTURE	* BROADBAND
* ARCHITECTURAL FLEXIBILITY	* LOW ABSORPTION

R&DD ORGANICS 3/88

ORGANIC MATERIALS IN INTEGRATED OPTICS

LOCKHEED

- CURRENT TECHNOLOGY: $TeLiNbO_3$
  - Materials Dev. Began in 1960s
- r = 32 pm/V
  - Larger Modulating Voltage
  - Little Improvement Expected
- LIMITED FABRICABILITY
  - 1000°C Processing
  - Depth Limited to 5 μm
  - Low Index Change Δn
  - Loss > 0.1 dB/cm
  - Optical Damage (Photorefractor)
- LARGE DIELECTRIC CONSTANT (28)
  - Longer Time Constants = RC
  - Large Velocity Mismatch in Traveling Wave Modulator
- MASS PRODUCTION DIFFICULT

- PROPERTIES OF POLYMERIC ORGANIC E-O MATERIALS
  - Materials Dev. Began 1975
- r = 14-53 pm/V (poled films*)
  - Lower Modulating Voltage
  - Potentially Much Larger r
- FLEXIBLE FABRICATION
  - Low Temperature Processing
  - Flexible Dimensions
  - Controllable Index Change Δn
  - Loss < 0.8 dB/cm**
  - High Optical Damage Threshold
- LOW DIELECTRIC CONSTANT (4)
  - Shorter Time Constants = RC
  - Smaller Velocity Mismatch
- POTENTIAL FOR MASS PRODUCTION

* See Proc. Materials Research Society, Boston MA (12/87)
** Current Lockheed/Hoechst Celanese Result

R&DD ORGANICS 3/88

ORGANIC MATERIALS IN OTHER DEVICES

LOCKHEED

ELECTRO-OPTIC DEVICES	ALL-OPTICAL DEVICES
* SPATIAL LIGHT MODULATORS, TUNABLE FILTERS, SHUTTERS	* ETALON SWITCHES, ALL-OPTICAL FILTERS, NONLINEAR WAVEGUIDE DEVICES
* MATERIALS WITH LARGE r AND LOW DIELECTRIC CONSTANTS EXIST AND ARE AVAILABLE	* NONRESONANT NONLINEARITIES ARE STILL FAR TOO SMALL FOR MICRON-SIZED DEVICES-RESONANT MATERIALS REQUIRED
* FABRICATION UNDERWAY IN THIS PROJECT	* NONRESONANT MATERIALS NEARLY ADEQUATE FOR GUIDED WAVE DEVICES

R&DD ORGANICS 3/88

ORGANIC E-O THIN-FILM WAVEGUIDE MODULATORS

LOCKHEED

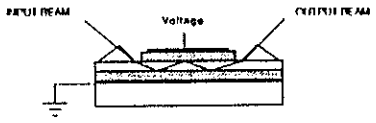

CONTACTS	BUFFER LAYERS	POLYMERS
COPPER	POLYSILOXANE RESIN	MNA/PMMA
ALUMINUM	UV CURABLE COATINGS	PC65
GOLD	SILICON DIOXIDE	C-22
ITO	2-COMPONENT EPOXY	HCC-1237 (new)

* TYPICAL LAYER THICKNESS OF ORDER 2 MICRONS
* POLING ACCOMPLISHED PRIOR TO FINAL ASSEMBLY

POLED ORGANIC E-O LAYER PREPARATION

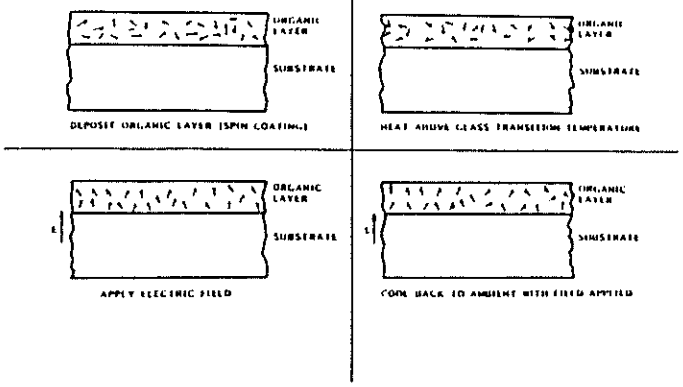

H&DD ORGANICS 3/88

POLED POLYMER FILMS AND SLAB WAVEGUIDE MODULATORS

LOCKHEED

(wavelength = 0.83 μm)	PC6S	C-22
E-O COEFFICIENT (pm/V)	2.8	14.0
TM REFRACTIVE INDEX (POLED)	1.7	1.58
TM INDEX DIFFERENCE (POLED-UNPOLED)	0.06	0.005
WG LENGTH (cm)	1.8	2.5
MEASURED LOSS (dB/cm)	3-4	0.8
HALF-WAVE VOLTAGE (volts)	48	7

H&DD ORGANICS 3/88

FABRICATION OF CHANNEL WAVEGUIDES BY SELECTIVE POLING

LOCKHEED

- SINGLE POLARIZATION BURIED CHANNEL WAVEGUIDES CAN BE FABRICATED BY SELECTIVE ELECTRIC FIELD POLING IN THIN FILM POLYMERS USING VERTICAL OR TRANSVERSE ELECTRODES
- POLING PRODUCES HIGHER-INDEX, E-O CHANNELS BURIED IN SURROUNDING, UNPOLED, LOWER INDEX POLYMER
- WAVEGUIDE PATTERN DEFINED BY PHOTOLITHOGRAPHY
- RELATIVELY LOW TEMPERATURE PROCESSING, 100-200 C
- FLEXIBLE DIMENSIONS IN HEIGHT AND WIDTH, 1-100 MICRONS
- VARIABLE INDEX DIFFERENCE Δn=0.001-0.05
- CAN MODE MATCH TO STANDARD SINGLE MODE FIBER
- CONCEPT PROVED IN DEVICE STRUCTURES: MACH-ZEHNDER INTERFEROMETER, COUPLER, TRAVELING WAVE MODULATOR

H&DD ORGANICS 3/88

VERTICAL AND TRANSVERSE POLING OF GLASSY POLYMER FILMS/WAVEGUIDES

LOCKHEED

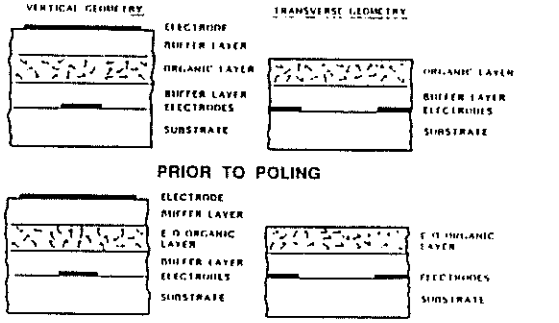

LOCKHEED

ORGANICS
1/88

INTEGRATED OPTIC MODULATOR FABRICATION

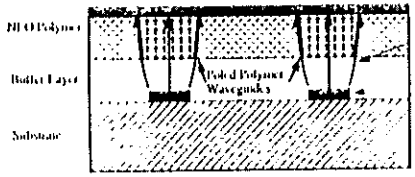

Fabrication of Poled Polymer Waveguide Structure

Top View of Modulator

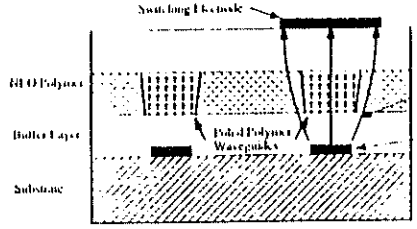

Optical Modulation By Electro-Optic Modulation

LOCKHEED

ORGANICS
3/88

CHANNEL BOUNDARY IN SELECTIVELY-POLED GUIDES

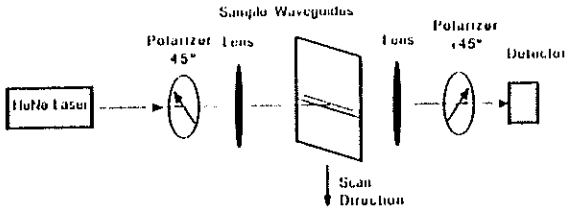

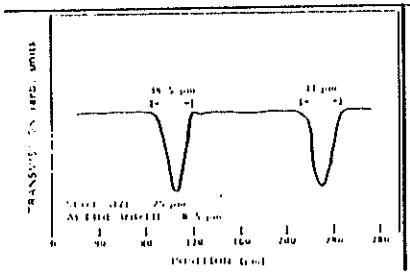

- Test of the Extent of Poling Beyond the Electrode Boundaries
- Sample Placed at 45° Between Crossed Polarizers
- Focused HeNe Spot Scanned Across Poled Waveguide Regions
- Poling Induced Birefringence at the Guide Boundary Would Cause Increased Signal
- Metallic Poling Electrode Blocks Beam and Causes a Dip in the Background Signal
- Poling Sharply Confined to the Electroded Region

R&DD
ORGANICS
3/88

LOCKHEED

FABRICATION AND OPERATION OF A SELECTIVELY-POLED M-Z INTERFEROMETER

ITO Switching Electrode

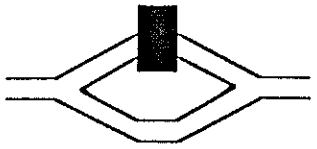

- POLED PC6S: 90° C, 5 MIN, 100 V/μm
- GOLD POLING ELECTRODE ON PC6S, REMOVED AFTER POLING
- 1° BRANCH ANGLE
- 780 nm LIGHT, TM MODE CONFINED
- GUIDE DIMENSIONS 2 x 7 μm

Device Structure After Poling Completed

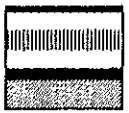

ITO switching electrode
3 μm epoxy buffer
2 μm PC6S E O polymer
3 μm UV curable coating
patterned aluminum electrode
glass substrate

INPUT Y-BRANCH

R&DD ORGANICS 3/88 — LOCKHEED

FABRICATION AND OPERATION OF A SELECTIVELY-POLED DIRECTIONAL COUPLER

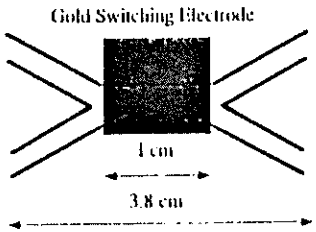

- POLED C-22; 105° C, 15 MIN., 90 V/μm
- 3° COUPLING ANGLE
- 830 nm LIGHT, TM MODE CONFINED
- INPUT/OUTPUT GUIDES 2 x 7 μm
- COMMON GUIDE 2 x 13 μm

Device Structure After Poling Completed

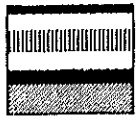

gold switching electrode
3 μm polysiloxane buffer
2 μm C-22 E-O polymer
3 μm UV curable coating
patterned aluminum electrode
glass substrate

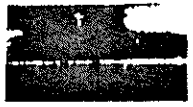

a) BAR STATE (120 V)

b) CROSS STATE (65 V)

R&DD ORGANICS 3/88 — LOCKHEED

TRAVELING WAVE INTEGRATED OPTIC PHASE MODULATOR

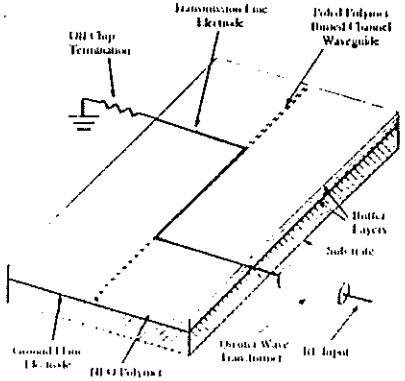

- POLED C-22 CHANNEL (100V/μm)
- ACTIVE PATH LENGTH 3 cm
- WAVELENGTH 830 nm
- DEVICE IMPEDANCE 9.5 ohms
- DRIVE SIGNAL 0.5 W (applied through transformer, 1/4 wave @250 MHz)

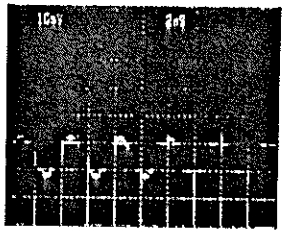

R&DD ORGANICS 3/88 — LOCKHEED

TRAVELING WAVE MODULATORS

- PHASE MODULATOR IN ONE ARM OF A MACH ZEHNDER INTERFEROMETER
- CALCULATED MODULATION DEPTH USING MEASURED AT LOW FREQUENCY EQUALS MEASURED MODULATION DEPTH AT HIGH FREQUENCY
- IMPEDANCE MATCHED, 9.5 Ω

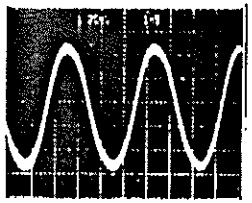

270 MHz

- PHASE MODULATOR IN ONE ARM OF A MACH ZEHNDER INTERFEROMETER
- RESPONSE SMEARED DUE TO IMPEDANCE MISMATCH, BUT
- CLEAR, GHz MODULATION IS OBSERVABLE

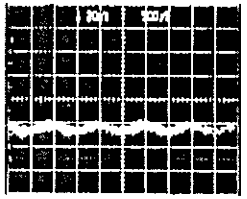

1 GHz

R&DD ORGANICS 3/88

SIGNIFICANCE OF ORGANIC E-O WAVEGUIDE RESEARCH — LOCKHEED

CRITICAL RESULTS	IMPLICATIONS
• POLED POLYMER WAVEGUIDE FAB IS CHEAP, FAST, AND SIMPLE	• MASS PRODUCTION POSSIBLE
• PATTERNS DETERMINED BY ORDINARY PHOTOLITHOGRAPHY	• COMPLEX DEVICES ON A CHIP
• E-O COEFFICIENTS NEARING LITHIUM NIOBATE LEVELS	• LOW DRIVING VOLTAGES COMPATIBLE WITH TTL
• DIELECTRIC CONSTANTS ARE 7-10 TIMES SMALLER THAN INORGANICS	• FASTER RESPONSE TIMES AND HIGHER SENSITIVITY
• MODULATION TO 1.3 GHz SHOWN, TO >>GHz ACHIEVABLE	• HIGH SPEED SWITCHING AND INTERCONNECTION
• DEVICES BUILT AND OPERATED: INTERFEROMETERS, COUPLERS, AND TW PHASE MODULATORS	• PROOF OF CONCEPT COMPLETE, CAN MOVE TO COMPLEX DEVICE FABRICATION

B. K. Nayar

British Telecom Research Laboratories, U. K.

ORGANIC NONLINEAR OPTICAL DEVICES AND MATERIAL CONSIDERATIONS

M. Thakur

AT&T

TOWARDS NONLINEAR OPTICAL APPLICATIONS OF POLYDIACETYLENES

R-2

TOWARD NONLINEAR OPTICAL APPLICATIONS OF POLYDIACETYLENES

M. THAKUR
AT&T BELL LABORATORIES

B. I. GREENE
J. ORENSTEIN
K. TAI
G. C. CHI
K. J. O'BRIEN
Y. SHANI
M. GOMEZ
H. TANAKA
A. TONELLI

TOPICS

- MATERIALS ASSESSMENT
- GROWTH OF THIN SINGLE CRYSTAL FILMS
- FABRICATION OF DEVICE STRUCTURES
- DEMONSTRATION OF CHANNEL WAVEGUIDING
- INTENSITY DEPENDENT PHASE-MODULATION

IMPORTANT PARAMETERS FOR MATERIALS SELECTION

- EXTENT OF CONVERSION (MONOMER → POLYMER)
- EXTENT OF CONJUGATION (PLANARITY)
- THERMAL STABILITY (THERMOCHROMISM)
- SOLUBILITY
- EASE OF CRYSTALLIZATION

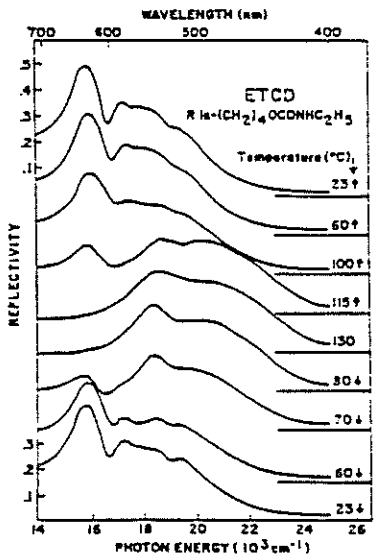

R-3

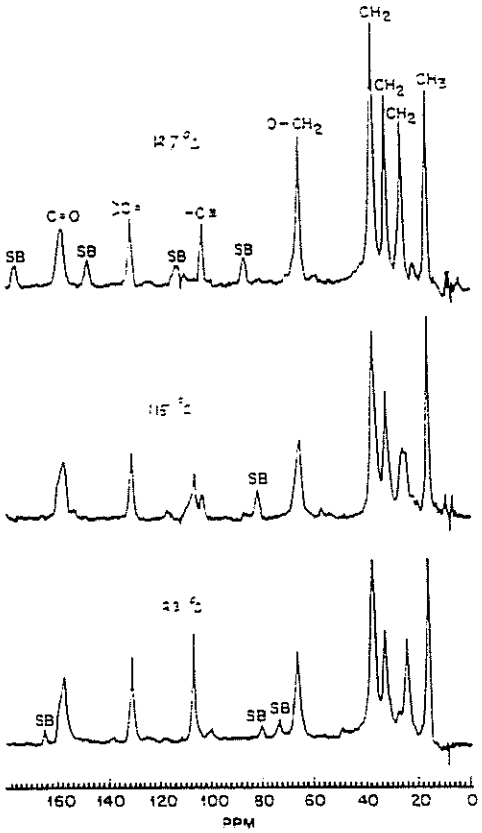

^{13}C Chemical Shifts of Polydiacetylenes

^{13}C, ppm vs. TMS

	C=O	≻C=	-C≡	α-CH_2	β-CH_2, γ-CH_2
ETCD (blue)	157.5	131.6	107.4	37.3	24.5
PTS-6 (blue)	—	131.3	107.1	—	—
PTS-12 (blue)	—	131.0	106	—	—
TCDU (blue)	—	—	107.3	—	—
ETCD (red)	158.3	132.0	103.6	37.8	26.4
TCDU (red)	155.8	131.5	102.9	37.9, 32.3	25.9, 21.8 28.0, 30.8
ETCD (melt)	158.1	130.8	102.5	37.3	27.2

CONCLUSIONS FROM NMR STUDIES

- THE CONJUGATION LENGTH IS DETERMINED BY THE EXTENT OF PLANARITY OF THE CHAIN-BACKBONE.
- INCREASE OF CHAIN LENGTH DOES NOT GUARANTEE INCREASE OF CONJUGATION LENGTH.
- THE ACETYLENIC FORM IS PREDOMINANT IN POLYDIACETYLENES INDEPENDENT OF PHASES.

R-4

SINGLE

GROWTH OF THIN FILM CRYSTALS

- THE SHEAR METHOD

  ORIENTATIONAL PRINCIPLES
  REQUIREMENTS ON MOLECULAR SHAPE
  GROWTH PARAMETERS
  CONTROL OF THICKNESS
  OPTICAL QUALITY OF FILMS

- COMPARISON WITH THE L-B METHOD

- ASSESSMENT OF APPLICABILITY

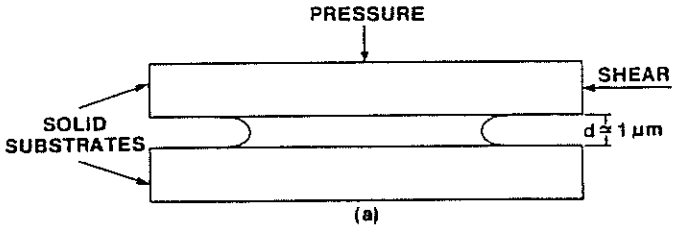

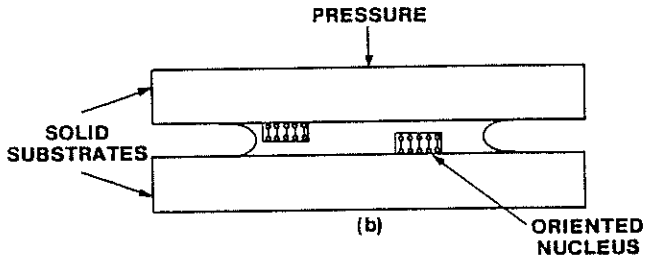

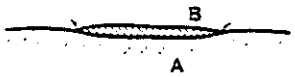

SPREADING COEFFICIENT

$$S_{B/A} = \gamma_A - \gamma_B - \gamma_{AB}$$

$$= W_{AB} - W_{BB}$$

γ = SURFACE TENSION
W_{AB} = WORK OF ADHESION
W_{BB} = WORK OF COHESION

FOR SPONTANEOUS SPREADING

$$S_{B/A} > 0$$

COMPARISON OF THE CALCULATED MOLECULAR LENGTHS WITH THE OBSERVED d-SPACINGS

MATERIALS	CALCULATED LENGTH L (Å)	COMPENSATED LENGTH $L\sin\phi$ (Å)	d-SPACINGS OF 1ST ORDER REFLECTIONS (Å)
$RC \equiv C - C \equiv CR$ WITH R			
1. $- CH_2 OH$	~8.1	8.1	8.05
2. $- (CH_2)_4 OCONH C_2H_5$	~17.9	17.9	17.87
3. $- (CH_2)_4 OCO NH C_6H_5$	~19.5	19.5	18.94
4. $- CH_2 OSO_2 C_6 H_4 CH_3$	~14.8	12.9	12.87
5. $- (CH_2) OCO NH CH_2COOC_4H_9$	~26.9	26.9	26.80
$NH_2 - C_6H_4 - C \equiv N$	~8.0	8.0	8.40
HO, HO, N, C_6H_4, NO_2	~10.5	10.5	10.05

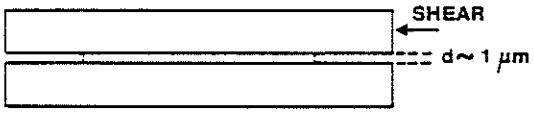

TOTAL SHEAR $T = T_{cap} + T_{ext}$
LATERAL PRESSURE $P \sim 10^7$ DYNES/cm^2
EQUILIBRIUM SPREADING PRESSURE OF A MONOLAYER
$P_{mono} \sim 10^7$ DYNES/cm^2

R-5

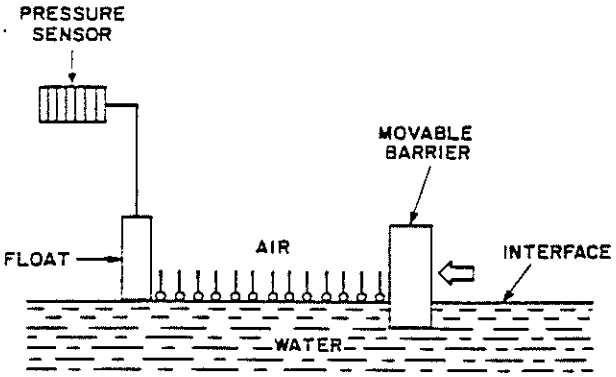

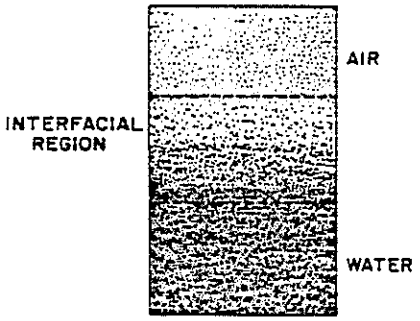

COMPARISON OF THE L-B AND THE SHEAR METHOD

- POLAR INTERACTIONS HAVE IMPORTANT ROLES IN BOTH THE METHODS.
- IN THE L-B TECHNIQUE A LIQUID IS USED AS THE SUBSTRATE. IN THE SHEAR METHOD SOLID SUBSTRATES ARE UTILIZED.
- THE L-B METHOD APPLIES TO AMPHIPHILIC MOLECULES ONLY. THE SHEAR METHOD IS APPLICABLE TO A BROADER RANGE OF MOLECULES.
- THE L-B METHOD PROVIDES ORDER ALONG ONE DIRECTION ONLY. THE SHEAR METHOD LEADS TO 3-D ORGANIZATION.
- THE L-B FILMS HAVE MICRO-DOMAIN MORPHOLOGY (POOR OPTICAL QUALITY). THE SHEAR-GROWN FILMS ARE UNIFORM SINGLE CRYSTALS (EXCELLENT OPTICAL QUALITY).

INTENSITY DEPENDENT PHASE MODULATION

$$n = n_0 + n_2 I$$

$$\Delta\phi = \frac{2\pi}{\lambda} n_2 I L \,, \quad L = \text{LENGTH OF PROPAGATION}$$

$\Delta\phi$ = PHASE SHIFT

FOR $\lambda \sim 0.8$ TO $2.0\,\mu$

n_2 OF PTS $\sim 7 \times 10^{-6}$ cm^2/MW (HERMANN AND SMITH, 1980)

IF OPTICAL PULSES ($\lambda \sim 1\,\mu$) OF PEAK POWER $\sim$ 500 mW ARE FOCUSSED ON A CROSS-SECTION $\sim 1\,\mu$m^2

$\Delta\phi \longrightarrow \pi$

FOR L $\sim$ 1.4 mm.

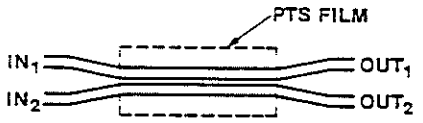

WITH SUBPICOSECOND PULSES
ENERGY REQUIREMENT < 1 pj/bit.
THE DATA-RATE THAT THE DEVICE COULD HANDLE $\sim$ 1 THz
NONABSORPTIVE ⟶ NO THERMAL DAMAGE.

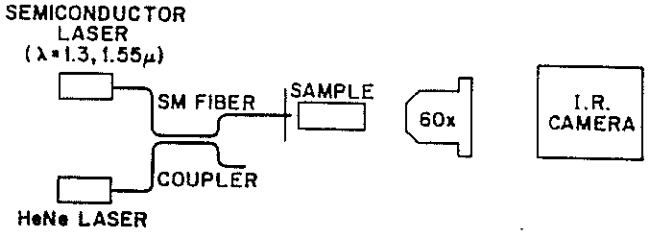

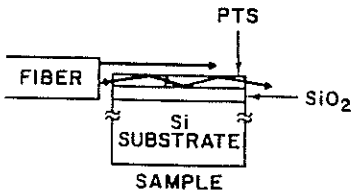

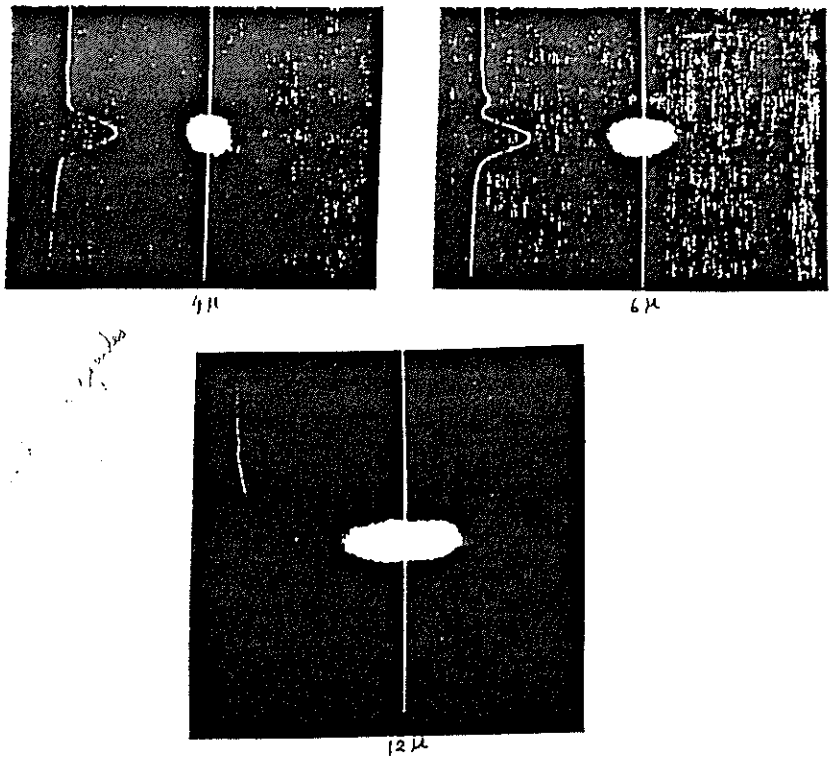

SUMMARY

- A COMPARATIVE EVALUATION IS MADE FOR DIFFERENT POLYDIACETYLENES IN RELATION TO NLO DEVICE APPLICATIONS.
- C^{13} – NMR RESULTS SHOW THAT THE CONJUGATION LENGTH IS DETERMINED BY THE EXTENT OF PLANARITY OF THE CHAIN BACKBONE AND NOT BY THE CHAIN LENGTH.
- THE ORIENTATIONAL PRINCIPLES OF THE SHEAR METHOD ARE DISCUSSED IN COMPARISON WITH THE L-B TECHNIQUE.

SUMMARY (Cont.)

- THE SUPERIORITY OF THE SHEAR METHOD IN PROVIDING GOOD OPTICAL QUALITY SINGLE CRYSTAL FILMS OF CONTROLLED THICKNESS AND ORIENTATION IS DEMONSTRATED WITH MANY EXAMPLES.
- CHANNEL WAVEGUIDING IS DEMONSTRATED (PROPAGATION > 5 mm) FOR SHEAR-GROWN PTS FILMS.
- PRELIMINARY RESULTS OF INTENSITY DEPENDENT PHASE CHANGE IN PTS WAVEGUIDES ARE DISCUSSED.

D. Haarer

Universitat Bayreuth, West Germany

HIGH RESOLUTION LASER SPECTROSCOPY IN POLYMERS

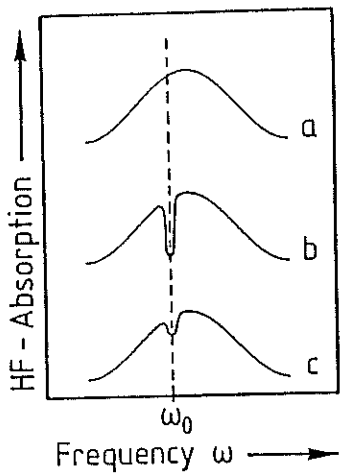

Fig.3.1. Local saturation of an NMR line at the frequency ω_0 (a) before, (b) during, and (c) after irradiation at ω_0 [3.1]

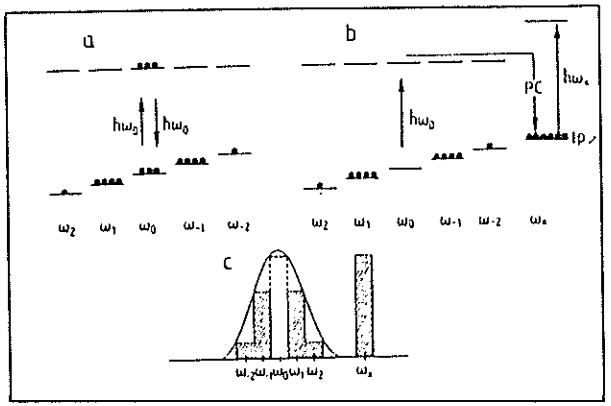

Fig.3.2. (a)Radiation saturation of an ensemble of five optical two-level systems at the center frequency ω_0. (b) Photochemical bleaching of an ensemble of five two-level systems at the center frequency ω_0. Creation of a photoproduct state absorbing at the frequency ω_x. (c) Absorption after photochemical bleaching as described in Fig.3.2b. The photoproduct shows up at the frequency ω_x

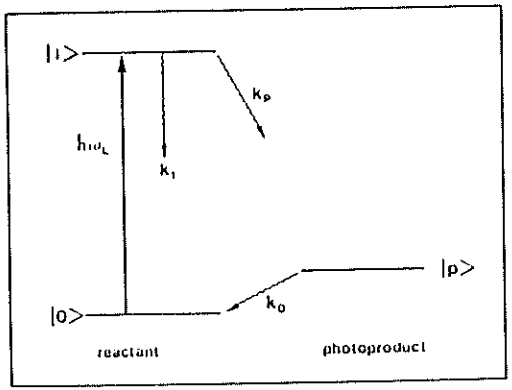

Fig.3.3. Three-level system with the reactant levels $|0\rangle$ and $|1\rangle$ and the photoproduct level $|p\rangle$. K_1, K_p and K_0 are the decay rate constants of the various states. ω_L is the hole-burning frequency

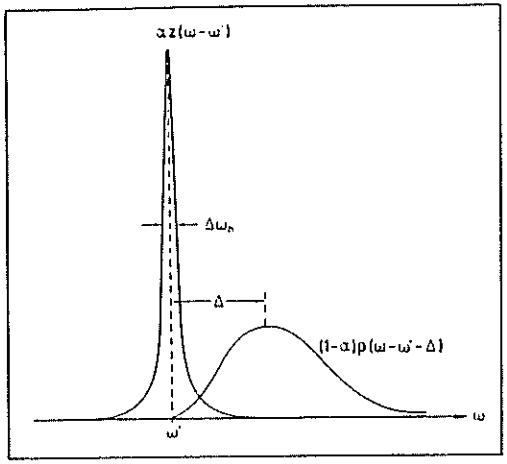

Fig.3.4. General lineshape function of an electronic excitation of a guest molecule in a solid host matrix: Schematic view of a zero-phonon line and its phonon sideband. The phonon sideband has an intensity of $(1-\alpha)$ and is displaced by the lineshift parameter Δ. The latter corresponds to half the "Stokes shift"

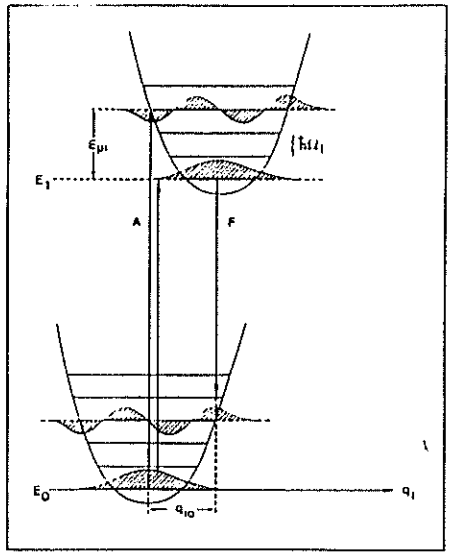

Fig.3.5. Energy diagram for interpreting phonon side-band spectra in terms of the excited state displacement q_{10}. The phonon frequency is Ω_1 The figure shows a zero-phonon and a three-phonon transition in absorption (A) and emission (F), respectively

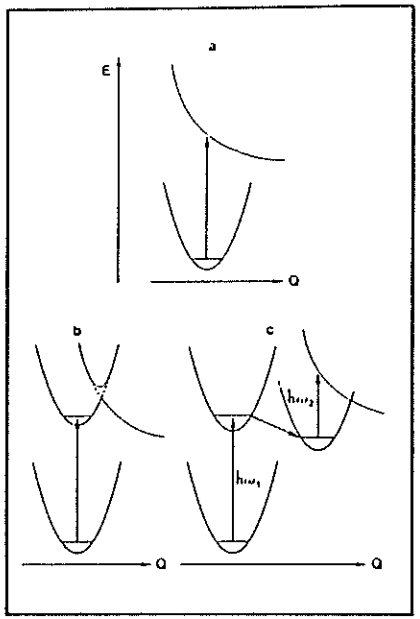

Fig.3.6a-c. Photochemical reaction schemes plotted as a function of one configurational coordinate Q. (a) Repulsive exciplex-like state. (b) Level-crossing from a "quasi-stable" excited state. (c) Two-photon reaction with photon energies $\hbar\omega_1$ and $\hbar\omega_2$. The level which absorbs the photon $\hbar\omega_2$ is a long-lived intermediate state

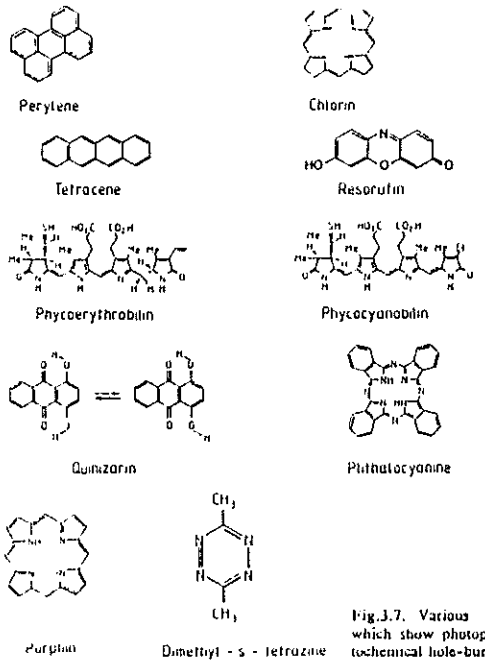

Fig.3.7. Various dye molecules which show photophysical and photochemical hole-burning

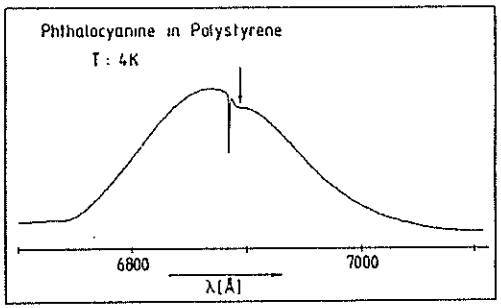

Fig.3.8. Experimental hole spectrum of phthalocyanine in polystyrene at 4 K. The pseudo-phonon wing is marked by the wavy arrow

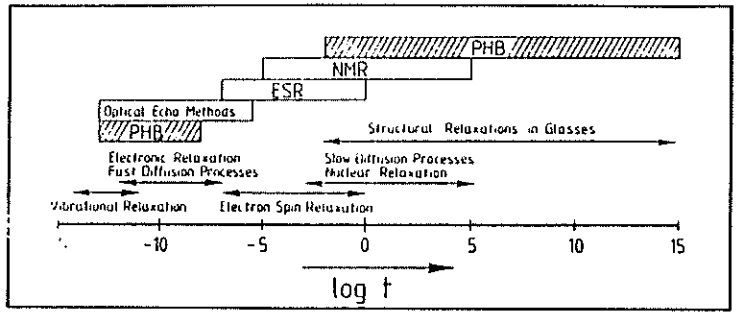

Fig.3.9. Logarithmic scale of relaxation times and of methods of measuring characteristic time constants. Hole-burning is especially well suited for very short and very long relaxation times (see text)

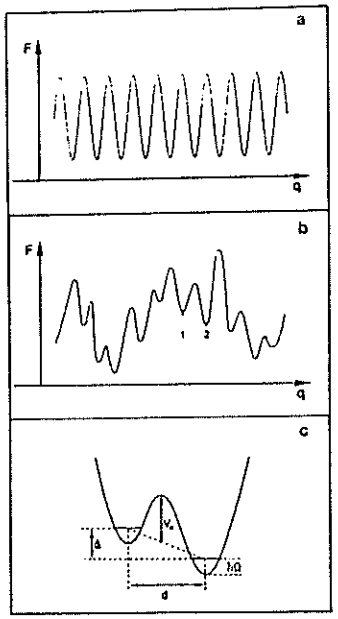

Fig.3.10. (a) Periodic potential of a crystalline solid. (b) Potential along a fictitious coordinate q of a glass: Note the lack of periodicity. (c) Idealized two level scheme with the two parameters Δ and V_0 (see text). The oscillators in the two wells are separated by the distance d and have a zero-point frequency on the order of Ω

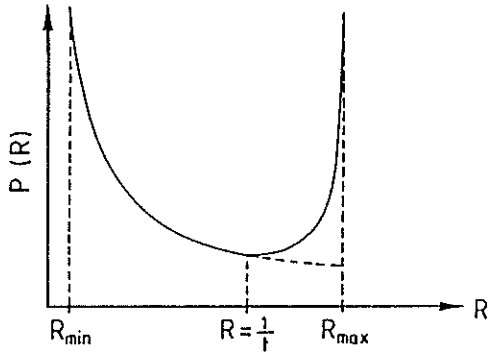

Fig.3.11. Rate distribution as calculated by *Jäckle* [3.98]. For the definition of the two limiting rates R_{min} and R_{max} see text

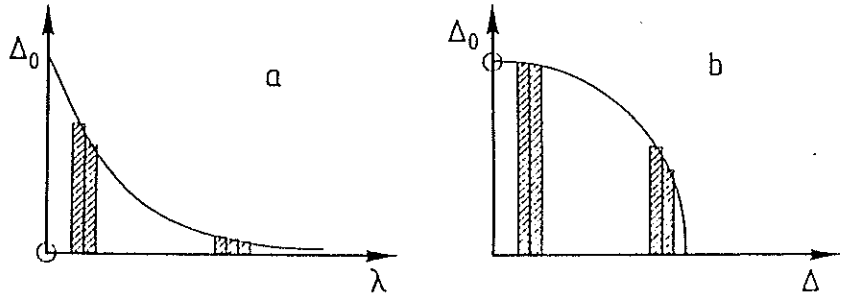

Fig.3.12. Functional dependence of the tunnelling matrix element Δ_0 on the TLS-parameters λ (Fig.3.12a) and Δ (Fig.3.12b) (see text)

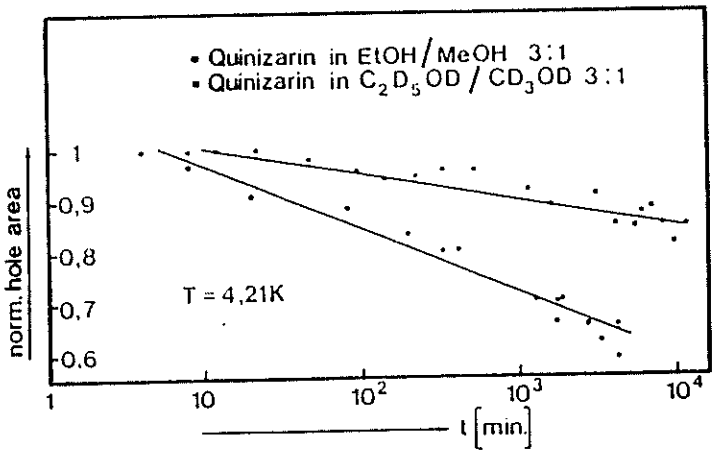

Fig.3.13. Time decay of the area of photochemical holes of quinizarin in alcohol glass for deuterated (*squares*) and protonated systems (*dots*)

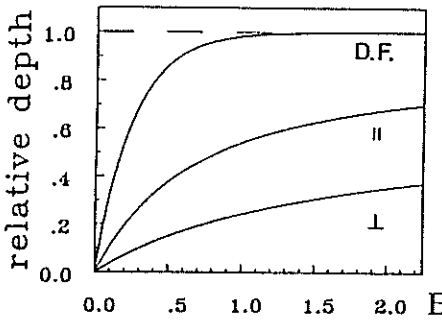

Fig.3.15. Dependence of the relative depth of a photochemical hole on the irradiated light dose B. The upper curve shows the maximally bleached distribution function with a polarization factor of unity. The two curves with parallel and perpendicular polarization are also shown [3.40]

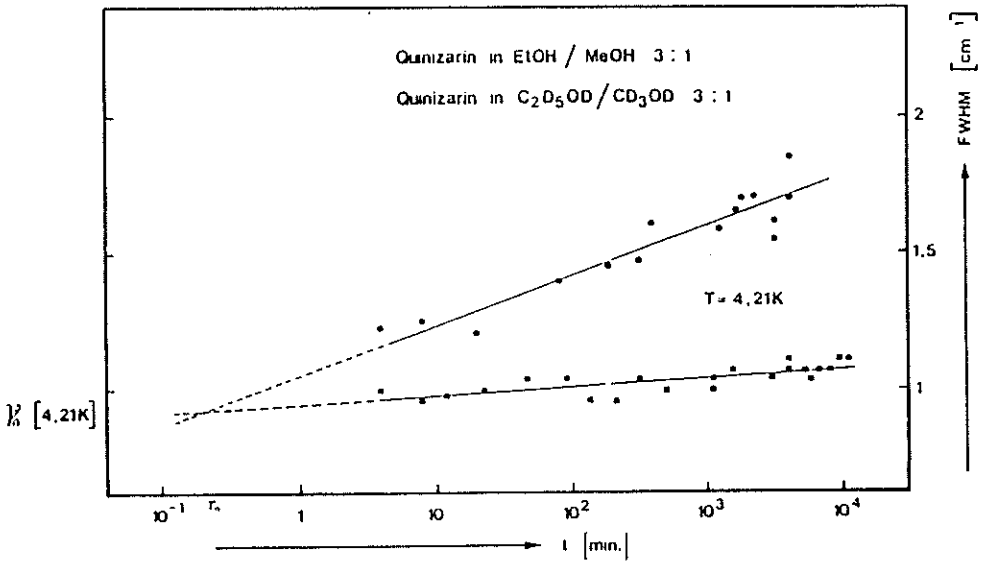

Fig.3.14. Line broadening of the photochemical holes of quinizarin in alcohol glass for deuterated (*squares*) and protonated systems (*dots*)

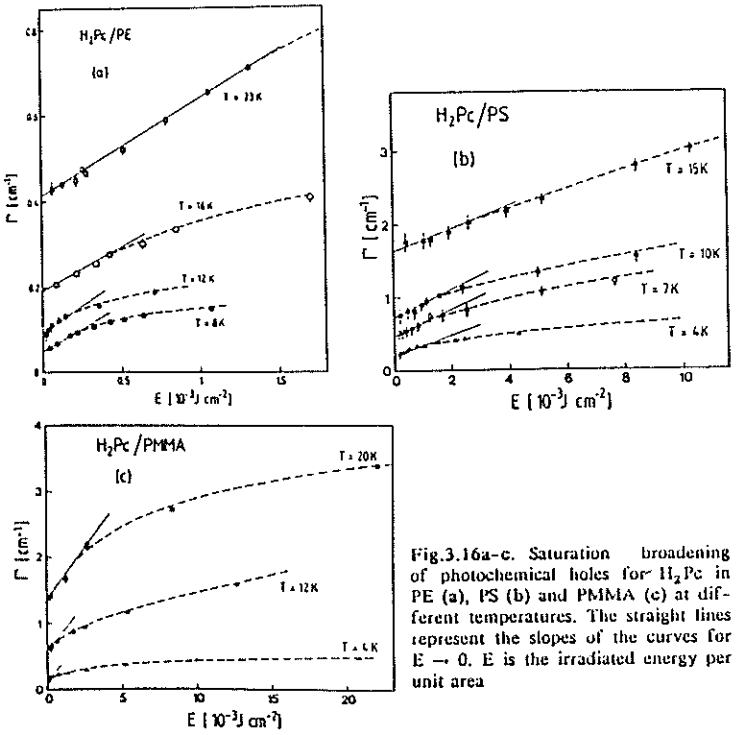

Fig.3.16a-c. Saturation broadening of photochemical holes for H_2Pc in PE (a), PS (b) and PMMA (c) at different temperatures. The straight lines represent the slopes of the curves for $E \to 0$. E is the irradiated energy per unit area

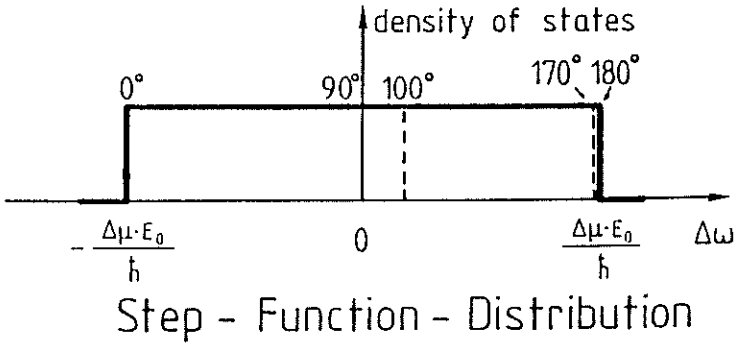

Fig.3.17. Distribution function of the absorption frequencies of guest molecules in an electric field E_0. All molecules absorb at the 0-frequency for E = 0; they have identical dipole moment changes $\Delta\mu$ but are oriented randomly with respect to the external E-field. The numbers indicate the orientation angles for some representative frequency shifts

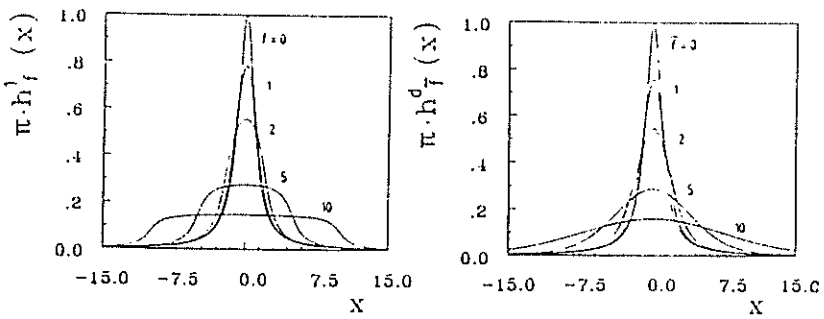

Fig.3.18. (a) Theoretical lineshape of a spectral hole for different external field strengths f. All absorbers have the same $\Delta\mu$ value. For a field value of f = 1, the Stark broadening equals the linewidth. (b) The same calculations as a) with a Gaussian distribution of $\Delta\mu$ values

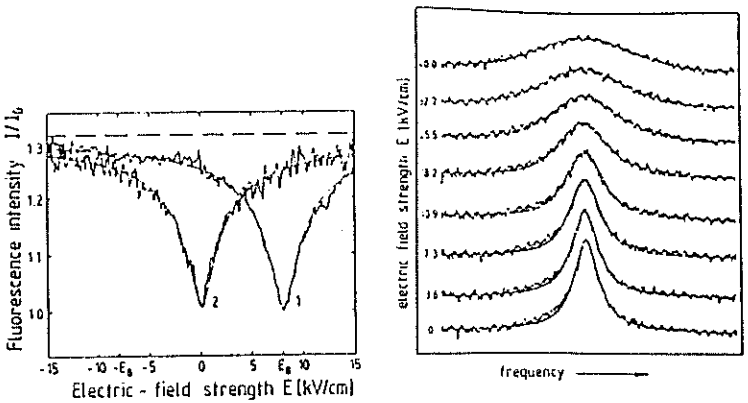

Fig.3.19. Fluorescence excitation spectra of two holes. One spectrum was burned at E = 0 and one was burned at the field E_0 [3.123]

Fig.3.20. Measured and calculated hole profiles for the system Zn-TBP $(C_6H_4CH_3)_4$ in polyvinylbutyral (see [3.124]). Here the average change in dipole moment is $\Delta\mu$ = 0.174 Debye units

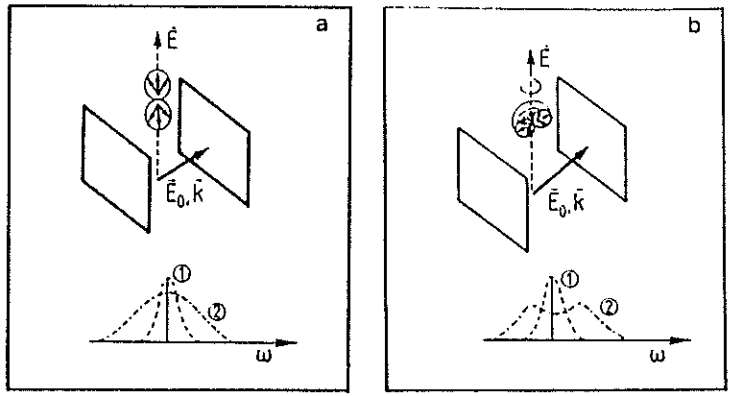

Fig.3.21. Dipolar $\Delta\mu$ configurations for $\Delta\mu$ parallel (a) and perpendicular (b) to the transition dipole moment. E_0 is the electric field strength and k is the wave vector of the incident light

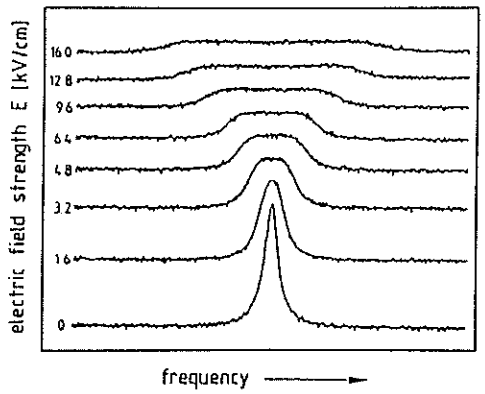

Fig.3.22. Measured and calculated hole profiles for H_2Ch in polyvinylbutyral [3.124]. Here the calculated $\Delta\mu$ value is $\Delta\mu$ = 0.214 Debye units

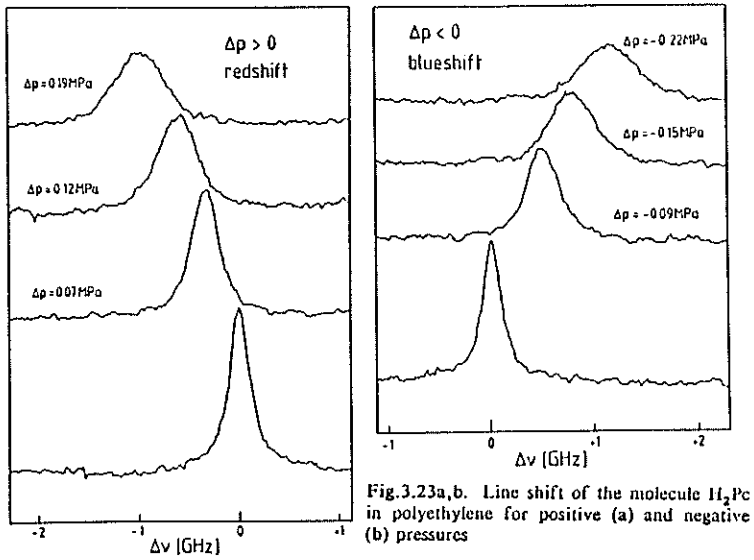

Fig.3.23a,b. Line shift of the molecule H_2Pc in polyethylene for positive (a) and negative (b) pressures

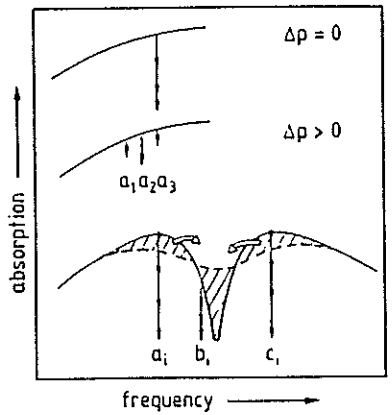

Fig.3.25. Line broadening of sites which had been site-selected at $\Delta p = 0$ and which drift apart at higher pressures $\Delta p \neq 0$. At higher pressures the frequency range of the absorbers extends from a_1 to a_2. The lower part of the figure shows the line broadening for various sets of molecules a_i, b_i and c_i

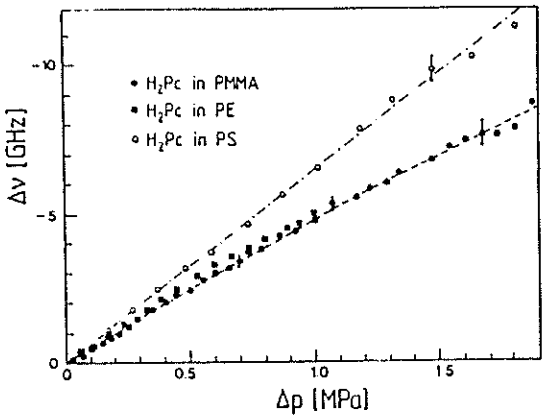

Fig.3.24. Line shifts of H_2Pc in PS, PE and PMMA in the low pressure regime

POSTER SESSION ABSTRACTS

Optical Kerr Measurements on some Ferrocene Derivatives.

C.S.Winter, J.D.Rush and S.N.Oliver.

British Telecom Research Labs.,
Martlesham Heath,
Ipswich IP5 7RE,
England.

We report here preliminary results from a study of the third order non-linearities in a range of organo-metallic compounds. These initial measurements have been carried out carried using the optical power limiter technique developed by Soileau *et al* [1], where the critical power for self-focusing is measured and used to calculate n_2. The materials measured were solutions of ferrocene in ethanol, varying from 10^{18} to 10^{19} molecules/cc and a liquid ferrocene derivative, bis(trimethylsilyl)ferrocene. A value of γ for ferrocene of 4.1×10^{-34} esu was found for the solution studies, in good agreement with that measured for the liquid derivative of 4.6×10^{-34} esu . The experiments were carried out at 1.06 μm with 10 ns pulses. We are currently repeating the measurements using other techniques and shorter pulses to distinguish the various possible contributions to the observed n_2.

(1) M.J.Soileau, W.E.Williams and E.W.Van Stryland;IEEE J Quant Elect.,QE-19,(1983),731.

Theoretical models for the second hyperpolarizability of novel conjugated polymers

David N. Beratan
Jet Propulsion Laboratory
California Institute of Technology
Pasadena, CA 91109

Theoretical models will be presented for the chain length dependence of the second electronic hyperpolarizability of simple polyenes, simple polyynes, and more complicated unsaturated organic materials. The hyperpolarizability of conjugated polymers which incorporate novel localized electronic states will be described as well. These materials present the possibility of achieving enhanced hyperpolarizabilities due to mixing of appropriate "gap states" with the delocalized states of the conjugated polymer. They also present the possibility of designing materials with "switchable" hyperpolarizabilities.

NONLINEAR OPTICAL PROPERTIES OF TRANSITION METAL POLY-YNES

E.A. Chauchard, M.P. Cockerham, P.L. Porter, S. Guha, C.C. Frazier
Martin Marietta Laboratories
1450 South Rolling Road
(301) 247-0700

Data from third harmonic generation (with a 1.06-μm fundamental), power limiting and four-wave mixing measurements of solutions and films of transition metal poly-ynes were used to verify that these compounds have large third-order optical susceptibilities. The large third-order nonlinearities observed in four-wave mixing studies of metal poly-yne solutions may originate, in part, from contributions from the real and imaginary components of intense two-photon absorptions associated with the metal-organic compounds. We will discuss our latest four wave mixing experiments and the direct observation of two-photon absorption in metal poly-ynes.

We will also discuss the correlation of polymer chain length and structure with third-order hyperpolarizability per repeat unit for several metal polymers and oligomers.

REVERSE SATURABLE ABSORBERS: INDANTHRONE AND ITS DERIVATIVES

R. S. Potember, R. C. Hoffman, and K. A. Stetyick
Johns Hopkins University Applied Physics Laboratory
Johns Hopkins Road
Laurel, MD 20707-6099

Indanthrone has been shown to exhibit the phenomenon of reverse saturable absorption.[1] The wavelengths at which indanthrone behaves in this fashion can be changed by structural modification of the indanthrone chromophore. The derivatives which have been synthesized have been shown to be more efficient reverse saturable absorbers than the parent chromophore.

It is advantageous to extend the range of nonlinear behavior to any desired portion of the spectrum, and this is best accomplished by substitution on the aromatic portion of the indanthrone molecule. We have demonstrated that oxidized indanthrone, monochloroindanthrone and an oligomer of indanthrone are more efficient saturable absorbers than the parent. Oxidized and monochloro-indanthrone exhibit reverse saturable absorption at both 1064 nm and 532 nm, whereas indanthrone itself exhibits the phenomenon at 532 nm only. The oligomer, which consists of three anthraquinone units, has proved to be an efficient reverse saturable absorber at 1064 nm as well as at 532 nm.

[1]C. R. Giuliano and L. D. Hess, IEEE J. Quantum Elec. QE-3, 338 (1966).

This work was supported in part by the Dept. of the Navy under Contract No. N00039-87-C-5301.

THE PREPARATION AND CHARACTERIZATION OF POLYMERIC MATERIALS WITH ENHANCED SECOND ORDER NONLINEARITIES. M.L. Schilling, H.E. Katz, D.I. Cox, AT&T Bell Laboratories, Murray Hill, NJ 07920.

We have recently introduced a new class of organic materials for second order nonlinear optics, consisting of poled films of dye-containing polymers. In the past year, some uncommon functional groups (di- and tricyanovinyl) have been shown to enhance the molecular susceptibilities of the nonlinear moieties when used instead of their more usual counterparts. Dyes with enhanced nonlinearities by virtue of the cyanovinyl substituents have been exploited in the preparation of bulk materials with some of the highest second order susceptibilities yet reported.

The synthesis of conformationally defined dye aggregates, whose subunit dipoles are constrained to be additive, is in progress. These dyes can then be incorporated into polymeric materials, taking advantage of their enhanced effective dipole moments for increased orientation in poling experiments. We will report some of the new synthetic organic chemistry that has been utilized in preparing our latest electro-optical materials.

Second Harmonic Generation in Doped Glassy Polymer Films as a Function of Physical Aging

Hilary L. Hampsch[a], Jian Yang[b], George K. Wong[b], and John. M. Torkelson[a,c]*

[a] Department of Materials Science and Engineering

[b] Department of Physics and Astronomy

[c] Department of Chemical Engineering and the Materials Research Center

Northwestern University

Evanston, Illinois

March 31, 1988

ABSTRACT

The temporal stability of second harmonic generation (SHG) intensity is measured in poly(methyl methacrylate) (PMMA) and bisphenol-A-polycarbonate (PC) doped with nonlinear optical dyes in electric field poled films. Doped PC films show slower SHG decay than doped PMMA films at times less than 8 hours. In PC+DANS films aged 10 hours at 25°C, there is no SHG decay over the first 8 hours, whereas in PMMA+DANS aged at 25°C and at 60°C the effect is much smaller. Two dopants show the effect of size on SHG decay, with the larger dopant showing increased temporal stability. Good agreement is obtained when decay curves are fit using a Williams-Watts stretched exponential.

* to whom correspondence should be addressed

ELECTRO-OPTIC, POLYMER CLAD, E-FIELD SENSOR

L. MICHAEL HAYDEN
GERALD F. SAUTER

UNISYS CORPORATION, CSD, St. Paul, MN, 55164

Abstract

There is a military need for sensor systems that combine high sensitivity, immunity to EMI/RFI, large bandwidth, and low power and cost. The hybridization of present day electronic components with optical components offers the promise of sensor systems that meet these requirements.

Unisys has been developing a PVDF-coated fiber optic, electric field sensor and now has expanded its program to include nonlinear organic polymers as cladding and waveguide material. This paper will report on progress using Guest/Host (GH) polymers as cladding material.

The concept of an all dielectric high frequency sensor is demonstrated. The sensor consists of a Ag^{+} exchange waveguide coated with a GH nonlinear polymer glass. The sensor is incorporated into one arm of a Mach-Zender interferometer and exhibits a figure of merit of 4 microradians/volt/meter/meter. The frequency response is flat from DC to our current instrumentation limit of 5 MHz.

This sensor design was chosen primarily as a vehicle that would allow an easy method to test and verify design parameters for fiber sensor systems. These parameters include index and depth of guide vs. index, thickness and E-O coefficients of the cladding. We will present a comparison of the results of this sensor with those from the PVDF sensor program.

MOLECULAR CONFORMATION AND THE STABILITY OF TICT STATE IN P,P'-DISUBSTITUTE-1,6-DIPHENYL-1,3,5-HEXATRIENES

C.T. Lin, H.W. Guan, R. K. McCoy and C. W. Spangler
Department of Chemistry
Northern Illinois University
DeKalb, IL 60115

ABSTRACT

The p,p'-disubstituted linear diphenyl polyenes are expected to have a high optical nonlinear susceptibility because of its large permanent dipole moment induced by the substituents. The photophysical properties for a series of p,p'-disubstituted-1,6-diphenyl-1,3,5-hexatrienes (referred as D,A-DPH) are investigated, where D and A are the electron-donating and - accepting groups of $-OCH_3$, $-N(CH_3)_2$ and $-NO_2$. In all solvents used, a dual fluorescence is observed for D,A-DPH containing the internal rotation groups of $-N(CH_3)_2$ and/or $-NO_2$, suggesting that the "a*" fluorescence (the locally excited state gives the normal "b*" fluorescence) is originated from a twisted intramolecular change transfer (TICT) state. The stability of TICT state is sensitive to the D and A substituents and their relative twisting angles. The observed results provide the evidence of the π-electron distortion and thus the enhancement of optical nonlinearity in this class of molecules.

Second and Third – Order Nonlinear Optical Properties of End – Capped Acetylenic Oligomers

Joseph W. Perry, Albert E. Stiegman, Seth R. Marder and Daniel R. Coulter

Jet Propulsion Laboratory, California Institute of Technology
4800 Oak Grove Drive, Pasadena, CA 91109

We have been investigating the second and third – order nonlinear optical properties of a variety of acetylenic oligomers. A series of symmetric acetylenic oligomers of the form

$$R-(C\equiv C)_n-R \qquad I$$

have been investigated for third – order nonlinear susceptibility. A series of new compounds of the form

$$D-(C\equiv C)_n-A \qquad II$$

where D and A are electron donor and acceptor groups, respectively, have been synthesized and investigated for second – order nonlinearity. Third – order nonlinear susceptibilities of series I molecules in solution have been measured using third harmonic generation (THG). THG susceptibilities at 1064 nm have been determined for various oligomer lengths and end – capping groups. X(3) increases with length and varies with the nature of the end – group. Series II compounds have been screened for second harmonic gener – ation by using the Kurtz powder method. Several samples show SHG efficien – cies comparable to urea. Characterization of molecular hyperpolarizabilities for the series is in progress.

Optical Field Induced Scattering in Polymer Dispersed Liquid Crystal Films

P. Palffy-Muhoray, Michael A. Lee and J.L. West
Liquid Crystal Institute
Kent State University
Kent, OH 44242

ABSTRACT

We report observations of optical field induced scattering in polymer dispersed liquid crystal films due to reorientation of the liquid crystal molecules by the optical field of a CW argon ion laser. These composite materials consist of nearly spherical liquid crystal droplets dispersed in a polymer binder. As previously reported [1,2,3], films of these materials may be switched from an opaque scattering state to a clear transparent state by application of a d.c. or low frequency a.c. electric field. An applied low frequency electric field is used to align the liquid crystal in an orientation such that the refractive index of the liquid crystal within the droplet is matched with that of the polymer binder. If a sufficiently intense optical field is applied to the transparent film, it will reorient the liquid crystal director, and give rise to a refractive index mismatch and hence scattering.

1. J.W. Doane, N.A. Vaz, B.-G. Wu and S. Zumer, App. Phys. Lett. 48, 269 (1986).

2. J.L West, Mol. Cryst. Liq. Cryst. (in press).

3. S. Zumer and J.W. Doane, Phys. Rev. A 34, 3373 (1986).

FABRICATION OF WAVEGUIDE STRUCTURES FROM SOLUBLE POLYDIACETYLENES. **G.L. Baker, N.E. Schlotter, J.L. Jackel, P. Townsend, S.Etemad, Bell Communications Research, Red Bank NJ 07701.**

Thin waveguide structures were fabricated from spun films of poly(3-BCMU) and poly(4-BCMU) by two separate processes. In the first, micron-sized features were patterned in polydiacetylene films using deep-UV lithography. This multilayer process utilizes a novel silicon-substituted polyacetylene as the resist layer, and can be used to generate sub-micron sized features in thick ($>1\mu m$) polydiacetylene films.

In the second method, composite waveguides were fabricated from a patterned glass substrate and an overlayer of the polydiacetylene. These composite structures are relatively simple to prepare and are mechanically robust. Guides constructed as described above performed well with minimal losses and single-moded behavior at laser wavelengths of 1-1.5 μm.